International Council
for Research and Innovation
in Building and Construction

A Systematic Review of

Passive Energy Conservation Measures and Probabilistic Assessment Under Changing Climate in Urban Settings

CIB Working Commission: W040

Heat and Moisture Transfer in Buildings

W040

A Systematic Review of Passive Energy Conservation Measures and Probabilistic Assessment Under Changing Climate in Urban Settings

CIB Working Commission: W040 Heat and Moisture Transfer in Buildings

Edited by

Lin Wang, National Research Council Canada, Canada

Magda Posani, Aalto University, Finland

Jiwei Zou, The Hong Kong Polytechnic University, China

Title:	A Systematic Review of Passive Energy Conservation Measures and Probabilistic Assessment Under Changing Climate in Urban Settings CIB
Serial No.	Publication 432
Edition:	1.0
Date:	30 July 2026
Authors:	Lin Wang, Magda Posani, Jiwei Zou et al.
Language:	English
Pages:	220
Key words:	Thermal insulation and moisture loads, Passive cooling and urban heat island, HAM tools and probabilistic assessment, Future climate and reference year, Decarbonization in built environment
ISBN/EAN	978-1-0678514-1-5
Publisher:	International Council for Research and Innovation in Building and Construction, AIBC Head Office Canada, 1-511 Lacolle Way, Suite #8312, Ottawa ON, K4A 5B6, Canada.

www.cibworld.org | secretariat@cibworld.org

FOREWORD

Founded in 1969, CIB W040 has witnessed half a century of development in heat and moisture transfer in buildings. In the end of the 1950s, the Glaser method was developed for interstitial condensation analysis of envelope systems in cold storage buildings. It was widely applied and standardized to analyze moisture performance of insulated building envelope systems amidst the energy crisis in the 1970s. Rooted in soil science, capillary theory was introduced into hygrothermal analysis of building materials in the 1960s. Together with vapor and heat transfer, this led to the development of the first dynamic hygrothermal computer simulation tool in the 1970s, which was validated against the data from a hot-box experimental work.

The 1980s saw a spring of hygrothermal model development, leading to the first international collaborative research program in the 1990s: ANNEX 24. ANNEX 24 covered five tasks: hygrothermal model development, interior and exterior climate conditions, material properties, experimental validation, as well as performance and practice. In almost the same period, ANNEX 21 evaluated 31 building thermal and energy simulation programs against field measurement data. However, moisture transfer was not included in these programs. Since then, simulation-based design has become a common practice in the building industry for renovation and new construction projects. This transition was driven by the advancement of simulation tools and by the increasing availability of datasets from lab and field measurement for benchmarking. It was further motivated by the establishment of the Intergovernmental Panel on Climate Change (IPCC), the international push towards the thermal retrofit of building envelope systems, and the growing recognition of moisture as a critical contributor to damage in buildings. ANNEX 41 attempted to couple hygrothermal envelope simulations with whole-building energy modelling, moving to whole-building heat, air and moisture (HAM) simulation tools in the early 2000s. In the same years, computational fluid dynamics (CFD) was adopted for wind-driven rain analysis, and relevant articles appeared in W040 conference proceedings (2004). These proceedings also covered topics of indoor air quality and thermal comfort, as well as HAM analysis from materials to wall systems and whole buildings.

The decade of the 2010s opened a new chapter of stochastic simulation and probabilistic analysis, which was driven by ANNEX 55, paving the way for the adoption of artificial intelligence for hygrothermal analysis in the 2020s. The increasing frequency of extreme weather events in the early 2020s led to growing public concern about the climate crisis. The goals of decarbonization set out in the Paris Agreement became increasingly challenging to meet, highlighting the need for international collaboration to accelerate the adoption of passive energy conservation measures (ECMs) to reach emissions reduction targets. The climate crisis, together with the urgent need to accelerate decarbonization, forms the primary motivation of the current W040 working program (2025-2028): probabilistic assessment of passive energy conservation measures under changing climate in urban settings.

Lin Wang
National Research Council Canada

EXECUTIVE SUMMARY

The working program for 2025-2028, developed to follow the conventional objectives of W040, focuses on application-oriented approaches to support climate change adaptation and decarbonization in the construction sector. This report marks the beginning of the 3-year working program and lays the foundation for the long-term research roadmap development.

In this report, a systematic review of the use of passive ECMs under a changing climate, in urban settings, is conducted. The topics cover most passive ECMs that regulate heat, air and moisture transfer in and around buildings. ECMs can be used to reduce heating and cooling demands of buildings, and help ensure the moisture safety, energy efficiency as well as thermal comfort performance of the buildings. These measures are hereby categorized into add-on insulation and passive cooling. Each ECM may be subject to different uncertainties, and its applicability is climate dependent. Therefore, the review in this report focuses on the benefits, uncertainties, potential risks as well as applicability of each passive energy conservation measure under changing climate in various urban environments. This review also includes the hygrothermal simulation tools and Monte Carlo-based stochastic modelling for probabilistic assessment, as such methods are widely used for building performance assessments. To account for the future impact of climate change on buildings, this report also discusses future climate data and reference year selection for building performance simulations.

The expected audience of this report is industrial practitioners who will develop the design or retrofit solutions to adapt buildings to a changing climate, while aiming to lower their operational emissions. Additionally, this report targets researchers who aim to advance the fundamental theory, knowledge, methodologies and innovative solutions needed to better support industrial practitioners in moving towards the design of a climate resilient, low-carbon built environment.

Authors (Alphabetical order of last name)

Name	Organization	Country
Jingjing An	Beijing University of Civil Engineering and Architecture	China
Elif Esra Aydin	Singapore University of Technology and Design	Singapore
Canan Bas	Istanbul Technical University	Turkey
Dario Bottino-Leone	Eurac Research	Italy
Fabiana Convertino	University of Bari Aldo Moro	Italy
Tayma Dadssi	Aalto University	Finland
Xinyuan Dang	KU Leuven/University College Dublin	Belgium/Ireland
Yifan Fan	Zhejiang University	China
Hua Ge	Concordia University	Canada
Payam Gholamalipour	Concordia University	Canada
Praveen Govindarajan	Singapore University of Technology and Design	Singapore
Max Junginger	Concordia University	Canada
Targo Kalamees	Tallinn University of Technology	Estonia
Aslihan Karatas	University of Illinois Chicago	USA
F. Peter Ortner	Singapore University of Technology and Design	Singapore
Magda Posani	Aalto University	Finland
Sina A. Shams	Concordia University	Canada
Zheng Tan	The Hong Kong Polytechnic University	China
Xiaoliang Teng	Zhejiang University	China
Nathan Van Den Bossche	Ghent University	Belgium
Stéphanie Van Linden	Ghent University	Belgium
Lin Wang	National Research Council Canada	Canada
Liangzhu (Leon) Wang	Concordia University	Canada
Da Yan	Tsinghua University	China
Shujie Yan	The Hong Kong Polytechnic University	China
Liqi Zhang	Kochi University	Japan
Xin Zhang	Kochi University	Japan
Jiwei Zou	The Hong Kong Polytechnic University	China

Acknowledgements

This report underwent peer review by a group of researchers from various fields. Their insightful comments and valuable suggestions were thoughtfully integrated into different sections of the report. This group of reviewers are duly acknowledged as international advisory board, their contributions are greatly appreciated.

International advisory board (Alphabetical order of last name)

Name	Organization	Country
Nickolaj Feldt Jensen	Aalborg University	Denmark
Targo Kalamees	Tallinn University of Technology	Estonia
Hideki Kikumoto	The University of Tokyo	Japan
Ronnen Levinson	Lawrence Berkeley National Laboratory	USA
Michael Lacasse	National Research Council Canada Concordia University	Canada
Valentina Marincioni	University College London	UK
Jonas Niklewski	Lund University	Sweden
Sareh Peyman	Stantec	Canada
Carsten Rode	Technical University of Denmark	Denmark
Mikael Salonvaara	Oak Ridge National Laboratory	USA
Nathan Van Den Bossche	Ghent University	Belgium
Evy Vereecken	KU Leuven	Belgium
Pieter de Wilde	Lund University	Sweden
Da Yan	Tsinghua University	China
Huibo Zhang	Shanghai Jiao Tong University	China

Contents

1 Introduction

1.1 Background

Climate change has become one of the most important global challenges that requires international collaboration to deal with. According to IPCC(IPCC, 2023), global warming (GW) has already reached 1.1°C in 2011-2020 as compared to the pre-industry level, and by 2050, it is likely to reach 1.5 °C given a very low greenhouse gas (GHG) emission scenario (Shared Socioeconomic Pathways, SSP1-1.9), whereas it is more likely to reach 2°C with moderate mitigation efforts (SSP2-4.5) which is considered the current pathway. Impacts of the climate change on settlements and human health are already visible including heatwaves, droughts, extreme precipitation, floods, storms, and increased heat-related human mortality and morbidity rates caused by increased frequency and intensity of extreme climate events. Considering the high levels of CO_2 emissions, energy use and urbanization with other drivers of vulnerability, the adverse impacts on well-being of people and projected risks on cities and urban aeras are expected to increase in the future (Chaudhry, 2024; Das et al., 2024; Jurgilevich et al., 2023). Rising temperatures and more frequent heavy precipitation events have already been increasing the environmental loads on buildings, and these loads are expected to intensify further in the future, exacerbating the risks to indoor overheating and moisture-related deterioration on buildings, as well, bring greater challenge of energy conservation (Athauda et al., 2023; Duan et al., 2025; Y. Lin et al., 2023; Waddicor et al., 2016).

It is well known that Greenhouse Gas (GHG) emission is the primary driver of climate change. Buildings are responsible for 31% of global CO_2 emissions (95% GHG emissions from buildings are CO_2 emissions) with 50% arising from energy use in residential buildings, 32% from energy use in non-residential buildings, and the remaining 18% from embodied emissions (Cabeza et al., 2022). Global CO_2 emissions from the building sector rose substantially between 1990 and 2019, driven not only by rising energy consumption of existing buildings but also by the rapid expansion of urban areas. Although in some countries, such as those in Northern America and Europe, the rate of urbanization has been stabilized in the past 30 years, the total energy use of existing buildings has continued to increase because of the growing use of household appliance, higher indoor quality standards as well as limited depth of retrofit (Berardi, 2017; González-Torres et al., 2022; Santamouris & Vasilakopoulou, 2021). In other countries, such as those in Eastern Asia and South America, the urbanization rate climbed steeply over the past three decades. In Eastern Asia, the urban expansion has been a major driver of rising energy consumption and CO_2 emissions in the building sector(Anwar et al., 2020; D. Li et al., 2024; X. Wang et al., 2012); in South America, building energy demand has grown with urban expansion, due to the increase of energy-using appliances, expanded floor space per capita. The increased demand of buildings and energy use has not been accompanied by efficient building design, given the countries in this region have not widely adopt unified and mandatory building energy codes (Asturias-Schaub & Gil-Alana, 2023; The World Bank, 2024; Van der Borght & Pallares Barbera, 2023).

Over the next three decades, many countries have committed to achieve net-zero carbon emissions by 2050 in line with the Paris Agreement and the goal of limiting global temperature rise to 1.5 °C above pre-industrial levels. Achieving this target is highly challenging, particularly under conditions of changing climate, intensified climate loads, and higher indoor environment quality expectations(IEA, 2024; Kutty et al., 2023; Liyanage et al., 2024a; Tajuddeen & Sajjadian, 2024). The challenge is even greater for the regions that are still anticipated to experience urban expansion in the next 30 years, such as Eastern Asia, South Asia, Africa and Latin America (IEA, 2023; United Nations Environment Programme, 2025). For countries where urbanization has stabilized—mainly in Europe, North America, Oceania and some developed countries in Asia—the energy retrofit of existing buildings is the most important strategy for achieving the goal of decarbonization. Retrofitting efforts must not only improve energy efficiency and reduce operational emissions, but also ensure indoor thermal comfort and prevent moisture-related deterioration or unintended hygrothermal side effects (Alazazmeh & Asif, 2021; Hilbrecht et al., 2025; Recart & Sturts Dossick, 2022; Schroderus et al., 2025). On the other hand, in regions with continuing urban expansion, decarbonization ought to consider combining energy-efficient retrofits with low-carbon urban planning and design—including passive design strategies, green infrastructure, and resilient urban landscapes—to ensure that both existing and newly built environments are sustainable, comfortable, and climate-adaptive, minimizing additional emissions (Liddo et al., 2025; Santamouris, 2014a; Seidu et al., 2025; UN-HABITAT, 2022).

1.2 Passive Energy Conservation Measures and Probabilistic Assessment

Passive energy conservation measures refer to design or retrofit strategies that rely on reducing energy demand of buildings, maintaining comfort indoor environment with minimized intervention of mechanical systems. Passive energy conservation measures could be achieved by upgrading thermal performance of building envelope systems, managing air flow between buildings and environment and modulating microclimate conditions in urban environment (Amaripadath & Sailor, 2024; Kokatnur et al., 2025; S. Yang et al., 2023). Passive energy conservation measures have many advantages over active measures, such as lower maintenance efforts and better durability, lower environmental impacts and improved resilience, less dependency on user's intervention, as well as lower life cycle cost (D'Agostino et al., 2023; Elaouzy & El Fadar, 2022; Panchalingam et al., 2024; Scherz et al., 2023). Although passive measures may generally require higher initial costs for materials and designs, once the measures are properly designed and implemented, they bring better return on investment through drastically reduced operational and maintenance expenses, thereby, lead to a lower life cycle cost (A. Sharbaf & Schneider-Marin, 2025; Elaouzy & El Fadar, 2022; Elnagar et al., 2024; Gangolells et al., 2020). However, the effectiveness of the passive energy conservation measures highly depend on environmental conditions, and every energy conservation measure could bring some side effects that may sacrifice other performance metrics of a building if it was not properly designed or implemented in an integrated approach. For example, although the primary purpose of adding insulation was to control heat flow of the building/environment interfaces, the moisture transfer behaviour may influence the effectiveness of this measure on reducing energy consumption and improving thermal comfort, depending on different climate zones.

This report provides a systematic review of some commonly used passive energy conservation measures including: add on thermal insulation, radiative cooling technology, green building envelope systems, natural ventilation, high performance glazing system and shading device, as well as urban-level measures to reduce urban heat island (UHI) effects and cooling energy demand of buildings. These measures were reviewed from the perspectives of: benefits, drawbacks and side effects, risk factors that impact the effectiveness of the measures, suitability of use in different climate zones, as well as applicability of large- scale implementation in an urban setting. For add on thermal insulation, this measure is generally used in heating-dominated regions(Kaczmarek, 2025; Kamel & Memari, 2022) , the moisture loads from indoor and outdoor environment are the most important risk factors that influence the effectiveness of reducing heating energy demand (Künzel & Dewsbury, 2022; Panico et al., 2023); for the passive cooling measures, they are generally applied in cooling-dominated regions, particularly in dense cities to against urban heat island effects; their effectiveness are highly dependent on local climate/microclimate conditions (H. Li et al., 2024; Rao et al., 2025; Santamouris et al., 2017; Synnefa et al., 2008). Therefore, two dedicated chapters were developed based on the measures that are generally used in heating or cooling dominated regions: Chapter 2 add on thermal insulation and moisture loads; Chapter 3 passive cooling and urban heat island. For performance assessment of these measures, simulation-based design/retrofit has been widely adopted in the past decades(Hens, 2015; Pan et al., 2023), probabilistic approach was also applied to address the uncertainties of influential factors and input parameters (Bayat Pour et al., 2024a; Hagentoft, 2017); as such, another chapter was established to review the HAM tools and probabilistic approach that could be used to assess various performance metrics of the passive ECMs, that is Chapter 4 HAM Tools and probabilistic approach. As climate change may influence the performance of the passive the passive energy conservation measures, these measures should be evaluated under future climate to guarantee their long-term performance(Kousis & Santamouris, 2025; Pajek et al., 2022). Future climate data is important to assess the performance of passive ECMs under future climate condition, therefore, the final chapter provides a review on acquisition of future climate data and different ways to derive reference years for building performance simulation, that is Chapter 5 Future climate data.

1.3 References

A. Sharbaf, S., & Schneider-Marin, P. (2025). Cost-benefit analysis of sustainable upgrades in existing buildings: A critical review. Energy and Buildings, 328, 115142. https://doi.org/10.1016/j.enbuild.2024.115142

Alazazmeh, A., & Asif, M. (2021). Commercial building retrofitting: Assessment of improvements in energy performance and indoor air quality. Case Studies in Thermal Engineering, 26, 100946. https://doi.org/10.1016/j.csite.2021.100946

Amaripadath, D., & Sailor, D. J. (2024). Reassessing energy-efficient passive retrofits in terms of indoor environmental quality in residential buildings in the United States. Energy and Buildings, 319, 114564. https://doi.org/10.1016/j.enbuild.2024.114564

Anwar, A., Younis, M., & Ullah, I. (2020). Impact of Urbanization and Economic Growth on CO2 Emission: A Case of Far East Asian Countries. International Journal of Environmental Research and Public Health, 17(7), 2531. https://doi.org/10.3390/ijerph17072531

Asturias-Schaub, L. R., & Gil-Alana, L. A. (2023). CO2 emissions in Latin America: a time series perspective based on fractional integration. Environmental Science and Pollution Research, 30(50), 109585–109605. https://doi.org/10.1007/s11356-023-29987-4

Athauda, R. S., Asmone, A. S., & Conejos, S. (2023). Climate Change Impacts on Facade Building Materials: A Qualitative Study. Sustainability, 15(10), 7893. https://doi.org/10.3390/su15107893

Bayat Pour, M., Niklewski, J., Naghibi, A., & Frühwald Hansson, E. (2024). A literature review of probabilistic hygrothermal assessment for building envelopes. Building and Environment, 261, 111756. https://doi.org/10.1016/j.buildenv.2024.111756

Berardi, U. (2017). A cross-country comparison of the building energy consumptions and their trends. Resources, Conservation and Recycling, 123, 230–241. https://doi.org/10.1016/j.resconrec.2016.03.014

Cabeza, L. F., Bai, Q., Bertoldi, P., Kihila, J. M., Lucena, A. F. P., Mata, E., Mirasgedis, S., Novikova, A., & Saheb, Y. (2022). Buildings. In P. R. Shukla, J. Skae, R. Slade, A. Al Khourdajie, R. Van Diemen, D. McCollum, M. Pathak, S. Some, P. Vyas, R. Fradera, M. Belkacemi, A. Hasija, G. Lisboa, S. Luz, & J. Malley (Eds.), Climate Change 2022 - Mitigation of Climate Change. Contribution of Working Group III to the Sixth Assessment Report of the Intergovernmental Panel on Climate Change (pp. 953–1048). Cambridge University Press. https://doi.org/10.1017/9781009157926.011

Chaudhry, D. (2024). Climate change and health of the urban poor: The role of environmental justice. The Journal of Climate Change and Health, 15, 100277. https://doi.org/10.1016/j.joclim.2023.100277

D'Agostino, D., Becchio, C., Crespi, G., & Corgnati, S. P. (2023). Assessment of passive and active buildings resilience to gas supply disruption in winter across European climates. Sustainable Cities and Society, 92, 104461. https://doi.org/10.1016/j.scs.2023.104461

Das, S., Choudhury, M. R., Chatterjee, B., Das, P., Bagri, S., Paul, D., Bera, M., & Dutta, S. (2024). Unraveling the urban climate crisis: Exploring the nexus of urbanization, climate change, and their impacts on the environment and human well-being – A global perspective. AIMS Public Health, 11(3), 963–1001. https://doi.org/10.3934/publichealth.2024050

Duan, Z., Omrany, H., & Zuo, J. (2025). Impact of climate change on energy performance and energy conservation measures effectiveness in Australian office buildings. Energy, 319, 134956. https://doi.org/10.1016/j.energy.2025.134956

Elaouzy, Y., & El Fadar, A. (2022). Energy, economic and environmental benefits of integrating passive design strategies into buildings: A review. Renewable and Sustainable Energy Reviews, 167, 112828. https://doi.org/10.1016/j.rser.2022.112828

Elnagar, E., Düvier, C., Batra, Z., Christoffersen, J., Mandin, C., Schweiker, M., & Wargocki, P. (2024). Creating a comprehensive framework for design, construction and management of healthy buildings. Energy and Buildings, 324, 114883. https://doi.org/10.1016/j.enbuild.2024.114883

Gangolells, M., Gaspar, K., Casals, M., Ferré-Bigorra, J., Forcada, N., & Macarulla, M. (2020). Life-cycle environmental and cost-effective energy retrofitting solutions for office stock. Sustainable Cities and Society, 61, 102319. https://doi.org/10.1016/j.scs.2020.102319

González-Torres, M., Pérez-Lombard, L., Coronel, J. F., Maestre, I. R., & Yan, D. (2022). A review on buildings energy information: Trends, end-uses, fuels and drivers. Energy Reports, 8, 626–637. https://doi.org/10.1016/j.egyr.2021.11.280

Hagentoft, C.-E. (2017). Reliability of energy efficient building retrofitting - probability assessment of performance and cost (Annex 55, RAP-RETRO). Energy and Buildings, 155, 166–171. https://doi.org/10.1016/j.enbuild.2017.09.007

Hens, H. L. S. C. (2015). Combined heat, air, moisture modelling: A look back, how, of help? Building and Environment, 91, 138–151. https://doi.org/10.1016/j.buildenv.2015.03.009

Hilbrecht, R., Cruickshank, C. A., Baldwin, C., & Scharf, N. (2025). A Rapid Review of Hygrothermal Performance Metrics for Innovative Materials in Building Envelope Retrofits. Energies, 18(18), 5016. https://doi.org/10.3390/en18185016

IEA. (2023). Net Zero Roadmap- A Global Pathway to Keep the 1.5 degree C Goal in Reach.

IEA. (2024). World energy outlook 2024.

IPCC. (2023). Climate Change 2023: Synthesis Report, Summary for Policymakers. Contribution of Working Groups I, II and III to the Sixth Assessment Report of the Intergovernmental Panel on Climate Change [Core Writing Team, H. Lee and J. Romero (eds.)]. IPCC, Geneva, Switzerland. https://doi.org/10.59327/IPCC/AR6-9789291691647.001

Jurgilevich, A., Käyhkö, J., Räsänen, A., Pörsti, S., Lagström, H., Käyhkö, J., & Juhola, S. (2023). Factors influencing vulnerability to climate change-related health impacts in cities – A conceptual framework. Environment International, 173, 107837. https://doi.org/10.1016/j.envint.2023.107837

Kaczmarek, A. (2025). A State-of-the-Art Review of Retrofit Interventions in Low-Emission School Buildings Located in Cool Temperate Climates. Buildings, 15(10), 1620. https://doi.org/10.3390/buildings15101620

Kamel, E., & Memari, A. (2022). Residential Building Envelope Energy Retrofit Methods, Simulation Tools, and Example Projects: A Review of the Literature. Buildings, 12(7), 954. https://doi.org/10.3390/buildings12070954

Kokatnur, T., Ferreira, S., Akkoç, B. K., Markarian, E., Nojedehi, P., Qiblawi, S., Sewraj, K., Gunay, B., O'Brien, W., Papineau, M., Schweiker, M., Harputlugil, G. U., & Azar, E. (2025). A review of passive design strategies and their effect on thermal resilience in low-income households. Energy and Buildings, 348, 116508. https://doi.org/10.1016/j.enbuild.2025.116508

Kousis, I., & Santamouris, M. (2025). Assessing long-term effectiveness of passive cooling strategies in the built environment under climate change. Solar Energy, 302, 114038. https://doi.org/10.1016/j.solener.2025.114038

Künzel, H., & Dewsbury, M. (2022). Moisture control design has to respond to all relevant hygrothermal loads. UCL Open Environment, 4. https://doi.org/10.14324/111.444/ucloe.000037

Kutty, N. A., Barakat, D., Darsaleh, A. O., & Kim, Y. K. (2023). A Systematic Review of Climate Change Implications on Building Energy Consumption: Impacts and Adaptation Measures in Hot Urban Desert Climates. Buildings, 14(1), 13. https://doi.org/10.3390/buildings14010013

Li, D., Han, P., Li, K., Di, Q., & Duan, Y. (2024). A Study on the Impact of Urbanization Level on Carbon Emissions Based on the STIRPAT Model: A Case Study of Five Major Urban Agglomerations in Northern China. Sustainability, 16(14), 6134. https://doi.org/10.3390/su16146134

Li, H., Zhao, Y., Wang, C., Ürge-Vorsatz, D., Carmeliet, J., & Bardhan, R. (2024). Cooling efficacy of trees across cities is determined by background climate, urban morphology, and tree trait. Communications Earth & Environment, 5(1), 754. https://doi.org/10.1038/s43247-024-01908-4

Liddo, F. Di, Amoruso, P., Tajani, F., Morano, P., & Stara, F. (2025). Urban redevelopment and decarbonization challenges. An overview from the real estate market perspective. Energy and Buildings, 343, 115914. https://doi.org/10.1016/j.enbuild.2025.115914

Lin, Y., Huang, T., Yang, W., Hu, X., & Li, C. (2023). A Review on the Impact of Outdoor Environment on Indoor Thermal Environment. Buildings, 13(10), 2600. https://doi.org/10.3390/buildings13102600

Liyanage, D. R., Hewage, K., Hussain, S. A., Razi, F., & Sadiq, R. (2024a). Climate adaptation of existing buildings: A critical review on planning energy retrofit strategies for future climate. Renewable and Sustainable Energy Reviews, 199, 114476. https://doi.org/10.1016/j.rser.2024.114476

Liyanage, D. R., Hewage, K., Hussain, S. A., Razi, F., & Sadiq, R. (2024b). Climate adaptation of existing buildings: A critical review on planning energy retrofit strategies for future climate. Renewable and Sustainable Energy Reviews, 199, 114476. https://doi.org/10.1016/j.rser.2024.114476

Pajek, L., Potočnik, J., & Košir, M. (2022). The effect of a warming climate on the relevance of passive design measures for heating and cooling of European single-family detached buildings. Energy and Buildings, 261, 111947. https://doi.org/10.1016/j.enbuild.2022.111947

Pan, Y., Zhu, M., Lv, Y., Yang, Y., Liang, Y., Yin, R., Yang, Y., Jia, X., Wang, X., Zeng, F., Huang, S., Hou, D., Xu, L., Yin, R., & Yuan, X. (2023). Building energy simulation and its application for building performance optimization: A review of methods, tools, and case studies. Advances in Applied Energy, 10, 100135. https://doi.org/10.1016/j.adapen.2023.100135

Panchalingam, K., Rasheed, E. O., & Rotimi, J. O. B. (2024). Cost-Related Drivers and Barriers of Passivhaus: A Systematic Literature Review. Sustainability, 16(15), 6510. https://doi.org/10.3390/su16156510

Panico, S., Larcher, M., Herrera Avellanosa, D., Baglivo, C., Troi, A., & Maria Congedo, P. (2023). Hygrothermal simulation challenges: Assessing boundary condition choices in retrofitting historic European buildings. Energy and Buildings, 297, 113464. https://doi.org/10.1016/j.enbuild.2023.113464

Rao, P., Torreggiani, D., Tassinari, P., Rötzer, T., Pauleit, S., & Rahman, M. A. (2025). Do urban green spaces cool cities differently across latitudes? Spatial variability and climatic drivers of vegetation-induced cooling. Sustainable Cities and Society, 130, 106513. https://doi.org/10.1016/j.scs.2025.106513

Recart, C., & Sturts Dossick, C. (2022). Hygrothermal behavior of post-retrofit housing: A review of the impacts of the energy efficiency upgrade strategies. Energy and Buildings, 262, 112001. https://doi.org/10.1016/j.enbuild.2022.112001

Santamouris, M. (2014). Cooling the cities – A review of reflective and green roof mitigation technologies to fight heat island and improve comfort in urban environments. Solar Energy, 103, 682–703. https://doi.org/10.1016/j.solener.2012.07.003

Santamouris, M., Ding, L., Fiorito, F., Oldfield, P., Osmond, P., Paolini, R., Prasad, D., & Synnefa, A. (2017). Passive and active cooling for the outdoor built environment – Analysis and assessment of the cooling potential of mitigation technologies using performance data from 220 large scale projects. Solar Energy, 154, 14–33. https://doi.org/10.1016/j.solener.2016.12.006

Santamouris, M., & Vasilakopoulou, K. (2021). Present and future energy consumption of buildings: Challenges and opportunities towards decarbonisation. E-Prime - Advances in Electrical Engineering, Electronics and Energy, 1, 100002. https://doi.org/10.1016/j.prime.2021.100002

Scherz, M., Hoxha, E., Maierhofer, D., Kreiner, H., & Passer, A. (2023). Strategies to improve building environmental and economic performance: an exploratory study on 37 residential building scenarios. The International Journal of Life Cycle Assessment, 28(7), 828–842. https://doi.org/10.1007/s11367-022-02073-6

Schroderus, S., Kuurola, P., Kempe, M., Fedorik, F., Leivo, V., & Haverinen-Shaughnessy, U. (2025). Impacts of building energy retrofits on energy consumption, indoor environment, and hygrothermal performance in future climate scenarios. Energy and Buildings, 347, 116413. https://doi.org/10.1016/j.enbuild.2025.116413

Seidu, S., Chan, D. W. M., & Taiwo, R. (2025). Integrating green and grey infrastructure systems in dense urban regions: a synthesis of critical barriers and effective implementation guidelines. Clean Technologies and Environmental Policy. https://doi.org/10.1007/s10098-025-03309-3

Synnefa, A., Dandou, A., Santamouris, M., Tombrou, M., & Soulakellis, N. (2008). On the Use of Cool Materials as a Heat Island Mitigation Strategy. Journal of Applied Meteorology and Climatology, 47(11), 2846–2856. https://doi.org/10.1175/2008JAMC1830.1

Tajuddeen, I., & Sajjadian, S. M. (2024). Climate change and the built environment - a systematic review. Environment, Development and Sustainability. https://doi.org/10.1007/s10668-024-04962-2

The World Bank. (2024). Mapping energy efficiency: a global dataset on building code effectiveness and compliance.

UN-HABITAT. (2022). World Cities Report 2022- Envisaging the Future of Cities.

United Nations Environment Programme. (2025). Global Status Report for Buildings and Construction 2024/2025.

Van der Borght, R., & Pallares Barbera, M. (2023). How urban spatial expansion influences CO2 emissions in Latin American countries. Cities, 139, 104389. https://doi.org/10.1016/j.cities.2023.104389

Waddicor, D. A., Fuentes, E., Sisó, L., Salom, J., Favre, B., Jiménez, C., & Azar, M. (2016). Climate change and building ageing impact on building energy performance and mitigation measures application: A case study in Turin, northern Italy. Building and Environment, 102, 13–25. https://doi.org/10.1016/j.buildenv.2016.03.003

Wang, X., Berrah, N., Mathur, S., & Vinuya, F. (2012). Winds of Change: East Asia's Sustainable Energy Future. World Bank.

Yang, S., Wang, L. (Leon), Stathopoulos, T., & Marey, A. M. (2023). Urban microclimate and its impact on built environment – A review. Building and Environment, 238, 110334. https://doi.org/10.1016/j.buildenv.2023.110334

2 Add on Insulation and Moisture Loads

2.1 Overview of Add on Insulations in Building Façade Systems

This section should be cited as:

Posani, M., Kalamees, T., Dadssi, T., Wang, L. (2026). Overview of add on insulation in building facade systems. In: A Systematic Review of Passive Energy Conservation Measures and Probabilistic Assessment under Changing Climate in Urban Settings, CIB W040 Report, CIB General Secretariat.

2.1.1 Add-on thermal insulation

In building physics, the term "thermal insulation" generally refers to a material or multilayer system that is designed to reduce the rate of heat transfer through the building envelope (Klemczak et al., 2024). Thermal insulation is a central measure for lowering heating demand in buildings and enabling the use of lower-capacity heating systems (Sadineni et al., 2011). The impact of insulation on cooling demand is less straightforward. Depending on the building characteristics and the local climate, insulation may either contribute to reduced cooling loads or, conversely, increase cooling demands by limiting heat release to the cool night air (Fosas et al., 2018; Posani, Veiga, & Freitas, 2023).

Most common insulation materials are designed to reduce heat transfer by conduction, leveraging low thermal conductivity (λ [W/(m·K)]). A widely accepted threshold is a thermal conductivity below 0.065 W/(m·K) (EOTA, 2013; Hyrkäs et al., 2025). A wide variety of insulation products meeting this criterion is available on the market. These materials are commonly grouped into four classes based on their origin (Grazieschi et al., 2021):

- Inorganic, mineral-derived materials (e.g., mineral wool, perlite, and vermiculite);
- Organic, petrochemical materials (e.g., EPS: expanded polystyrene, XPS: extruded polystyrene, PUR: polyurethane, and PIR: polyisocyanurate);
- Bio-based and natural materials, of plant or animal origin (e.g., wood fibre, hemp, and sheep wool);
- Innovative technologies (e.g., aerogels and VIP: vacuum insulation panels).

For this last class of materials, thermal conductivity can reach values below 0.026 W/(m·K) (Nosrati & Berardi, 2018). Materials exhibiting such high insulating performance are commonly referred to as super insulators (Posani et al., 2021). Thermal insulation materials are often available in different formats on the market. Common ones include blankets, such as batts and rolls, rigid boards and blocks, while some materials can be available as loose fill (e.g, for blown-in application). Other solutions can be foamed in-place or sprayed on surfaces (Grazieschi et al., 2021).

During renovation works, add-on thermal insulation is most commonly used with the main goal to reduce heat loss and improve thermal comfort during the heating season (Eugenia & Marin, 2025; Kuusk et al., 2014; Simona et al., 2017). It typically targets envelope components that are poorly insulated or uninsulated. Envelope elements that can be considered during thermal retrofit works with add-on insulation include external walls, roofs, intermediate floors, and partition walls separating spaces with different heating setpoints or adjacent to unheated zones, as well as underground walls and ground contact slabs (Eugenia & Marin, 2025; Fedorik et al., 2019). Add-on insulation is most often applied to either the interior or exterior surface of existing envelope components (Harberg et al., 2025; H. Li et al., 2025). The addition of insulation within the core of an existing element, such as cavity wall insulation, is an alternative solution to interior and exterior insulation. This approach has lower versatility, as it is restricted to buildings with suitable pre-existing, uninsulated cavities in the envelope. Although such constructions are relatively common in specific building stocks, for example cavity-wall buildings widely constructed in Europe during the 20th century (Magrini et al., 2022), this insulation strategy is not addressed further in this work due to its more limited applicability.

2.1.1.1 Recent scientific literature

To investigate the current state of the art regarding the use of add-on insulation in the retrofit of energy-inefficient buildings, a systematic literature review was conducted using SCOPUS database. The search query was constructed as follows and a schematic overview of its structure is provided in Figure 2.1.1: TITLE("insulat*" OR "post-insulat*") AND TITLE-ABS-KEY((("energy" AND "retrofit") OR "renovation" OR "upgrade" OR "rehabil*" OR ("thermal" AND "retrofit") OR "resilien*" OR "refurbish*" OR "post-insulat*") AND ("hygrothermal" OR "moisture" OR "heat" OR ("heat" AND "moisture") OR "HAM" OR "energy") AND ("risk*" OR "durability" OR "damage*" OR ("thermal" AND "performance") OR "comfort*" OR ("climat*" AND "chang*") OR "efficien*" OR "consumption*") AND ("roof*" OR "floor*" OR "wall*" OR "building*" OR "window*" OR "glasing*" OR "glazing*" OR "envelop*")).

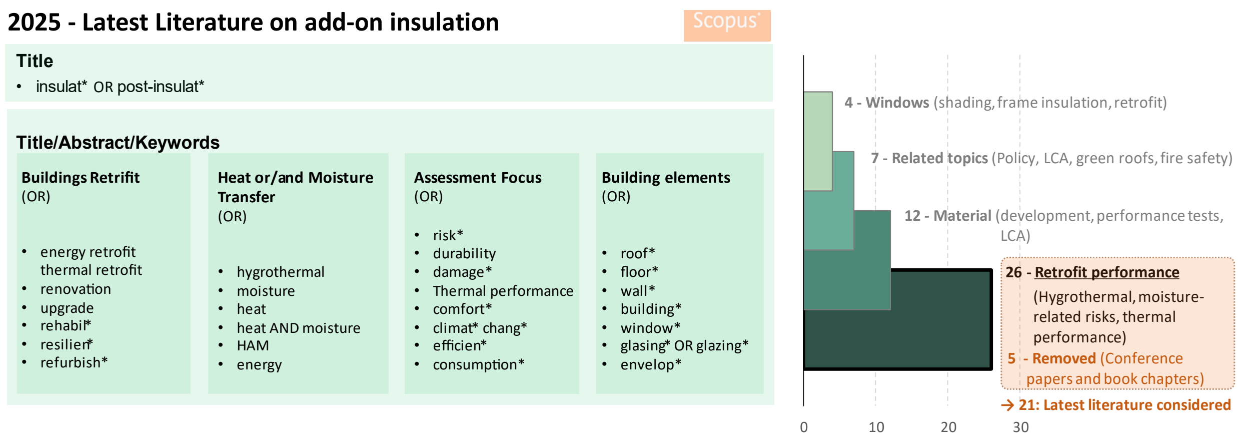

Figure 2.1.1 Identification of the 2025 literature on add-on insulation for renovation: (left) SCOPUS search query; (right) paper selection process, from 49 identified manuscripts to 21 journal articles selected.

The most recent articles identified through the literature search for the year 2025, as available on 10 December 2025, were included in the review. In total, 44 journal articles were identified. Four addressed the thermal upgrade of windows, while seven focused on policy making, life cycle assessment, green roofs, and fire safety. Twelve manuscripts investigated only the material scale, concentrating on material development and performance rather than on their application in building renovation. The remaining 21 manuscripts were considered relevant, as they examined the use of thermal insulation in building renovation, typically addressing hygrothermal behaviour, moisture related degradation risks, thermal performance, and energy efficiency.

The final 2025-review therefore focuses on 21 journal articles, which are discussed in the following paragraphs. These studies were analysed with respect to the following research questions:

- Which materials are most commonly considered?
- Which building envelope components are retrofitted?
- Which performance aspects are assessed, and which methods are used?
- Do the assessments primarily address coupled heat and moisture transfer, or thermal performance alone?
- Do the studies consider future climate conditions and environmental impacts?

2.1.1.2 Thermal insulation materials and use in envelope renovation

When looking at the thermal insulation market, data for the European Union are publicly available. They show that the market is dominated by a few conventional materials, although sustainable and bio-based alternatives are gaining attention, likely due to environmental concerns. As shown in Figure 2.1.2, data from 2014 (Pavel & Blagoeva, 2018) indicate that the share of EU market, by volume of thermal insulation material, was dominated by mineral wool (about 60 %, with roughly 36 % and 22 % being glass wool and stone wool, respectively), and Expanded Polystyrene (EPS, with almost 30 %). A further 14 % was taken by other petrochemical foams and finally about 1% included other insulation materials. A more recent evaluation (IAL Consultants, 2023) shows that in 2022 the market for building Insulation materials was still dominated by mineral wool and EPS, with similar shares, but slight increase in “other materials”. Specifically, mineral wool was still found to cover about 60% of the market by volume and EPS covering almost 25% of the market. A further 20% was taken by other petrochemical foams and 3% included other insulation materials. Interestingly, this 3% is for its majority (2/3) composed of renewable materials, suggesting a growing interest in solutions aligned with a more environmentally sustainable trajectory. Another interesting aspect is that only about 0.1% of the market volume is covered by emerging innovative technologies, such as aerogels and vacuum insulation panels (VIPs).

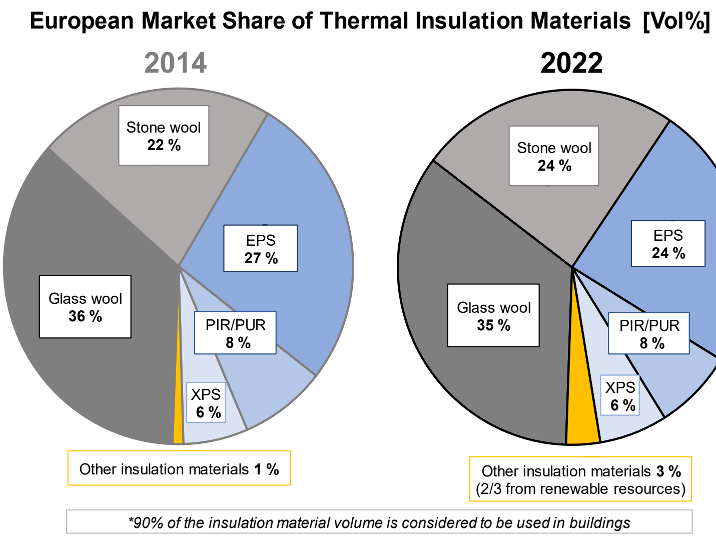

Figure 2.1.2 European thermal insulation market share by material, shown as volume percentage [Vol%] for the years 2014 (Pavel & Blagoeva, 2018) and 2022 (IAL Consultants, 2023).

Finally, an EU technical report (IAL Consultants, 2023) indicates that wall insulation is the largest application in the building thermal insulation market (by value) with about 47 %, followed by roof (37 %) and floor (15 %), as per 2017 data. Also, in scientific literature, most add-on renovation solutions appear to focus on walls. A 2019 review on thermal retrofit of historic buildings (Posani et al., 2019) found 145 mentioned interventions about add-on thermal insulation, 67% of which referring to the retrofitting of external walls. This share was composed of a minority (18%) of interventions considering exterior insulation, and a vast majority (49%) focusing on interior insulation. The preference for interior insulation is to be expected, as historic and heritage buildings are often protected by preservation mandates, which strongly restricts the possibility of applying add-on insulation on the exterior surface of outer walls (Posani et al., 2021). Similarly, in the most recent literature (2025 articles selected in section 2.1.1.1), the majority of research considers add-on insulation for the application on external walls. Indeed, wall insulation is considered in about 80% of the articles, with 40% referring to interior insulation (Ballerini et al., 2025; Harberg et al., 2025; Kang & Kim, 2025; Massafra et al., 2025; Mathews & Charde, 2025; Sahyoun et al., 2025; Yuk et al., 2025; Zhang et al., 2025) and 25% to exterior insulation (Arbulu et al., 2025; Eugenia & Marin, 2025; H. Li et al., 2025; Xu et al., 2025; H. Zhou et al., 2026). Also in this case, the literature mostly focuses on interior insulation of outer walls, rather than exterior. This is probably due to the interesting high complexity of the former intervention, which is prone to moisture degradation risks such as accumulation of moisture from interstitial condensation. Finally, 15% of the papers do not mention which is the side selected for add-on insulation on outer walls, which is the case of research focusing on the final thermal transmittance (Mohammed et al., 2025; Teng et al., 2025) and one study considering a solution that can be used in either interior or exterior add-on insulation (Borodinecs et al., 2025). Additionally, 40% of the studies consider insulation applied to roofs (Arbulu et al., 2025; Ballerini et al., 2025; Eugenia & Marin, 2025; Mathews & Charde, 2025; Mohammed et al., 2025). Insulation of floor structures or slabs in contact with the ground is addressed in 15% of the articles (Eugenia & Marin, 2025; Liu et al., 2025; Mohammed et al., 2025). The latter three articles also consider window upgrades, including glazing, frames, or reduction of thermal bridges, while only two of them consider HVAC upgrades. The sum of these percentages (80% wall insulation, 40% roof insulation, and 15% floor/slab insulation) exceeds 100%, as several articles investigate combined renovation strategies, including the insulation of multiple envelope components. Finally, it is interesting to notice that among all the papers, about 25% (5/21) focuses on historic or heritage buildings, considering the preservation mandates limiting the add-on insulation intervention. The materials considered in the 2025 literature are reported in Figure 2.1.3, which quantifies how many papers mention each insulation material. Across the 21 reviewed articles, specific insulation materials are mentioned 44 times in total, reflecting the fact that several studies consider multiple insulation solutions.

Overall, the 2025 literature reflects EU market trends for the most common insulation materials, with mineral wool and EPS dominating both. In the reviewed studies from 2025, these materials are the most frequently mentioned, appearing in approximately 50% (10/21) and 40% (8/21) of the papers, respectively. At the same time, bio-based materials account for around 15% of all mentions (6/44) and are considered in 25% of the papers (5/21), while new technology solutions represent about 10% of mentions (5/44) and are addressed in 20% of the studies (4/21). Bio-based and new technology materials are proportionally more prominent in research, rather than on the EU market trends. The stronger interest of research on these material typologies is expected since they are often costly or not yet widely familiar to practitioners, limiting their market penetration while attracting substantial academic interest for further development and optimisation. The bio-based materials discussed include wood fiber insulation, cellulose, reed, and hemp. New technology solutions range from high-tech façade panels and VIP to hybrid systems combining conventional insulation with phase change materials and radiative cooling materials. Other solutions include Calcium Silicate (CaSi), a mineral material considered in one paper (Sahyoun et al., 2025), as well as newly developed materials in research, such as a bio-based composite insulation panel made from recycled cardboard aggregates and a mix of binding agents (corn starch, lime, and clay) (Mathews & Charde, 2025), as well as an insulation material made from recycled surgical masks (following the COVID-19 pandemic) (Ballerini et al., 2025).

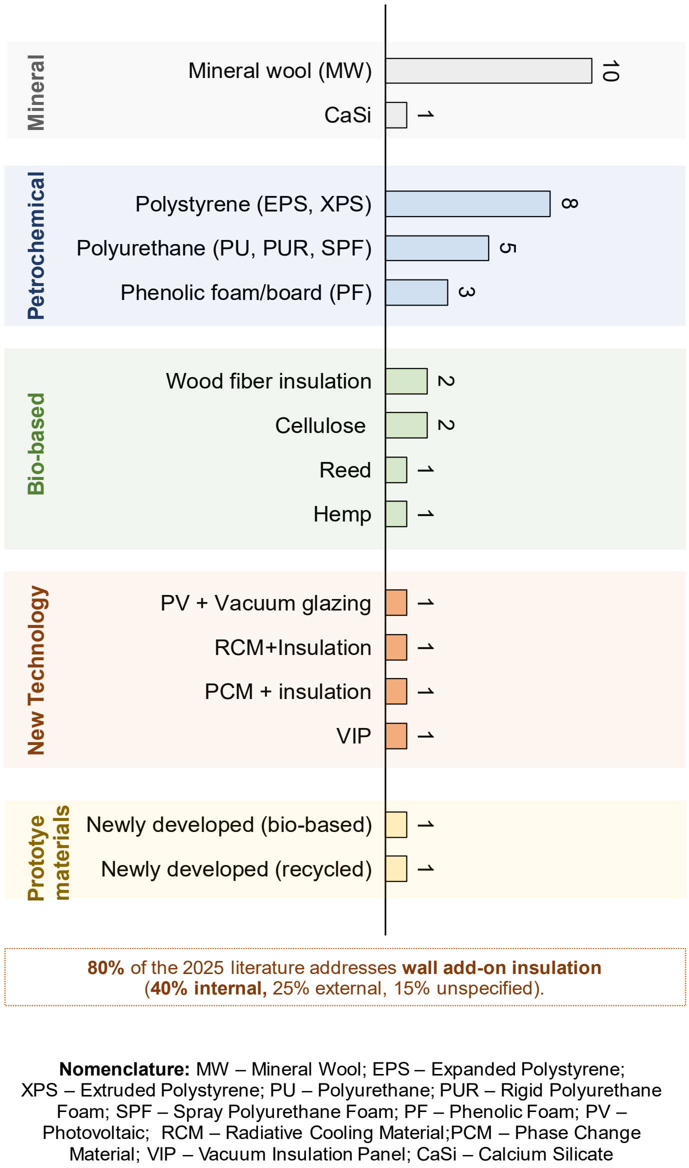

Figure 2.1.3 Thermal insulation materials and number of articles mentioning each of them, in the 2025 literature on add-on insulation. Across the 21 reviewed articles, materials are mentioned 44 times in total, as several studies consider more than one insulation material.

2.1.2 Performance assessment

When assessing the performance of add-on insulation in buildings, most of the literature focuses on walls. This intervention can be particularly challenging for several reasons, some of them related to heat transfer, some to moisture accumulation, and others to both.

2.1.2.1 Thermal transmittance

When applying insulation on external walls, there are a few challenges related to thermal performance. A classic assessment of the performance of post-insulated walls regards the thermal transmittance and reduction of winter heat losses. The thermal transmittance quantifies the rate of heat flow through the wall per square meter of surface, and for each degree of temperature difference between the inside and outside air boundary layers (Posani et al., 2021). Thus, in principle the lower the thermal transmittance, the larger the reduction of winter heat losses through the wall. The thermal transmittance of post-insulated walls can be evaluated by experimental means, for instance measurements on site using heat flux and temperature sensors (O'Hegarty et al., 2021), or via numerical assessment. A simplified assessment can be performed using steady-state calculations of thermal transmittance according to ISO 6946 (2017). In this approach, the thermal transmittance (or U-value) is determined from the declared dry thermal conductivity of each material layer, their thicknesses, and standard internal and external surface thermal resistances. However, this simplified method is more suited for practical early design of renovations, rather than research. More comprehensive methods from scientific literature include the use of dynamic hygrothermal simulations, so to assess the effect of moisture transfer and boundary climatic conditions on the monthly thermal transmittance and dynamic heat loss rates in renovated walls (Amorim et al., 2020, 2023; Maia et al., 2018). This type of assessment allows evaluating the loss of thermal performance due, for instance, to moisture accumulation in the colder wall when interior insulation is used or due to condensate accumulation in the interior insulation (Bottino-Leone et al., 2019; Vereecken et al., 2015; Vereecken & Roels, 2015), while other studies consider the effect of moisture content in exterior insulation like external thermal insulation composite system (ETICS) used in external walls renovation (Maia et al., 2018). Notable results were observed by Amorim et al. (Amorim et al., 2020), who concluded that the moisture content due to wind-driven rain can increase the heat loss of a wall retrofitted with internal mineral wool insulation by up to 40% in the climate condition of Porto (maritime temperate climate), while only 8% in the climate condition of Krakow (continental temperate climate). Similarly, Vereecken et al. (2015) evaluated the hygrothermal performance of a masonry wall retrofitted with interior insulation, comparing the performance of a capillary active insulation system and a vapour tight insulation system, in the climate conditions of Essen, Bremerhaven and Munich. They found that a capillary active interior insulation system had higher winter heat losses than a vapour tight system, likely due to the moisture content influence of the thermal conductivity. Further studies show the degradation of thermal performance due to the presence of moisture in insulated walls under different climate zones (Amorim et al., 2023; F. Li et al., 2021).

2.1.2.2 Increased overheating and cooling demand

Another aspect that is often considered when insulating existing walls is the potential undesirable effect of increased overheating discomfort and higher cooling demand during summer (Posani, Veiga, & Freitas, 2023). This issue is particularly relevant when interventions involve walls with high thermal mass (Posani, Veiga, & Freitas, 2023; Verbeke & Audenaert, 2018). It is well established that adding insulation to thermally heavy walls can significantly reduce the passive cooling effect associated with thermal inertia (Posani, Veiga, & Freitas, 2023; Verbeke & Audenaert, 2018). The magnitude of this reduction depends strongly on the location of the insulation layer, with exterior insulation having a less detrimental impact on thermal inertia than interior insulation (Al-Sanea et al., 2012; Posani, Veiga, & Freitas, 2023; Saldanha & Piñon, 2013). This effect is commonly assessed using dynamic thermal or hygrothermal simulations. For example, one-dimensional simulations can be used to quantify changes in parameters such as time lag, decrement factor, and cooling transmission load (Al-Sanea et al., 2012). These parameters respectively describe the delay between peak outdoor and indoor surface temperatures during summer, the ratio between the amplitude of temperature fluctuations at the inner and outer wall surfaces, and the influence of the wall design on cooling energy demand during warm periods (Al-Sanea et al., 2012). Whole building dynamic energy or hygrothermal simulations can instead be used to evaluate impacts such as changes in cooling energy demand when indoor conditions are mechanically controlled (Posani, Veiga, & Freitas, 2023; Saldanha & Piñon, 2013), as well as overheating hours and overheating discomfort intensity under free floating indoor conditions (Posani, Veiga, & Freitas, 2023). The issue of increased overheating due to add-on insulation can also affect lightweight structures, where thermal insulation can both decrease and increase overheating issues depending on the specific case study at hand (Fosas et al., 2018). The first outcome is mainly due to the reduction of transmission of heat from the warm outdoor surface to the colder indoor one, characteristic of summertime air-conditioned spaces. The other is related to effects like the reduced ability of the envelope to dissipate internal heat gains. The combination of positive and negative aspects results in an overall increase or decrease of overheating which depends on many factors, including the outdoor climate, ventilation rate and control, building typology, orientation, thermal transmittance and thermal mass of the opaque envelope before renovation, shading, windows size and performance, and internal heat gains (Fosas et al., 2018). This type of assessment is typically conducted using whole building dynamic simulations, e.g. through building energy simulation modelling and assessing cooling needs and/or overheating discomfort (Curado & de Freitas, 2019; Fosas et al., 2018; Posani, Veiga, & Freitas, 2023). An alternative to numerical studies is to monitor indoor environmental conditions (e.g., indoor air temperature and surface temperatures) before and after the renovation in reference test buildings (Tink et al., 2018). Field measurements are highly valuable as they provide direct evidence of the effect of insulation on overheating, however they are costly in both economic and time efforts, and as so application in research is limited compared to simulation studies. This statement is generally true for all performance and moisture-related assessments discussed in this paragraph.

2.1.2.3 Moisture-related degradation risks

Moisture is one of the main drivers of degradation in buildings (Posani, Habert, et al., 2025). Entering the building envelope through sources such as driving rain, groundwater, air leakage, or originating within the construction, for instance due to pipe leakages, it can lead to a series of degradation issues that threaten the durability of constructions. Accordingly, alongside thermal considerations, a range of moisture-related degradation risks should be addressed when evaluating add-on insulation interventions. The risks most commonly considered in literature are schematically illustrated in Figure 2.1.4. When insulation is applied on the interior side of existing walls, relevant risks include frost damage, rotting of wooden beam ends embedded in the wall, moisture accumulation due to reduced drying ability, and mould growth at internal and interlayer surfaces. In the case of exterior insulation systems, such as ETICS, the main concerns relate to moisture accumulation within the wall caused by reduced drying potential, as well as the proliferation of mould and algae on the exterior surface. Other moisture-driven deterioration mechanisms, including corrosion and salt efflorescence, may also occur. However, these are less frequently addressed in the literature and are therefore not considered further here,

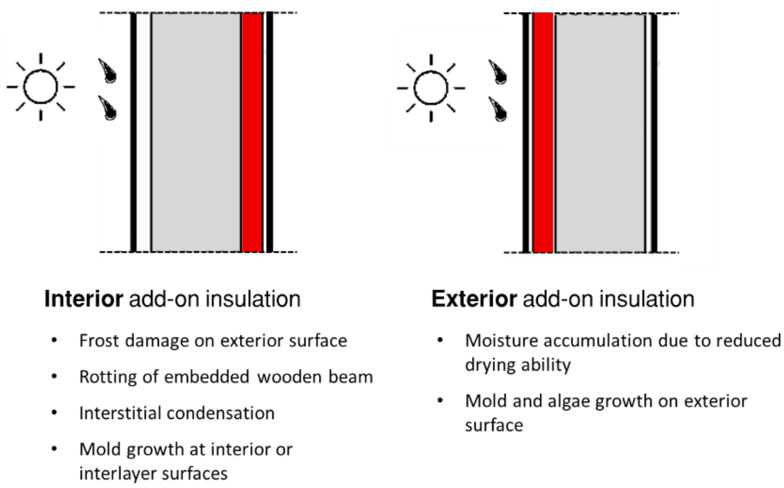

Figure 2.1.4 Moisture-related risks commonly addressed in the literature for interior and exterior add-on insulation interventions on walls.

although additional information can be found in a recent study (Janssens, Vandemeulebroucke, et al., 2024). These risks are most commonly assessed using dynamic hygrothermal simulations, typically applied at the component level through one-dimensional or two-dimensional models. Such analyses are generally carried out using software from the WUFI (Fraunhofer Institute for Building Physics IBP, 2024b, 2024a) or Delphin (Bauklimatik-Dresden, 2024) families. Although less related to add-on insulation, it is worth mentioning that moisture-related risks can also be mitigated through the use of ventilated facades, where the outer cladding acts as the primary barrier or rain screen, thus providing a first deflection device that reduces the risk of rainwater penetration by keeping water off the building structure. Similarly, hydrophobic treatment can be implemented to reduce rainwater penetration. While several studies (Abdul Hamid & Wallentén, 2017; Jensen et al., 2021a; Soulios et al., 2021; X. Zhou et al., 2018) have shown positive effects from hydrophobic treatments, other studies point out several limitations. These include problems such as overall coverage and surface defects (e.g. cracks and holes) potentially creating “moisture hot spots” (Charola, 1995; Drive, 2008; Hilbert et al., 2014; Soulios et al., 2020), the adhesion of the hydrophobising treatment in relation to mineral composition (Hansen, 2018), and exacerbating rising damp issues due to reduced drying potential (Møller, 2004). Longer-term concerns involve durability and the feasibility of reapplication (Appelbaum, 1987), as well as the treatments' irreversibility or difficult removal after adverse effects arise (Appelbaum, 1987; Wendler & Von Plehwe-Leisen, 2008).

2.1.2.4 Frost damage risk

Frost damage may increase following the application of interior insulation, as this intervention leads to lower temperatures in the exterior cladding, during the heating season. The associated risk is commonly assessed by comparing the hygrothermal behaviour of wall assemblies before and after insulation, typically using one-dimensional simulations (Prignon et al., 2023; X. Zhou et al., 2017), and focusing on temperature and moisture content at a critical location on the exterior side of the wall.

For instance, literature on masonry walls most often considers a point located 0.5 cm from the exterior surface (X. Zhou et al., 2017). This position is regarded as sufficiently close to the exterior to experience a high number of freeze thaw cycles, while being far enough from the surface to be less sensitive to short-term exterior climate fluctuations and therefore more representative for evaluating freeze thaw damage (X. Zhou et al., 2017). Alternatively, some studies suggest that a depth of 1 cm from the exterior surface of masonry walls may in certain cases be more representative and exposed to higher risks (Prignon et al., 2023). Frost damage can be assessed using a range of indicators, with common ones being exposure-based, related to the Time-of-Frost, Amount-of-Frozen-Water and Number of Freeze-Thaw Cycles (Feng et al., 2019; Prignon et al., 2023). The computation of frost-damage indicators usually requires fixing values for the critical temperature (T_L) and moisture content (w_L) (Prignon et al., 2023). T_L is the temperature below which liquid water in the pores is assumed to turn into ice, which depends on pore size distribution and salt content, and is often set in the range 0 to -2 °C (Prignon et al., 2023). w_L is the minimum amount of water that must be present for frost damage to be possible, which is considered to possibly span between 25% and 90% (Sahyoun et al., 2025), depending on the materials used in the building fabric. For brickwork masonry, WTA Merkblatt 6-5 (WTA, 2014) suggests using a value of 30% of the moisture content at saturation (w_s) for simulation purposes. This reference value has been used in the literature (Prignon et al., 2023) to quantify freeze thaw cycles (elaborated into an indicative freeze thaw cycle indicator), assuming frost damage risk when the temperature falls below the critical value and the moisture content exceeds the critical threshold at the selected assessment point. Alternative indicators have also been proposed. One approach previously used for brick masonry defines critical freeze thaw cycles based on a moisture threshold corresponding to an ice mass density exceeding 25 percent of the open porosity (Prignon et al., 2023). Another approach consists of considering a freeze thaw damage risk index called the FTDR index (X. Zhou et al., 2017). Unlike other indicators, the FTDR index accounts for both the number of freeze thaw cycles and the variation in ice content during each cycle. It is defined as the cumulative difference between the maximum and minimum degree of ice saturation over each complete or incomplete freeze thaw cycle. According to the literature, even a limited number of freeze thaw cycles can lead to significant degradation of brick masonry walls, and the threshold number of cycles associated with damage should be selected based on the specific material properties of wall layers at risk (Sahyoun et al., 2025). Some studies classify damage risk using a ranking based on number of moist freeze-thaw cycles (where both critical temperature and critical saturation degree or ice volume thresholds are exceeded simultaneously), for instance for masonry walls two studies considered the following classification (Choidis et al., 2023; Sahyoun et al., 2025): 1–5 Damage possible; 6–35 Damage likely; >35 Observable damage. Finally, recent research (Janssens, Feng, et al., 2024) proposes the Ω-factor method, which applies experimentally determined elastic modulus loss (Ω-factor curves) at representative saturation degrees and freezing temperatures, as a material-specific damage threshold to be used to assess simulation results in terms of damage risk.

It should be noted that prediction of freeze-thaw damage via numerical simulations remains a highly debated topic and no consensus has been reached on the reliability of the assessment methods (Janssens, Feng, et al., 2024). Because of the limited reliability and potentially inconsistent results obtained using different methods (Janssens, Feng, et al., 2024), freeze-thaw damage evaluations should be approached carefully and mainly for comparative assessments of relative frost damage risk between retrofit scenarios (before/after insulation) rather than to predict damage occurrence.

2.1.2.5 Risk of rotting of wooden beam ends

Rotting of wooden beam ends becomes a significant concern in masonry walls with add-on interior insulation, as the lowered drying potential raises moisture levels around embedded joists, potentially accelerating decay processes. This rotting risk can be roughly evaluated from the results of 1D simulations, but a 2D approach is more complete and recommended (Vereecken et al., 2015). Examples from the literature include simplified approaches using 1D hygrothermal simulations. For instance, in one evaluation (Vereecken et al., 2015), the point located 5 cm behind the insulation system, within the masonry wall, was taken to represent the end of an embedded wooden beam (simplification, with no wooden beam included in the modelling). The number of hours during which relative humidity at this location exceeded 95% was then calculated over a relevant assessment period (January in the specific study). Another research (Janssens, Vandemeulebroucke, et al., 2024) considered relative humidity at 10 cm depth from the interior masonry surface, considered as corresponding to the minimum structural support required for timber joists embedded in masonry walls. Wood mass loss was estimated using the dose-response relationship of Brischke and Rapp, while decay severity was classified according to EN 252 (CEN, 2014), using a decay index ranging from no attack (0) to failure (4). To limit decay risk, the decay index was required to remain below level 1 (slight attack) over a 30-year period, corresponding to the minimum service life of wooden beams. An example of a more detailed study (Guizzardi et al., 2015) employed 2D simulations. Risk assessment was performed using the VTT wood decay model (Viitanen, Toratti, et al., 2010), to post-process simulation results. The model is built on a 2-phases degradation assumption based on experimental observations. The first phase is an activation period, when varying temperature and RH contribute to the initiation of the process. Once the mechanism is activated, the decay proceeds and the rate of mass loss is dependent on the temperature and RH conditions in the microclimate. It should be noted that several wood decay models (including the VTT model) have generally been found to be rather conservative in their risk predictions (Jensen, 2021; Johansson et al., 2019; Kvist Hansen et al., 2020). Similar wood decay issues can also appear in multilayered walls containing wooden layers, for instance insulated CLT wall assemblies, as investigated by Libralato et al. (Libralato et al., 2021) using the assessment model from European standard EN252 (CEN, 2014). A few studies (Hansen et al., 2018; Harrestrup & Svendsen, 2015; Odgaard et al., 2018) have included an un-insulated gap or a material with a higher thermal conductivity (e.g. aerated concrete block) below and/or above the floor partition to create a deliberate thermal bridge to improve the hygrothermal conditions in the wooden beam ends. This allows more heat to reach the beam ends, leading to increased temperatures and lower relative humidity levels in the beam ends, resulting in reduced wood decay risk. Odgaard et al. (2018) observed reduced VTT wood decay risk in embedded wooden elements by including the material with a higher thermal conductivity below the floor partition.

2.1.2.6 Risk of interstitial condensation

Condensation is a phenomenon where water vapour (gaseous state) in the air changes into liquid water. This can occur due to heat and moisture transfer mechanisms, with many studies focusing on the risk of interstitial condensation at the thermal bridges and exterior side of interior insulation systems added to existing walls. For instance, one study (Vereecken et al., 2015) assessed the number of hours during which the relative humidity at the interface between the masonry wall and the insulation exceeds 99.9%RH, often with a focus on critical winter months such as January. Other approaches (Xue et al., 2022) classify condensation risk using relative humidity ranges, with 95-100%RH indicating near saturation, 90-95%RH associated with likely condensation under minor disturbances, 85-90%RH indicating possible condensation under rapid environmental changes such as radiant cooling, and values below 85%RH considered low risk. More detailed evaluations related to this topic are commonly undertaken in studies on capillary active insulation materials, with analyses of moisture dynamics used to characterise absorption, redistribution, and drying processes enabled by such systems when condensation at the critical cold interface behind the insulation occurs (Vereecken & Roels, 2015, 2016; Zhao et al., 2017). It is worth mentioning that condensation is not a degradation risk, but it is a moisture-related issue often studied in the field as condensate accumulation leads to increased moisture content in building materials, which can in turn lead to moisture-related degradation risks (e.g. mould growth), as well as loss of thermal resistance.

2.1.2.7 Mould degradation risk

Mould growth is considered a critical degradation risk which can develop before condensation, when relatively high humidity conditions affect surfaces or interfaces within the construction assemblies (Harberg et al., 2025). Critical locations include interior building surfaces and cold surfaces behind interior insulation added to existing walls, as well as at layers interface (e.g., between wind barriers and adjacent materials) (Harberg et al., 2025). Common assessment approaches include postprocessing hourly hygrothermal results from numerical simulations, at critical points, for instance using the Finnish mould model (Lähdesmäki et al., 2008; Viitanen et al., 2011; Viitanen, Vinha, et al., 2010), Isopleths approach (Sedlbauer, 2001), or simplified assessments (Harberg et al., 2025). The Finnish mould model predicts mould growth risk as a function of temperature, relative humidity, exposure time, material sensitivity, and surface conditions. It is used to calculate a mould index, ranging from 0 to 6, with higher index indicating heavier mould spread and null indicating none. The model explicitly accounts for the effect of unfavorable environmental conditions on the slowdown of mould growth risk. However, the process of mould set back during unfavorable environmental conditions still needs further experimental verification (Isaksson et al., 2010). For example, mould may not grow under unfavourable conditions, but they could remain dormant for a rather long period of time, and then start germination when conditions become favorable (Jensen et al., 2021b). In addition, the model does not account for processes such as substrate condition outside nutrient availability (e.g. age and pH) and previously colonised materials, which may remain susceptible to renewed growth when favourable conditions return (Ojanen et al., 2007). The isopleth approach is a threshold-based analysis that relies on Sedlbauer's isopleths (Sedlbauer, 2001): curves describing combinations of temperature and relative humidity under which mould growth becomes possible for a given type of substrate, which was constructed based on hygrothermal conditions suitable for the growth of mould types commonly found in buildings (Havinga & Schellen, 2018). Different isopleth systems are defined for categories of materials representing substrates that are more or less prone to mould growth (M. Krus, 2007). Mould risk is assessed by comparing simulated transient surface conditions with the relevant isopleths, with mould growth becoming possible when favourable conditions persist over time (Havinga & Schellen, 2018). More simplified assessments occasionally refer to a threshold relative humidity (RH) as a risk indicator. For instance, a study in Norway (Harberg et al., 2025) used a threshold of RH>80 %, referring to the European standard EN ISO 13788 (CEN, 2012), concurrent to temperatures in the range T=5-30 °C. The risk was then evaluated based on the continuous period of favorable mould conditions, with high risk occurring when conditions persisted for 2 days or longer. Other simplified approaches refer to the 30-day moving average of surface relative humidity. For instance, in Havinga & Schellen (2018) the authors considered a moving average below 80%RH to exclude mould growth risks, for surfaces with a moving average surface temperature between 5 °C and 40 °C, based on standards ASHRAE Standard 160 (ASHRAE, 2009) and ISO 13788 (ISO, 2012). Additionally, the study considered no mould growth risk if 24-h, 7-day and 30-day moving average of surface relative humidity did not surpass 100%, 98% and 80%, respectively. In the context of moisture-related risks assessment for add-on interior insulation interventions, it is worth noting that most studies considering mould growth and/or condensation disregard convective vapour transfer due to air leakages (Havinga & Schellen, 2019). However, Havinga and Schellen (2018) demonstrated that this limitation can be critical, particularly when vapour barriers are used in interior insulation systems for lightweight constructions. In such cases, damage or imperfect installation of the vapour barrier can compromise airtightness and lead to air leakage. Air leakages and the associated convective vapour transfer were shown to substantially increase the risk of mould growth and condensation in internally insulated lightweight walls. This outcome highlights that the limitations associated with neglecting air leakage through vapour barriers should be carefully considered when assessing moisture-related risks due to add-on interior insulation systems. Also, Vereecken and Roels (2017) found a significant impact of convective moisture transport, resulting in increased mould risk, in their study on wooden beam ends in combination with interior insulation systems. They emphasize the importance of preventing both air exfiltration and air circulation near the wooden beam. For mineral wool, a soft insulation material that can be more easily pressed against the beam ends, the impact of convective vapour transport was less pronounced. Finally, it should be noted that the method used in the mould growth assessment should be carefully selected, as different methods might lead to incomparable results (Vereecken & Roels, 2012).

2.1.2.8 Moisture accumulation and algae growth risk with add-on in exterior insulation

When adding exterior insulation to external walls, moisture-related degradation risks are generally lower than in the case of interior insulation. A well-designed exterior insulation system can reduce thermal bridges and associated cold-spot moisture risks, while also limiting wind-driven rain exposure of the existing wall. At the same time, the addition of exterior insulation may significantly reduce the wall's drying potential, particularly when materials with high resistance to water vapour diffusion are used. Previous studies have shown that exterior insulation alters both the wetting and drying behaviour of wall assemblies, highlighting the need to achieve an appropriate balance between moisture protection and drying capacity (Posani, Veiga, & de Freitas, 2023). These effects are typically assessed by analysing moisture accumulation within the wall assembly through transient hygrothermal simulations, for example by evaluating the temporal evolution of water content in the wall layers over multiple years (Posani, Veiga, & de Freitas, 2023). Further studies show that, in walls with added external thermal insulation systems, night-time overcooling can be a major driver of algae growth on facades, resulting in surface defacement (Barreira et al., 2013; Barreira & de Freitas, 2013). This risk arises from long wave radiative heat loss from the insulated exterior surface to the night sky, which can lower surface temperatures below ambient air temperature. The resulting cold surfaces experience prolonged periods of elevated surface relative humidity and frequent moisture availability, creating favourable conditions for algae growth. This phenomenon can be studied through dynamic hygrothermal simulations, via an accurate modelling of radiation balance at the wall surface (Maia et al., 2018). One study (Maia et al., 2018) assessed the problem by postprocessing the results from hygrothermal simulations and using prolonged surface condensation as an indicator for algae growth. The analysis quantified the accumulated condensation potential by evaluating periods in which the water vapour partial pressure in the adjacent air exceeded the saturation vapour pressure at the surface.

Similarly, results can be postprocessed to analyse mould growth risk in those cases where this is considered as a more critical issue on the façade compared to algae (Parracha et al., 2024).

2.1.2.9 Performance assessment in 2025 literature

Focusing on the 21 papers selected in the 2025 literature review, ten studies focus on heat transfer and energy simulations while neglecting moisture transport. Two of these use TRNSYS. One (Liu et al., 2025) evaluates the payback time of renovation alternatives based on costs and heating demand reduction for well and poorly insulated apartments in the temperate oceanic climate of Utrecht in the Netherlands. The other (Arbulu et al., 2025) investigates overheating risks associated with add-on insulation in typical multifamily residential buildings from the 1960s and 1970s in different regions of Spain. Another study (H. Li et al., 2025), addressing cooling demand reduction, employs DeST simulation software with an embedded equivalent sky radiation temperature module to assess the combined use of radiative cooling materials and conventional insulation, in the cooling dominated climates of Guangzhou, Hong Kong, Taipei, Miami, and Cairo. Five studies use EnergyPlus dynamic energy simulations to quantify the impact of add-on insulation on heating and or cooling energy demands (Ballerini et al., 2025; Mathews & Charde, 2025; Mohammed et al., 2025), with several also including economic assessments of payback time based on intervention costs and operational energy savings (Kang & Kim, 2025; Zhang et al., 2025). Two additional studies extend thermal performance analyses to carbon assessments. One (Teng et al., 2025) applies a BIM based workflow using ArchiCAD to evaluate energy use, as well as embodied and operational carbon emissions, for the thermal retrofit of an apartment building in Japan. The other (Eugenia & Marin, 2025) adopts simplified heat transfer calculations for post-insulated components of a secondary public school and introduces a carbon index to quantify emission reductions associated with lower heating demand. Four studies rely primarily on mono-dimensional dynamic hygrothermal simulations. Two use Delphin for case studies in continental climates with cold winters. One (Sahyoun et al., 2025) examines freeze-thaw damage risks associated with interior insulation applied to masonry walls, while the other (Borodinecs et al., 2025) analyses humidity levels, condensation, and mould growth risk in an insulated timber frame element intended for insulation and thermal renovation applications. Another study (Harberg et al., 2025) uses WUFI Pro simulations to evaluate combinations of insulation materials and vapour retarders for interior insulation of timber plank frame walls, with the aim of preventing mould growth. Another study (Xu et al., 2025) integrates hygrothermal wall simulations with assessments of heating and cooling loads and payback time, accounting for the influence of moisture on thermal performance, as well as reduction in heating demands and associated reduction in operational carbon emissions. Three studies explicitly use both whole building energy simulations and hygrothermal calculations for envelope components. One study (Yuk et al., 2025) investigates the application of internal add-on insulation in the walls of heritage buildings in Seoul, South Korea, using dynamic energy modelling in EnergyPlus to evaluate heating and cooling demands and to estimate payback periods, while separately employing WUFI one-dimensional simulations to analyse condensation risk within the walls. Another study (Massafra et al., 2025) uses EnergyPlus to assess the impact of add-on insulation on building energy consumption and complements this with simplified condensation risk calculations based on the vapour diffusion resistance of the wall layers, while neglecting other moisture transport mechanisms. Finally, one study employs IDA ICE whole building energy simulations coupled with envelope hygrothermal calculations to evaluate both energy demand and mould growth risk in retrofitted envelope components, within the context of a renovation targeting nearly zero energy performance (Kalamees et al., 2025).

2.1.2.10 Effect of climate change and environmental considerations

In terms of climate change, some literature is currently available, including studies addressing the effect of the changing climate on moisture-related degradation in building envelope component and the effect of add-on insulation (Defo & Lacasse, 2020; Janssens, Vandemeulebroucke, et al., 2024; Lu et al., 2021; Schroderus et al., 2025), as well as the effect of add-on insulation and increased thermal resistance of building envelope on increased overheating under future climatic conditions (Ayikoe Tettey & Gustavsson, 2020; Hao et al., 2022; Rodrigues & Fernandes, 2020). However, among the most recent literature considered for the year 2025, only one study was found to account for the effect of climate change when assessing add-on insulation, specifically in a study focusing on freeze-thaw damage in add-on interior insulation for historic brick masonry walls in Ottawa, Canada (Sahyoun et al., 2025).

Most 2025 literature reviewed is composed of deterministic studies relying on numerical simulations. As simulation inputs are affected by relevant uncertainty, e.g. climatic boundary conditions and material properties, a common approach in literature is to use parametric or sensitivity analyses, where selected input variables are varied systematically to compare design options and identify influential parameters on the matter addressed. Parametric and sensitivity analyses are hereby regarded as deterministic approaches as they rely on varying selected inputs to identify influential parameters and benchmark outcome ranges, while they do not explicitly quantify probability distributions or characterize result uncertainties, hence they remaining scenario-based rather than probabilistic.

In 2025 literature, only one study considers the uncertainty of input parameters by using a Monte Carlo Analysis (MCA) to calculate probability distributions for uncertain inputs (heating price, investment in insulation measures, and percentage of subsidies) for assessing the likelihood of different payback times (PBTs) and understanding the uncertainty associated with investment decisions in energy efficiency measures (Liu et al., 2025). Overall, probabilistic assessments are highly valuable when assessing energy performance and moisture-related degradation risks related to add-on insulation, alas not very common in the literature. The relevance of adopting probabilistic assessments in this field and possible methodologies are described in previous literature (Galimshina et al., 2020; Ilomets et al., 2018; Marincioni et al., 2018; Vereecken et al., 2015; Zhao et al., 2021), and addressed in more detail in section 4 of this report.

Finally, the 2025 literature showcases that environmental sustainability is often considered only in very generalist terms, for instance, assuming bio-based materials to be a more-sustainable alternative to conventional mineral and petrochemical insulation. Only very few studies quantitatively assess environmental sustainability (Eugenia & Marin, 2025; Teng et al., 2025; Xu et al., 2025), combining hygrothermal or energy calculations with carbon footprint evaluation. Specifically, two studies (Eugenia & Marin, 2025; Xu et al., 2025) were found to account for the reduction of operational carbon emissions related to decreased energy consumption due to add-on insulation, and only one (Teng et al., 2025) considered both the embodied emissions in the materials for the renovation and the reduction of operational emission following the decreased energy consumptions.

2.1.3 Closing remarks

Overall, the existing literature provides a range of methods to assess the hygrothermal and energy performance of add-on insulation in renovations, with most studies focusing on the thermal retrofit of walls. Based on both recent (2025) and earlier literature, more studies that explicitly account for the impact of climate change on the performance of post-insulated envelopes are considered as a valuable addition to future literature, as well as more studies adopting probabilistic approaches. Further progress could be achieved by improving the way hygrothermal and energy assessments are integrated with environmental sustainability assessments. This is particularly meaningful when viewed in the context of the climate crisis and shift towards climate-neutral targets. While thermal insulation is intended to improve energy efficiency and reduce operational energy demand, the direction of recent decades has been shifting towards a broader sustainability perspective, including not only operational energy reductions but also minimisation of embodied carbon in construction materials (Galimshina et al., 2024; Recast, 2010). In this context, the use of bio-based thermal insulation has been recognised as one of the most promising solutions to reach carbon targets, and effectively store biogenic carbon in building renovations (Priore et al., 2026). Future valuable approaches could therefore attempt to integrate full life cycle assessment (LCA), including embodied and operational emissions, and considering end of life scenarios (Posani, Voney, et al., 2025). Such approaches could additionally benefit from addressing not only the use of low-carbon insulation solutions but also considering the potential for biogenic carbon storage in bio-based insulation materials (Kuittinen & Häkkinen, 2020; Priore et al., 2023, 2025).

2.1.4 References

Abdul Hamid, A., & Wallentén, P. (2017). Hygrothermal assessment of internally added thermal insulation on external brick walls in Swedish multifamily buildings. *Building and Environment*. https://doi.org/10.1016/j.buildenv.2017.05.019

Al-Sanea, S. A., Zedan, M. F., & Al-Hussain, S. N. (2012). Effect of thermal mass on performance of insulated building walls and the concept of energy savings potential. *Applied Energy*. https://doi.org/10.1016/j.apenergy.2011.08.009

Amorim, M., de Freitas, V. P., & Torres, I. (2023). Influence of Moisture on the Energy Performance of Retrofitted Walls - Experimental Assessment and Validation of an Hygrothermal Model. *International Journal of Architectural Heritage*. https://doi.org/10.1080/15583058.2022.2157777

Amorim, M., Freitas, V. P. de, Torres, I., Kisilewicz, T., & Berardi, U. (2020). The influence of moisture on the energy performance of retrofitted walls. *MATEC Web of Conferences*. https://doi.org/10.1051/matecconf/202032201035

Appelbaum, B. (1987). Criteria for treatment: Reversibility. *Journal of the American Institute for Conservation*, *26*(2). https://doi.org/10.1179/019713687806027852

Arbulu, M., Otaegi, J., Rodríguez-Vidal, I., & Oregi, X. (2025). Overheating Risk Assessment in Insulation-Based Energy Renovations in Spain. *Environmental and Climate Technologies*, *29*(1). https://doi.org/10.2478/rtuect-2025-0030

ASHRAE. (2009). *ASHRAE Standard 160-2009 - "Criteria for Moisture-Control Design Analysis in Buildings."*

Ayikoe Tettey, U. Y., & Gustavsson, L. (2020). Energy savings and overheating risk of deep energy renovation of a multi-storey residential building in a cold climate under climate change. *Energy*, *202*. https://doi.org/10.1016/j.energy.2020.117578

Ballerini, V., Valdiserri, P., Neri, M., Kašpar, J., Pilotelli, M., Piana, E., & Di Schio, E. R. (2025). Analysis of Energy Consumption of a Building Placed in Milan by Adopting Common Building Insulation Materials and Recycled Surgical Masks. *Building Simulation Applications*. https://doi.org/10.13124/9788860462022_43

Barreira, E., & de Freitas, V. P. (2013). Experimental study of the hygrothermal behaviour of External Thermal Insulation Composite Systems (ETICS). *Building and Environment*. https://doi.org/10.1016/j.buildenv.2013.02.001

Barreira, E., Delgado, J. M. P. Q., Ramos, N. M. M., & de Freitas, V. P. (2013). Exterior condensations on façades: Numerical simulation of the undercooling phenomenon. *Journal of Building Performance Simulation*, *6*(5). https://doi.org/10.1080/19401493.2011.560685

Bauklimatik-Dresden. (2024). *DELPHIN*. https://bauklimatik-dresden.de/delphin/index.php

Borodinecs, A., Jacnevs, V., Ákos, L., & Gendelis, S. (2025). Hygrothermal performance of well-insulated wood-frame walls in Baltic climatic conditions. *Case Studies in Thermal Engineering*, *66*. https://doi.org/10.1016/j.csite.2025.105772

Bottino-Leone, D., Larcher, M., Herrera-Avellanosa, D., Haas, F., & Troi, A. (2019). Evaluation of natural-based internal insulation systems in historic buildings through a holistic approach. *Energy*. https://doi.org/10.1016/j.energy.2019.05.139

CEN. (2012). *ISO 13788:2012 - " Hygrothermal performance of building components and building elements — Internal surface temperature to avoid critical surface humidity and interstitial condensation — Calculation methods."*

CEN. (2014). *EN 252:2014 - "Field test method for determining the relative protective effectiveness of a wood preservative in ground contact."*

Charola, A. E. (1995). Water-Repellent Treatments for Building Stones: A Practical Overview. *APT Bulletin*, *26*(2/3). https://doi.org/10.2307/1504480

Choidis, P., Coelho, G. B. A., & Kraniotis, D. (2023). Assessment of frost damage risk in a historic masonry wall due to climate change. *Advances in Geosciences*, *58*. https://doi.org/10.5194/adgeo-58-157-2023

Curado, A., & de Freitas, V. P. (2019). Influence of thermal insulation of facades on the performance of retrofitted social housing buildings in Southern European countries. *Sustainable Cities and Society*, *48*. https://doi.org/10.1016/j.scs.2019.101534

Defo, M., & Lacasse, M. (2020). Resilience of Canadian homes and small buildings to the effects of climate change - Risk of deterioration due to condensation within wall assemblies. *E3S Web of Conferences*, *172*. https://doi.org/10.1051/e3sconf/202017202002

Drive, C. P. (2008). Colorless Coatings for Brick Masonry. *Coating*, (August).

EOTA. (2013). *ETAG 004:2013 - "Guideline for european technical approval of external thermal insulation composite systems (ETICS) with rendering."*

Eugenia, T., & Marin, B. (2025). Contributions Regarding the Energy Efficiency of Public Buildings Through Thermal Insulation. *Advances in Science and Technology*, *163 AST*. https://doi.org/10.4028/p-JnDg89

Fedorik, F., Heiskanen, R., Laukkarinen, A., & Vinha, J. (2019). Impacts of multiple refurbishment strategies on hygrothermal behaviour of basement walls. *Journal of Building Engineering*, *26*. https://doi.org/10.1016/j.jobe.2019.100902

Feng, C., Roels, S., & Janssen, H. (2019). Towards a more representative assessment of frost damage to porous building materials. *Building and Environment*, *164*. https://doi.org/10.1016/j.buildenv.2019.106343

Fosas, D., Coley, D. A., Natarajan, S., Herrera, M., Fosas de Pando, M., & Ramallo-Gonzalez, A. (2018). Mitigation versus adaptation: Does insulating dwellings increase overheating risk? *Building and Environment*, *143*. https://doi.org/10.1016/j.buildenv.2018.07.033

Fraunhofer Institute for Building Physics IBP. (2024a). *WUFI 2D*. https://wufi.de/en/software/wufi-2d/

Fraunhofer Institute for Building Physics IBP. (2024b). *WUFI Pro*. https://wufi.de/en/software/wufi-pro/

Galimshina, A., Moustapha, M., Hollberg, A., Lasvaux, S., Sudret, B., & Habert, G. (2024). Strategies for robust renovation of residential buildings in Switzerland. *Nature Communications*, *15*(1), 2227.

Galimshina, A., Moustapha, M., Hollberg, A., Padey, P., Lasvaux, S., Sudret, B., & Habert, G. (2020). Statistical method to identify robust building renovation choices for environmental and economic performance. *Building and Environment*, *183*. https://doi.org/10.1016/j.buildenv.2020.107143

Grazieschi, G., Asdrubali, F., & Thomas, G. (2021). Embodied energy and carbon of building insulating materials: A critical review. *Cleaner Environmental Systems*, *2*. https://doi.org/10.1016/j.cesys.2021.100032

Guizzardi, M., Carmeliet, J., & Derome, D. (2015). Risk analysis of biodeterioration of wooden beams embedded in internally insulated masonry walls. *Construction and Building Materials*, *99*. https://doi.org/10.1016/j.conbuildmat.2015.08.022

Hansen, T. K. (2018). Hygrothermal performance of internal insulation in historic buildings. In *Phd thesis*. Technical University of Denmark.

Hansen, T. K., Bjarløv, S. P., Peuhkuri, R. H., & Harrestrup, M. (2018). Long term in situ measurements of hygrothermal conditions at critical points in four cases of internally insulated historic solid masonry walls. *Energy and Buildings*, *172*. https://doi.org/10.1016/j.enbuild.2018.05.001

Hao, L., Herrera-Avellanosa, D., Del Pero, C., & Troi, A. (2022). Overheating Risks and Adaptation Strategies of Energy Retrofitted Historic Buildings under the Impact of Climate Change: Case Studies in Alpine Region. *Applied Sciences (Switzerland)*, *12*(14). https://doi.org/10.3390/app12147162

Harberg, M. E., Asphaug, S. K., & Kvande, T. (2025). Mould Growth Risk for Internal Retrofit Insulation of Heritage-Protected Timber Plank Frame Walls. *Heritage*, *8*(7). https://doi.org/10.3390/heritage8070278

Harrestrup, M., & Svendsen, S. (2015). Full-scale test of an old heritage multi-storey building undergoing energy retrofitting with focus on internal insulation and moisture. *Building and Environment*, *85*. https://doi.org/10.1016/j.buildenv.2014.12.005

Havinga, L., & Schellen, H. (2018). Applying internal insulation in post-war prefab housing: Understanding and mitigating the hygrothermal risks. *Building and Environment*, *144*(August), 631–647. https://doi.org/10.1016/j.buildenv.2018.08.035

Havinga, L., & Schellen, H. (2019). The impact of convective vapour transport on the hygrothermal risk of the internal insulation of post-war lightweight prefab housing. *Energy and Buildings*, *204*. https://doi.org/10.1016/j.enbuild.2019.109418

Hilbert, G., Neumann, H.-H., & Wendler, E. (2014). Hydrophobization – One Target, Several Possibilities. *Restoration of Buildings and Monuments*, *18*(1). https://doi.org/10.1515/rbm-2012-6495

Hyrkäs, J., Kuittinen, M., & Posani, M. (2025, October). Ultralight Earth: A Preliminary Look into Thermal Performance of Locally Sourced Fibre-Earth Composites . *1st RILEM YouthSymposium (RYS2025).*

IAL_Consultants. (2023). The European market for thermal insulation products . In *PRESS RELEASE December 2023*. Aavailable online at: https://www.ialconsultants.com/media/1118/thermal-insulation-press-release-2023.pdf (accessed on 17.12.2025).

Ilomets, S., Kalamees, T., & Vinha, J. (2018). Indoor hygrothermal loads for the deterministic and stochastic design of the building envelope for dwellings in cold climates. *Journal of Building Physics*, *41*(6). https://doi.org/10.1177/1744259117718442

Isaksson, T., Thelandersson, S., Ekstrand-Tobin, A., & Johansson, P. (2010). Critical conditions for onset of mould growth under varying climate conditions. *Building and Environment*, *45*(7). https://doi.org/10.1016/j.buildenv.2010.01.023

ISO. (2017). *ISO 6946:2017 - Building components and building elements — Thermal resistance and thermal transmittance — Calculation methods properties.*

ISO (International Organization for Standardization). (2012). *EN ISO 13788:2012 Hygrothermal performance of building components and building elements – Internal surface temperature to avoid critical surface humidity and interstitial condensation – Calculation methods. Geneva, Switzerland.*

Janssens, K., Feng, C., Marincioni, V., & Van Den Bossche, N. (2024). Comparison of different frost models with hygrothermal simulations to better understand frost damage in porous building materials. *Building and Environment*, *255*. https://doi.org/10.1016/j.buildenv.2024.111399

Janssens, K., Vandemeulebroucke, I., Marincioni, V., & Van Den Bossche, N. (2024). Hygrothermal risk assessment tool for brick walls in a changing climate. *Journal of Building Physics*, *48*(3). https://doi.org/10.1177/17442591241266484

Jensen, N. F. (2021). *Robust solutions of design of internal insulation in historic buildings with regards to hygrothermal performance*. Technical University of Denmark.

Jensen, N. F., Bjarløv, S. P., Rode, C., Andersen, B., & Møller, E. B. (2021a). Hygrothermal performance of six insulation systems for internal retrofitting solid masonry walls. *Journal of Building Physics*, *44*(6). https://doi.org/10.1177/1744259120988745

Jensen, N. F., Bjarløv, S. P., Rode, C., Andersen, B., & Møller, E. B. (2021b). Laboratory-based investigation of the materials' water activity and pH relative to fungal growth in internally insulated solid masonry walls. *Indoor Air*, *31*(4). https://doi.org/10.1111/ina.12796

Johansson, P., Lång, L., Capener, C.-M., Møller, E. B., Quagliarini, E., D'Orazio, M., Gianangeli, A., Janssen, H., Feng, C., & Langmans, J. (2019). *RIBuild (Robust Internal Thermal Insulation of Historic Buildings, EU Project) - Report on Threshold values for failure, linked to types of building structures and failure modes (Deliverable no. D2.2)*. https://www.ribuild.eu/s/RIBuild_D22_v10_1.pdf

Kalamees, T., Kalbe, K., Kodi, G. M., Pihelo, P., Simson, R., & Arumägi, E. (2025). Moisture Safety Strategies for Renovations of a Roof with Prefabricated Additional Insulation Elements: A Whole Building Heat, Air, and Moisture Simulation Approach. *Lecture Notes in Civil Engineering*, *552 LNCE*. https://doi.org/10.1007/978-981-97-8305-2_36

Kang, Y., & Kim, S. (2025). Sustainable Retrofit of a Historic Building Using Wall Insulation: Balancing Heritage Preservation and Energy Performance. *International Journal of Thermophysics*, *46*(9). https://doi.org/10.1007/s10765-025-03602-9

Klemczak, B., Kucharczyk-Brus, B., Sulimowska, A., & Radziewicz-Winnicki, R. (2024). Historical Evolution and Current Developments in Building Thermal Insulation Materials—A Review. In *Energies* (Vol. 17, Number 22). https://doi.org/10.3390/en17225535

Kuittinen, M., & Häkkinen, T. (2020). Reduced carbon footprints of buildings: new Finnish standards and assessments. *Buildings and Cities*, *1*(1). https://doi.org/10.5334/bc.30

Kuusk, K., Kalamees, T., & Maivel, M. (2014). Cost effectiveness of energy performance improvements in Estonian brick apartment buildings. *Energy and Buildings*, *77*. https://doi.org/10.1016/j.enbuild.2014.03.026

Kvist Hansen, T., Feldt Jensen, N., Møller, E., Jan De Place Hansen, E., & Peuhkuri, R. (2020). Monitored conditions in wooden wall plates in relation to mold and wood decaying fungi. *E3S Web of Conferences*, *172*. https://doi.org/10.1051/e3sconf/202017220004

Lähdesmäki, K., Vinha, J., Viitanen, H., Salminen, K., Peuhkuri, R., Ojanen, T., Paajanen, L., Iitti, H., & Strander, T. (2008). Development of an improved model for mould growth: Laboratory and field experiments . In *Symposium on Building Physics in the Nordic Countries, NSB 2008* .

Li, F., Li, Q., Meng, Q., Liu, J., Mao, H., Xie, J., & Liu, J. (2021). Effect of moisture on the thermal performance of exterior walls in the tropical islands of the South China Sea. *Applied Thermal Engineering*, *186*. https://doi.org/10.1016/j.applthermaleng.2020.116505

Li, H., An, J., Wang, C., & Yan, D. (2025). Simulation analysis on synergistic energy-saving effect of building envelope insulation and radiative cooling technology. *Energy and Buildings*, *339*. https://doi.org/10.1016/j.enbuild.2025.115759

Libralato, M., De Angelis, A., Saro, O., Qin, M., & Rode, C. (2021). Effects of considering moisture hysteresis on wood decay risk simulations of building envelopes. *Journal of Building Engineering*, *42*. https://doi.org/10.1016/j.jobe.2021.102444

Liu, W., Harmsen, R., Yang, T., & Kramer, G. J. (2025). The role of behavior on variation in domestic space heating demand in similar dwellings: What does it mean for the payback period of re-insulation? *Energy*, *335*. https://doi.org/10.1016/j.energy.2025.138013

Lu, J., Marincioni, V., Orr, S. A., & Altamirano-Medina, H. (2021). Climate resilience of internally-insulated historic masonry assemblies: Comparison of moisture risk under current and future climate scenarios. *Minerals*, *11*(3). https://doi.org/10.3390/min11030271

M. Krus, R. K. and K. S. (2007). M ould growth prediction by computational simulation on historic buildings. *Museum Microclimates*.

Magrini, A., Marenco, L., Leoni, V., & Gamba, R. (2022). Air Cavity Building Walls: A Discussion on the Opportunity of Filling Insulation to Support Energy Performance Improvement Strategies. *Energies*, *15*(23). https://doi.org/10.3390/en15238916

Maia, J., Ramos, N. M. M., & Veiga, R. (2018). Evaluation of the hygrothermal properties of thermal rendering systems. *Building and Environment*. https://doi.org/10.1016/j.buildenv.2018.08.055

Marincioni, V., Marra, G., & Altamirano-Medina, H. (2018). Development of predictive models for the probabilistic moisture risk assessment of internal wall insulation. *Building and Environment*, *137*. https://doi.org/10.1016/j.buildenv.2018.04.001

Massafra, A., Mattioli, L., Kozlova, I., Mazzoli, C., Predari, G., & Gulli, R. (2025). HBIM-Based Multicriteria Method for Assessing Internal Insulation in Heritage Buildings. *Heritage*, *8*(7). https://doi.org/10.3390/heritage8070259

Mathews, J. M., & Charde, M. (2025). Thermal insulation panels fabricated using recycled cardboard for energy efficiency in buildings: retrofit performance evaluation in hot climate. *International Journal of Sustainable Energy*, *44*(1). https://doi.org/10.1080/14786451.2024.2432280

Mohammed, A. S., Atiyah, I. K., Mohammed, A. K., & Al-Abbas, A. H. (2025). Evaluation and improvement of thermal insulation systems in residential buildings through thermal modeling. *Advances in Science and Technology Research Journal*, *19*(9). https://doi.org/10.12913/22998624/207605

Møller, E. B. (2004). *Hygrothermal performance and soiling of exterior building surfaces*. Technical University of Denmark.

Nosrati, R. H., & Berardi, U. (2018). Hygrothermal characteristics of aerogel-enhanced insulating materials under different humidity and temperature conditions. *Energy and Buildings*. https://doi.org/10.1016/j.enbuild.2017.09.079

Odgaard, T., Bjarløv, S. P., & Rode, C. (2018). Influence of hydrophobation and deliberate thermal bridge on hygrothermal conditions of internally insulated historic solid masonry walls with built-in wood. *Energy and Buildings*, *173*. https://doi.org/10.1016/j.enbuild.2018.05.053

O'Hegarty, R., Kinnane, O., Lennon, D., & Colclough, S. (2021). In-situ U-value monitoring of highly insulated building envelopes: Review and experimental investigation. *Energy and Buildings*, *252*. https://doi.org/10.1016/j.enbuild.2021.111447

Ojanen, T., Viitanen, H., & Peuhkuri, R. (2007). Modelling of mould growth in building envelopes. *IEA-Annex Meeting Porto*.

Parracha, J. L., Veiga, R., Gomes, M. G., Flores-Colen, I., & Nunes, L. (2024). Hygrothermal behaviour of external thermal insulation composite systems (ETICS) to withstand biological colonisation. *Journal of Building Engineering*, *86*. https://doi.org/10.1016/j.jobe.2024.108932

Pavel, C. C., & Blagoeva, D. T. (2018). Competitive landscape of the EU's insulation materials industry for energy-efficient buildings. *Publications Office of the European Union*.

Posani, M., Habert, G., Yannick, I., Fogue, D., Du, Y., Vereecken, E., Estève-Bourrel, P., Pinchard, L., Losini, A., Coelho, G., Ben-Alon, L., Carcassi, O. B., Dormohmadi, M., Rios, A., Kamath, M., Libralato, M., Maia, J., Makoundou, C., Malet-Damour, B., … Brás, A. (2025). Bio-stabilised earthen materials: a perspective on the potential contribution to climate change adaptation and mitigation. *1st RILEM Youth Symposium (RYS2025)*.

Posani, M., Veiga, M. D. R., & de Freitas, V. P. (2019). Towards Resilience and Sustainability for Historic Buildings: A Review of Envelope Retrofit Possibilities and a Discussion on Hygric Compatibility of Thermal Insulations. *International Journal of Architectural Heritage*. https://doi.org/10.1080/15583058.2019.1650133

Posani, M., Veiga, R., & de Freitas, V. P. (2021). Retrofitting Historic Walls: Feasibility of Thermal Insulation and Suitability of Thermal Mortars. *Heritage*, *4*(3), 2009–2022. https://doi.org/https://doi.org/10.3390/heritage4030114

Posani, M., Veiga, R., & de Freitas, V. P. (2023). Thermal renders for traditional and historic masonry walls: Comparative study and recommendations for hygric compatibility. *Building and Environment*, *228*, 109737. https://doi.org/10.1016/J.BUILDENV.2022.109737

Posani, M., Veiga, R., & Freitas, V. (2023). Post-Insulating Traditional Massive Walls in Southern Europe: A moderate thermal resistance can be more effective than you think. *Energy and Buildings*. https://doi.org/10.1016/j.enbuild.2023.113299

Posani, M., Voney, V., Odaglia, P., Du, Y., Komkova, A., Brumaud, C., Dillenburger, B., & Habert, G. (2025). Low-carbon indoor humidity regulation via 3D-printed superhygroscopic building components. *Nature Communications*, *16*(1), 425.

Prignon, M., Mets, T. De, Vereecken, E., & Tilmans, A. (2023). Frost Damage Risk in Insulated Masonry Walls: Challenges in Analysing Large Number of Numerical Simulations. *Journal of Physics: Conference Series*, *2654*(1). https://doi.org/10.1088/1742-6596/2654/1/012015

Priore, Y. D., Delmenico, S., Rinquet, L., Habert, G., & Jusselme, T. (2026). Potential contribution of biogenic materials in new and renovated buildings towards carbon budgets and storage in Switzerland. *Journal of Cleaner Production*, *541*, 147558.

Priore, Y. D., Habert, G., & Jusselme, T. (2023). Exploring the gap between carbon-budget-compatible buildings and existing solutions–A Swiss case study. *Energy and Buildings*, *278*, 112598.

Priore, Y. D., Schulthess, L., Delmenico, S., Rinquet, L., Habert, G., & Jusselme, T. (2025). Potential for biogenic carbon storage towards a net-zero built environment in Switzerland. *Sustainable Production and Consumption*.

Recast, E. (2010). Directive 2010/31/EU of the European Parliament and of the Council of 19 May 2010 on the energy performance of buildings (recast). *Official Journal of the European Union*, *18*(06), 2010.

Rodrigues, E., & Fernandes, M. S. (2020). Overheating risk in Mediterranean residential buildings: Comparison of current and future climate scenarios. *Applied Energy*, *259*. https://doi.org/10.1016/j.apenergy.2019.114110

Sadineni, S. B., Madala, S., & Boehm, R. F. (2011). Passive building energy savings: A review of building envelope components. *Renewable and Sustainable Energy Reviews*. https://doi.org/10.1016/j.rser.2011.07.014

Sahyoun, S., Ge, H., & Lacasse, M. A. (2025). Freeze-thaw damage assessment of internally insulated historic brick masonry walls under a changing climate. *Journal of Building Engineering*, *102*. https://doi.org/10.1016/j.jobe.2025.111900

Saldanha, C. M., & Piñon, J. P. (2013). Influence of building design on energy benefit of thermal mass compared to prescriptive U-factors. *Thermal Performance of the Exterior Envelopes of Whole Buildings - 12th International Conference*.

Schroderus, S., Lähteenmäki, V. M., Barbero-López, A., Haapala, A., & Fedorik, F. (2025). Effect of climate change on hygrothermal performance of timber framed wall with different insulation materials. *Building and Environment*, *269*. https://doi.org/10.1016/j.buildenv.2024.112438

SCOPUS - Available Online at: https://www.scopus.com// [Accessed on 02-07-2025]. (n.d.).

Sedlbauer, K. (2001). Prediction of mould fungus formation on the surface of and inside building components. *Fraunhofer Institute for Building Physics*, *9*(2), 75–141.

Simona, P. L., Spiru, P., & Ion, I. V. (2017). Increasing the energy efficiency of buildings by thermal insulation. *Energy Procedia*, *128*. https://doi.org/10.1016/j.egypro.2017.09.044

Soulios, V., Jan de Place Hansen, E., Feng, C., & Janssen, H. (2020). Hygric behavior of hydrophobized brick and mortar samples. *Building and Environment*, *176*. https://doi.org/10.1016/j.buildenv.2020.106843

Soulios, V., Jan de Place Hansen, E., & Peuhkuri, R. (2021). Hygrothermal performance of hydrophobized and internally insulated masonry walls - Simulating the impact of hydrophobization based on experimental results. *Building and Environment*, *187*. https://doi.org/10.1016/j.buildenv.2020.107410

Teng, X., Shen, Z., & Tutuko, D. C. S. (2025). Evaluating the Impact of Insulation Materials on Energy Efficiency Using BIM-Based Simulation for Existing Building Retrofits: Case Study of an Apartment Building in Kanazawa, Japan. *Buildings*, *15*(4). https://doi.org/10.3390/buildings15040570

Tink, V., Porritt, S., Allinson, D., & Loveday, D. (2018). Measuring and mitigating overheating risk in solid wall dwellings retrofitted with internal wall insulation. *Building and Environment*, *141*. https://doi.org/10.1016/j.buildenv.2018.05.062

Verbeke, S., & Audenaert, A. (2018). Thermal inertia in buildings: A review of impacts across climate and building use. In *Renewable and Sustainable Energy Reviews*. https://doi.org/10.1016/j.rser.2017.08.083

Vereecken, E., & Roels, S. (2012). Review of mould prediction models and their influence on mould risk evaluation. *Building and Environment*, *51*. https://doi.org/10.1016/j.buildenv.2011.11.003

Vereecken, E., & Roels, S. (2015). Capillary active interior insulation: do the advantages really offset potential disadvantages? *Materials and Structures*, *48*(9), 3009–3021.

Vereecken, E., & Roels, S. (2016). Capillary Active Interior Insulation Systems for Wall Retrofitting: A More Nuanced Story. *International Journal of Architectural Heritage*, *10*(5), 558–569. https://doi.org/10.1080/15583058.2015.1009575

Vereecken, E., & Roels, S. (2017). Wooden beam ends in combination with interior insulation: the importance of an airtight sealing. Energy Procedia. 132, 664-669. https://doi.org/10.1016/j.egypro.2017.10.003

Vereecken, E., Van Gelder, L., Janssen, H., & Roels, S. (2015). Interior insulation for wall retrofitting–A probabilistic analysis of energy savings and hygrothermal risks. *Energy and Buildings*, *89*, 231–244.

Viitanen, H., Ojanen, T., Peuhkuri, R., Vinha, J., Lähdesmäki, K., & Salminen, K. M. (2011). Mould growth modelling to evaluate the durability of materials. *Proceedings to 12th International Conference on Durability of Building Materials and Components: 12-15th April 2011. Porto, Portugal*.

Viitanen, H., Toratti, T., Makkonen, L., Peuhkuri, R., Ojanen, T., Ruokolainen, L., & Räisänen, J. (2010). Towards modelling of decay risk of wooden materials. *European Journal of Wood and Wood Products*, *68*(3). https://doi.org/10.1007/s00107-010-0450-x

Viitanen, H., Vinha, J., Salminen, K., Ojanen, T., Peuhkuri, R., Paajanen, L., & Lähdesmäki, K. (2010). Moisture and bio-deterioration risk of building materials and structures. *Journal of Building Physics*, *33*(3). https://doi.org/10.1177/1744259109343511

Wendler, E., & Von Plehwe-Leisen, E. (2008). Water repellent treatment of porous materials. A new edition of the WTA leaflet. *Hydrophobe V, Fifth International Conference on Water Repellent Treatment of Building Materials, April 15-16 2008, Brussels, Belgium*.

WTA. (2014). *WTA Merkblatt, '6-5: Innendämmung nach WTA II: Nachweis von Innendämmsystemen mittels numerischer Berechnungsverfahren.'*

Xu, C., Shao, S., Wei, W., Qin, Y., & Li, N. (2025). A study on optimum insulation thickness of building walls in hot summer and warm winter zone in China. *Scientific Reports*, *15*(1). https://doi.org/10.1038/s41598-025-93945-y

Xue, Y., Fan, Y., Wang, Z., Gao, W., Sun, Z., & Ge, J. (2022). Facilitator of moisture accumulation in building envelopes and its influences on condensation and mould growth. *Energy and Buildings*, *277*. https://doi.org/10.1016/j.enbuild.2022.112528

Yuk, H., Park, J. H., Kang, Y., & Kim, S. (2025). Advancing retrofitting practices for heritage masonry: The role of insulation materials in thermal and hygrothermal performance. *Applied Thermal Engineering*, *279*. https://doi.org/10.1016/j.applthermaleng.2025.127570

Zhang, Y., Omer, S., & Hu, R. (2025). Combination of Wall Insulation and PCMs in External Walls of Typical Residential Buildings in the UK and Their Impact on Building Energy Consumption. *Buildings*, *15*(6). https://doi.org/10.3390/buildings15060854

Zhao, J., Grunewald, J., Ruisinger, U., & Feng, S. (2017). Evaluation of capillary-active mineral insulation systems for interior retrofit solution. *Building and Environment*. https://doi.org/10.1016/j.buildenv.2017.01.004

Zhao, J., Zhang, J. "Jensen," Grunewald, J., & Feng, S. (2021). A probabilistic-based method to evaluate hygrothermal performance of an internally insulated brick wall. *Building Simulation*, *14*(2). https://doi.org/10.1007/s12273-020-0702-6

Zhou, H., Peng, J., & Yang, H. (2026). Experimental study on thermal, electrical and energy performance of solar PV vacuum glazing (SVG) insulated walls in hot climates. *Renewable Energy*, *256*. https://doi.org/10.1016/j.renene.2025.124166

Zhou, X., Carmeliet, J., & Derome, D. (2018). Influence of envelope properties on interior insulation solutions for masonry walls. *Building and Environment*, *135*. https://doi.org/10.1016/j.buildenv.2018.02.047

Zhou, X., Derome, D., & Carmeliet, J. (2017). Hygrothermal modeling and evaluation of freeze-thaw damage risk of masonry walls retrofitted with internal insulation. *Building and Environment*, *125*. https://doi.org/10.1016/j.buildenv.2017.08.001

2.2 Hygrothermal Material Properties in Probabilistic Assessments of Passive Energy Conservation Measures

This section should be cited as:

Dang, X. (2026). Hygrothermal material properties in probabilistic assessment of passive energy conservation measures. In: A Systematic Review of Passive Energy Conservation Measures and Probabilistic Assessment under Changing Climate in Urban Settings, CIB W040 Report, CIB General Secretariat.

2.2.1 Introduction

Probabilistic building performance assessment frameworks for passive energy conservation measures increasingly account for uncertainties in future climate projections and urban microclimates, particularly under climate change and urban heat island conditions (Shen et al., 2025; Kousis and Santamouris 2025). Moreover, stochastic representations of occupant behavior are progressively integrated into such frameworks to better capture variability in building energy demand (Cipolla et al., 2026). However, despite this growing attention to external and operational uncertainties, the uncertainties associated with hygrothermal material properties—although fundamental to heat and moisture transfer within building envelopes—are still commonly simplified or treated as deterministic constants (Pour et al., 2024). Under climate change, these processes are expected to intensify due to rising temperatures, altered humidity regimes, and more frequent extreme precipitation events. This treatment overlooks the fact that material properties are not peripheral inputs but constitutive parameters that fundamentally shape the dynamic response of passive systems to climatic stresses.

Passive strategies such as ex-/in-ternal insulation systems, moisture buffering materials, ventilated facades and climate-adaptive retrofits are inherently sensitive to transient hygrothermal processes (Pagoni et al., 2025). As a result, the reliability of predictions related to energy savings, overheating risk, indoor comfort and envelope durability increasingly depends on how accurately hygrothermal material properties are characterized and represented within simulation models.

Uncertainties in material properties arise from a chain of epistemic and aleatory factors extending from laboratory testing to model implementation, rather than from measurement variability alone (Feng et al., 2015). Recognizing hygrothermal properties as a distinct contributor to overall uncertainty is thus critical (Dang 2025). Because passive measures derive their performance not solely from thermal resistance but from coupled heat–moisture interactions, uncertainties in these properties can propagate nonlinearly through simulation outputs (Xue et al., 2025). This affects predictions of moisture accumulation, thermal mass effect, long-term degradation and overall energy performance, particularly under intensified climatic loads (Wang et al., 2025). Consequently, a rigorous probabilistic treatment of passive energy measures must explicitly incorporate the uncertainties inherent in hygrothermal material properties rather than relegating them to fixed or implicitly defined inputs.

2.2.2 Overview of hygrothermal properties and their impact

In transient hygrothermal analysis, material properties are most effectively described through a functional classification that reflects their role in coupled heat and moisture transfer (Janssen et al., 2007). This approach highlights how different property groups govern storage, transport and exchange processes within porous building materials, and how these processes interact to shape the overall hygrothermal response of envelope systems. The key hygrothermal properties relevant to modeling and performance assessment can be organized into four functional categories: heat storage properties, heat transport properties, moisture storage properties and moisture transport properties (Künzel, 1995).

2.2.2.1 Thermal properties

Heat storage and transport properties govern how building materials absorb, retain and conduct heat, shaping the thermal inertia and peak-load moderation of passive envelope systems. Thermal conductivity is commonly modeled as a function of moisture content and temperature to capture the well-documented degradation of insulation performance under elevated moisture levels and varied temperatures, and it may also vary with ageing-related changes in microstructure. Likewise, heat capacity is not strictly constant but exhibits temperature dependence, which becomes particularly pronounced in materials undergoing phase transitions or containing heterogeneous microstructures. Phase-change materials represent an extreme case of such behavior: their apparent heat capacity shows strong peaks within a narrow temperature range, enabling latent-heat storage and additional peak-load reduction, while also introducing greater sensitivity to boundary conditions and parameter uncertainty. As heat and moisture transfers are intrinsically coupled, variations in these thermal parameters can propagate through the system whenever moisture levels fluctuate, altering both temperature fields and drying potentials. This interaction becomes especially relevant in probabilistic analyses, where uncertainties in thermal behavior interact with moisture-related parameters to influence the spread of predicted outcomes. Under future climates, the effective thermal behavior of envelope components may deviate from nominal observations, making the coupling between heat and moisture properties increasingly important for assessing passive performance and retrofit strategies (Vandemeulebroucke et al., 2024).

2.2.2.2 Hygric properties

Moisture storage properties describe how porous materials retain water under varying moisture driving potentials, typically expressed through sorption isotherms or moisture retention curves. These relationships define the material's capacity to buffer humidity fluctuations and mediate latent heat exchanges, both of which are central to the passive moderation of indoor environments. Beyond local buffering, moisture storage characteristics influence how moisture transport across multilayer assemblies, affecting the onset of interstitial condensation and the availability of drying pathways. In transient hygrothermal simulations, these properties determine the transitions between hygroscopic and capillary regimes and thus shape the overall moisture dynamics of the envelope. These storage properties also determine the material response under more irregular moisture loads, including unexpected liquid water intrusion such as rain leakage or condensation triggered by air exfiltration, where the balance between capillary uptake and redistribution becomes particularly critical (Gutland et al., 2021; Van den Bossche et al., 2025). Sorption hysteresis, i.e., the difference between adsorption and desorption branches, is an inherent feature of most porous building materials and can influence predicted moisture contents, particularly under cyclic boundary conditions. In probabilistic analyses under climate change, the representation of hysteresis becomes an additional source of uncertainty in sorption behavior and contributes to variability in predicted moisture accumulation and thus affect assessments of retrofit robustness and long-term durability (Panico et al., 2023). Moisture transport properties control the mechanisms and rates by which water vapor and liquid water migrate through porous materials. As moisture movement directly governs the accumulation and dissipation of water within envelope components, transport properties often constitute a crucial source of uncertainty in probabilistic hygrothermal analyses. This is especially true for liquid transport parameters, which strongly influence the speed of wetting during rain exposure and the subsequent drying behavior. The overall performance of passive envelope systems depends on maintaining low and stable moisture levels. Variations in moisture transport properties can therefore lead to substantial discrepancies in predicted hygric responses, such as drying times and the duration of high humidity states, deviating from the actual behavior. These discrepancies can be further amplified under externally imposed moisture loads, including high ambient humidity, wind-driven rain and condensation generated by air exfiltration, and are expected to become even more pronounced under the intensified wetting–drying cycles projected for future climates (Dang et al., 2024a; Ksit et al., 2025). This makes accurate characterization and uncertainty quantification of moisture transport essential for evaluating passive retrofit measures and long-term resilience.

2.2.3 Measurement uncertainty: limits of material characterization

2.2.3.1 Inherent constraints of laboratory measurements

Hygrothermal material properties are fundamentally shaped by the limitations of the laboratory methods used to obtain them. Sorption isotherms, for example, are typically measured under controlled relative humidity conditions using gravimetric or climatic-chamber techniques, whereas moisture retention curves rely on pressure plate or suction-controlled methods to capture the over-hygroscopic range (Feng and Janssen, 2021). Because these techniques operate under different thermodynamic constraints, they may produce partially inconsistent or non-overlapping segments (Dang et al., 2024b). This discontinuity complicates the construction of continuous material functions for hygrothermal models and introduces structural uncertainty that cannot be resolved through additional measurement alone.

Moisture transport properties face even more fundamental measurement limitations. Advanced imaging techniques such as X-ray CT or NMR can capture spatial and temporal moisture distributions with high fidelity, but they do not directly yield transport coefficients; these must be inferred through inverse modeling (Carmeliet et al., 2004). As such imaging methods are not always available, alternative approaches, such as the ruler method, the multi-step method and Künzel's empirical formula, are commonly used instead (Ren et al., 2019). However, these techniques are constrained by material-specific applicability, demanding sample conditioning procedures, or strong simplifying assumptions and therefore do not consistently achieve stable accuracy across different materials and moisture regimes (Feng and Janssen, 2021). Combined with the strong nonlinearity of liquid transport and the inherent heterogeneity of porous materials, these methodological constraints result in substantial uncertainty in liquid transport parameters even before probabilistic analysis is applied (Zhao, 2012).

2.2.3.2 Repeatability, reproducibility and material heterogeneity

Beyond methodological limitations, uncertainty in hygrothermal material properties arises from three structurally distinct sources: repeatability, reproducibility and material heterogeneity (Feng et al., 2015). Repeatability reflects the variability observed when the same operator, equipment and laboratory conditions are used; reproducibility captures differences across laboratories, test setups and procedural interpretations; and material heterogeneity represents intrinsic variability within and between production batches. Across published datasets, material heterogeneity and inter-laboratory reproducibility consistently emerge as the dominant contributors to overall uncertainty. This is particularly consequential for passive retrofitting materials—such as bio-based insulation, mineral-based renders or recycled composites—whose microstructure and pore network can vary substantially even when products are nominally classified under the same material type (Huang et al., 2023). As a result, the "true" hygrothermal behavior of such materials is better represented as a distribution rather than a single deterministic curve (Wang et al., 2024). For probabilistic hygrothermal modeling and climate-resilient retrofit assessment, acknowledging and quantifying these sources of variability is therefore essential, as they directly influence the spread of predicted moisture loads, drying behavior and long-term performance outcomes (Tutmez, 2023).

2.2.4 Transformation and simplification: from measurements to model inputs

Measured hygrothermal properties rarely enter numerical models in their raw form. Instead, they must undergo a series of transformations to produce continuous, model-compatible functions. Moisture storage data, for instance, often require curve fitting, smoothing or extrapolation to cover the full hygroscopic and over-hygroscopic ranges. Transport properties may need to be reformulated to match the driving potentials used in the model—such as converting between relative humidity–based and capillary pressure–based formulations—or expressed in parameter formats compatible with the governing equations (Dang et al., 2025a).

These transformations are not merely technical adjustments; they embed assumptions that can meaningfully alter the resulting material functions. Enforcing monotonicity, omitting sorption hysteresis or extending curves into poorly measured moisture ranges all reshape the material response, particularly near saturation where measurement data are sparse, and uncertainties are highest (Dang et al., 2026). This is also the regime where coupled heat–moisture interactions intensify and where climate-change-driven increases in wetting and humidity make accurate representation especially critical. As a result, the transformation process itself becomes a non-negligible source of epistemic uncertainty that must be acknowledged in probabilistic analyses.

Beyond data transformation, inherent simplifications are frequently introduced to reduce computational burden or to satisfy the requirements of specific hygrothermal models. Such simplifications can be justified for routine simulations or for materials operating within moderate environmental ranges, where moisture gradients are small and transient effects are limited. However, these reductions can introduce systematic bias when applied to conditions characterized by strong nonlinearity and rapid moisture fluctuations. Under extreme weather events or future climate scenarios—where driving forces become more intense, wetting–drying cycles accelerate, and materials operate closer to saturation—the neglected details of moisture storage and transport behavior become increasingly influential (Ksit et al., 2025). Simplified representations may therefore under- or over-estimate moisture accumulation, mis predict drying time or distort the coupling between heat and moisture transfer. For probabilistic modeling and the assessment of passive retrofit strategies, such inherent simplifications can narrow the apparent uncertainty range while masking the true variability of system performance.

2.2.5 Implementation uncertainties: model- and user-dependent effects

2.2.5.1 Model-dependent formulations

Even when identical material datasets are supplied, hygrothermal simulation models can yield substantially different results because they implement equivalent governing equations with different simplifications and numerical treatments (Dang, 2025). Each implementation reflects specific assumptions about dominant transport mechanisms and their interactions, which can shift predicted moisture responses. Such model-level differences can lead to divergent predictions of heat fluxes, moisture accumulation, drying behavior and phase-change dynamics, particularly under transient or high-moisture conditions. These discrepancies are not merely numerical artifacts but reflect structural choices embedded in the model architecture. As a result, model-dependent uncertainty becomes an intrinsic component of the overall uncertainty chain, especially when assessing passive retrofit strategies or future climate scenarios where coupled heat–moisture processes intensify.

2.2.5.2 User-dependent implementation choices

A significant share of implementation uncertainty arises not from the model itself but from user decisions during setup (Yamamoto and Takada, 2022). In practice, complete hygrothermal datasets are rarely available, prompting users to substitute materials from default libraries or to select "similar" materials based on a limited subset of properties (Dang et al., 2025b). This implicitly assumes that similarity in a few parameters implies similarity in full hygrothermal behavior, an assumption that often fails for materials with nonlinear sorption characteristics or complex pore structures. These practical limitations highlight the need for large, systematically curated databases and data-driven models capable of estimating missing properties. Instead of relying on ad-hoc material substitution, users could infer unavailable parameters through machine-learning models trained on comprehensive datasets, thereby reducing subjective judgment and improving the consistency of simulation inputs. Additional uncertainty arises from incorrect or inconsistent interpretations of parameter definitions. One example concerns the definition of “saturation”, where experimental protocols range from multi-day full submersion to short-term partial immersion, leading to either vacuum saturation or capillary saturation as the terminal point of the moisture storage curves applied in HAM models. For moisture-transport properties, both over- and under-representation may occur—for example, double-counting liquid-phase contribution in vapor and liquid transport functions, or omitting liquid transport entirely in moisture-sensitive assemblies (Dang et al., 2025a). These choices introduce systematic biases rather than random noise, and such biases persist across simulations. In probabilistic analyses, they may artificially narrow the apparent uncertainty range while masking structural misrepresentation of material behavior (Gan et al., 2025).

2.2.6 Conclusion

From a probabilistic perspective, uncertainties associated with hygrothermal material properties arise from both systematic and stochastic sources, each influencing model outputs in distinct ways (Pour et al., 2024). Systematic uncertainties originate from model-structure assumptions, parameterization choices, and simplifications embedded in simulation tools. These uncertainties shift predictions in a consistent direction and are difficult to detect through conventional sensitivity analysis (Panico et al., 2023). Stochastic uncertainties, by contrast, arise from measurement variability, material heterogeneity and operator-dependent effects during laboratory characterization (Feng et al., 2015). While they increase the spread of predicted outcomes, their influence does not necessarily diminish across ensembles due to the nonlinear nature of moisture transport.

Distinguishing between these uncertainty types is essential for interpreting probabilistic results. Systematic uncertainties are particularly problematic because they can produce a narrow distribution centered around a biased mean, creating a misleading impression of robustness. This issue becomes more consequential when evaluating passive energy conservation strategies under future climate conditions, where moisture loads, wetting–drying cycles, and thermal stresses deviate from historical norms. If material properties are biased due to simplifications or implementation choices, probabilistic simulations may systematically under- or over-estimate both energy- and moisture-related vulnerabilities, thereby distorting the simulation outcomes and misleading the assessment of energy and moisture performance (Shams et al., 2026).

In sum, hygrothermal material properties constitute a structurally distinct and insufficiently addressed source of uncertainty in probabilistic assessments of passive strategies. Treating these properties deterministically—or assigning simplistic variability without accounting for the measurement, transformation, and implementation pathways through which they are derived—risks masking the true range of possible outcomes. At the urban scale, where building-level uncertainties propagate across large stocks and interact with microclimatic effects, this omission becomes even more consequential (Pasandi et al., 2024). A robust probabilistic framework must therefore minimize systematic error while explicitly incorporating stochastic uncertainty, ensuring that assessments of passive performance and climate resilience reflect the full multi-layered uncertainty chain associated with hygrothermal material properties.

2.2.7 References

Carmeliet, J., Hens, H., Roels, S., Adan, O., Brocken, H., Cerny, R., Pavlik, Z., Hall, C., Kumaran, K., & Pel, L. (2004). Determination of the liquid water diffusivity from transient moisture transfer experiments. Journal of Thermal Envelope and Building Science, 27(4), 277–305.

Cipolla, G., Buonomano, A., Pernigotto, G., & Gasparella, A. (2026). Energy flexibility strategies in urban areas: A sustainable energy consumption and production balance under a stochastic framework. Renewable and Sustainable Energy Reviews, 230, 116678.

Dang, X. (2025). Quality assessment of heat, air and moisture (HAM) models to predict the hygrothermal response of building components. PhD thesis, KU Leuven, Belgium.

Dang, X., Guimarães, A. S., Sarkany, A., Laukkarinen, A., Xu, B., Vanderschelden, B., ... & Roels, S. (2025a). A state-of-the-art empirical round robin validation of heat, air and moisture (HAM) models. Building and Environment, 276, 112867.

Dang, X., Vereecken, E., Janssen, H., & Roels, S. (2024a). Impact of semi-empirical methods implemented in heat, air, and moisture (HAM) models on predicted wind-driven rain (WDR) loads and hygrothermal responses. Building and Environment, 262, 111770.

Dang, X., Janssen, H., & Roels, S. (2024b). A comprehensive benchmark dataset for the validation of building component heat, air, and moisture (HAM) models. Building Simulation, 17(11), 1893–1907.

Dang, X., Janssen, H., & Roels, S. (2025b). User preferences, biases and/or mistakes as uncertainties in hygrothermal simulations: Insights from a round robin test. In U. Berardi (Ed.), Multiphysics and multiscale building physics (Vol. 552, pp. 68–75). Springer.

Dang, X., Janssen, H., & Roels, S. (2026). Implementation strategies and uncertainties of moisture transport properties in heat, air and moisture (HAM) models: Comparative insights from WUFI and DELPHIN. Journal of Building Physics. http://doi.org/10.1177/17442591261425558

Feng, C., & Janssen, H. (2021). Hygric properties of porous building materials (VII): Full-range benchmark characterizations of three materials. Building and Environment, 195, 107727.

Feng, C., Janssen, H., Feng, Y., & Meng, Q. (2015). Hygric properties of porous building materials: Analysis of measurement repeatability and reproducibility. Building and Environment, 85, 160–172.

Gan, W., Li, X., Fang, J., & Feng, C. (2025). Influence of input uncertainty on the 1-D hygrothermal simulation of composite walls in China. Building Simulation, 18, 19–32.

Gutland, M., Bucking, S., & Santana Quintero, M. (2021). A methodology for hygrothermal modelling of imperfect masonry interfaces. Journal of Building Physics, 44(6), 485-509.

Huang, G., Abou-Chakra, A., Geoffroy, S., & Absi, J. (2023). A multiscale homogenization model on thermal conductivity of bio-based building composite considering anisotropy, imperfect interface and moisture. Construction and Building Materials, 377, 131156.

Janssen, H., Blocken, B., & Carmeliet, J. (2007). Conservative modelling of the moisture and heat transfer in building components under atmospheric excitation. International Journal of Heat and Mass Transfer, 50(5–6), 1128–1140.

Kousis, I., & Santamouris, M. (2025). Assessing long-term effectiveness of passive cooling strategies in the built environment under climate change. Solar Energy, 302, 114038.

Ksit, B., Szymczak-Graczyk, A., Orlik-Kożdoń, B., & Garbowski, T. (2025). Numerical and surrogate modeling of drying processes in building envelopes under variable climatic conditions. Energy, 139014.

Künzel, H. M. (1995). Simultaneous heat & moisture transport in building components. PhD thesis, IRB Verlag, Germany.

Pagoni, P., Møller, E. B., Peuhkuri, R. H., & Jensen, N. F. (2025). Evaluation of the performance of different internal insulation systems in real-life conditions: A case study. Building and Environment, 267, 112319.

Panico, S., Larcher, M., Avellanosa, D. H., Baglivo, C., Troi, A., & Congedo, P. M. (2023). Hygrothermal simulation challenges: Assessing boundary condition choices in retrofitting historic European buildings. Energy and Buildings, 297, 113464.

Panico, S., Larcher, M., Marincioni, V., Troi, A., Baglivo, C., & Congedo, P. M. (2023). Identifying key parameters through a sensitivity analysis for realistic hygrothermal simulations at wall level supported by monitored data. Building and Environment, 229, 109969.

Pasandi, L., Qian, Z., Woo, W. L., & Palacin, R. (2024). A comprehensive review of applications and feedback impact of microclimate on building operation and energy. Building and Environment, 263, 111855.

Pour, M. B., Niklewski, J., Naghibi, A., & Hansson, E. F. (2024). A literature review of probabilistic hygrothermal assessment for building envelopes. Building and Environment, 261, 111756.

Ren, P., Feng, C., & Janssen, H. (2019). Hygric properties of porous building materials (V): Comparison of different methods to determine moisture diffusivity. Building and Environment, 164, 106344.

Shams, S. A., Ge, H., & Wang, L. (2026). Incorporating hysteresis in hygrothermal modeling of cross-laminated timber walls: Model development, validation and moisture risk analysis. Journal of Building Engineering, 118, 115158.

Shen, P., Li, Y., Gao, X., Chen, S., Cui, X., Zhang, Y., ... & Wang, M. (2025). Climate adaptability of building passive strategies to changing future urban climate: A review. Nexus, 2(2).

Tutmez, B. (2023). Relative uncertainty-based Bayesian interlaboratory consensus building. Science of the Total Environment, 870, 161977.

Vandemeulebroucke, I., Vanderschelden, B., Janssens, K., Caluwaerts, S., & Van Den Bossche, N. (2024). The impact of climate change on degradation in historical building envelopes: Progress in research using hygrothermal models. Journal of Cultural Heritage, 70, 345–363.

Van den Bossche, R., Vanderschelden, B., Van Den Bossche, N., & Steeman, M. (2025). Experimental investigation of rainwater absorption and infiltration in different types of masonry with lime hemp interior insulation. Construction and Building Materials, 495, 143704.

Wang, S., Li, H., & Liu, L. (2024). Development of a multifunctional bio-based insulation material with corncob and silica aerogel. Energy and Buildings, 323, 114817.

Wang, X., Jie, P., Zhu, K., et al. (2025). Integration of moisture effects into urban building energy modeling. Building Simulation, 18, 663–678.

Xue, Y., Gao, T., Fan, Y., Lu, J., & Ge, J. (2025). A coupled hygrothermal transfer model with driving potential of moisture content for multilayer envelopes: Feasibility analysis and advantages demonstration. Journal of Building Engineering, 113530.

Yamamoto, H., & Takada, S. (2022). Influence of variability in hygrothermal properties on analytical results of simultaneous heat and moisture transfer in porous materials. Journal of Building Physics, 45(6), 757–773.

Zhao, J. (2012). Development of a novel statistical method and procedure for material characterization and a probabilistic approach to assessing the hygrothermal performance of building enclosure assemblies. Syracuse University.

2.3 Rainwater Infiltration Rates in Facade Systems: Review and Modelling Approach

This section should be cited as:

Van Den Bossche, N., Van Linden, S. (2026). Rainwater Infiltration Rates in Façade Systems: Review and Modelling Approach. In: A Systematic Review of Passive Energy Conservation Measures and Probabilistic Assessment under Changing Climate in Urban Settings, CIB W040 Report, CIB General Secretariat.

Rainwater management in façade systems is studied by means of full-scale experiments, as current modelling approaches do not allow to predict rainwater ingress and drainage. The interaction of kinetic energy, capillary forces, surface tension, hydrostatic pressure, air currents and pressure difference is too complex to handle at this point. For a range of wall configurations, experimental work has been carried out to quantify rainwater ingress and water transfer when a wall is subjected to different combinations of rain loads and driving rain wind pressures.

This section first provides a short review of infiltration rates as have been determined for sidings, ETICS, stucco, masonry and cladding panels with open joints for which the infiltration rates have been reported as a percentage of the applied water spray rate. When possible, there is a differentiation between the total amount of water that penetrated the cladding, and the amount of water that crosses the cavity (if present). For a more detailed review, please refer to Van Linden & Van Den Bossche (2022).

Thereafter, a methodology is presented to provide a more generic approach to quantify infiltration rates through different types of wall systems. Finally, the implementation of rainwater infiltration rates in hygrothermal simulations is discussed.

2.3.1 Siding

Sidings, such as vinyl or painted wood, are inherently water-resistant and are designed to repel rainwater when installed with overlapping joints. However, water intrusion can occur through cracks in the siding or poorly executed joints. Boardman and Glass (2013) examined water penetration at horizontal lap joints under simulated wind-driven rain conditions. Well-installed sidings with an 11 mm cavity showed no leakage, but defects introduced via wedges allowed infiltration once pressure exceeded 30.4 Pa, increasing with wind speed. At 48 Pa, infiltration reached 0.046% of sprayed water. Ngudjiharto (2015) conducted a seven-month field study on Dutch-lap vinyl siding, recording a maximum infiltration of 0.27% of wind-driven rain. Water entry was linked to runoff above windows, where J-trims redirected moisture behind the siding, underscoring the necessity of proper flashing installation. Collectively, these studies highlight that infiltration rates are rather low, but the quality of the detailing and installation significantly influence siding performance under wind-driven rain conditions.

2.3.2 Exterior Thermal Insulation Composite Systems (ETICS) & Stucco

External Thermal Insulation Composite Systems (ETICS), known in North America as Exterior Insulation and Finish Systems (EIFS), comprise an insulation panel, reinforced base coat, and finish coat. Due to the low capillary absorption of the finish layer, water penetration through intact EIFS surfaces is highly unlikely. However, cracks caused by hygric stresses, ageing, or structural movement—particularly near openings, thickness transitions, or poorly reinforced joints—are almost unavoidable (Barreira & De Freitas, 2013). Historically introduced in Germany on solid masonry walls during the 1950s for post-war retrofits, EIFS gained popularity during the 1970s energy crisis and were later applied to wood-frame constructions in North America, where moisture intrusion led to severe damage such as sheathing rot (Rousseau, 1999). Consequently, in North America, drainage cavities are now mandatory in such assemblies. Despite these challenges, EIFS remain prevalent due to cost-effectiveness and high insulation potential (Parracha et al, 2021). Experimental studies confirm that the presence of cracks in the wall assembly significantly increase water infiltration under pressure differences. Ullet and Brown (1996) reported infiltration rising from 0.06% at zero pressure to 1.15% at 500 Pa in cracked specimens (without deficiencies it was only half that much). Molnar et al. (2017) conducted qualitative analysis on the impact of cracks, and observed water transport along render-insulation interfaces, but also infiltration through the joints between insulation panels towards the load bearing structure.

Traditional hardcoat stucco consists of three cementitious layers applied over masonry or metal lath installed over building paper and sheathing. These systems absorb rainwater and provide buffering capacity; once saturated, water drains along the stucco–building paper interface. In contrast, synthetic stuccos incorporate fibers and acrylics for strength and flexibility, making them more water-repellent. However, similar to EIFS, cracks caused by ageing or movement create pathways for infiltration. Paint finishes can reduce absorptivity but fail to bridge micro-cracks. Laboratory tests by Saber et al. (2014) showed no infiltration without pressure difference, but water infiltration increased with higher pressure and water spray rates, with the highest percentage infiltration occurring at the lowest spray rate. Field tests by Ngudjiharto (2015) on stucco walls without drainage cavities recorded up to 2.3% of wind-driven rain infiltrating over a month, primarily at window-wall interfaces despite no intentional defects.

2.3.3 Masonry

Historically, thick masonry walls of stone or mortared bricks relied on their buffering capacity to absorb and redistribute rainwater, preventing interior wetting. Modern masonry walls, however, are thinner, increasing the risk of water infiltration. During rain events, most impinging water is absorbed by the masonry. Kahangi Shahreza et al. (2021) reported that 76–92% of water applied at spray rates of 2–3.8 $l/m^2 \cdot h$ was absorbed within the first 3.5 hours. Surface saturation time depends on absorptivity of the masonry and water spray rate. Once the masonry is saturated, runoff occurs, and water may infiltrate through cracks or mortar joints via capillary suction, which can generate pressures of 75–750 Pa for crack widths of 0.1–1.0 mm (Straube, 1998). Hydrostatic pressure in vertical joints (e.g., 60 mm head joint) can reach 600 Pa, sufficient to overcome meniscus resistance in cracks as small as 0.125 mm (Straube, 1998).

Water infiltration primarily occurs at brick–mortar interfaces, especially vertical head joints (Kahangi et al., 2021). Chiovitti et al. (1998) and Hens et al. (2004) observed quasi-linear infiltration over time once interior runoff began. Water infiltration through masonry walls is strongly influenced by workmanship, wall thickness, and material properties. Poor workmanship combined with cracks significantly increases infiltration; Calle et al. (2020) reported a 94% rise in infiltration for cracked, poorly executed specimens compared to those with normal workmanship. Wall thickness also plays a critical role: triple wythe masonry exhibited infiltration rates of only 1.30% of the spray rate versus 21% for single wythe walls, and required 360 minutes to reach saturation compared to 48 minutes (Calle, 2020). Air permeability further affects performance; (Hens et al., 2004).

Joint sealing and bonding methods are decisive as regards water infiltration of wall assemblies. Laboratory tests showed glued concrete blocks allowed 70% infiltration compared to 0.39% for mortared blocks, whereas this trend for field tests was reversed: glued blocks infiltrated 0.82% as compared to 3.37% for mortared blocks due to differences in pressure reduction by airtight inner walls (Hens et al., 2004). Mortar type also matters; lime mortar improves watertightness compared to cement mortar, and pointing mortars further enhance resistance (Calle, 2020). Surface treatments can also reduce infiltration of masonry walls. Brown (1982) observed reductions of 64% for clay bricks and 96% for concrete blocks with water-repellent coatings, though Chiovitti et al. (1998) noted performance declines over time due to microcracking. These findings underscore the combined influence of workmanship, detailing, and protective treatments on masonry durability.

2.3.4 Cladding panels with open joints

Facades with open joints, commonly composed of fibre-cement, stone, or wood panels mounted on metal or timber framework, allow rainwater to infiltrate primarily through the joints rather than the panel surfaces. While most raindrops deposited on the façade surface splash back (≈49.7%), or form runoff films (≈22.5%), under typical conditions about 27.8% infiltrates through joints (Recatala et al., 2018). Pressure equalization can minimize infiltration caused by pressure differences. Killip and Cheetham (1984) demonstrated that 99% equalization occurs when the ratio of exterior openings to air-barrier openings exceeds 25–40. Recatala et al. (2018) confirmed this effect, observing only 10 Pa pressure difference even under 750 Pa applied pressure, eliminating pressure-driven infiltration.

Joint geometry strongly influences infiltration. Mas et al. (2011) found that non-planar edges (grooved profiles) reduce infiltration for joints <8 mm by limiting capillary action, whereas for joints ≥8 mm, gravity and raindrop impact dominate. Horizontal joints are particularly vulnerable; taping them reduced infiltration from 27.8% to 0.7% (Recatala et al., 2018). The Association of Ventilated Curtain Wall Facades (n.d.) measured 5.4% infiltration through 8 mm horizontal joints and 17% through combined horizontal and vertical joints, whereas Mas et al. (2011) reported up to 45% infiltration for 8 mm joints with 40 mm panel thickness—differences likely due to variations in spray angle, rate, and test setup.

These findings highlight that infiltration through open-joint facades is highly sensitive to joint design, detailing, and test conditions. While pressure equalization can mitigate one driving force, capillary action and gravity remain dominant for narrow and wide joints, respectively.

2.3.5 Quantification of infiltration rates

In the studies as have been reviewed, various types of cladding were subjected to wind simulated by an air pressure difference over the test specimen and to rain by spraying water directly onto the specimen. The total amount of water infiltrating through the exterior cladding surface, reaching a drainage cavity, WRB and/or materials that are not intended to get wet, were weighed and reported. The review showed that the dependency of the infiltration rates on the applied pressure difference and spray rate, was affected by the type of cladding and the presence of openings.

A constant water infiltration percentage for increasing pressure was observed for specimens which included a pressure equalized cavity reducing the pressure difference over the cladding. To obtain effective pressure equalization (PEP > 90%), the airtightness of the air barrier should be at least ten times higher than the airtightness of the cladding (Van Den Bossche et al., 2020). The other cladding types showed an increase of the infiltration percentage for increasing pressure difference.

The larger the openings in the exterior cladding surface, the smaller the pressure required for water to infiltrate and the higher the infiltration percentages. This was apparent for the panel cladding with open joints, the glued concrete blocks with open head joints and mortared masonry. Even without a pressure difference over the specimen, infiltration occurred. Water running off a saturated masonry exterior surface may cause a hydrostatic pressure onto the surface and combined with capillary suction, water may be forced through cracks, in particular at the mortar-brick interface. The smaller the openings, cracks or deficiencies in the exterior surface or in case of concealed openings, the larger the pressure needs to be before infiltration occurs (Van Den Bossche et al., 2012). A pressure threshold first needs to be exceeded before infiltration occurs, for example, through sidings, ETICS and stucco. It should be noted that most of the infiltration percentages reported in literature are only valid for saturated wall cladding, which may not be typical for masonry walls. Façade materials with a high porosity and moisture absorption capacity often store a considerable part of the wind driven rain load, which will depend on the wetting and drying sequence in a specific climate. Standardized watertightness tests were typically designed to evaluate the potential to withstand extreme combinations of rain and wind. Consequently, the infiltration rates in literature should be considered as worst-case. Most experimental results reported in the literature are derived from single-instance test configurations, with limited or no replication across independent samples. While repeated measurements on one specimen may reduce measurement noise, they do not capture construction-related variability. From a methodological standpoint, statistically meaningful inference requires both repeatability—through tests on multiple identical specimens—and reproducibility, achieved by independent validation in different laboratory settings. At this point, there is a lack of data to develop an evidence-based probabilistic infiltration model.

Evidently, when a cavity of more than 10 mm is present in the wall assembly, only a portion of the infiltrated water reaches the interior side of the cavity. Water may reach the interior side of, for example, masonry cavity walls due to splashing on extruded mortar joints or water drops being transported along wall ties angled towards the interior. Calle et al. (2020) found that the ratio of water reaching the interior side of the cavity and the residual part of infiltrated water, which in most cases drains along the interior side of the cladding, was dependent on the applied pressure difference. For increasing pressure difference, an increased portion of infiltrated water reached the interior side of the cavity. Ratios between 0.2% and 2.9% were found for pressure differences of 0 and 300 Pa respectively and a cavity width of 30 mm. For masonry walls with normal workmanship and a cavity width of 30 mm, this results in 1.3% of the sprayed water reaching the interior side of the cavity and 45.3% being drained along the interior side of the cladding at a pressure difference of 300 Pa. Similarly, Recatala et al. (2018) reported that 0.5% of the sprayed water reached the interior side of a 100 mm cavity behind panel cladding with open joints and 27.3% either drained along the interior side of the cladding or drained in the cavity. None of the other studies differentiated between the percentage of water draining along the interior side of the cladding or reaching the interior side of the cavity.

2.3.6 Water entry functions

To conduct hygrothermal simulations from which to ascertain the water management of the facade, it is, however, of importance to determine the portion of water that either drains along the interior side of the cladding or in the drainage cavity or reaches the WRB or the interior side of the cavity. Besides the pressure difference, the portion of water crossing the cavity is also affected by the cavity width and whether water drops can infiltrate directly through large openings in the cladding in an unobstructed manner.

In simulations, a moisture load should be defined representing the infiltrated water in a wall assembly. The previously reported studies showed that the infiltration rates and percentages are dependent on the applied spray rate and pressure difference over the wall assembly. Therefore in reality, the infiltration percentages will be dependent on the wind-driven rain (WDR) and driving rain wind pressure (DRWP). As the WDR and DRWP values vary over time and for different locations, it is essential to provide a water entry function as moisture load which includes the combined effect of WDR (or spray rate) and DRWP (or pressure difference).

Sahal and Lacasse (2005) established a water entry function based on infiltration rates in the stud cavity of hardboard siding-clad walls. They derived a linear function that relates the water entry rate to the spray rate for each static pressure difference. In contrast with what is presented by Sahal and Lacasse, the reviewed studies in this chapter showed a non-linear relation between the water infiltration rate and the spray rate and a maximum infiltration rate for a certain spray rate. Moore et al. (2019) also derived a water entry function to calculate the water entry for a given quantity of WDR and wind-induced pressure. There the water entry is linear with the WDR, but the effect of pressure difference is incorporated by means of a power law. However, the power function implies that no water entry occurs at zero wind-induced pressure, whereas the reviewed studies showed that water entry may occur without any induced wind-pressure but only due to a hydrostatic pressure. Xiao et al. (2023) advanced the approach developed by Moore et al. by adding the spray rate as a parameter in the water entry function. These functions were derived from experiments on different wall configurations, and provides one of the few examples where a probabilistic approach might be feasible. These water entry functions may thus be used as input for hygrothermal simulations. However, to obtain these water entry functions it is necessary to conduct laboratory tests at different spray rates and pressure levels. These kind of tests are not available for every type of cladding and façade detail and it is not always preferable to conduct new tests when a building is designed. ASHRAE Standard 160 (ASHRAE, 2016) therefore, proposed a default infiltration rate of 1%. However, based on the presented review it is clear that infiltration percentages differ for different cladding types and that 1% is not always a reasonable assumption.

To gain insight in the expected infiltration percentages for a cladding type during the design phase, without performing additional laboratory studies, a categorization of exterior cladding surfaces has been developed. During the design phase, one can look up information either for the specific preferred cladding type, for similar cladding materials or for a category with similar characteristics, depending on the available information. Figure 2.3.1 provides an overview of the infiltration rates found in literature, and 7 categories are introduced to generalize the results. When possible the detailed results reported in literature can be used, but for other cases the category that corresponds best to the cladding type can be adopted to estimate the infiltration rates.

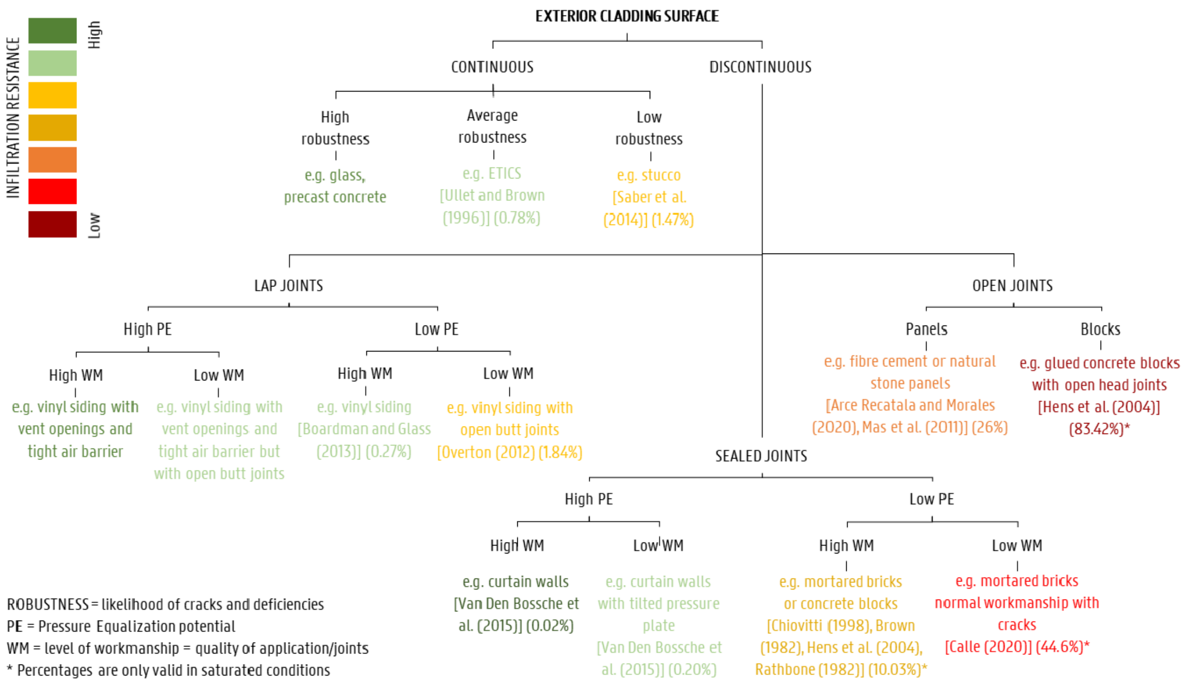

Figure 2.3.1 Categorization and colour rating of exterior cladding surfaces based on their resistance to water infiltration. Examples are provided for each category and a colour rating is assigned to each category based on infiltration percentages found in literature. Infiltration percentages at a pressure of 300 Pa are provided when available in literature

The initial categorization is whether the cladding surface is continuous or discontinuous:

- A continuous cladding system does not include joints between different cladding elements, and joints at façade details such as windows or ducts are not taken into account. At the exterior these claddings are perceived as a continuous surface. Water infiltration through continuous cladding systems is most likely to occur through cracks in the surface.
    - ETICS: 0.06 – 0.74%, increasing to 4.2 – 6.6% considering façade details
    - Stucco: 0 - 1.5%, increasing to 3 – 6% (façade details)
- Discontinuous cladding - Lap joints: an overlap is present between the different cladding elements. Lap joints may be present in different ways; for example, one element is applied on top of the other element in an overlapping manner or two elements are connected with shiplap joints. As well, in this type of cladding, there are no openings that provide a direct horizontal path for infiltrating water towards the interior. Water infiltration is most likely to occur through deficiencies in the lap joint by capillary action.
    - High pressure equalisation: no data
    - Low pressure equalisation: 0 – 0.05% (vinyl sidings), 3.2 - 4% (façade details)
- Discontinuous cladding - Sealed joints: All joints between the cladding elements are sealed by means of, for example, mortar, elastomeric sealant, foam sealing tape, or other sealing products. Water infiltration is most likely to occur through deficiencies at the interface between the joint sealing material and the substrate.
    - High pressure equalisation: 0.021 – 0.27% (curtain wall)

- Low pressure equalisation: 0.05% (mortared brick, good workmanship), 7 – 34% (mortared brick, poor workmanship), 15% (mortared concrete blocks), 2.1 – 3.5% (façade details).

- Discontinuous cladding - Open joints: Either horizontal, vertical or all joints between cladding elements are open providing a direct path for water to infiltrate. Open joints may either be present between panels or blocks. Blocks are defined as elements which have a thickness that is within the same order of magnitude as either the width or height of the elements. Panels are defined as elements with a thickness several times smaller than the width or height of the elements. It is assumed that the total length of joints for facades composed of blocks will be several times larger than the total length of joints between panels.
    - High pressure equalisation: 23% (fibre cement panels), 24% (natural stone panels)
    - Low pressure equalisation: 20 – 70% (glued concrete blocks with open head joints)

Discontinuous exterior cladding surfaces with lap joints and sealed joints are further subdivided based on the pressure equalization potential of the wall assembly which implies determining whether, or not, a significant pressure difference can be expected to occur across the cladding. High pressure equalization (PE) is considered when the pressure equalization potential is more than 90% which may be achieved when the airtightness of the air barrier is at least ten times higher than the airtightness of the cladding (Van Den Bossche et al., 2020). A high pressure equalization will result in less infiltration as the pressure difference is reduced as a driving force. It is assumed that the pressure equalization potential of continuous claddings will always be low as the number of intentional openings will be low. In contrast, it is assumed that the pressure equalization potential for claddings with open joints will always be high.

2.3.7 Modelling Infiltration Rates

The water entry functions and reported infiltration rates provide a basis to implement water ingress in hygrothermal simulations. This is often done by implementing a moisture source in numerical simulation models, and more specifically by adopting a fraction of the WDR as moisture load in one, or more, cells of the numerical configuration. Typically, 1% of the wind-driven rain load is chosen as source term as proposed by the ASHRAE Standard 160. The findings in this review, however, have shown that 1% of the wind-driven rain load as a moisture source can be an over- or underestimation of the infiltration percentages depending on the characteristics of the wall assembly and whether or not drainage and water retention are accounted for. It should be noted that to the knowledge of the authors, no simulation models exist that explicitly account for the effect of drainage inside building components. However, when water is supplied by the source term to one or more gird cells in subsequent time steps, very often the supply exceeds the redistribution rate within the construction. That may cause a very quick increase in the moisture content of those cells, often well above the open porosity of the material which is physically not possible. Hence, these models have implicit or explicit cut-off values that prevent the moisture content to rise above a certain threshold value, and hence the moisture source is by default removed from the moisture balance in the model. By consequence, this effect can also be used by the modeler to implement the effect of drainage in a wall assembly. Infiltrated rainwater that crosses a cavity will partly adhere to that surface and partly drain to the outside. The modeller can define a specific layer with a storage capacity that corresponds to the amount of water that adheres on the surface, whereas the automatic cut-off of the moisture content mimics the drainage effect. In some cases it can even be advisable to split up materials layers and change, for example, the open porosity to accommodate implementing the source term in a more realistic way. When implementing water ingress in hygrothermal simulations by means of water entry functions, it is important to consider how this is implemented in the simulation model. Whenever a source term is implemented in a hygrothermal model, it is key to determine what exactly is occurring in the model, to what extent moisture is, in fact, removed from the equation, as explained above, and to what extent drainage occurs, in reality. It should be noted that these results are highly sensitive to the location, material, and number of grid cells in which the source term is implemented.

Finally, the infiltration rates reported in literature, and by consequence those in this review, are representative of saturated cladding materials. The spray rates adopted in test standards are extremely high, and often the infiltration rates are only determined once a stationary infiltration rate is recorded (which implies that saturation is achieved). In the case of, for example, capillary materials, this will lead to an overestimation of water entry at the beginning of a rain event. In reality, saturation may be extremely rare in some cases, leading to a significant overestimation of infiltration rates (Van Den Bossche et al., 2025). Commercial models currently do not allow rendering the infiltration rate function of the saturation level of certain layers or cells.

To include the effect of rainwater infiltration in hygrothermal simulation, different aspects need to be considered:

- Rainwater infiltration locations

- Rainwater infiltration to drained layers

- Retention of rainwater in drained layers

- Rainwater infiltration to undrained layers

2.3.7.1 Rainwater infiltration locations

Rainwater may infiltrate to several locations in the wall assembly, which include the: interior side of the cladding (1); exterior side of the WRB, or drainage barrier (2), and; interior side of the WRB, or drainage barrier (3) (Figure 2.3.2). Whether, or not, water will infiltrate to each of these locations in an assembly will depend on the WDR load, the DRWP, the water management of the wall system and rain water reaching the openings or deficiencies. Each of these locations may either be defined by a drained or undrained layer and for each location a moisture load may be implemented in the simulations. For example, in a typical brick cavity wall in Europe without WRB (Figure 2.3.2 left), water may infiltrate the brick cladding and reach the interior side of the wall assembly (1). Evidently, whether or not there needs to be a WRB, and whether there are specific requirements on the insulation type will depend a.o. on the building traditions, climate, and exposure. A portion of the infiltrated water may cross the cavity and reach the exterior side of the drainage barrier (2), which may, for example, be the insulation and which, again, is considered as a drainage layer. When deficiencies are present in the drainage barrier, for example, an open joint between two insulation panels, water may infiltrate through this joint and reach the interior side of the drainage barrier (3). In case of an assembly where no drainage is provided, for example, direct-applied siding (Figure 2.3.2 right), the interior side of the cladding (1) and the exterior side of the WRB (2) coincide, and consequently, this location should be considered as an undrained layer.

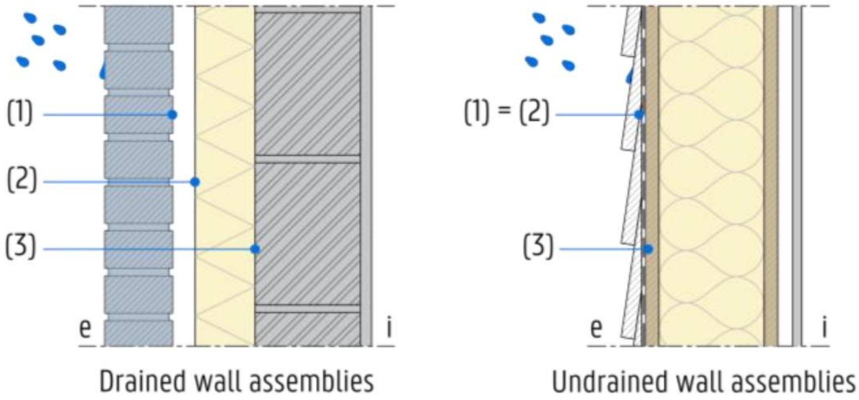

Figure 2.3.2 Rainwater infiltration locations in drained and undrained wall assemblies: (1) interior side of cladding, (2) exterior side of drainage barrier, (3) interior side of drainage barrier.

2.3.7.2 Rainwater infiltration to drained layers

A number of wall configurations comprise drainage layers, and these layers are supposed to adequately manage both the infiltration and evacuation of rainwater. As discussed above, the modelling approach should reflect the actual behaviour of the wall, and the concept of drainage can be replicated by considering the combination of moisture source and moisture storage in a dedicated layer in the model. It should be noted that this approach was conceived for 1D simulations: drainage and accumulation of infiltrated rainwater at the bottom of a construction requires a completely different approach.

2.3.7.3 Retention of rainwater in drained layers

Infiltrated rainwater will be drained to some extent, and some water will be retained by the drainage layer. The retention can be seen as a maximum value, and when the rainwater infiltration rate is sufficiently high, this maximum retention value will be reached, and any additional supply will be drained. The retention will depend on the rainwater supply, and the material properties of the drainage layer and the cavity. In hygrothermal simulations the retention can be simulated by supplying the infiltration rate to a material with a moisture storage function. For materials with open pores this is automatically the case; for other types of materials, a fictitious material layer can be added to simulate the moisture storage. Evidently, this layer should not affect other storage and transport phenomena in the wall configuration.

2.3.7.4 Rainwater infiltration to undrained layers

Water infiltration to undrained layers typically refers to unintentional rainwater ingress, e.g. through deficiencies in the wall assembly. The ASHRAE 1% rule was designed to represent the infiltration into drained cavities and should not be used to account for the impact of unintended leakages to assess, for example, the robustness of a wall assembly. When a drainage layer is present, it can be assumed that the infiltration to an underlying undrained layer can be expressed as a percentage of the infiltration rate to the drained layer: when there is a tear in a WRB, only a part of the rainwater reaching the WRB will in fact infiltrate through that deficiency. Given that there are no drainage provisions in the subsequent layer, it can conservatively be assumed that all infiltrating water reaching the undrained layer will be stored, and there is no "maximum retention". Again, the rainwater infiltration rate will depend on the WDR load, the DRWP, the water management of the wall system, and the supply to openings or deficiencies. In hygrothermal simulations the rainwater infiltration rate can be calculated as a percentage of the WDR, or a separate source file can be used.

2.3.8 References

ASHRAE. (2016). ASHRAE 160: Criteria for moisture-control design analysis in buildings. American Society of Heating, Refrigerating and Air-Conditioning Engineers.

Barreira, E., & de Freitas, V. P. (2013). Experimental study of the hygrothermal behaviour of External Thermal Insulation Composite Systems (ETICS). Building and Environment, 63, 31–39. https://doi.org/10.1016/j.buildenv.2013.02.001

Boardman, C. R., & Glass, S. V. (2013). Investigating wind-driven rain intrusion in walls with the CARWASh. Thermal Performance of the Exterior Envelopes of Whole Buildings XII International Conference, 11.

Brown, R. H. (1982). Initial effects of clear coatings on water permeance of masonry. ASTM International, 16.

Calle, K., Coupillie, C., Janssens, A., & Van Den Bossche, N. (2020). Implementation of rainwater infiltration measurements in hygrothermal modelling of non-insulated brick cavity walls. Journal of Building Physics, 43, 477–502. https://doi.org/10.1177/1744259119883909

Calle, K. (2020). Renovatie van historische gevels: redding of doodsteek? [Doctoral dissertation, Ghent University].

Chiovitti, D., Gonçalves, M., & Renzullo, A. (1998). Performance evaluation of water repellents for above grade masonry. Journal of Thermal Envelope and Building Science, 22, 156–168. https://doi.org/10.1177/109719639802200208

FVHF. (n.d.). Properties of rear-ventilated facades. Retrieved October 16, 2025, from https://www.fvhf.de/facade/VHF-System/Merkmale.php

Hens, H., Roels, S., & Desadeleer, W. (2004). Rain leakage through veneer walls, built with concrete blocks. CIB W40 Meeting, Glasgow, United Kingdom.

Kahangi Shahreza, S., Niklewski, J., & Molnár, M. (2021). Experimental investigation of water absorption and penetration in clay brick masonry under simulated uniform water spray exposure. Journal of Building Engineering, 43, 102583. https://doi.org/10.1016/j.jobe.2021.102583

Killip, I. R., & Cheetham, D. W. (1984). The prevention of rain penetration through external walls and joints by means of pressure equalization. Building and Environment, 19, 81–91. https://doi.org/10.1016/0360-1323(84)90033-7

Mas, Á., Gutiérrez, J., Gil, E., Gil, A., & Galvañ, V. (2011). Design and construction recommendations to improve impermeability in rainscreen walls built with natural stone coverings. Construction and Building Materials, 25, 1753–1761. https://doi.org/10.1016/j.conbuildmat.2010.11.091

Molnar, M., Jönsson, J., & Rosenkvist, P.-O. (2017). Development of experimental methods to evaluate infiltration of wind-driven rain into external thermal insulation composite systems (ETICS). 14th International Conference on Durability and Building Materials, 12.

Moore, T. V., & Lacasse, M. A. (2019). Determining moisture source due to wind driven rain for input to hygrothermal simulations using experimental methods. Thermal Performance of the Exterior Envelopes of Whole Buildings XIV International Conference, Florida.

Ngudjiharto, E. (2015). Field study of wind driven rain penetration into vinyl sidings and stucco-clad wood-frame wall systems at window sill (Master's thesis, Concordia University).

Parracha, J. L., Borsoi, G., Flores-Colen, I., Veiga, R., Nunes, L., Dionísio, A., Gomes, M. G., & Faria, P. (2021). Performance parameters of ETICS: Correlating water resistance, bio-susceptibility and surface properties. Construction and Building Materials, 272, 121956. https://doi.org/10.1016/j.conbuildmat.2020.121956

Recatala, M. A., Morales, S. G., & Van Den Bossche, N. (2018). Experimental assessment of rainwater management of a ventilated façade. Journal of Building Physics, 42, 38–67. https://doi.org/10.1177/1744259117719077

Rousseau, M. (1999). An overview of the survey of building envelope failures in the coastal climate of British Columbia, performed by Morrisson-Hershfield Limited for CMHC. Journal of Thermal Envelope and Building Science, 22, 364–367. https://doi.org/10.1177/109719639902200411

Saber, H., Lacasse, M., Moore, T., & Nicholls, M. (2014). Mid-rise wood constructions: Investigation of water penetration through cladding and deficiencies. National Research Council of Canada. https://doi.org/10.4224/21274581

Sahal, N., & Lacasse, M. A. (2005). Water entry function of a hardboard siding-clad wood stud wall. Building and Environment, 40, 1479–1491. https://doi.org/10.1016/j.buildenv.2004.11.019

Straube, J., & Burnett, E. F. P. (1998). Driving rain and masonry veneer. Water Leakage through Building Facades (ASTM STP 1314).

Ullet, J. M., & Brown, W. C. (1996). Measured pressure equalized performance of an exterior insulation finish system (EIFS) specimen. National Research Council Canada, Ottawa, Canada.

Van Linden, S., & Van Den Bossche, N. (2022). Review of rainwater infiltration rates in wall assemblies. Building and Environment, 219, 109213. https://doi.org/10.1016/j.buildenv.2022.109213

Van Den Bossche, N., Lacasse, M., Moore, T., & Janssens, A. (2012). Water infiltration through openings in a vertical plane under static boundary conditions. Proceedings of the 5th International Building Physics Conference, Kyoto, Japan.

Van Den Bossche, N., Janssens, A., Moore, T., & Lacasse, M. (2020). Development of numerical model for determination of pressure equalization in facades during wet conditions. Building and Environment, 178, 106919. https://doi.org/10.1016/j.buildenv.2020.106919

Van den Bossche, R., Vanderschelden, B., Van Den Bossche, N., & Steeman, M. (2025). Experimental investigation of rainwater absorption and infiltration in different types of masonry with lime hemp interior insulation. Construction and Building Materials, 495, 143704. https://doi.org/10.1016/j.conbuildmat.2025.143704

Xiao Z., Defo M., Lacasse M., Wang L, Moore T., Assessment of Moisture Loads in Wall Assemblies from Watertightness Tests. Results on Wind-Driven Rain Analysis and Water Entry Tests. CRBE-Report_FY22-23_Water entry tests. National Research Council Canada.

2.4 The Impact of Air Leakage on Hygrothermal Performance of Building Façade Systems

This section should be cited as:

Junginger, M. (2026). The Impact of air leakage on hygrothermal performance of building façade systems. In: A Systematic Review of Passive Energy Conservation Measures and Probabilistic Assessment under Changing Climate in Urban Settings, CIB W040 Report, CIB General Secretariat.

2.4.1 Air leakage

For quite an amount of time, vapor diffusion was considered the main source of moisture and this could lead to condensation and bio deterioration of sensitive materials. Around 1960, however, it was understood that air leakage was the most important source of water migration (Quirouette, 1989) and researchers found out that the most of the moisture was due to air leakage instead of vapor diffusion (Kumaran & Haysom, 2000).

While vapor diffusion happens because of vapor pressure differences, Garden (1965) explains that:

> *Air leakage is the uncontrolled movement of air through walls and roofs, both into a building (infiltration) and out of it (exfiltration), and the interchange of air from the building with that in spaces in the building envelope. Pressure differences that cause infiltration and exfiltration are produced by wind, chimney effect, and the operation of mechanical ventilation systems.*

CMHC (1992), Bomberg & Brown (1993) and Bomberg & Onysko (2002) explained that the understanding of the performance of walls came mainly from the extreme climate in the Prairies of North America, where the climate magnifies any fault in the ability of the wall to maintain environmental control. After extensive research in the University of Minnesota in the 1930s, building paper was accepted as a weather barrier, limiting the movement of air and rain. Vapor barriers were introduced, and homes built as early as the 1940s already included weather resistive barriers outside and vapor barriers inside. Vapor barriers are special building papers, membranes, or coatings designed to avoid vapor diffusion due to vapor pressure differences. Whereas a few building materials are impervious to vapor, like glass and metal, a considerable amount of materials provide sufficient resistance to be used for vapor control purposes (Handegord, 1960).

Kumaran & Haysom (2000) mentioned that the use of vapor barriers was introduced in the 1930s to control vapor diffusion into walls and attics; however, when interior humification started in 1950s, moisture accumulation again became a problem in many houses. The same view is given by Hutcheon (1989), who says that commercial and institutional buildings in the 1950s which had traditionally been operated at low indoor relative humidities started having problems after being humidified during winter.

Condensation problems have not been widespread and those that have occurred have usually been associated with holes and gaps in the interior cladding and vapor barrier, which may be due to the installation of electrical wiring (Hutcheon & Handegord, 1980). By then, a common complaint from the occupants during winter was about cold air leakage into the house through electrical receptacles in exterior walls. Hutcheon (1953) explains:

> *The flows of heat, moisture and air in walls have implications not only by themselves, but for all the other considerations listed. Air merits major consideration mainly because of its influence on heat and moisture flow. The overall transmission of heat, air and moisture through a wall can affect the ease with which the desired environmental conditions may be maintained, and so may have a marked influence on cost of operation of a building.*

Due to this air movement, Handegord (1960) mentioned that "the most impermeable, most durable vapor barrier may be rendered virtually ineffective by the presence of accidental or intentional openings … and will result in excessive condensation within the wall". This statement matches with ASHRAE ASHRAE (2017, p. 26.6), which says air leakage is far more important than vapor diffusion.

When analysing a situation with air leakage through a 30 cm thick unplastered brick wall with no inside finish, Wilson & Garden (1965) explained that, while the moisture accumulation due to vapor diffusion reaches the amount of only 0.22 kg/m^2, air leakage might lead to a much higher amount of 36 kg/m^2 under the same conditions. So, a system of caulking would increase air tightness and help solving the problem; Hutcheon (1963) said that this action can reduce the air leakage by a factor of as much as 100. In another example, with brickwork and cracks, Latta (1976) explains that air leakage has a much greater potential for carrying moisture than vapor diffusion even when neglecting the cracks at the columns (Figure 2.4.1).

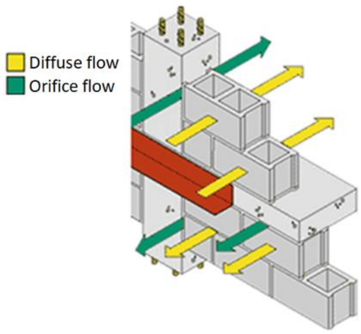

Figure 2.4.1 Water vapor transport through diffusion and air leakage

Another situation is shown by Rousseau (1984): a 1 m^2 painted gypsum wall, one continuous and the other with a 4 cm^2 hole under a pressure difference of 10 Pa. The air leakage through the hole carries about 100 times more moisture than diffusion alone (**Error! Reference source not found.**). Some years later, Rousseau & Brown (1995) complemented:

> *It is now well established that air movement is the dominant means of moisture transport through the building envelope as well as a major component of heat transfer. A high proportion of the problems associated with building envelope deterioration can be attributed to inadequate control of air leakage. The air-barrier system is the assembly installed to provide a*

continuous barrier to the movement of air. Its performance and durability are of prime importance to the durability of the whole building envelope.

Simpson & O´Connor (1994) tested a 2.8 m high assembly in two conditions: continuous vapor barrier and intentionally perforated vapor barrier. Compared to the intact vapor barrier, there was no important increase in moisture accumulation with the damaged barrier under dry indoor conditions (25% RH), but a substantial increase under wet indoor conditions (60%RH). Handegord (1982) said that a vapor barrier is still effective even with small holes on it; however, if this vapor barrier is also an air barrier, those holes will allow much greater moisture transfer and accumulation under an air pressure difference. A few small holes and cracks do not add much to the vapor transfer by diffusion because the area is small even though the permeability may be large, but under small pressures these holes are a free way for the air to move and carry an important amount of moisture (Hutcheon, 1963).

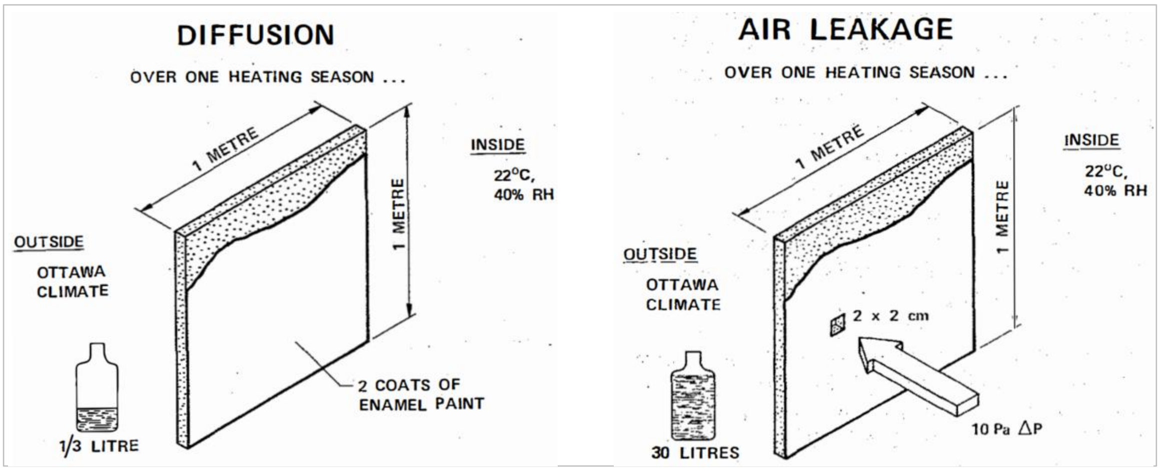

Figure 2.4.2 Moisture accumulation comparing diffusion and air leakage (Rousseau, 1984).

Tsongas (1995) compared the efficacy of a vapor barrier in a wall subjected to an air leakage rate of 0.15 L/s.m^2 and concluded "… exfiltration essentially diminishes the effectiveness of the vapor retarder. When exfiltration is present it is much more important than diffusion as a moisture migration mechanism". Ojanen & Kumaran (1996), in a simple calculation considering a 2 cm diameter hole, show that the amount of moisture due to air leakage through that single hole can be 100 times greater than the amount due to diffusion only. ASHRAE (2017, p. 26.6) states: "calculations of water vapor flow, interstitial condensation, and related moisture accumulation using only water vapor resistances are useless when airflow is involved".

The National Building Code incorporated the science behind air leakage in the 1995 version, acknowledging that air movement is dominant factor in the transport of moisture through building envelope assemblies. Also, due to the high influence of air movement on heat transfer, the importance of an air barrier would be also recognized in the 1997 version of the National Energy Code (Brown et al., 1998). This knowledge is present in the current version of the NBC (NRCC, 2025), which says:

The majority of moisture problems resulting from condensation of water vapor in walls and ceiling/attic spaces are caused by the leakage of moist interior

> *heated air into these spaces rather than by the diffusion of water vapor through the building envelope.*

When considering air leakage at low rates, the heat flux is also low and there is almost no influence on the temperature of the leakage path and the components around it. However, at higher air leakage rates, heat flux has a greater contribution to the temperature variations of the wall components and they become so warm that the condition for condensation cease to exist (Ojanen & Kumaran, 1992). Old and leaky walls are so warm that condensation cannot occur; however, there will be a price to pay related to energy efficiency (Bomberg & Onysko, 2002; Kumaran & Haysom, 2000).

Figure 2.4.3 shows the simulation results of moisture accumulation and outdoor temperature in different cities (nine in Canada and three in Finland) for the same air leakage rate (0.98 L/s.m^2 at 21°C and 30% RH): in general, the coldest the city, the highest the amount of moisture, but this might vary because of winter duration and other factors (Ojanen & Kumaran, 1992). The geometry of the wall and the air leakage path are shown at the top of the figure.

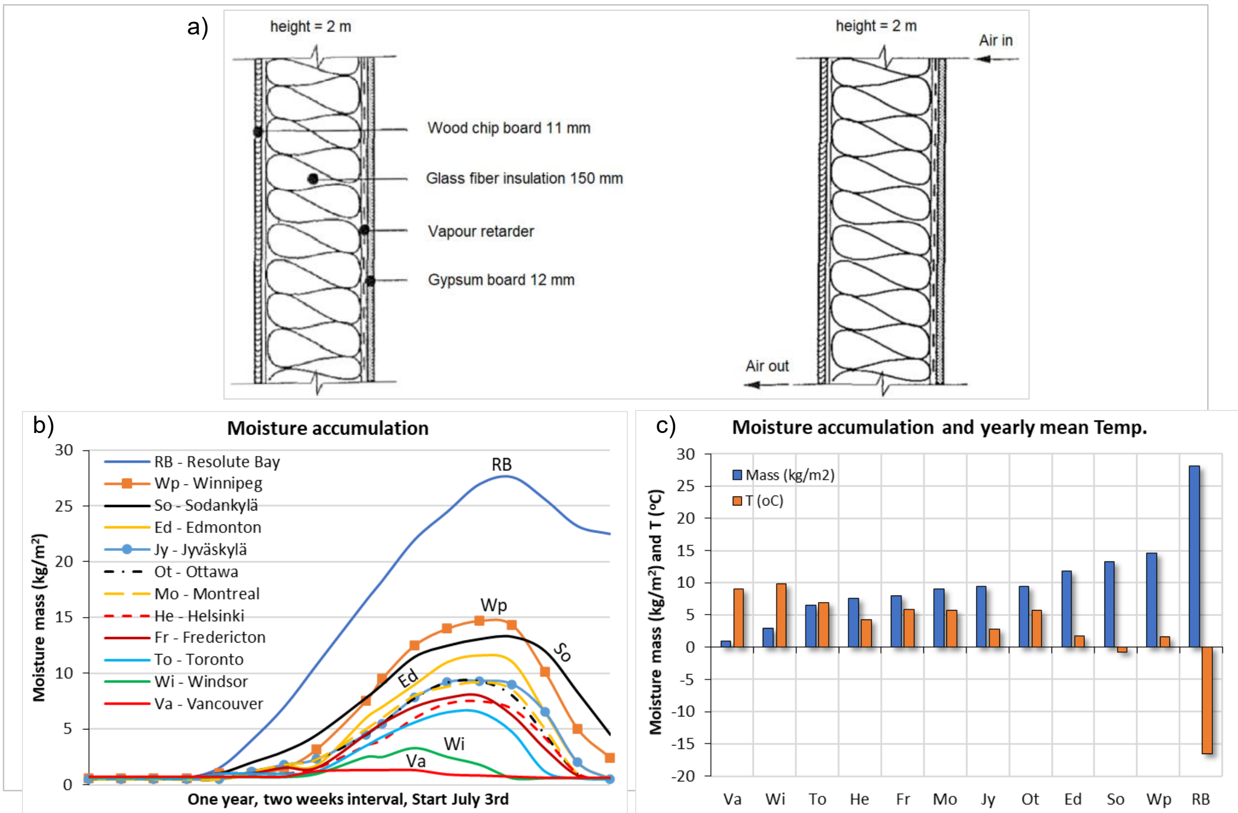

Figure 2.4.3 a) wall configuration; b) mass of moisture per surface area as a function of time; c) moisture accumulation and outdoor temperature for different cities (adapted from Ojanen & Kumaran (1992)).

For different indoor conditions, 36% RH at 21°C and 48% RH at 21°C, Figure 2.4.4 shows that moisture accumulation at 48% RH is higher than at 36%. That means the tolerable air leakage rate will strongly be related to the humidity level of the indoor air (Ojanen & Kumaran, 1996). It is possible to see the heat flux is the same for both cases since the air enthalpy does not vary much between 36% and 48% RH.

Common openings in residential walls are represented by electrical boxes: power outlets (at bottom) and light switches (middle height). When analyzing the correlation between air leakage paths and hygrothermal performance, Ojanen & Kumaran (1996) came up with Figure 2.4.5, with five possibilities: number 5 is one of the worst cases in terms of moisture accumulation and conveys the idea of air leakage entering through the power outlet, diffusing through the insulated cavity and managing its way out at the top of the wall. Underneath each path there is a bar showing a comparison among all moisture accumulations: paths 1 and 5 are the worst cases, 3 and 4 are in between and 2 is the best case. So, path number 5 has been adopted in other studies (Chown & Mukhopadhyaya, 2005; Defo & Lacasse, 2020; Desmarais et al., 2000; Junginger et al., 2020; Kayll et al., 2020; Saber, 2014).

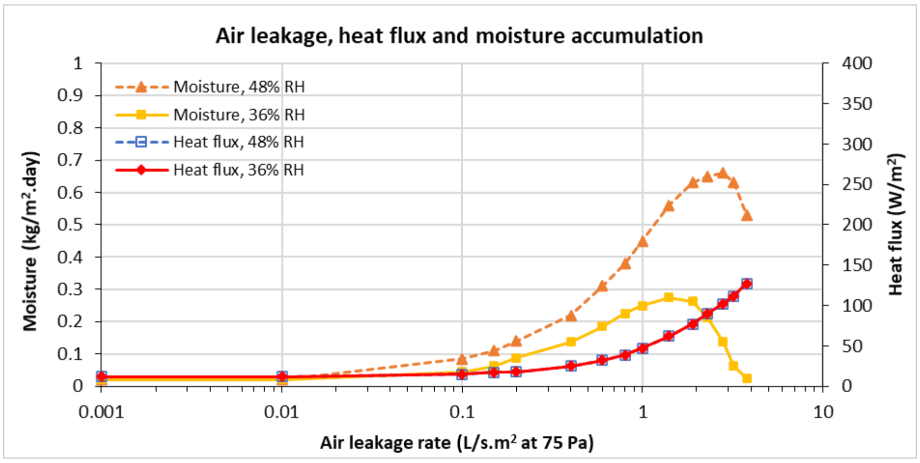

Figure 2.4.4 Correlation between air leakage rate, heat flux and moisture accumulation, indoor conditions at 21°C, 36% RH and 21°C, 48% RH (adapted from Ojanen & Kumaran (1996)).

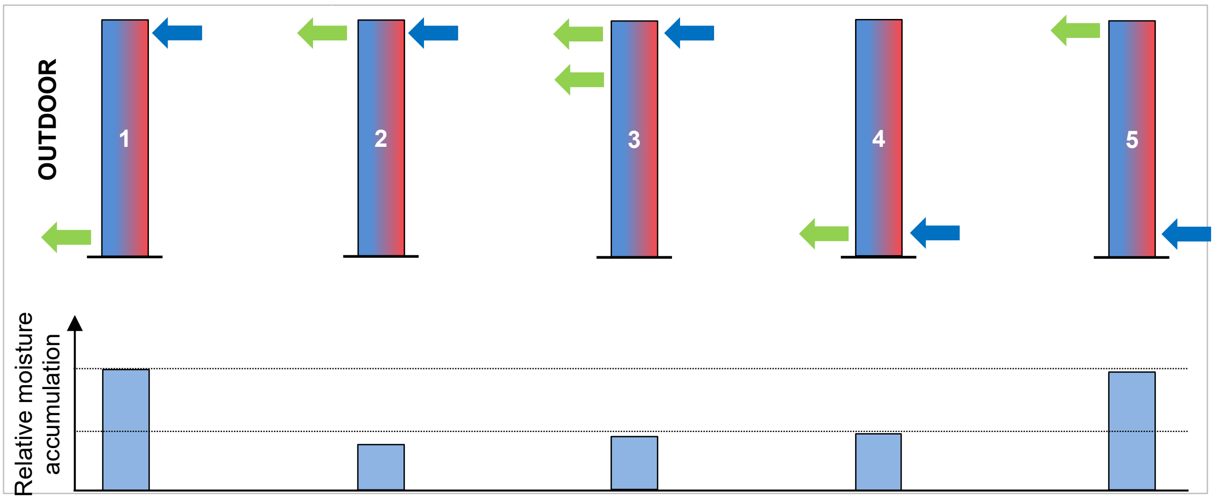

Figure 2.4.5. Five possible paths of exfiltration (top) and relative moisture accumulation (bottom), adapted from Ojanen and Kumaran (1996).

Figure 2.4.5 shows that the exfiltrated air leaves a warm environment and goes towards a cold environment. So, the longer it stays close to the cold side of the assembly, the higher the risk of condensation since there is more time for the air to get colder. While in paths 2, 3 and 4 the air needs to cross about only 150mm, in paths 1 and 5 the way is roughly 15 times longer, about the height of the wall.

The influence of air leakage on the long-term performance of assemblies is related to many different factors, for instance pressure difference, indoor and outdoor relative humidity and temperature, the composition of the assembly itself, the position and size of the air entry. Moreover, inside the assembly the air flux may go through random paths due to unintended voids and permeability of the insulation: inactive paths at low pressure may become active under higher pressures. Therefore, the best solution to be evaluated depends on a risk analysis which encompasses the situation most likely to occur in practice.

Basically, air leakage through the building envelope is a consequence of pressure difference, which happens either due to mechanical pressurization, wind speed, stack effect or a combination thereof. The air flow that develops is then a function of the resistance between the air entry and the air exit: different types of insulation, construction details, position of the studs, gaps between the insulation and the structural frame, all these parameters have an impact on how the air moves inside the assemblies. For instance, air flow may dissipate all over an air permeable insulation but may penetrate through a specific crack/gap if the insulation poses high resistance to air movement. Moreover, the air path may change according to the pressure difference, since inactive gaps under low pressures might become active under higher pressures and once diffuse flows can become more concentrated through a specific path.

On the other hand, sheathing conditions are much easier to map under controlled environment in a laboratory: imposing a known air flow rate through pre-positioned holes, moisture content can be measured and used to validate computational models, which can be further used to predict the hygrothermal behavior of other assemblies with reasonable similarities (Bunkholt et al., 2021; Desmarais et al., 2000; P. Kölsch et al., 2016; Pallin et al., 2015). Figure 2.4.6, for instance, shows the results of an experiment where the authors varied the number, size and position of the air entries, the permeability of the insulation, and the pressure difference. The main conclusions were: high density insulations retain more moisture than low density ones and then reduce the condensation at the sheathing; different arrangements of holes change completely the moisture profile; holes close to the studs lead to a higher airflow because of the recess of the insulation at the corner.

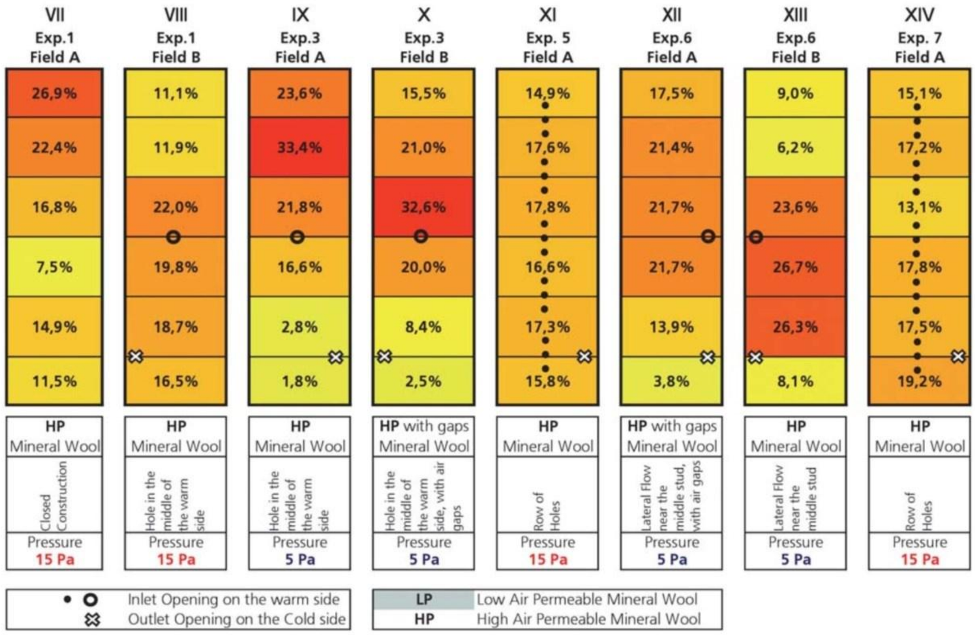

Figure 2.4.6 Moisture distribution in the paper sheets for the experiments with high air permeable mineral wool, view from the cold side (P. Kölsch et al., 2016).

In cold climates, exfiltration of warm air is usually of concern, since it might induce moisture problems and it is a way of losing energy. In this case, it might be possible to detect the leak from the outside by using different techniques, even though the path of the air flow remains unknown. If sufficient heat is transferred through the building envelope in the form of localized airflow, thermal imaging may be able to identify the corresponding exterior location. In some cases, it is reasonable to assume that the interior source is located near the detected exterior area. However, with brick cladding or siding, for instance, the air layer behind them makes this assumption impractical.

Another way of identifying leaks is the use of acoustic cameras, which consist of a series of microphones on the outside of the building capturing the sound of omnidirectional speakers inside the building; it is basically a sound leakage detector (B. Kölsch et al., 2023). This method does not detect thermal bridges, while thermography does; the combination of both can be a promising technology after further research is done.

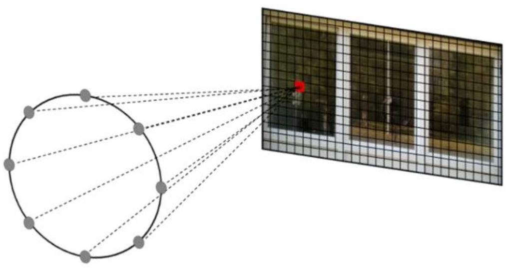

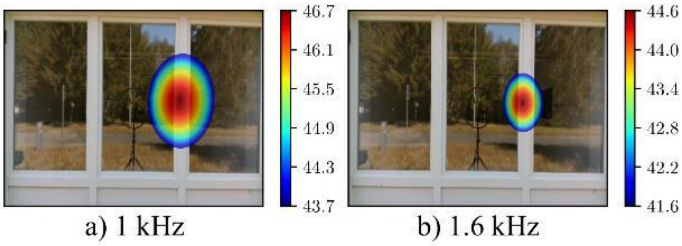

Figure 2.4.7 Scanning process through microphone arrays and the output image (B. Kölsch et al., 2023).

An on-going research (Hargather, 2026) is also focusing on real-time air leakage detection and the objective is to develop a system to optically characterize building envelope air leakage; the background of the technology uses different refraction indices of a transparent fluid via the distortion of the background pattern. In air, this technique allows the direct visualization of plumes with an air density or temperature different from the ambient (Figure 2.4.8).

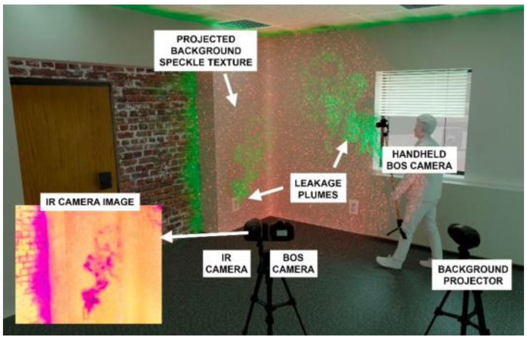

Figure 2.4.8. Air Leakage Visualizer (ALV) system (Hargather, 2026).

As technology advances, new methods for detecting air leakage may become available; it is important to emphasize, however, that it is not possible to build a flawless assembly which remains this way for the lifespan of the building. Hence, controlling indoor relative humidity and keeping the exterior sheathing above the dew point of the indoor air will always be a good strategy when possible.

2.4.2 References

ASHRAE. (2017). *ASHRAE Handbook of fundamentals*. American Society of Heating, Refrigerating and Air-Conditioning Engineers, Inc.

Bomberg, M., & Brown, W. C. (1993). Building envelope: heat, air and moisture interactions. *Journal of Thermal Insulation and Building Envelopes*, *16*(April), 306–311. https://doi.org/https://doi.org/10.1177%2F109719639301600402

Bomberg, M., & Onysko, D. (2002). Heat, Air and Moisture Control in the Historic Basis for Current Practices. *Journal of Thermal Envelope and Building Science*, *26*(1), 3–31. https://doi.org/10.1106/109719602025857

Brown, W. C., Lawton, M., Poirier, G. ., & Di Lenardo, B. (1998). An Evaluation guide for performance assessment of air barrier systems. *Thermal Performance of the Exterior Envelopes of Whole Buildings VII International Conference*, 773–780.

Bunkholt, N. S., Rüther, P., Gullbrekken, L., & Geving, S. (2021). Effect of forced convection on the hygrothermal performance of a wood frame wall with wood fibre insulation. *Building and Environment*, *195*(March). https://doi.org/10.1016/j.buildenv.2021.107748

Chown, G. ., & Mukhopadhyaya, P. (2005). NBC 9.25.1.2: The on-going development of building code requirements to address low air and vapour permeance materials. *10th Canadian Conference on Building Science and Technology "Building Science and the Integrated Design Process,"* 45–58. https://nrc-publications.canada.ca/eng/view/object/?id=1b3c3eda-1374-42bc-b20c-d031912b7d41

CMHC. (1992). *Moisture in Canadian Wood-Frame House Construction: Problems, Research and Practice*.

Defo, M., & Lacasse, M. A. (2020). Resilience of Canadian homes and small buildings to the effects of climate change - Risk of deterioration due to condensation within wall assemblies. *E3S Web of Conferences*, *172*, 1–10. https://doi.org/10.1051/e3sconf/202017202002

Desmarais, G., Derome, D., & Fazio, P. (2000). Mapping of Air Leakage in Exterior Wall Assemblies. *Journal of Building Physics*, *24*(2), 132–154. https://doi.org/10.1106/BWH8-9D3J-R939-957E

Garden, G. K. (1965, December). CBD 72 - Control of air leakage is important. *Canadian Building Digest*.

Handegord, G. O. (1960, September). CBD 9 - Vapour barriers in home construction. *Canadian Building Digest*.

Handegord, G. O. (1982). Air Leakage, Ventilation, and Moisture Control in Buildings. In M. Lieff & H. R. Trechsel (Eds.), *Moisture Migration in Buildings, ASTM STP 779* (pp. 223–233). ASTM International.

Hargather, M. (2026). *Real-Time Building Air Leakage Visualizer*. https://www.energy.gov/cmei/buildings/articles/real-time-building-air-leakage-visualizer

Hutcheon, N. B. (1953). Fundamental considerations in the design of exterior walls for buildings - technical report #13. *67th Anjual General and Professional Meeting of the Engineering Institute of Canada*, 1–25.

Hutcheon, N. B. (1963, June). CBD 42 - Humidified buildings. *Canadian Building Digest*.

Hutcheon, N. B. (1989). 40 years of vapor barriers. In H. R. Trechsel & M. Bomberg (Eds.), *ASTM STP 1039 - WaterVapor Transmission Through Building Materials and Systems: Mechanisms and Measuremen* (pp. 5–7). American Society for testing and materials.

Hutcheon, N. B., & Handegord, G. O. (1980). Evolution of the insulated wood-frame wall in Canada. *8th CIB Triennial Congress*, 434–438.

Junginger, M., Defo, M., Moore, T., Lacasse, M. A., & John, V. (2020). Assessment of Moisture Performance of National Building Code Canada Compliant Wall Assemblies under Climate Change. In C. Serrat, J. R. Casas, & V. Gibert (Eds.), *XV DBMC - Current topics and trends on durability of building materials and components*. International Center for Numerical Methods in Engineering (CIMNE). https://doi.org/10.23967/dbmc.2020.012

Kayll, D., Defo, M., Moore, T. V., & Lacasse, M. A. (2020). A Methodology for Assessment of Building Assembly Air Leakage Moisture Response, Condensation Risk, and Expected Durability When Subjected to Projected Future Climate Loads. In C. Serrat, J. R. Casas, & V. Gibert (Eds.), *XV DBMC - Current topics and trends on durability of building materials and components* (pp. 51–58). International Center for Numerical Methods in Engineering (CIMNE).

Kölsch, B., Tiddens, A., Estevam Schmiedt, J., Schiricke, B., & Hoffschmidt, B. (2023). Detection of air leakage in building envelopes using microphone arrays. *41st AIVC/ASHRAE IAQ- 9th TightVent - 7th Venticool Conference*, 9. https://doi.org/10.1520/STP161520180022

Kölsch, P., Zegowitz, A., Nusser, B., Zirkelbach, D., Künzel, H., & Wagner, R. (2016). Airflow through lightweight wall assemblies - influence of size and location of leakages. *Thermal Performance of the Exterior Envelopes of Whole Buildings XIII International Conference*, 459–484.

Kumaran, M. K., & Haysom, J. C. (2000). *Low-Permeance Materials in Building Envelopes* (pp. 1–6). National Research Council Canada.

Latta, J. K. (1976, March). CBD 175: Vapour Barriers: What are they? Are they effective? *Canadian Building Digest*.

NRCC. (2025). *NBCC - National Building Code of Canada*. National Research Council Canada.

Ojanen, T., & Kumaran, K. (1996). Effect of exfiltration on the hygrothermal behaviour of a residential wall assembly: Results from calculations and computer simulations. *Journal of Thermal Envelope and Building Science*, *19*(1), 215–227. https://doi.org/https://doi.org/10.1177/109719639601900303

Ojanen, T., & Kumaran, M. K. (1992). Air Exfiltration and Moisture Accumulation in Residential Wall Cavities. *Thermal Perfomance of the Exterior Envelopes of Buildings V*, 491–500.

Pallin, S., Boudreaux, P., Kehrer, M., Hun, D. E., Jackson, R. K., & Desjarlais, A. O. (2015). *Moisture Durability Assessment of Selected Well-insulated Wall Assemblies (ORNL/TM-2015/645)* (Number December). Oak Ridge National Lab.

Quirouette, R. L. (1989). The air barrier defined. *Building Science Insight ´86*, 1–6.

Rousseau, M. Z. (1984). Control of surface and concealed condensation. *Building Science Insight '83 - Humidity, Condensation and Ventilation in Houses*, 29–40.

Rousseau, M. Z., & Brown, W. C. (1995). Research update on heat, air and moisture flows in exterior walls. *Building Envelope Performance and Durability, IRC Technical Seminar*, 1–7. https://nrc-publications.canada.ca/eng/view/object/?id=3a4773ab-d418-488e-acf2-f73d2f6d2431

Saber, H. (2014). *Report on Properties and Position of Materials in the Building Envelope for Housing and Small Buildings*. National Research Council Canada.

Simpson, A., & O'connor, D. E. (1994). Timber frame wall: Hygrothermal properties and vapour barrier damage. *Building Services Engineering Research & Technology*, *15*(3), 179–184. https://doi.org/10.1177/014362449401500309

Tsongas, G., Burch, D., & Cunningham, M. (1995). A parametric study of wall moisture contents using a revised variable indoor relative humidity version of the "Moist" transient heat and moisture transfer model. *Thermal Performance of the Exterior Envelopes of Whole Buildings VI*, 307–320.

Wilson, A. G., & Garden, G. K. (1965). Moisture accumulation in walls due to air leakage. *RILEM/CIB Symposium - Moisture Problems in Buildings*. https://nrc-publications.canada.ca/eng/view/object/?id=aebbca87-8deb-4f03-9ca9-ba27712f9297

2.5 The Impact of Key Parameters on Wind-Driven Rain in Urban Area

This section should be cited as:

Gholamalipour, P. (2026). The impact of key parameters on wind-driven rain in urban area. In: A Systematic Review of Passive Energy Conservation Measures and Probabilistic Assessment under Changing Climate in Urban Settings, CIB W040 Report, CIB General Secretariat.

2.5.1 The impact of WDR on building performance

Wind-driven rain (WDR), defined as the combined action of wind and rainfall, is a critical environmental loading on building facades. It is recognized as one of the most important moisture sources affecting facades, roofs, and other exterior components of the wall assemblies. WDR exposure can result in a variety of problems, including water penetration through cracks and joints, frost damage, salt efflorescence, and degradation of facade materials (Erkal et al., 2012). Previous studies highlight the severity of WDR-related damages. In Vancouver, repair costs from rain penetration in the 1990s were estimated at nearly one billion Canadian dollars (Kayll, 2001). In the UK and Australia, about half of facades built in the mid-1980s experienced rain leakage, with one-third deteriorating before reaching their expected service life (Matthews et al., 1996). Beyond durability issues, WDR also influences building energy performance and indoor comfort, since uncontrolled moisture entrance may compromise insulation effectiveness and increase heating (e.g. 18.7%) or cooling demands (S. Yu et al., 2023). Moreover, moisture accumulation caused by WDR can create favorable conditions for mold growth within building envelopes, which may deteriorate indoor air quality and pose potential health risks to occupants (Abuku et al., 2009). For example, hygrothermal simulations showed that rain exposure increased the moisture content of exterior wood fiberboard from about 3% to 52% depending on the cladding material, highlighting the strong influence of WDR on envelope moisture conditions and associated mold growth risk (Bastien & Winther-Gaasvig, 2018). Hu et al., (2023) further demonstrated that dynamic WDR absorption significantly affects surface moisture flux and hygrothermal performance, which can exacerbate indoor humidity levels and indirectly promote mold proliferation. Such mold growth can significantly compromise indoor air quality and occupant health. Accurate assessment of WDR is therefore essential not only for designing resilient and durable building envelopes but also for ensuring efficient energy performance and healthy indoor environments.

2.5.2 WDR Classification

The study of wind-driven rain can be viewed from two main perspectives, as shown in Figure 2.5.1 (Gholamalipour et al., 2022). The first addresses WDR impinging on the facade, where it is considered an external WDR load. This perspective emphasizes the amount and distribution of rainfall droplets deposited on building surfaces, governed primarily by meteorological and geometrical parameters. The second perspective focuses on the response of the facade to WDR impinging, which depends on the building facade characteristics (Blocken & Carmeliet, 2004). In this case, several phenomena are considered such as splashing, bouncing, adhesion, spreading, absorption, evaporation, film formation, and runoff. Together, these perspectives provide a comprehensive understanding of both the exposure of facades to WDR and their behavior under this WDR loading.

Figure 2.5.1 shows that the WDR load on a building facade is controlled primarily by two groups of influential parameters. 1) Meteorological parameters: approaching wind speed, wind direction (angle of incidence), and rainfall intensity/raindrop-size distribution. 2) Geometrical parameters: building configuration (stand-alone, street canyon, building-array, urban area), building shape/size/height, facade details (overhangs, balconies, recesses) and roof form.

As highlighted in a recent review (Gholamalipour et al., 2022), building configuration has been identified as the most influential parameter affecting WDR distribution, as it strongly governs both the pattern and magnitude of rain deposition. Approximately 70% of WDR studies since 2000 have focused on stand-alone (isolated) buildings. In contrast, only a small fraction of research (around 8 - 13%) has addressed more complex configurations, including street canyons (Gholamalipour et al., 2024b; Kubilay et al., 2015), building arrays (Kubilay et al., 2014a, 2014b; H. Yu, Zhang, & Feng, 2025; H. Yu & Zhang, 2025), and urban areas (Ge, 2015; Gholamalipour et al., 2024a). This limited coverage emphasizes the need for further investigation of WDR in complex urban settings, where surrounding buildings vary in size and arrangement around.

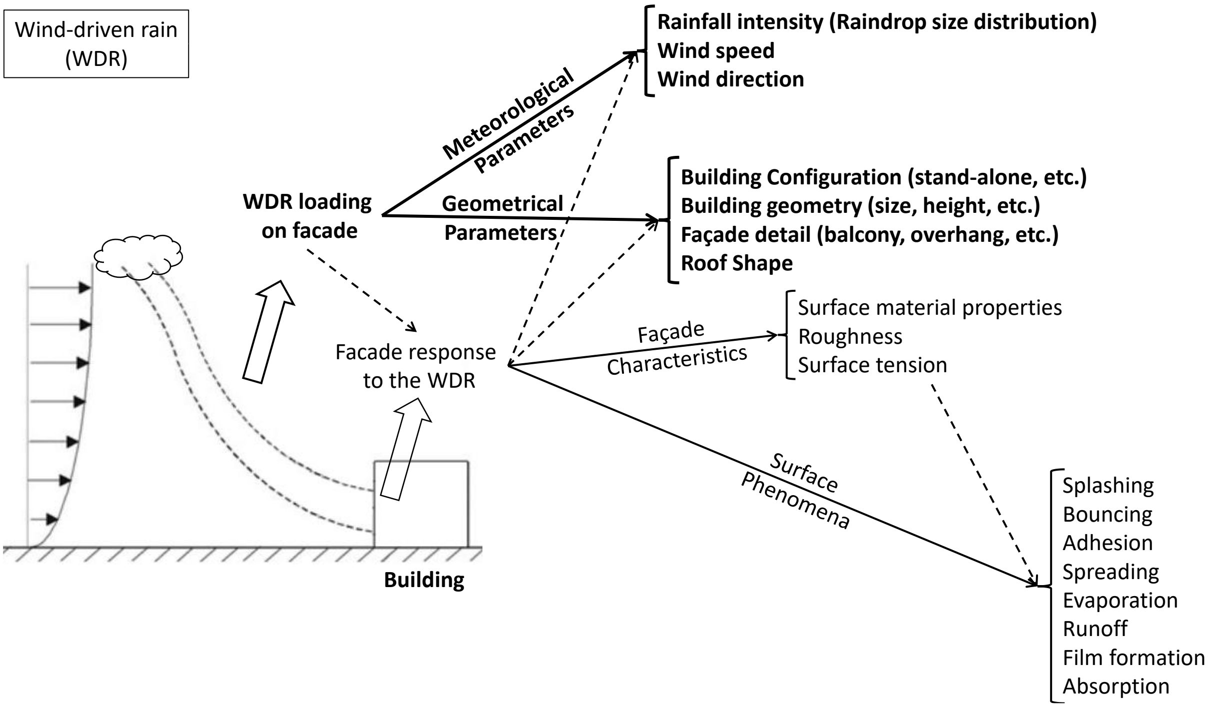

Figure 2.5.1 Overview of WDR studies and key influential parameters (Gholamalipour et al., 2022)

2.5.3 Key parameters on WDR

2.5.3.1 Impact of meteorological parameters

WDR on facades is influenced by meteorological factors such as rainfall intensity, wind speed, and wind direction. In meteorology, rainfall intensity (denoted by Rh in the following text) directly impact on the raindrop size distribution, with higher intensities corresponding to a wider range of raindrop sizes. The catch ratio, a common metric for WDR deposition, is defined as the spatial distribution of the ratio of total WDR on a surface to the total horizontal rainfall.

Figure 2.5.2b shows that catch ratios have only slight variations for rainfall intensities between 2 and 10 mm/h along the central vertical line of a windward facade of a model building (at the building height, H = 10 m, U_{10} = 5 m/s). Similar trends have been reported by Blocken and Carmeliet (2006). Figure 2.5.2c and 2.5.2d show the effects of wind speed at 10 meters height (denoted by U_{10}) and wind direction on WDR loading of the windward facade (H = 10 m). As shown in Figure 2.5.2c, catch ratio values along the central vertical line of the windward facade can increase by up to 100% when wind speed rises from 2 m/s to 10 m/s (Rh = 5 mm/h). Thus, increasing upstream wind speed significantly raises WDR deposition. Regarding the impact of wind direction of WDR, Figure 2.5.2d shows the highest catch ratios occur when the wind is perpendicular to the facade (θ = 0°), while values decrease significantly as the incident angle increases, a trend that continues for angles beyond 45° (Blocken & Carmeliet, 2000; Foroushani et al., 2014).

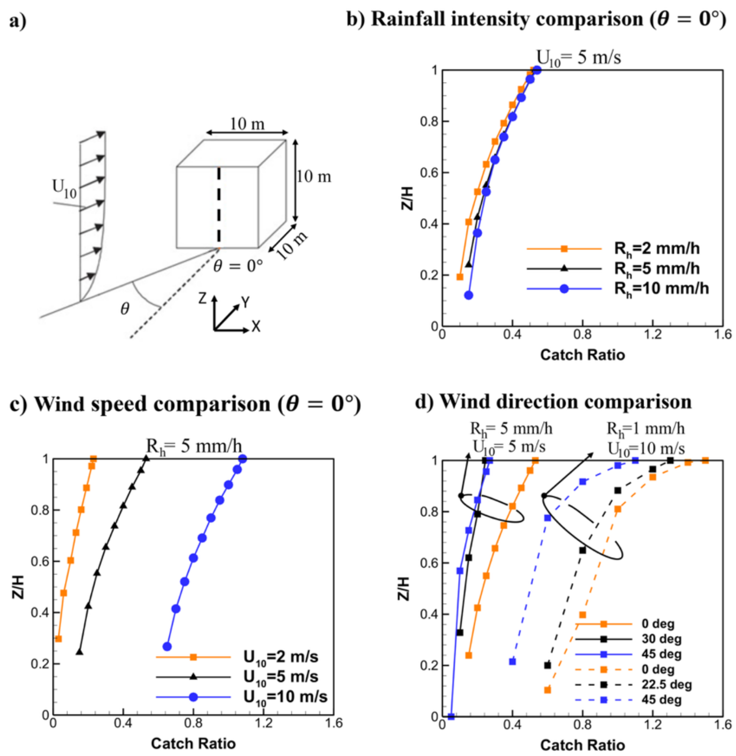

Figure 2.5.2 Catch ratio variation along the vertical dashed line at the center of the windward facade of a 10 m × 10 m × 10 m building. a) Geometry and coordinate system, b) Effect of rainfall intensity, R_h, for θ = 0° and U_{10} = 5 m/s, c) Effect of wind speed, U_{10}, for R_h = 5 mm/h and θ = 0°, and d) Effect of wind direction, θ. for two different dataset (R_h = 5 mm/h, U_{10} = 5 m/s), and (R_h = 1 mm/h, U_{10} = 10 m/s). Here, R_h is rainfall intensity, U_{10} is wind speed at 10 m height, Z is vertical facade height, and H is building height. (based on (Blocken & Carmeliet, 2000; Foroushani et al., 2014; Gholamalipour et al., 2022))

2.5.3.2 Impact of geometrical parameters

Differences in WDR distribution are primarily driven by the wind flow fields formed around different building configurations. Due to the acceleration of wind over buildings' roof, higher catch ratios are typically observed near the upper portion of the windward facade. In contrast, vortices forming in front of and between buildings reduce WDR on the middle and lower parts of the façade (H. Yu & Zhang, 2025). Figure 2.5.3 shows the four primary configurations: stand-alone, street canyon, building-array, and urban area. Buildings geometry plays a major role in shaping WDR distribution, particularly through wind-blocking effects, where taller or wider buildings reduce upstream wind speed and consequently receive lower WDR amounts, while low-rise buildings may experience higher WDR due to weaker wind-blocking (Blocken & Carmeliet, 2006). In the other three configurations, WDR loading is strongly influenced by upstream buildings, whose presence may increase, decrease, or have a neutral effect on the distribution across different portions of the downstream building facade.

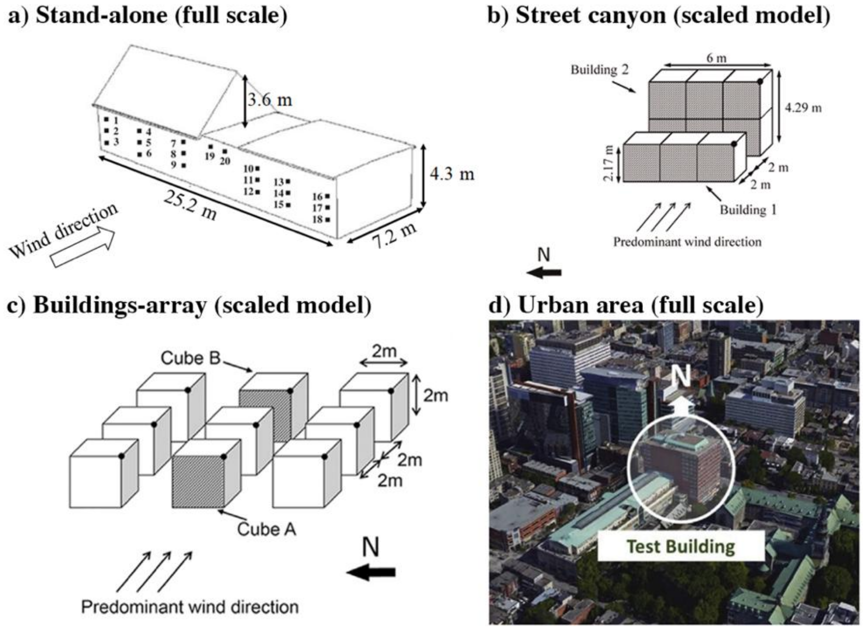

Figure 2.5.3 Building configurations a) stand-alone (Blocken & Carmeliet, 2007) b) street canyon (Kubilay et al., 2015) c) buildings-arrays (Kubilay et al., 2014a), and d) urban area (Ge, Deb Nath, et al., 2017)

A recent CFD-based study by Gholamalipour et al. (2024b) investigated 12 configurations to assess the impact of upstream buildings. These analyses focus on perpendicular wind direction, in which the windward facade experiences the highest WDR. To quantify this effect, the Obstruction Factor is defined as:

$$O\ [-] = \frac{\eta_{Presence\ of\ upstream\ buildings}}{\eta_{Stand-alone}} \tag{2.5.1}$$

where η denotes the catch ratio on the windward facade of the downstream building. This factor compares WDR loads in the presence of upstream buildings against those of a stand-alone case. As an example, Figure 2.5.4 shows the effect of upstream building height on wind velocity and Obstruction Factor. In Figure 2.5.4a and d (lower upstream building), the upstream height accelerates the flow, creating a high-velocity region (U/U_H = 0.8 [-]) near the windward facade of the downstream building, especially near the roofline. Here, U represents the local wind speed and U_H the reference wind speed at the building height. This corresponds with a strong red-zone (O > 1 [-]) in the Obstruction Factor, indicating higher WDR loading. In Figure. 2.5.4b and e (same building height), the flow pattern resembles a typical street canyon, with a low-velocity wake (U/U_H = 0.1 [-]) behind the upstream building, which result in an Obstruction Factor that gradually increases with height, reaching O = 1 [-] near the roof edge. In Figure2.5.4c and f (higher upstream building), the downstream building is fully immersed in the upstream wake, resulting in uniformly low velocities (U/U_H = 0.1 [-]) across the windward facade, and the Obstruction Factor remains nearly zero, showing a strong shielding effect. Overall, these cases highlight the critical role of relative upstream–downstream height differences in shaping wind flow and WDR deposition.

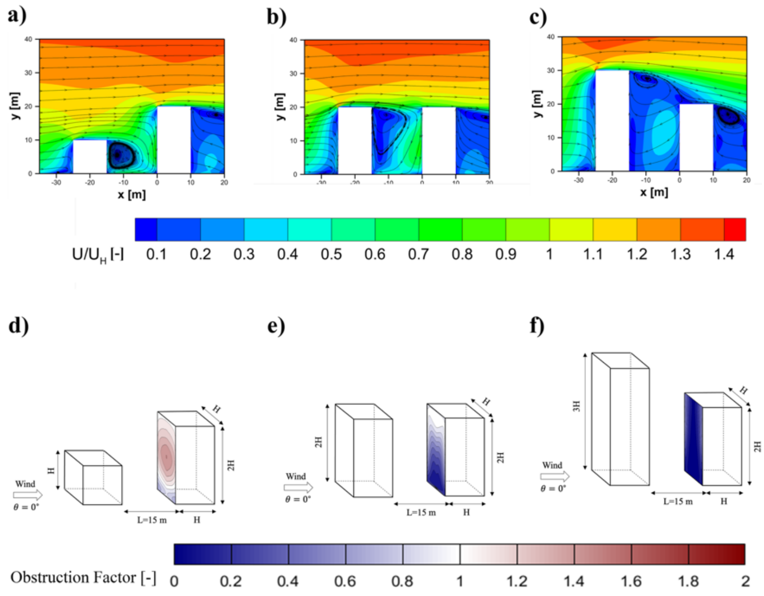

Figure 2.5.4 Normalized mean velocity, U/U_H [−], contours and streamlines along vertical mid-plane (z/H = 0.0) and, d - f) Obstruction Factor, O [−], contours (obtain from CFD for 3 different building configurations, for Rh = 1 [mm/h], U_H = 5 [m/s], and $\theta = 0°$) (Gholamalipour et al., 2024b)

Table 2.5.1 summarizes the findings, highlighting how upstream buildings change WDR loading, specifically on the top 20% of the facade, where deposition is most occurred. It is also found that the meteorological parameters such as wind speed and rainfall intensity have limited influence on the top 20% of the facade. Moreover, Gholamalipour et al. (2024b) findings show that when multiple upstream buildings exist, only the nearest one significantly affects WDR loading. These insights provide a useful foundation for extending WDR assessment to more complex configurations such as building arrays and urban areas.

Moreover, the overhang is the next most important geometrical parameters influencing WDR deposition after building configuration, as it creates a sheltering effect that reduces rain exposure on the upper facade, with its impact varying based on depth, wind conditions, and rainfall intensity (Ge, Chiu, et al., 2017; Gholamalipour et al., 2025).

Table 2.5.1 Obstruction Factor on top 20% of the windward facade of the downstream building based on CFD (Gholamalipour et al., 2024b)

Building configuration	**Obstruction Factor, O [-]**
Same building height ($H_U = H_D$)	$0.9 < O < 1.1$
Higher upstream building height ($H_U > H_D$)	$O \approx 0\ (L \leq H_D)$ $O \approx 1\ (L \gg H_D)$
Lower upstream building height ($H_U < H_D$)	$O > 1\ (L \leq H_D)$ $O \approx 1\ (L \gg H_D)$
Wide street canyon ($H_U = H_D < W$)	$0.6 < O < 1.25$

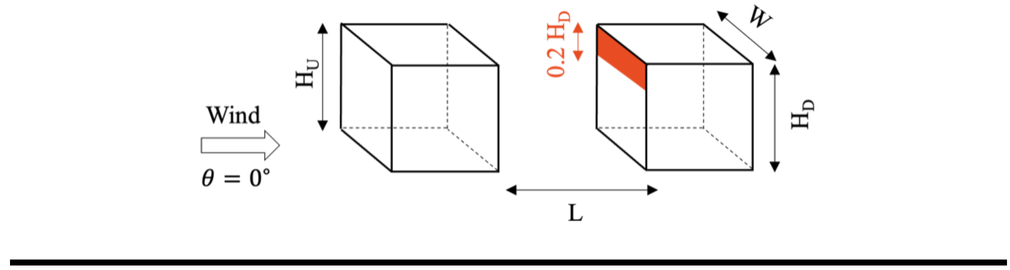

2.5.4 knowledge gaps and future work

Refinement of semi-empirical models: Semi-empirical models such as ISO remain widely used in design practice due to their simplicity. Although, there several studies highlighting the ISO model limitations and proposed refined Obstruction and Wall Factors, Future work could extend this by improving other empirical coefficients, such as Roughness and Topography. This would enhance the practical applicability of semi-empirical models without sacrificing accuracy.

Expansion of data-driven WDR modeling: Exploring ML models and architectures using hybrid CFD-ML approach could improve WDR predictions and provide insights into the rain deposition on facades.

Extreme rainfall and high wind-speed events: Field measurements during severe weather events are scarce due to logistical challenges, yet these conditions can significantly impact building envelope performance. Future studies should focus on capturing and modeling high wind-speed rainfall events, both experimentally and numerically, to better understand their influence on WDR loads. Such research would support the design of resilient building envelopes under extreme climatic conditions.

These directions aim to enhance the accuracy, applicability, and physical understanding of WDR prediction methods for resilient building design.

2.5.5 Reference

Abuku, M., Janssen, H., & Roels, S. (2009). Impact of wind-driven rain on historic brick wall buildings in a moderately cold and humid climate: Numerical analyses of mould growth risk, indoor climate and energy consumption. Energy and Buildings, 41(1), 101–110. https://doi.org/10.1016/j.enbuild.2008.07.011

Bastien, D., & Winther-Gaasvig, M. (2018). Influence of driving rain and vapour diffusion on the hygrothermal performance of a hygroscopic and permeable building envelope. Energy, 164(46), 288–297. https://doi.org/10.1016/j.energy.2018.07.195

Blocken, B., & Carmeliet, J. (2000). Driving rain on building envelopes-I. Numerical estimation and full-scale experimental verification. Journal of Thermal Envelope and Building Science, 24(1), 61–85.

Blocken, B., & Carmeliet, J. (2004). A review of wind-driven rain research in building science. Journal of Wind Engineering and Industrial Aerodynamics, 92, 1079–1130. https://doi.org/10.1016/j.jweia.2004.06.003

Blocken, B., & Carmeliet, J. (2006). The influence of the wind-blocking effect by a building on its wind-driven rain exposure. Journal of Wind Engineering and Industrial Aerodynamics, 94(2), 101–127. https://doi.org/10.1016/j.jweia.2005.11.001

Blocken, B., & Carmeliet, J. (2007). Validation of CFD simulations of wind-driven rain on a low-rise building facade. Building and Environment, 42(7), 2530–2548. https://doi.org/10.1016/j.buildenv.2006.07.032

Erkal, A., D'Ayala, D., & Sequeira, L. (2012). Assessment of wind-driven rain impact, related surface erosion and surface strength reduction of historic building materials. Building and Environment, 57, 336–348. https://doi.org/10.1016/j.buildenv.2012.05.004

Foroushani, S. S. M., Ge, H., & Naylor, D. (2014). Effects of roof overhangs on wind-driven rain wetting of a low-rise cubic building: A numerical study. Journal of Wind Engineering and Industrial Aerodynamics, 125, 38–51. https://doi.org/10.1016/j.jweia.2013.10.007

Ge, H. (2015). Influence of time resolution and averaging techniques of meteorological data on the estimation of wind-driven rain load on building facades for Canadian climates. Journal of Wind Engineering and Industrial Aerodynamics, 143, 50–61. https://doi.org/10.1016/j.jweia.2015.04.019

Ge, H., Chiu, V., & Stathopoulos, T. (2017). Effect of overhang on wind-driven rain wetting of facades on a mid- rise building : Field measurements. Building and Environment, 118, 234–250. https://doi.org/10.1016/j.buildenv.2017.03.034

Ge, H., Deb Nath, U. K., & Chiu, V. (2017). Field measurements of wind-driven rain on mid-and high-rise buildings in three Canadian regions. Building and Environment, 116, 228–245. https://doi.org/10.1016/j.buildenv.2017.02.016

Gholamalipour, P., Ge, H., & Stathopoulos, T. (2022). Wind-driven rain (WDR) loading on building facades: A state-of-the-art review. Building and Environment, 221, 109314. https://doi.org/10.1016/j.buildenv.2022.109314

Gholamalipour, P., Ge, H., & Stathopoulos, T. (2024a). CFD modeling of Wind-Driven Rain (WDR) on a mid-rise building in an urban area. Journal of Wind Engineering and Industrial Aerodynamics, 245. https://doi.org/10.1016/j.jweia.2023.105637

Gholamalipour, P., Ge, H., & Stathopoulos, T. (2024b). Impact of upstream buildings on Wind-Driven Rain Loading: Refining Obstruction Factor in ISO semi-empirical model based on CFD. Journal of Building Engineering, 97, 110717. https://doi.org/10.1016/J.JOBE.2024.110717

Gholamalipour, P., Stathopoulos, T., & Ge, H. (2025). Refined ISO model for Wind-Driven Rain (WDR) on buildings: Machine Learning-based approach. Building and Environment, 113522. https://doi.org/10.1016/j.buildenv.2025.113522

Hu, X., Zhang, H., & Yu, H. (2023). Numerical simulation study on the hygrothermal performance of building exterior walls under dynamic wind-driven rain condition. Building Simulation 2023 17:2, 17(2), 207–221. https://doi.org/10.1007/s12273-023-1076-3

Kayll, D. G. (2001). The role of the building envelope professional in the aftermath of Vancouver's Leaky Condominium Crisis. Thermal Performance of the Exterior Envelopes of Whole Buildings, 1–5.

Kubilay, A., Derome, D., Blocken, B., & Carmeliet, J. (2014a). High-resolution field measurements of wind-driven rain on an array of low-rise cubic buildings. Building and Environment, 78, 1–13. https://doi.org/10.1016/j.buildenv.2014.04.004

Kubilay, A., Derome, D., Blocken, B., & Carmeliet, J. (2014b). Numerical simulations of wind-driven rain on an array of low-rise cubic buildings and validation by field measurements. Building and Environment, 81, 283–295. https://doi.org/10.1016/J.BUILDENV.2014.07.008

Kubilay, A., Derome, D., Blocken, B., & Carmeliet, J. (2015). Wind-driven rain on two parallel wide buildings: field measurements and CFD simulations. Journal of Wind Engineering and Industrial Aerodynamics, 146, 11–28. https://doi.org/10.1016/j.jweia.2015.07.006

Matthews, R. S., Bury, M. R. C., & Redfearn, D. (1996). Investigation of dynamic water penetration tests for curtain walling. Journal of Wind Engineering and Industrial Aerodynamics, 60(1–3), 1–16. https://doi.org/10.1016/0167-6105(96)00020-7

Yu, H., & Zhang, H. (2025). A new method for predicting wind-driven rain catch ratios on building facades in urban residential areas using machine learning models. Building and Environment, 270, 112467. https://doi.org/10.1016/j.buildenv.2024.112467

Yu, H., Zhang, H., & Feng, C. (2025). Wind-driven rain under typhoon conditions: distribution analysis, semi-empirical model optimization, and predictive model development. Building and Environment, 283(8046), 113394. https://doi.org/10.1016/j.buildenv.2025.113394

Yu, S., Liu, X., Li, Y., He, S., Yao, Y., & Sun, S. (2023). Experimental and numerical simulation study on hygrothermal migration of damaged envelope walls during wind-driven rain. Building and Environment, 243, 110653. https://doi.org/10.1016/J.BUILDENV.2023.110653

3 Passive Cooling and Urban Heat Island

3.1 Green Building Envelope Systems

This section should be cited as:

Convertino, F. (2026). Vegetated building envelope systems. In: A Systematic Review of Passive Energy Conservation Measures and Probabilistic Assessment under Changing Climate in Urban Settings, CIB W040 Report, CIB General Secretariat.

3.1.1 Types of greenery systems for buildings

Greenery systems for buildings can be applied to both the horizontal (or tilted) and vertical components of the envelope and are defined as green roofs and green walls, respectively.

Green roofs are rooftop systems including a growing medium and plants (Vijayaraghavan, 2016). Roof waterproofing, drainage and roots barrier are essential for their proper functioning, duration and to prevent damage. Green roofs can be classified according to the substrate depth and consequent vegetation type as extensive, semi-intensive and intensive (Table 3.1.1, Figure 3.1.1). Extensive green roofs are characterized by a shallow substrate, low-maintenance sedums/grass mixes and light weight. These are mainly used for stormwater retention, biodiversity and insulation. Intensive types have deeper substrate and can support shrubs and small trees. These involve a higher structural load and maintenance requirements. Intensive green roofs are used as accessible roof gardens. In the case of intermediate substrate depth and plant species, green roofs are defined as semi-intensive or hybrid (Kotze et al., 2020).

Table 3.1.1 Main characteristics of extensive and intensive green roofs.

Feature	Extensive	Intensive
Vegetation	Mosses, grasses, herbaceous plants, sedums, creating a carpet and stress tolerant	No restrictions; from small plants to higher trees, as in roof gardens
Substrate depth	≤ 20 cm	≤ 100 cm
Weight	≤ 150 kg m-2, at maximum water capacity	≤ 500 kg m-2, at maximum water capacity
Use	Stormwater management, thermal insulation, fireproofing, pollutant abatement, aesthetic benefits; usually accessible only for maintenance.	Accessible gardens, with multiple specific functions.
Maintenance	Low maintenance, no or sporadic irrigation.	High, as for gardens. Weeding, fertilizing, irrigation and constant maintenance are required.

Green walls or vertical greenery systems can be classified as green façades and living walls (Manso & Castro-Gomes, 2015). Green façades can be direct or indirect, depending on the absence or presence of an air gap between the wall and the greenery (Figure 3.1.1). The plants used can be climbing or cascading, evergreen or deciduous, and rooted at the base, at the top of the façade, or placed at different heights along the façade. In the direct type, the plants are attached directly to the wall, while in the indirect, a supporting structure is needed to assist plants growth. Green façades do not require high technology and high costs and are mainly used for shading and biodiversity purposes. Living walls are modular systems, based on engineered panels, or continuous, based on trays and felt pockets. Both systems are equipped with substrate and irrigation. Living walls feature more advanced technology, allow for denser planting and more design control, but have higher costs and maintenance needs.

3.1.2 Main benefits associated with green envelopes

Greenery systems for buildings can provide several benefits, from different perspectives and on different scales, from the building to the urban level. These can be grouped mainly into environmental, social and economic advantages (Table 3.1.2).

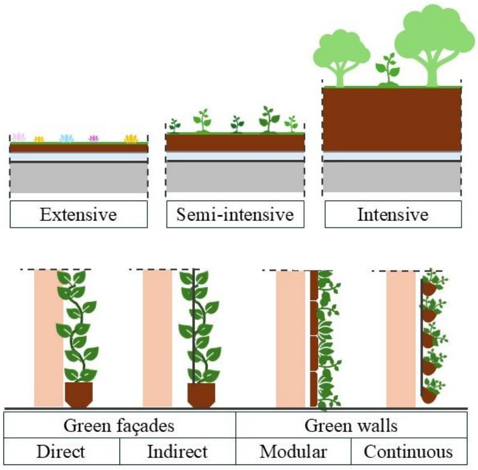

Figure 3.1.1 Schematic representation of green roofs (above) and green walls (below) typologies.

Table 3.1.2 Main benefits derived from greenery systems application.

Category of benefits	**Specific contributions**	
	At urban scale	At building scale
Environmental	Mitigation of the urban heat island effect, improvement of air quality and stormwater management, increase in biodiversity	Increased thermal comfort and energy efficiency, noise insulation
Social	Improvement in the inhabitants' quality of life and health, creation of new natural areas	More user-friendly buildings and access to nature
Economic	Creation of new jobs, expansion of urban agriculture	Increased real estate value, longer lifespan of building components, and reduced fire risk, if well maintained

From a broad environmental perspective, green roofs and walls contribute to building thermal regulation and energy efficiency, by providing surface and air cooling, through shading and evapotranspiration, thus reducing cooling demand, and by providing extra thermal insulation, reducing heating demand (Harbiankova & Manso, 2025). Regarding green roofs, some studies pointed out that, depending on the specific application, they can reduce the maximum daily surface temperature of the roof by an average of 15-25 °C, compared to a bare roof (Peng et al., 2019). In the case of vertical greenery systems, depending on the context, constructive specifications and wall orientation, the temperature reduction of the wall external surface can reach 20 °C (Chen et al., 2013).

Greenery systems, by absorbing and scattering sound, promote noise reduction at the urban level and also inside buildings (Azkorra et al., 2015). Overall, reductions in the range 1-15 dB were found.

Green building envelopes, especially green roofs, also contribute to stormwater management, by retaining rainfall and promoting infiltration and evapotranspiration (Yan et al., 2022).

Available research suggests cumulative runoff retention rates of between 40 and 90%, depending on the context and characteristics of the greenery system (Liu et al., 2022).

The foliage of vegetation on roofs and walls improves air quality both indoors and outdoors by filtering, absorbing and retaining pollutant particles. The positive effects are related to dust and particulate matter reduction, but also to carbon sequestration and indirect CO2 reduction, as a result of reduced air conditioning systems usage and related emissions (Viecco et al., 2021).

A very important environmental contribution is the increase in urban biodiversity, by enhancing native species richness, providing habitat for fauna and creating ecological networks (Tiago et al., 2024).

Greenery systems contribute to physical and psychological wellbeing (Ode Sang et al., 2022). This aspect emerged particularly in the post-pandemic period. The spread of green envelopes in cities, mitigating the urban heat island effect, contributes to the pedestrian thermal comfort and the reduction of heat stress accidents.

Finally, from an economic point of view, greenery can protect building envelope components, such as the waterproofing, protection from solar radiation and temperature fluctuations, thereby extending their lifespan. The improvement in stormwater management decreases the urban drainage load, offering long-term economic benefits. Moreover, green envelopes enhance the architectural quality and property value of buildings.

3.1.3 Green envelopes applications across different climate contexts

Climate is a key parameter, crucial for understanding how green roofs and walls perform and which systems or plants are the most appropriate and viable (Table 3.1.3). Examining different application contexts can help clarify this aspect.

Table 3.1.3. Suitability matrix for greenery systems across climate zones and specific requirements. Green, yellow and red indicate that the system is highly suitable, suitable with design adaptation, and not recommended without major technical measures, respectively.

Climate zone	Green roofs			Green walls	
	Extensive	Semi-intensive	Intensive	Green façades	Living walls
Arid (hot, dry, scarce rain)	Drought-tolerant species or irrigation	Drought-tolerant species or irrigation	High irrigation	Drought-tolerant species	Proper irrigation systems, UV-resistant panels
Tropical/Sub-tropical (hot, humid, heavy rain)	Fungal growth control	Reinforced structure	Optimal drainage, reinforced structure	Corrosion resistant structures, ventilation gap	Irrigation, resistant structures, moisture membrane
Mediterranean/Semi-arid (hot dry summer, mild winter)	Drought-tolerant species	Drought-tolerant species, seasonal irrigation	Irrigation	Drought-tolerant species	Proper irrigation systems

Temperate/Oceanic (mild weather, moderate rain)	No particular issues	No particular issues	No particular issues	No particular issues	No particular issues
Cold/Continental (long winter, low temperature, snow)	Cold-hardy species	Cold-hardy species	Snow load design	Cold-hardy species	Cold-hardy species, anti-freezing measures

In arid climates, the main problem is extreme heat and scarce rainfall, so when installing green roofs and walls, the irrigation management is crucial, possibly considering the grey water reuse and the stormwater storage, as well as the selection of stress-resistant plant species. Succulents are mainly grown on roofs, while drought-tolerant climbing native and vines plants are generally used for vertical applications. Indoor vertical solutions may be more appropriate. If well irrigated, greenery systems provide benefits in terms of significant reduction of roof and wall surface temperatures and of mean radiant temperature (El Menchawy et al., 2025).

In tropical and subtropical areas, characterized by a hot, very humid climate with intense and frequent precipitation, there is no problem with plant growth and survival, in fact vegetation grows rapidly. In this context, it is recommended to use local species, and the main issues concern the vegetation and structures maintenance, which must be frequent. The vegetation most commonly applied on roofs includes species of Portulacaceae (es. Portulaca grandiflora) and Commelinaceae (es. Tradescantia spathacea). For vegetating walls, species of Ficus or of the Araceae family, like Epipremnum aureum, are often used. The main advantages of greenery application are related to shading and evapotranspiration, leading to indoor air and surface temperature reduction and consequent energy saving (Zhang et al., 2022).

Mediterranean and semi-arid climates are characterized by hot, dry summers and mild winters, so the main problem is water scarcity. Consequently, to ensure the survival of vegetation and the proper functioning of greenery systems, it is important to select drought-tolerant species and to set up a good irrigation system and plan. Common plants in these areas are sedum and herbs, for roofs, and climbing plants, such as species of Bougainvillaea, Jasminum, and Lonicera, for walls. Green roofs and walls can reduce surface and air temperatures in summer and improve thermal insulation in winter, thus providing energy saving in both warm and cold seasons (Vox et al., 2022).

In temperate and oceanic climate areas, with mild temperatures and moderate rainfall, greenery systems can be easily managed, with limited irrigation. Vegetation, especially in the case of green roofs, can significantly contribute to stormwater retention. At the same time, greenery systems contribute to surface cooling, heat transfer reduction and urban heat island mitigation (Ouldboukhitine et al., 2025). A variety of plants can be used in these contexts, including several species of Crassulaceae and Lamiaceae for roofs, and Vitaceae (as Parthenocissus tricuspidata) and Araliaceae (as Hedera helix) for vertical applications.

Cold and continental climates are characterized by harsh winters, heavy snowfall, and short growing seasons. In these extreme conditions, plant survival is the main concern, thus cold-hardy species and eventually frost protection must be used. Some sedum species are applied on roofs, and both perennial and deciduous plants, such as Vinca minor and Parthenocissus quinquefolia, are grown in vertical systems. Low-tech and resilient systems are the preferred ones. The main positive effect in this climate is related to additional thermal insulation and, consequently, winter energy efficiency (Collins et al., 2017). Snow cover on intensive green roofs is particularly critical, as snow accumulation adds a significant load to an already heavy system. The roof structure design must avoid any risk of structural damage or deformation. Furthermore, it is important to keep in mind that snow cover reduces the thermal benefits of green roofs compared to bare roofs.

Overall, there are some general design considerations to take into account for applying greenery in any climate. As for vegetation, the best strategy is to use native, region-specific species, due to their resilience, possibly mixing them. Regarding water, rainwater harvesting is a very effective strategy as the use of soil moisture sensors to optimize irrigation. The necessary structural requirements include a proper load-bearing structure, a drainage system, and a root barrier.

3.1.4 Main risk factors influencing green envelope effectiveness

Green envelopes must be carefully applied, considering many issues that may compromise their effectiveness, or posing risks.

From an engineering (design and construction) perspective, the main risks are related to the additional weight of the greenery. This could cause structural failure if the building cannot support it, especially in saturated conditions. Another relevant issue is related to water, as inadequate waterproofing or drainage can cause leaks, water pooling or root rot. This happened, for example, in February 2011, at the Aquascape headquarters (St. Charles, Illinois, USA) having a large green roof with native Illinois plants. After a heavy snowstorm, followed by freeze-thaw cycles, the roof drainage overwhelmed, became clogged, water accumulated, causing part of the roof to collapse. This is a clear case of inadequate drainage design for extreme weather conditions. Water problems can also be a consequence of missing or damaged root barriers. Roots can penetrate the system layers, causing leaks and even structural issues. In addition, systems could be ineffective and short-lived if the substrate layer is not of proper depth or composition and if wrong vegetation is selected. These risks can be mitigated following strategies based on careful structural assessments, proper layers design and selection of high-quality materials (Shafique et al., 2018).

Closely related are issues of maintenance and management (Tabatabaee et al., 2022). Structural risks may arise if the necessary maintenance activities are not properly and periodically carried out on the green system and, particularly, on the supporting structures. Maintenance problems are often due to the difficulty of carrying out activities because of limited accessibility to roofs and walls. Vegetation issues could mainly result from inadequate watering. Insufficient irrigation could be responsible for plant stress and mortality, especially in dry seasons. Over-watering could cause waterlogging, nutrient leaching and possible structural damage. In this regard, the case of Paradise Park Children’s Centre, in London (UK) is significant. The building was equipped with a large vertical garden in 2009, and after only three years, the installation deteriorated due to irrigation system issues and inadequate maintenance (Terblanche, 2025). Vegetation can be also stressed by weeds and pests, with serious harm and risks to its survival. An efficient monitoring system could be an effective way to address these issues. In addition, implementing a scheduled maintenance plan, providing safe access for staff and including automation are crucial to avoid or, at least, reduce risks.

Environmental and climate conditions are crucial factors for green evelopes performance and, indeed, for their durability. Extreme weather conditions, such as drought, heavy rainfall, hail and strong winds can cause damage to plants and structures. Too high or too low temperatures, excessive or insufficient solar radiation could stress vegetation, especially if inappropriate species are used. And dry vegetation can become a fire hazard, especially in arid climates (Bielawski et al., 2024). There are some documented real cases of fire propagation in buildings equipped with greenery. For example, this happened in a block of flats in Ealing (London, UK) on August 5, 2018. A fire destroyed a living wall and witnesses reported that the fire spread fast due to dry vegetation burning (Kotzen et al., 2023). These risks can be mitigated as well. Choosing the most climate-appropriate species, such as the native ones, is likely the most important strategy. Eventually, the selected plants should also be fire-resistant and maintain adequate moisture levels.

Furthermore, many other application aspects must be considered. Some are biological, as the cited spread of invasive species, pests and disease, but there could be also allergen concerns due to plants release of pollen or other organic volatile compounds. To limit these risks, the proper plant choice and monitoring is very important. Similarly, operational risks are noteworthy. These include insufficient expertise in designing and/or maintaining greenery systems by untrained personnel. At the same time, a lack of long-term planning could compromise the project success, as green solutions require funding and monitoring. Budget constraints pose problems in the construction phase (e.g., the use of cheaper, low-performing materials) and in the following maintenance period. In this regard, the evaluation of the life-cycle-costs, potential savings and cost-benefit analysis can be useful (Manso et al., 2021). There are also issues related to regulatory or compliance gaps. These relate to non-compliance with building codes, fire safety standards, and stormwater management. Verifying local codes and standards is essential as well as integrating firebreaks and following local safety standards.

A summary of the main risks and possible mitigation strategies is provided in Table 3.1.4.

Table 3.1.4. Main risks associated with greenery systems application and related mitigation measures.

Risk category	Specific risk	Mitigation measure
Constructive	Additional weight on structures	Careful structural analysis and consequent adequate design of load-bearing structures
	Waterproofing failure, with roots and water damage	Use of high-performance material layers and periodic monitoring
	Drainage issues	Proper design and regular maintenance

Environmental	Poor performance due to inadequate species selection	Use of local, climate-appropriate plants
	Damages to vegetation and structures due to weather events	Use of resilient species and technical tips, such as windbreaks
	Fire hazard due to dry vegetation	Use of fire-resistant plants, maintain adequate moisture and vegetation care
Maintenance/Operational	Low performance and issues due to low maintenance	Establish a scheduled maintenance plan and guarantee access
	Vegetation death due to design or maintenance issues of irrigation systems	Use of automated irrigation systems provided with sensors
	Difficult to access roofs or walls for maintenance	Careful design including safe access points for maintenance activities
Biological	Pests attack and mold or fungi growth	Regular monitoring, biological pathogens control, air circulation
	Spread of invasive species outside the site, with harm for local ecosystems	Use of native vegetation
	Allergen issues for the occupants due to pollen release	Selection of hypoallergenic species
Economic	Difficulty in covering costs for installation and maintenance	Performing feasibility and cost-benefit analysis before implementation and maintenance plan with related costs

3.1.5 Green building envelopes in urban contexts under changing climate

A noteworthy focus relates to implementation and effects, under changing climate, on larger scale (neighbourhood and city). In recent years, large-scale implementations have been growing, supported by specific urban regulations and development plans. This is the case of the city of Copenhagen (Denmark), where a "Green-roof" policy programme was implemented in 2008. This aimed at promoting the installation of green envelopes to tackle urban environmental challenges and led to a widespread presence of green roofs. The "Skyrise Greenery" initiative was undertaken in Singapore in 2009, leading to the incorporation of greenery into the city landscape in a variety of ways, including green roofs and walls. The same was done in the city of Toronto (Canada) from 2010 to 2025. The "Green roof bylaw" promoted the installation of more than 1200 green roofs across the city, based on evidence that these can deliver significant environmental benefits.

When focusing on the urban scale application of green envelopes, the main considerations related to induced effects derive from modelling and simulation studies rather than real implementations (Ji et al., 2024a). Recent studies are also considering different climate changing scenarios in modelling, thus enabling evaluations of possible future performance. The use of climate projections in urban scale models is important to ensure that green interventions remain effective under warmer and drier future scenarios (Jia et al., 2024). Modelling studies suggest that the effectiveness of green solutions strongly depends on coverage, urban form, climate, and integration with other measures. For example, the average air cooling in neighbourhoods due to green roofs and green walls implementation can reach up to 2 °C, depending on the case (W. Chen et al., 2026). The combination of different types of green envelopes connected by green corridors can provide the greatest benefits. However, the actual situation reveals that such integration and spread are still far from being realized, unless targeted policies are adopted.

3.1.6 Uncertainties influencing performance of buildings with greenery systems

Realizing green envelopes is challenging and many uncertainties characterize their implementation.

In terms of design factors, the first issue is related to the choice of the most suitable engineering green solution. An important choice concerns the substrate properties in terms of depth, density, porosity, and water retention. These affect not only the plant growth and status, but also the thermal resistance and hydrological behaviour of the system (Chabada & Juras, 2025). Construction defects and degradation of building elements over time alter thermal and moisture performance.

Other uncertainties are related to biological and ecological issues. The selection of plant species influences their survival and adaptation to climate conditions and, thus, the life duration of the greenery system. This choice directly effects evapotranspiration and albedo and, therefore, cooling effect and thermal insulation. Seasonal variations in leaf coverage result in alteration in shading, latent cooling and insulation fluctuations (Y. Zhang et al., 2022).

Climate and environmental factors are very relevant variables. Weather variability throughout the year, in terms of solar radiation, air temperature and humidity and rainfall, affects greenery systems metrics and therefore the building performance. Closely related to this issue is that of the climate change projections. Future scenarios may alter the effectiveness of green roofs and green walls. In urban contexts, another uncertainty factor is the urban microclimate and its variability. Specifically, wind patterns, shading, and surrounding albedo, variable across cities and even neighbourhoods, influence localized performance.

Operational and maintenance uncertainties relate to irrigation management (de Oliveira Santos et al., 2024). Maintenance and good status of the green envelopes are essential for long-term performance and effectiveness.

Last but not least, a fundamental and critical issue is that of thermal modelling (Blanco & Convertino, 2023). The knowledge of green envelopes physical functioning is necessary for optimizing their design and application and for maximizing benefits. Therefore, uncertainties related to this aspect are very relevant. The results strongly depend on the assumed thermal properties, evapotranspiration coefficients and boundary conditions. Simplified models are usually adopted, often neglecting dynamic and microclimate factors. The collection of long-term empirical data, for validating models and evaluating effects could help reducing these uncertainties. However, further research is needed about this.

3.1.7 References

Azkorra, Z., Pérez, G., Coma, J., Cabeza, L. F., Bures, S., Álvaro, J. E., Erkoreka, A., & Urrestarazu, M. (2015). Evaluation of green walls as a passive acoustic insulation system for buildings. Applied Acoustics, 89, 46–56. https://doi.org/10.1016/J.APACOUST.2014.09.010

Bielawski, J., Papis, B. K., Krajewski, G., & Węgrzyński, W. (2024). An exploratory investigation into moisture content and wind impact on the fire behaviour of modular living walls. Fire Safety Journal, 142, 104024. https://doi.org/10.1016/J.FIRESAF.2023.104024

Blanco, I., & Convertino, F. (2023). Thermal performance of green façades: research trends analysis using a science mapping approach. Sustainability, 15(13), 9981. https://doi.org/10.3390/su15139981

Chabada, M., & Juras, P. (2025). Numerical Study: Substrate Thickness and Type of Roof Structure and Their Impact on the Thermal Behavior of Green Roofs. Buildings 2025, Vol. 15, Page 3240, 15(17), 3240. https://doi.org/10.3390/BUILDINGS15173240

Chen, Q., Li, B., & Liu, X. (2013). An experimental evaluation of the living wall system in hot and humid climate. Energy and Buildings, 61, 298–307. https://doi.org/10.1016/j.enbuild.2013.02.030

Chen, W., Pan, J., Quan, J., Wei, H., & Wang, W. (2026). Scalable impact of urban green infrastructure on urban climate: A critical review. In Renewable and Sustainable Energy Reviews (Vol. 226). Elsevier Ltd. https://doi.org/10.1016/j.rser.2025.116259

Collins, S., Kuoppamäki, K., Kotze, D. J., & Lü, X. (2017). Thermal behavior of green roofs under Nordic winter conditions. Building and Environment, 122, 206–214. https://doi.org/10.1016/J.BUILDENV.2017.06.020

de Oliveira Santos, T. D., Pacheco, F. A. L., & Fernandes, L. F. S. (2024). A systematic analysis on the efficiency and sustainability of green facades and roofs. Science of The Total Environment, 932, 173107. https://doi.org/10.1016/J.SCITOTENV.2024.173107

El Menchawy, A. S., Elkholy, M. A., & Mohamed, A. F. A. (2025). Applying green roof in an educational building in the hot arid zone to achieve thermal comfort. Journal of Umm Al-Qura University for Engineering and Architecture 2025, 1–15. https://doi.org/10.1007/S43995-025-00209-X

Harbiankova, A., & Manso, M. (2025). Integrating green roofs and green walls to enhance buildings thermal performance: A literature review. Building and Environment, 270, 112524. https://doi.org/10.1016/J.BUILDENV.2025.112524

Ji, L., Shu, C., Gaur, A., Wang, L., & Lacasse, M. (2024). A state-of-the-art review of studies on urban green infrastructure for thermal resilient communities. Building and Environment, 257, 111524. https://doi.org/10.1016/J.BUILDENV.2024.111524

Jia, S., Weng, Q., Yoo, C., Xiao, H., & Zhong, Q. (2024). Building energy savings by green roofs and cool roofs in current and future climates. Npj Urban Sustainability 2024 4:1, 4(1), 1–13. https://doi.org/10.1038/s42949-024-00159-8

Kotze, D. J., Kuoppamäki, K., Niemikapee, J., Mesimäki, M., Vaurola, V., & Lehvävirta, S. (2020). A revised terminology for vegetated rooftops based on function and vegetation. Urban Forestry and Urban Greening, 49, 126644. https://doi.org/10.1016/j.ufug.2020.126644

Kotzen, B., Galea, E. R., Mosco, S., Wang, Z., Ewer, J., & Jia, F. (2023). Fire safety risks of external living walls and implications for regulatory guidance in England. Fire Safety Journal, 139(1), 103816. https://doi.org/10.1016/j.firesaf.2023.103816

Liu, W., Engel, B. A., Feng, Q., & Li, R. (2022). Simulating annual runoff retention performance of extensive green roofs: A comparison of four climatic regions in China. Journal of Hydrology, 610, 127871. https://doi.org/10.1016/j.jhydrol.2022.127871

Manso, M., & Castro-Gomes, J. (2015). Green wall systems: A review of their characteristics. Renewable and Sustainable Energy Reviews, 41, 863–871. https://doi.org/10.1016/J.RSER.2014.07.203

Manso, M., Teotónio, I., Silva, C. M., & Cruz, C. O. (2021). Green roof and green wall benefits and costs: A review of the quantitative evidence. Renewable and Sustainable Energy Reviews, 135, 110111. https://doi.org/10.1016/j.rser.2020.110111

Ode Sang, Å., Thorpert, P., & Fransson, A. M. (2022). Planning, Designing, and Managing Green Roofs and Green Walls for Public Health – An Ecosystem Services Approach. Frontiers in Ecology and Evolution, 10, 804500. https://doi.org/10.3389/FEVO.2022.804500/FULL

Ouldboukhitine, S. E., Bakkour, A., Khiati, S., & Belarbi, R. (2025). Modular green walls: A sustainable architectural solution for energy efficiency in oceanic climates. Energy and Buildings, 342, 115850. https://doi.org/10.1016/J.ENBUILD.2025.115850

Peng, L. L. H., Yang, X., He, Y., Hu, Z., Xu, T., Jiang, Z., & Yao, L. (2019). Thermal and energy performance of two distinct green roofs: Temporal pattern and underlying factors in a subtropical climate. Energy and Buildings, 185, 247–258. https://doi.org/10.1016/j.enbuild.2018.12.040

Shafique, M., Kim, R., & Rafiq, M. (2018). Green roof benefits, opportunities and challenges – A review. Renewable and Sustainable Energy Reviews, 90, 757–773. https://doi.org/10.1016/j.rser.2018.04.006

Tabatabaee, S., Ashour, M., Mohandes, S. R., Sadeghi, H., Mahdiyar, A., Hosseini, M. R., & Ismail, S. (2022). Deterrents to the adoption of green walls: a hybrid fuzzy-based approach. Engineering, Construction and Architectural Management, 29(9), 3460–3479. https://doi.org/10.1108/ECAM-04-2021-0286

Terblanche, R. (2025). Incorporating Vegetation into Building Design. In Sustainable Built Environment for People and Society (4). IntechOpen. https://doi.org/10.5772/intechopen.1010089

Tiago, P., Leal, A. I., & Silva, C. M. (2024). Assessing Ecological Gains: A Review of How Arthropods, Bats and Birds Benefit from Green Roofs and Walls. Environments, 11(4), 76. https://doi.org/10.3390/ENVIRONMENTS11040076/S1

Viecco, M., Jorquera, H., Sharma, A., Bustamante, W., Fernando, H. J. S., & Vera, S. (2021). Green roofs and green walls layouts for improved urban air quality by mitigating particulate matter. Building and Environment, 204, 108120. https://doi.org/10.1016/J.BUILDENV.2021.108120

Vijayaraghavan, K. (2016). Green roofs: A critical review on the role of components, benefits, limitations and trends. Renewable and Sustainable Energy Reviews, (57), 740–752. https://doi.org/10.1016/j.rser.2015.12.119

Vox, G., Blanco, I., Convertino, F., & Schettini, E. (2022). Heat transfer reduction in building envelope with green façade system: A year-round balance in Mediterranean climate conditions. Energy and Buildings, 274, 112439. https://doi.org/10.1016/j.enbuild.2022.112439

Yan, J., Zhang, S., Zhang, J., Zhang, S., Zhang, C., Yang, H., Wang, R., & Wei, L. (2022). Stormwater retention performance of green roofs with various configurations in different climatic zones. Journal of Environmental Management, 319, 115447. https://doi.org/10.1016/J.JENVMAN.2022.115447

Zhang, K., Garg, A., Mei, G., Jiang, M., Wang, H., Huang, S., & Gan, L. (2022). Thermal performance and energy consumption analysis of eight types of extensive green roofs in subtropical monsoon climate. Building and Environment, 216, 108982. https://doi.org/10.1016/J.BUILDENV.2022.108982

Zhang, Y., Yang, Y., Zhang, L., Zhao, C., Yan, J., Liu, M., & Zhao, L. (2022). Seasonal variation in leaf area index and its impact on the shading effects of vertical green facades in subtropical areas. Building and Environment, 225, 109629. https://doi.org/10.1016/J.BUILDENV.2022.109629

3.2 Radiative Cooling Technologies

This section should be cited as:

An, J., Yan, D. (2026). Radiative cooling technologies. In: A Systematic Review of Passive Energy Conservation Measures and Probabilistic Assessment under Changing Climate in Urban Settings, CIB W040 Report, CIB General Secretariat.

Daytime radiative cooling (RC) technology has recently attracted growing attention in the building sector due to its passive operation and zero-emission characteristics. The core of this technology lies in the spectral selectivity of materials, which simultaneously exhibit high infrared emittance within the 8–13 μm atmospheric window and high solar reflectance in the 0.3–2.5 μm range (Liu et al., 2024). RC materials reduce daytime solar heat gain by maintaining low solar absorptivity. Moreover, spectrally selective radiative properties play a key role in daytime radiative cooling. High thermal emittance within the atmospheric window enhances radiative heat loss to outer space, while reduced radiative exchange outside the atmospheric window helps reduce radiative coupling with the warmer atmosphere. However, because the atmospheric window is not fully transparent, the cooling effectiveness of this spectral design still depends on atmospheric conditions. Under favourable sky conditions (e.g., clear and dry), decreased atmospheric absorption and reduced downwelling long-wave radiation enhance radiative heat loss to outer space, whereas humid or cloudy conditions weaken radiative cooling performance (Yin et al., 2020). Surface temperature also affects radiative cooling performance because radiative heat emission increases with surface temperature RC materials

3.2.1 RC materials

With the advancement of nanophotonics (manipulation of light at the nanoscale) and metamaterials (artificially structured materials with tailored electromagnetic properties), RC materials have developed rapidly with tailored spectral properties for radiative cooling applications. Static RC materials can be broadly categorized into several representative types based on their underlying design strategies for tailoring radiative properties, including: (i) multilayer photonic structures, (ii) porous polymers, and (iii) particle–polymer composites.

Multilayer photonic structures rely on ordered periodic architectures to achieve spectral selectivity via optical interference and/or photonic bandgap effects, thereby enabling high solar rejection and strong emission within the atmospheric window. Raman et al. (2014) proposed a seven-layer HfO_2/SiO_2 photonic structure that reflects 97% of incident sunlight while selectively emitting within the atmospheric window. In rooftop tests conducted at Stanford University on a clear winter day, with the apparatus tilted 30° towards the south, the radiative cooler achieved an exterior surface temperature 4.9 °C below ambient air temperature under direct sunlight exceeding 850 W/m² and delivered 40.1 W/m² of cooling power at ambient air temperature. Rephaeli et al. (2013) proposed a hybrid photonic crystal design combining a SiO_2/SiC emitter with a TiO_2/MgF_2 reflector on an Ag substrate. Numerical simulations showed that it can achieve a net cooling power exceeding 100 W/m^2 at ambient temperature under AM1.5 global tilt solar illumination (964 W/m^2) in clear-sky conditions. Here, net cooling power is defined as the emitted thermal radiation minus the absorbed heat fluxes, including atmospheric radiation, solar irradiance, and non-radiative heat transfer. Although photonic structures provide the spectral selectivity required for sub-ambient cooling, their practical application at the building scale is limited by high fabrication costs and stringent nanometer-scale manufacturing requirements (Morales-Inzunza et al., 2023; Aili et al., 2024).

Porous polymers are a disordered scattering approach for radiative cooling, where randomly distributed micro-, nano-, or macro-pores enhance broadband solar backscattering at air–polymer interfaces. Meanwhile, the polymer matrix provides high infrared emittance in the atmospheric window; in many porous polymers, this high emittance extends over a broader thermal infrared range beyond the atmospheric window. The air-filled porous network can further lower the effective thermal conductivity relative to the solid polymer matrix, helping reduce conductive heat transfer through the layer. These materials can be implemented either as radiative films or coatings, representing a mature and practical technology well suited for application on building exterior surfaces. Mandal et al. (2018) proposed a passive daytime RC strategy based on hierarchically porous poly(vinylidene fluoride-co-hexafluoropropene) [P(VdF-HFP)] coatings, achieving high solar reflectance (about 0.96) and high infrared emittance (about 0.97) in the atmospheric window. In outdoor tests across different climates, the coating achieved a sub-ambient temperature drop of approximately 6 °C under clear-sky, low-humidity conditions in Phoenix with a peak solar irradiance of approximately 890 W/m^2, and provided a cooling power of about 96 W/m^2 under a solar irradiance of about 750 W/m^2. Zhong et al. (2021) developed a passive daytime RC approach using microfiber-based films with hierarchical hollow and porous structures, achieving a substrate-independent hemispherical solar reflectance of 0.94 and an infrared emittance of 0.94 in the atmospheric window. Under a solar irradiance of 900 W/m^2 in clear-sky outdoor conditions, the film achieved a temperature reduction of around 9 °C and a cooling power of about 85 W/m^2.

Particle–polymer composites (often termed polymer nanocomposites when nano-fillers dominate) are another class of disordered RC materials, where randomly distributed particles embedded in the polymer matrix enhance solar reflectance primarily through Mie scattering introduced by refractive-index contrast between fillers and the polymer matrix. Their performance can be tuned through filler type, size, loading, and dispersion, enabling scalable coating and film-based fabrication. Zhai et al. (2017) developed a scalable glass–polymer hybrid metamaterial consisting of randomly distributed SiO_2 microspheres embedded in a transparent poly(4-methyl-1-pentene) (TPX) matrix, backed by a 200 nm Ag layer. This material exhibited a solar reflectance of 0.96 and an infrared emittance above 0.93 in the atmospheric window, while also exhibiting relatively high infrared emittance over a wider infrared range outside the atmospheric window, albeit at lower levels. In a 72-h outdoor test conducted in Cave Creek, Arizona, under direct sunlight, it achieved an average noontime cooling power of 93 W/m^2 (11:00–14:00), with peak values exceeding 110 W/m^2 at solar irradiance exceeding 900 W/m^2. This metamaterial can be fabricated using scalable manufacturing processes and realized as thin polymer films, suggesting potential for large-area building applications. Zhao et al. (2024)

proposed a scalable superhydrophobic bilayer RC coating, consisting of a TiO_2/acrylic resin bottom layer for solar reflection and a SiO_2/P(VdF-HFP) top layer for superhydrophobicity and enhanced reflection in the solar ultraviolet spectrum (0.3–0.4 µm). The coating achieved a solar reflectance of 0.94 and an infrared emittance of 0.97 in the atmospheric window. In outdoor experiments under direct sunlight, with average solar irradiance exceeding 700 W/m^2, the coating reached temperatures 5.8 °C lower than a commercial white paint used as a reference surface in this experiment, and 2.7 °C below ambient. Recent research has focused on improving the durability (Jiang et al., 2023; Xu et al., 2024), self-cleaning properties (Zhao et al., 2024; Sun et al., 2022), and scalable fabrication (Zhai et al., 2017; Zhao et al., 2024) of RC materials, aiming to facilitate the practical implementation of RC technologies in real-world applications.

Static RC materials are suitable for regions where cooling is the primary requirement. However, the performance of static RC materials is often limited by seasonal trade-offs between cooling and heating demands. To address this limitation, dynamic and tunable RC materials, which respond to thermal (Tang et al., 2021), electrical (Banerjee et al., 2023), mechanical (Wang et al., 2023), and other stimuli, have become an increasingly active research direction due to their wider applicability in diverse climatic conditions. These materials offer enhanced flexibility and adaptability, enabling more effective thermal management across a range of environments. For example, Tang et al. (2021) developed a temperature-adaptive radiative coating that dynamically switches emissivity for all-season thermal regulation, while Wang et al. (2021) demonstrated thermochromic smart windows capable of combining solar modulation with passive radiative cooling. These adaptive systems provide a pathway to mitigate the fundamental trade-off between radiative cooling under warm conditions and unwanted heat loss under cool conditions inherent in static RC materials.

3.2.2 Application of RC in buildings

Although RC materials applied to building exteriors can effectively reduce surface temperatures, their impact on indoor temperature (in free-running buildings) and cooling energy use (in air-conditioned buildings) is governed by a combination of climatic conditions, building characteristics, and operational modes. Among these factors, solar radiation and ambient temperature are the primary drivers, while internal heat gains and envelope properties further influence its effectiveness.

Field experiments have been widely used to evaluate the real-world cooling performance of radiative cooling materials under outdoor conditions. Yi et al. (2021) conducted outdoor experiments using two identical model boxes [1.0 m (L) × 0.6 m (W) × 1.2 m (H)] with and without a transparent radiative cooling film in Ningbo, China, under summer conditions, demonstrating a maximum internal air temperature reduction of 21.6 °C. Yang et al. (2021) further performed outdoor measurements using a small-scale room-simulating device in Nanjing under strong solar irradiation (~860 W/m^2), showing that the RC material reduced the internal air temperature to 44–45 °C, compared with 60.4 °C for conventional materials, while the outdoor air temperature was approximately 50 °C. At a larger scale, Wang et al. (2022) applied a RC film to the roof of a large, air-conditioned commercial warehouse [152 m (L) × 54 m (W) × 11.5 m (H)] with a conventional steel roof in Guangxi, China, and conducted a field experiment under comparable sunny weather conditions. The RC film reduced roof temperature, mitigated indoor thermal stratification, and decreased daily cooling electricity consumption from 449 to 249 kWh (about 44%), equivalent to a cooling-electricity saving of approximately 0.024 kWh/(m²·day) when expressed per unit treated roof area. Yuan et al. (2022) conducted outdoor experiments on a full-scale experimental house [4 m (L) × 3 m (W) × 2.4 m (H)] representing a free-running indoor space in a subtropical climate. The RC-film envelope achieved sustained sub-ambient roof temperatures of 2–9 °C below ambient and indoor air temperature reductions of 2–14 °C. The corresponding area-weighted radiative cooling power over the exposed RC envelope area (including the roof and walls) ranged from 5 to 55 W/m², calculated as the difference between emitted long-wave radiation and the sum of absorbed atmospheric radiation and absorbed solar radiation.

In parallel, simulation studies have been widely used to quantify the building-scale energy impacts of RC under typical meteorological conditions. Fang et al. (2022) evaluated a metamaterial-based RC roof across different International Energy Conservation Code (IECC) climate zones, including Tucson, Arizona (2B, hot-dry), Los Angeles, California (3B, warm-dry), and Orlando, Florida (2A, hot-humid), showing that it can reduce cooling electricity consumption by 113–144 kWh/(m²·yr) per unit roof area modified compared with conventional shingle roofs. Extending the analysis to different building operation modes, Chen et al. (2021) reported that RC roofs can reduce rooftop temperatures by over 30 °C and decrease roof-bottom temperature by up to 13.8 °C in free-running buildings. In the air-conditioned buildings, annual HVAC energy savings of up to 9.3% were achieved, particularly in cooling-dominated climates where reductions in cooling demand outweigh the increase in heating energy demand. Cui et al. (2022) showed that the energy-saving performance of RC varies substantially across climates, with annual cooling-energy savings ranging from 6.8% to 64.3%, corresponding to 21.9–52.7 kWh/(m².yr) based on floor area; in high heat-density buildings, such as telecommunication base stations, cooling demand remained dominant throughout the year because of the large internal heat gains. As a result, cool roofs did not introduce a heating penalty, and the energy savings were primarily driven by reductions in solar heat gain and enhanced heat dissipation through the envelope.

Consistently, Peoples et al. (2022) conducted a comprehensive assessment of the building energy-saving performance of RC across all ASHRAE climate zones. The study considered typical single-story residential buildings with RC applied to all exterior surfaces. They reported annual cooling electricity savings exceeding 12% for typical residential buildings and 7% for high-efficiency residential buildings across all studied ASHRAE climate zones, although the absolute electricity reductions in colder northern climates were comparatively small. Savings in warm climates reached up to 46% and 22% for the typical building and high-efficiency residential buildings, respectively. This trend is further confirmed at the global scale by Wang et al. (2024), who reported annual HVAC energy savings (considering both cooling and heating) in most climates, although increased heating energy demand may occur in colder regions.

These results collectively highlight the strong dependence of RC performance on climatic conditions. RC is most effective in cooling-dominated regions, whereas in heating-dominated climates, increased heating demand may offset or even outweigh its benefits. This seasonal trade-off arises because RC materials absorb less solar radiation than conventional dark surfaces, which reduces cooling demand during warm periods but may increase heating demand during cold periods. Enhanced long-wave heat loss to the sky can further contribute to winter heating penalties. Atmospheric factors further modulate this effect. High humidity and cloud cover reduce atmospheric transparency and weaken long-wave radiative cooling performance, while cloud cover can also reduce incident solar radiation and associated solar heat gains (Chen and Lu, 2021; Bijarniya et al., 2020).

While RC is most effectively applied on roofs because roofs typically receive greater solar radiation and maintain a larger sky view factor for long-wave radiative heat dissipation than vertical facades. However, in high-rise buildings, the energy-saving potential of roof-based RC may be limited because the available roof area becomes small compared with the overall building envelope area. This limitation has motivated the extension of RC applications to building facades. However, compared with roofs, facade performance is more sensitive to shading from surrounding buildings and self-shading architectural elements (e.g., overhangs), as well as to variations in solar radiation with orientation and time of day. Xu et al. (2024) evaluated the application of cool materials (solar reflectance SR=0.80, thermal emittance TE=0.90) and super-cool materials (SR=0.96, TE=0.96) on the roofs and facades of residential buildings in Nanjing, using conventional building surfaces (SR=0.20, TE=0.80) as the reference. The results showed that roof-only application of cool materials reduced annual HVAC energy consumption by about 1.0 %, whereas combining roof and facade applications increased savings to up to 3.4% for cool materials and 4.3% for super-cool materials. Cool-material application on the west, east, and north facades provided annual HVAC energy savings of about 0.55%–0.86%, 0.39%–0.60%, and 0.43%–0.91%, respectively, while application on the south facade provided little or even negative annual HVAC savings because winter heating penalties offset part of the summer cooling savings.

The performance of RC is also strongly influenced by its interaction with other envelope technologies, particularly insulation. In general, increased insulation reduces the effectiveness of RC by limiting heat transfer from the indoor space to the exterior. This trend has been consistently observed across simulation studies for various building types (Cui et al., 2022; Yang et al., 2024; Wang et al., 2024; Zhao et al., 2019), and further confirmed by Feng et al. (2022), who showed that increased insulation may even lead to an increase in overall energy consumption in cooling-dominated climates. Similarly, Tian et al. (2024) showed that RC performs more effectively on roofs with lower thermal resistance, and field experiments by Wang et al. (2025) confirmed that RC coatings enhance heat transfer from indoors to outdoors, particularly in buildings with poorly insulated walls. Li et al. (2025) further demonstrated that the optimal insulation level depends on building operating conditions: reduced insulation is beneficial under high internal heat gains or elevated cooling setpoint temperatures, as it facilitates heat transfer to the exterior, whereas higher insulation becomes advantageous when internal heat gains are low or cooling setpoints are lower, as it helps retain cooling and reduce heat gain. These results suggest that optimizing the thermal performance of the envelope, particularly conductive heat transfer through the envelope, may further improve RC performance.

In addition, phase-change materials (PCM) have been explored as a complementary strategy to enhance RC performance. By absorbing and releasing heat, these materials can mitigate both daytime overheating and night-time overcooling, leading to more stable indoor temperatures. Liu et al. (2024) proposed an RC–PCM composite roof and experimentally compared ordinary roofs (OR), phase-change roofs (PCR), and RC-PCM roofs (RC-PCR) using outdoor test chambers (1 m × 1 m × 1 m) in Ganzhou, China. Under free-running conditions, PCR reduced peak interior underside temperature by 0.5–1.1 °C and peak indoor air temperature by 0.3–0.8 °C compared with OR, whereas RC-PCR achieved reductions of 4.8–5.1 °C in peak roof underside temperature and 2.9–3.7 °C peak indoor air temperature. Compared with the PCM-only roof, the RC–PCM roof increased the estimated reduction in cooling energy consumption from approximately 48–61% to 133–143%, both relative to the OR case. The cooling energy reduction was calculated from the reduction in roof-to-indoor heat flux based on the temperature difference between the interior roof surface and indoor air, indicating a clear synergistic effect between radiative cooling and thermal storage. However, the absence of an RC-only case limits the ability to quantify the individual contribution of radiative cooling. Wang (2025) used EnergyPlus to analyze the annual energy consumption of a single-story building with an RC–PCM roof in Marrakesh, Morocco. Compared with an RC-only roof, the RC-PCM roof reduced annual heating energy consumption by about 15% by mitigating winter overcooling, while slightly weakening the cooling performance of the RC roof due to the thermal storage effect of PCM. Other simulation-based studies (Jiang et al., 2024; Li et al., 2025; Han et al., 2025) conducted across different climate zones have reported similar trends, indicating that PCM can help regulate thermal performance and improve the overall energy performance of RC systems.

3.2.3 Brief summary

As summarized in Table 3.2.1, spectrally selective RC has demonstrated significant advantages in regions or building types dominated by cooling loads. While roof-based systems remain the primary application, spectrally selective RC applied to opaque building facades is attracting increasing attention. Moreover, the interaction between RC and insulation is strongly coupled and depends on building thermal characteristics and operating conditions. In many cooling-dominated cases, the cooling benefits of RC are often more pronounced in poorly insulated envelopes, where reductions in solar heat gains more directly translate into indoor load reduction; in contrast, in well-insulated buildings, the incremental benefit of RC may be reduced. However, the optimal insulation level may still vary depending on factors such as internal heat gains, cooling setpoints, and HVAC operation modes. Beyond insulation interactions, integrating RC with PCMs has been shown to moderate roof and indoor temperature fluctuations by utilizing the latent heat storage capacity of PCMs. These findings highlight the importance of a holistic approach to RC implementation that accounts for both envelope properties and material interactions. RC should therefore be understood as part of an integrated envelope system involving material properties, climatic conditions, and building operation.

These findings highlight several key challenges for the practical implementation of RC technologies, including material scalability and performance stability under real varying environmental conditions. It should also be noted that RC may increase heating energy consumption in buildings, which can limit its applicability and energy-saving potential. As discussed above, dynamic RC systems provide a promising pathway to mitigate overcooling and improve the adaptability of RC technologies under varying environmental conditions.

Table 3.2.1 Summary of thermal and energy performance of RC materials in building applications

Ref.	**Method**	**Climate /Location**	**Building Type**	**RC materials**	**Performance**		
					Surface temperature reduction	**Indoor air temperature reduction**	**Energy impacts compared with baseline**
Wang et al. (2022)	Simulation	Greenville, SC, USA; Cairo, Egypt; Jimma, Ethiopia; Mexico City, Mexico	Large-scale warehouse	Metamaterial-based RC roof ($\rho \approx 0.7$, $\varepsilon \approx 0.85$)	NA	NA	22% (Greenville, SC, USA); 21% (Cairo); 53% (Jimma); 65% (Mexico City) (annual cooling electricity savings)
	Experiment	Guangxi, China (hot summer and warm winter, HSWW)		Metamaterial-based RC roof ($\rho \approx 0.92$, $\varepsilon \approx 0.91$)	Max $\Delta T \approx 20.9$ °C (roof, vs baseline)	$\Delta T = 0.8$ °C (vs baseline, 1.5 m) $\Delta T = 2.7$ °C (vs baseline, 10 m)	44% (daily cooling energy savings)
Yi et al. (2021)	Experiment	Ningbo, China (hot summer and cold winter, HSCW)	Small-scale model boxes	T-RC film on rooftop glass ($\rho \approx 0.6$, $\varepsilon \approx 0.9$)	NA	Max $\Delta T \approx 22$ °C (vs baseline)	NA
	Simulation	Multiple cities, China (HSCW, and HSWW zones)	Exhibition building with roof glazing		NA	$\Delta T =$ 9–12 °C (vs baseline)	41–52% (HSCW); 55–63% (HSWW) (annual cooling electricity savings)
Yuan et al. (2022)	Experiment	Zhejiang, China	Full-scale experimental house	RC film on full envelope ($\rho \approx 0.97$, $\varepsilon \approx 0.93$)	$\Delta T \approx$ 2-9 °C (exterior surface of roof, vs ambient, daytime)	$\Delta T \approx$ 4-12 °C (vs baseline)	NA
Hong et al. (2019)	Simulation	Tucson, AZ, USA; Los Angeles, CA, USA; Orlando, FL, USA	Commercial building	Metamaterial-based RC roof	NA	NA	113-144 kWh/m^2·yr (annual cooling power over the roof-and-wall RC surfaces
Chen and Lu (2021)	Simulation	Harbin, Beijing, Shanghai, Hong Kong, Kunming, China	Simplified mid-size commercial building	Idealized RC roof (varying ρ and ε)	Max $\Delta T \approx$ 29–34 °C (roof, vs baseline, across climates)	NA	0.6% (Harbin); 3.3% (Beijing); 4.1% (Shanghai); 9.3% (Kunming); 7.1% (Hong Kong) (annual HVAC energy savings)
Yang et al. (2021)	Simulation	Nanjing, China	Simplified building	Porous polypropylene-based RC roof ($\rho \approx 0.97$, $\varepsilon \approx$ 0.67–0.81)	NA	Max $\Delta T \approx 3.6$ °C (vs baseline)	~200 W (cooling load reduction on a typical summer day)
	Experiment				NA	$\Delta T \approx$ 15.4–16.4 °C (vs baseline)	NA
Cui et al. (2022)	Simulation	Harbin, Urumqi, Beijing, Guiyang, Kunming, Shanghai, and Guangzhou, China	Telecommunication base station (single-zone, high internal heat)	RC film on roofs and walls ($\rho \approx 0.96$, $\varepsilon \approx 0.95$)	NA	NA	6.8%–64.3%, and 21.9-52.7 kWh/m^2·yr (annual AC electricity, across cities)

Xu et al. (2024)	Simulation	Nanjing, China	Six typical residential neighborhoods	Cool materials (ρ≈0.8, ε≈0.9), and super cool materials (ρ≈0.96, ε ≈ 0.96) on roof and facades	NA	NA	Up to 1% (cool roof only); up to 3.4%/ 4.3% (cool or super cool, roof + façades); lower in high-rise: ~0.2 (cool roof only), and 2% (all cool surfaces) (annual HVAC energy savings)
Peoples et al. (2022)	Simulation	16 U.S. cities (all ASHRAE climate zones)	single-story residential building (typical & high-efficiency)	RC paint on full envelope (ρ ≈ 0.96, ε≈0.92)	NA	NA	>7% (high-efficiency), >12% (typical); up to 22% (high-efficiency) and 46% (typical) in warm climates (annual cooling electricity savings)
Bijarniya et al. (2020)	Simulation	Varanasi (composite), Mumbai (humid), Kolkata (humid), Delhi (composite), Jaisalmer (dry), India	Single-zone AC room	Photonic RC roof (four types)	Max ΔT≈17-21 °C (exterior surface of roof, vs ambient)	NA	≈36% in low-humidity climates (cooling load reduction)
Wang et al. (2024)	Simulation	250 locations worldwide (all ASHRAE climate zones)	Two-floor single-family detached house (low / medium / high U values: 0.3 / 0.5 / 1.0 W/m²/K)	RC coating on full envelope (ρ ≈ 0.96, ε ≈ 0.97)	NA	NA	12–49% (warm climates); <1% (cold climates) (annual HVAC energy savings)

Note: ρ denotes solar reflectance and ε denotes thermal emittance

3.2.4 References

Aili, A., Jiang, T., Chen, J., Wen, Y., Yang, R., Yin, X., & Tan, G. (2024). Passive daytime radiative cooling: Moving beyond materials towards real-world applications. Next Energy, 3, 100121. https://doi.org/10.1016/J.NXENER.2024.100121.

Banerjee, D., Hallberg, T., Chen, S., Kuang, C., Liao, M., Kariis, H., & Jonsson, M. P. (2023). Electrical tuning of radiative cooling at ambient conditions. Cell Reports Physical Science, 4(2), 101274. https://doi.org/10.1016/j.xcrp.2023.101274.

Bijarniya, J. P., Sarkar, J., & Maiti, P. (2020). Environmental effect on the performance of passive daytime photonic radiative cooling and building energy-saving potential. Journal of Cleaner Production, 274, 123119. https://doi.org/10.1016/j.jclepro.2020.123119

Chen, J., & Lu, L. (2021). Comprehensive evaluation of thermal and energy performance of radiative roof cooling in buildings. Journal of Building Engineering, 33, 101631. https://doi.org/10.1016/j.jobe.2020.101631.

Cui, Z. K., Guo, C. Y., & Zhao, D. L. (2022). Energy-saving and economic analysis of passive radiative sky cooling for telecommunication base station in China. Building Simulation, 15(10), 1775–1787. https://doi.org/10.1007/s12273-022-0894-z.

Feng, J., Saliari, M., Gao, K., & Santamouris, M. (2022). On the cooling energy conservation potential of super cool roofs. Energy and Buildings, 264, 112076. https://doi.org/10.1016/j.enbuild.2022.112076

Hong, F., Zhao, D. L., Yuan, J. C., Aili, A., Yin, X. B., Yang, R. G., & Tan, G. (2019). Performance evaluation of a metamaterial-based new cool roof using improved roof thermal transfer value model. Applied Energy, 248, 589–599. https://doi.org/10.1016/j.apenergy.2019.04.116.

Jiang, T., Fan, W., & Wang, F. (2023). Long-lasting self-cleaning daytime radiative cooling paint for building. Colloids and Surfaces A: Physicochemical and Engineering Aspects, 666, 131296. https://doi.org/10.1016/j.colsurfa.2023.131296

Li, H., An, J.J., Wang, C., Yan, D., 2025. Simulation analysis on synergistic energy-saving effect of building envelope insulation and radiative cooling technology. Energy and Buildings, 339, 115759. https://doi.org/10.1016/j.enbuild.2025.115759.

Liu, R., Wang, S., Zhou, Z., Zhang, K., Wang, G., Chen, C., & Long, Y. (2024). Materials in radiative cooling technologies. Advanced Materials, 2401577. https://doi.org/10.1002/ADMA.202401577.

Mandal, J., Fu, Y., Overvig, A. C., Jia, M., Sun, K., Shi, N. N., Zhou, H., Xiao, X., Yu, N., & Yang, Y. (2018). Hierarchically porous polymer coatings for highly efficient passive daytime radiative cooling. Science, 362(6412), 315–319. https://doi.org/10.1126/SCIENCE.AAT9513.

Morales-Inzunza, S., González-Trevizo, M. E., Martínez-Torres, K. E., Luna-León, A., Tamayo-Pérez, U. J., Fernández-Melchor, F., & Santamouris, M. (2023). On the potential of cool materials in the urban heat island context: Scalability challenges and technological setbacks towards building decarbonization. Energy and Buildings, 296, 113330. https://doi.org/10.1016/J.ENBUILD.2023.113330.

Peoples, J., Hung, Y.-W., Fang, Z., Braun, J. E., Horton, W. T., & Ruan, X. (2022). Energy savings of radiative cooling paints applied to residential buildings. International Journal of Heat and Mass Transfer, 194, 123001. https://doi.org/10.1016/j.ijheatmasstransfer.2022.123001

Raman, A. P., Anoma, M. A., Zhu, L., Rephaeli, E., & Fan, S. (2014). Passive radiative cooling below ambient air temperature under direct sunlight. Nature, 515(7528), 540–544. https://doi.org/10.1038/nature13883.

Rephaeli, E., Raman, A., & Fan, S. (2013). Ultrabroadband photonic structures to achieve high-performance daytime radiative cooling. Nano Letters, 13(4), 1457–1461. https://doi.org/10.1021/NL4004283.

Sun, Y., Javed, M., Yi, I., et al. (2022). Design and preparation of flexible double-layered daytime radiative cooling composite film with antifouling property. Solar Energy Materials and Solar Cells, 245, 111836. https://doi.org/10.1016/j.solmat.2022.111836

Tang, K., Dong, K., Li, J., Gordon, M. P., Reichertz, F. G., Kim, H., Rho, Y., Wang, Q., Lin, C.-Y., Grigoropoulos, C. P., Javey, A., Urban, J. J., Yao, J., Levinson, R., & Wu, J. (2021). Temperature-adaptive radiative coating for all-season household thermal regulation. Science, 374(6574), 1504–1509. https://doi.org/10.1126/science.abf7136.

Tian, L., Li, Z., & Zhao, X. (2024). Effect of thermal resistance and infrared transparency on radiative cooling efficiency. Energy and Buildings, 323, 114801. https://doi.org/10.1016/j.enbuild.2024.114801.

Wang, J., Li, Z., Zhou, T., Deng, W., Liang, R., Lun, I. Y.-F., Li, Y., & Bao, R. (2024). Global assessment of radiative cooling and low-emissivity coatings for energy efficiency in buildings across all climate zones. Energy and Buildings, 317, 114402. https://doi.org/10.1016/j.enbuild.2024.114402

Wang, N. S., Lv, Y. Y., Zhao, D. L., Zhao, W. B., Xu, J. T., & Yang, R. G. (2022). Performance evaluation of radiative cooling for commercial-scale warehouse. Materials Today Energy, 24, 100927. https://doi.org/10.1016/j.mtener.2021.100927.

Wang, S., Dong, Y., Li, Y., Ryu, K., Dong, Z., Chen, J., Dai, Z., Ke, Y., Yin, J., & Long, Y. (2023). A solar/radiative cooling dual-regulation smart window based on shape-morphing kirigami structures. Materials Horizons, 10(10), 4243–4250. https://doi.org/10.1039/D3MH00671A.

Wang, S., Jiang, T., Meng, Y., Yang, R., Tan, G., & Long, Y. (2021). Scalable thermochromic smart windows with passive radiative cooling regulation. Science, 374(6574), 1501–1504. https://doi.org/10.1016/j.apenergy.2024.124961

Wang, Z. Y., Wu, X., Qu, M. L., Fan, L. W., Yu, Z. T., Chen, S. Q., Ge, J., Wang, L., & Dai, S. J. (2025). A field test and evaluation of radiative cooling performance as applied on the sidewall surfaces of residential buildings in China, 379, 124961. https://doi.org/10.1016/j.apenergy.2024.124961

Xu, F. S., Tian, D. D., Gao, Z., & Zhang, J. J. (2024). The effects of cool materials, façade orientation, and morphological parameters on energy consumption at the residential neighborhood scale. Building Simulation, 17(4), 525–542. https://doi.org/10.1007/s12273-023-1096-z.

Xu, X., Zhang, H., Kang, X., et al. (2024). High-performance, superhydrophobic, durable photonic structure coating for efficient passive daytime radiative cooling. Materials Today Physics, 48, 101556. https://doi.org/10.1016/j.mtphys.2024.101556

Yang, Y., Zhang, G., & Rong, L. (2024). Assessing energy saving potential of wavelength-dependent passive daytime radiative cooler implemented with EnergyPlus by a roof model. Heliyon, 10(5), e26428. https://doi.org/10.1016/j.heliyon.2024.e26428.

Yang, Z., Sun, H., Xi, Y., et al. (2021). Bio-inspired structure using random, three-dimensional pores in the polymeric matrix for daytime radiative cooling. Solar Energy Materials and Solar Cells, 227, 111101. https://doi.org/10.1016/j.solmat.2021.111101

Yi, Z., Lv, Y., Xu, D., Xu, J., Qian, H., Zhao, D., & Yang, R. (2021). Energy saving analysis of a transparent radiative cooling film for buildings with roof glazing. Energy and Built Environment, 2(2), 214–222. https://doi.org/10.1016/j.enbenv.2020.07.003.

Yin, X., Yang, R., Tan, G., et al. (2020). Terrestrial radiative cooling: Using the cold universe as a renewable and sustainable energy source. Science, 370(6518), 786–791. DOI: 10.1126/science.abb0971

Yuan, J., Yin, H., Yuan, D., Yang, Y., & Xu, S. (2022). On daytime radiative cooling using spectrally selective metamaterial based building envelopes. Energy, 242, 122779. https://doi.org/10.1016/j.energy.2021.122779

Zhai, Y., Ma, Y., David, S. N., Zhao, D., Lou, R., Tan, G., Yang, R., & Yin, X. (2017). Scalable-manufactured randomized glass-polymer hybrid metamaterial for daytime radiative cooling. Science, 355(6329), 1062–1066. https://doi.org/10.1126/SCIENCE.AAI7899.

Zhao, B., Xu, C., Jin, C., Lu, K., Chen, K., Li, X., Li, L., & Pei, G. (2024). Superhydrophobic bilayer coating for passive daytime radiative cooling. Nanophotonics, 13(5), 583–591. https://doi.org/10.1515/nanoph-2023-0511.

Zhao, D., Aili, A., Yin, X., Tan, G., & Yang, R. (2019). Roof-integrated radiative air-cooling system to achieve cooler attic for building energy saving. Energy and Buildings, 203, 109453. https://doi.org/10.1016/j.enbuild.2019.109453.

Zhong, H., Li, Y., Zhang, P., Gao, S., Liu, B., Wang, Y., Meng, T., Zhou, Y., Hou, H., Xue, C., Zhao, Y., & Wang, Z. (2021). Hierarchically hollow microfibers as a scalable and effective thermal insulating cooler for buildings. ACS Nano, 15(6), 10076–10083. https://doi.org/10.1021/ACSNANO.1C01814.

3.3 High Performance Windows and Shading Device in Building Retrofit

This section should be cited as:

Bottino-Leone, D. (2026). High performance windows and shading device in building retrofit. In: A Systematic Review of Passive Energy Conservation Measures and Probabilistic Assessment under Changing Climate in Urban Settings, CIB W040 Report, CIB General Secretariat.

Improving the performance of building envelopes is a key strategy to reduce energy consumption and greenhouse gas emissions in the existing building stock. Windows and shading devices play a critical role due to their impact on heat transfer, solar gains, daylighting, and occupant comfort. This review analyses the state-of-the-art technologies in high-performance windows and shading systems, focusing on their application in retrofit interventions.

3.3.1 High performance window technologies

High-performance window systems for retrofit are defined by the combined optimization of thermal transmittance (U-value), solar heat gain coefficient (SHGC or g-value), visible transmittance (Tvis), airtightness, and durability (ISO, 2017a; ISO, 2017b). Technologies can be grouped into glazing systems, frames, and adaptive (dynamic) solutions.

3.3.1.1 Glazing system

Double and Triple Low-E Glazing (Readiness: strong). Insulating glazing units (IGUs) consist of two or more glass panes separated by sealed cavities and assembled into a single unit. The cavities are typically filled with air or inert gases (e.g., argon or krypton) and are hermetically sealed to reduce convective and conductive heat transfer. In insulating glazing units, one of the cavity-facing glass surfaces is coated with a low-emissivity (low-E) thin film, typically composed of metallic or metal-oxide layers, to reduce radiative heat transfer by reflecting long-wave infrared radiation while maintaining high visible light transmission. The position of the low-E coating depends on the climatic context: in hot or cooling-dominated climates, it is typically applied to the inner surface of the outer pane, whereas in cold or heating-dominated climates it is generally placed on the outer surface of the inner pane. In spectrally selective configurations, these coatings are engineered to allow most of the visible spectrum (daylight) to pass through while reflecting a substantial portion of near-infrared solar radiation, thus decoupling daylight availability from solar heat gains. From a physical perspective, heat transfer through glazing occurs via conduction (through glass and gas layers), convection (within the cavity), and radiation (between pane surfaces). Low-e coatings primarily target the radiative component, while multiple panes and gas fills reduce conductive and convective heat transfer. The overall thermal performance is quantified by the U-value, while solar performance is described by SHGC (or g-value) and optical performance by visible transmittance (Tvis) (Jelle et al., 2012; ISO, 2017b). The current baseline for retrofit is insulating glazing units (IGUs) with low-emissivity (low-e) coatings (Jelle et al., 2012). Double glazing (U ≈ 1.0–1.4 W/m^2K) is widely used where cost constraints exist, while triple glazing (U ≈ 0.5–0.8 W/m^2K) is preferred in colder climates (Grynning et al., 2013). Low-e coatings reduce long-wave radiative heat transfer; spectrally selective coatings are tuned to maximize Tvis (≈0.6–0.75) while limiting SHGC (≈0.25–0.5) (Jelle et al., 2012).

Gas-Filled Cavities (Readiness: strong). Gas-filled cavities are a fundamental component of insulating glazing units (IGUs), consisting of the space between two or more glass panes that is filled with a gas having lower thermal conductivity than air. The primary function of the gas layer is to reduce heat transfer through the glazing system by limiting both conduction and convection within the cavity. The performance of this layer depends on gas type, cavity thickness, and sealing quality. From a physical standpoint, heat transfer within the cavity occurs through gas conduction and natural convection. By replacing air with inert gases such as argon or krypton, which have lower thermal conductivity, the conductive heat transfer is reduced. Additionally, optimizing the cavity thickness (typically 12–16 mm for argon) minimizes convective loops, further improving insulation performance. Krypton is often used in thinner cavities due to its superior insulating properties, making it suitable for high-performance or space-constrained applications (Aguilar-Santana et al., 2020). Argon is the most commonly used gas due to its balance between performance and cost, while krypton is used for higher-performance applications despite its higher cost (Aguila-Santana et al., 2020). Proper edge sealing is critical to prevent gas leakage over time, as degradation of gas concentration leads to reduced thermal performance (ISO, 2017b).

Warm Edge Spacers (Readiness: strong). Warm edge spacers are components used at the perimeter of insulating glazing units (IGUs) to separate the glass panes and seal the cavity, replacing traditional aluminium spacers with materials of lower thermal conductivity. Their primary function is structural (maintaining pane and ensuring hermetic sealing), but they also play a critical role in reducing thermal bridges along the edge of the glazing system. From a heat transfer perspective, the spacer region is one of the weakest points in an IGU, where linear thermal transmittance (Ψ-value) can significantly degrade overall window performance. Conventional aluminum spacers exhibit high thermal conductivity, leading to increased heat loss, lower internal surface temperatures, and higher risk of condensation at the glass edge. Warm edge spacers, typically made of stainless steel, thermoplastic materials, or composite polymers, reduce conductive heat flow across the edge and improve the temperature distribution across the glazing unit (ISO, 2017a). In addition to thermal benefits, warm edge spacers contribute to improved durability by accommodating differential thermal expansion between glass panes and maintaining long-term gas retention within the cavity. They also enhance indoor comfort by reducing cold downdrafts and condensation risk near window edges. Quantitatively, the use of warm edge spacers can reduce linear thermal transmittance (Ψ) by up to 40–80% compared to aluminium spacers, leading to measurable improvements in whole-window U-values, particularly in high-performance glazing systems (ISO, 2017a; ISO, 2017b).

Vacuum Insulated Glazing (VIG) (Readiness: medium). Vacuum Insulated Glazing (VIG) is an advanced glazing technology consisting of two glass panes separated by an ultra-thin evacuated cavity (typically <1 mm), in which the air has been removed to create a near-vacuum condition. The panes are held apart by a grid of micro-scale support pillars, while the perimeter is sealed using specialized edge seals to maintain the vacuum over time. From a heat transfer perspective, the vacuum cavity virtually eliminates conductive and convective heat transfer, as there is no gas medium to support these mechanisms. As a result, thermal transmission is dominated by radiative heat exchange between the internal glass surfaces, which is minimized through the application of low-emissivity (low-e) coatings. This combination allows VIG units to achieve very low U-values (typically in the range of 0.3–0.5 W/m²K) despite having a total thickness comparable to or even lower than conventional double glazing (ISO, 2017b). One of the key advantages of VIG is its compactness, making it particularly suitable for retrofit applications where frame depth and façade constraints limit the use of thicker triple glazing systems. This is especially relevant in historic buildings, where maintaining the original appearance of window frames is required. However, several technical challenges remain. These include long-term durability of the edge seal (which must maintain vacuum integrity over decades), potential thermal bridging through the support pillars, and higher manufacturing costs compared to conventional IGUs. Additionally, optical artifacts caused by the pillar array may affect visual quality in certain configurations.

Aerogel and Advanced Fill Materials (Readiness: emerging). Aerogel-based glazing systems use highly porous solid materials (typically silica aerogels) inserted within the cavity of glazing units to enhance thermal insulation. Aerogels are characterized by extremely low density and very low thermal conductivity (≈0.012–0.020 W/m·K), resulting from their nanostructured network that significantly limits heat transfer through both conduction and convection. In glazing applications, aerogels can be used in granular form (filling the cavity) or as monolithic translucent panels. From a heat transfer perspective, aerogels reduce conductive heat transfer through the solid matrix while suppressing convective heat transfer due to their nanoscale pore structure, which prevents air movement. Radiative heat transfer can also be reduced depending on the optical properties and any additional coatings applied. As a result, aerogel glazing systems can achieve very low U-values, comparable to or better than high-performance triple glazing, while maintaining reduced thickness (Grynning et al., 2013). A key advantage of aerogel glazing is its ability to provide diffuse daylight transmission, which can improve daylight uniformity and reduce glare. However, this comes at the expense of visual clarity, as aerogels typically introduce haze and limit direct visual connection with the exterior. Therefore, they are often applied in areas where daylighting is prioritized overview (e.g., skylights, façades with limited visual requirements). Despite their promising performance, aerogel-based systems remain in the emerging stage due to several limitations, including high material and manufacturing costs, challenges in large-scale production, durability concerns, and limited standardization. Integration into conventional IGU manufacturing processes is still under development.

Solar Control and Spectrally Selective Coatings (Readiness: strong). Solar control and spectrally selective coatings are thin-film layers, typically composed of metal or metal-oxide stacks, deposited on glass surfaces to tailor the spectral transmission and reflection properties of glazing systems. These coatings are designed to selectively manage solar radiation by allowing high transmittance of visible light (for daylighting) while reducing the transmission of near-infrared radiation responsible for heat gains. From a physical standpoint, solar radiation consists of ultraviolet (UV), visible (VIS), and near-infrared (NIR) components. Spectrally selective coatings are engineered to maximize transmittance in the visible range (≈380–780 nm) while reflecting or absorbing a significant portion of NIR radiation (≈780–2500 nm). This selective behavior enables a decoupling between daylight availability (Tvis) and solar heat gain (SHGC), which is a key objective in high-performance façade design (Grynning et al., 2013).

These coatings are typically applied to specific glass surfaces within IGUs to optimize both thermal and solar performance. In addition to reducing solar gains, many of these coatings also exhibit low-emissivity properties, thereby contributing to reduced radiative heat transfer and improved U-values. The performance of solar control coatings is characterized by parameters such as the solar heat gain coefficient (SHGC, also referred to as g-value), visible transmittance (Tvis), and selectivity ratio. High selectivity coatings are particularly effective in cooling-dominated climates or highly glazed buildings, where limiting solar gains without compromising daylight is critical. In retrofit applications, these coatings are widely adopted due to their compatibility with standard glazing manufacturing processes and their ability to significantly improve energy performance without major changes to window geometry.

Secondary Glazing (Retrofit Solution) (Readiness: medium). Secondary glazing is a retrofit solution consisting of the installation of an additional glazing layer on the interior side of an existing window, creating a sealed or semi-sealed air cavity between the original and the new pane. Unlike full window replacement, this approach preserves the original window frame and façade appearance, making it particularly suitable for historic and heritage buildings where external modifications are restricted. From a physical perspective, the addition of a secondary pane increases the overall thermal resistance of the window system by introducing an additional air layer that reduces conductive and convective heat transfer. The performance of secondary glazing depends on several factors, including cavity thickness, airtightness of the system, and the properties of the added glazing (e.g., presence of low-e coatings). When properly sealed, the air gap can significantly reduce heat losses, approaching the performance of double glazing systems. In addition to thermal improvements, secondary glazing enhances airtightness by reducing infiltration through existing window frames, which is often a major source of heat loss in older buildings. It also contributes to improved acoustic insulation and condensation control by increasing the internal surface temperature of the glazing system. However, the performance of secondary glazing is highly dependent on installation quality. Poor sealing can lead to air leakage and moisture accumulation within the cavity, reducing thermal effectiveness and potentially causing condensation issues. Furthermore, this solution may reduce the usability of windows (e.g., opening mechanisms) and can introduce maintenance challenges.

3.3.1.2 Frame technologies

PVC Frames (Readiness: strong). PVC (polyvinyl chloride) window frames are widely used in high-performance glazing systems due to their low thermal conductivity, durability, and cost-effectiveness. Modern PVC frames are typically designed with multi-chamber profiles, where internal cavities trap air and reduce heat transfer through the frame, significantly improving thermal insulation compared to solid materials. From a heat transfer perspective, PVC has inherently low thermal conductivity (≈0.16–0.19 W/m·K), which limits conductive heat flow across the frame. The multi-chamber geometry further enhances insulation by introducing air layers that reduce both conduction and convection. This design allows PVC frames to achieve relatively low frame U-values ($U_f \approx 1.0–1.4$ W/m²K), contributing positively to overall window performance (Grynning et al., 2013). Structural reinforcement is often required, particularly for larger window elements. This is typically achieved through the integration of steel or fiberglass inserts within the profile. While steel reinforcement can slightly increase thermal conductivity, optimized designs minimize this impact through thermal breaks and positioning strategies. PVC frames also offer high levels of airtightness due to precision manufacturing and the use of multiple sealing gaskets, which reduce air infiltration and improve overall energy performance. Additionally, they are resistant to moisture, corrosion, and UV degradation, making them suitable for long-term applications with limited maintenance requirements. From a retrofit perspective, PVC frames are widely adopted due to their compatibility with standard glazing systems, ease of installation, and favorable cost-performance ratio.

Timber Frames (Readiness: strong). Timber window frames are traditional yet high-performing solutions characterized by low thermal conductivity and good hygroscopic properties. Wood is a natural material with good thermal performance, which limits conductive heat transfer through the frame (Grynning et al., 2013). From a physical perspective, the cellular structure of wood contains air-filled pores that reduce heat conduction, while its moisture-buffering capacity helps regulate indoor humidity and surface temperatures. This contributes to improved thermal comfort and reduced condensation risk at the frame–glazing interface. Timber frames are particularly suitable for heritage and retrofit applications due to their aesthetic compatibility with historic façades. Modern timber frames are often treated or engineered (e.g., laminated wood) to enhance durability, dimensional stability, and resistance to moisture and biological degradation. However, timber requires periodic maintenance (e.g., painting, sealing) to ensure long-term performance. When properly maintained, it offers excellent durability and environmental benefits due to its renewable nature. Timber frames provide good insulation and are suitable for heritage applications (Grynning et al., 2013).

Thermally Broken Aluminium (Readiness: strong). Aluminium frames are widely used in commercial and high-performance façade systems due to their high structural strength, durability, and ability to support large glazing areas. However, aluminium has high thermal conductivity (≈160–200 W/m·K), which would result in significant heat losses if not properly mitigated. To address this, thermally broken aluminium frames incorporate insulating barriers (typically polyamide strips) between the interior and exterior sections of the frame. From a heat transfer perspective, the thermal break interrupts the conductive heat flow path, significantly reducing overall thermal transmittance. The effectiveness of the system depends on the width and material properties of the thermal break, as well as the overall frame geometry. Modern systems can achieve Uf values in the range of ≈1.6–2.5 W/m²K, with advanced designs reaching lower values (Aguilar-Santana et al., 2020). Thermally broken aluminium frames offer excellent dimensional stability, resistance to weathering, and low maintenance requirements. They are particularly suited for curtain walls and large-span glazing systems, where structural performance is critical. In retrofit applications, aluminium frames are often used in non-residential buildings or where architectural constraints require slim profiles and high structural capacity.

Composite Frames (e.g., Wood–Aluminium, Fiberglass) (Readiness: medium). Composite window frames combine different materials to leverage their respective advantages, typically pairing an insulating material (e.g., wood or fiberglass) on the interior side with a durable, weather-resistant material (e.g., aluminium) on the exterior. This hybrid approach aims to optimize both thermal performance and long-term durability. From a thermal standpoint, the insulating core (wood or fiberglass) reduces conductive heat transfer, while the external aluminium cladding provides protection against environmental exposure without significantly compromising thermal performance due to separation from the interior layer. Fiberglass, in particular, offers low thermal conductivity (≈0.03–0.04 W/m·K) and low thermal expansion, resulting in stable performance across temperature variations. Composite frames can achieve frame U-values comparable to high-performance PVC or timber systems (≈1.0–1.4 W/m²K), while offering improved durability and reduced maintenance compared to pure timber solutions (Grynning et al., 2013). These systems are particularly attractive in retrofit contexts where both performance and façade durability are critical, although their adoption is still less widespread compared to conventional materials due to higher costs and more complex manufacturing processes.

3.3.1.3 Dynamic and Smart Glazing

Electrochromic (EC) Glazing (Readiness: strong). Electrochromic glazing is an active smart window technology that modulates optical and solar properties through a reversible electrochemical reaction triggered by a low electrical voltage. EC devices typically consist of multilayer thin-film stacks deposited on glass, including transparent conductive layers, electrochromic materials (e.g., tungsten oxide), ion storage layers, and an electrolyte. From a physical standpoint, when voltage is applied, ions (typically Li+ or H+) migrate between layers, altering the optical properties of the electrochromic material. This changes both visible transmittance (Tvis) and solar heat gain coefficient (SHGC), allowing dynamic control of solar radiation and daylight. In the bleached state, the glazing is highly transparent; in the colored state, it significantly reduces solar and visible transmission. EC glazing directly controls radiative heat gains and glare without relying on external shading. It can reduce cooling loads, improve visual comfort, and maintain external view. Typical performance ranges include Tvis modulation from ~0.6 to <0.05, with corresponding reductions in SHGC (Baetens et al., 2010; Jelle et al., 2012). Limitations include switching speed (typically minutes), potential non-uniform coloration in large panes, cost, and the need for control systems integration.

Thermochromic (TC) Glazing (Readiness: emerging). Thermochromic glazing is a passive smart window technology that changes its optical properties in response to temperature variations. Typically based on materials such as vanadium dioxide (VO_2), TC glazing undergoes a phase transition at a specific temperature, resulting in reduced solar transmittance when the material heats up. From a physical perspective, the phase transition modifies the material's interaction with near-infrared radiation, reducing solar heat gains under high-temperature conditions while maintaining partial visible transmittance. This allows TC glazing to passively limit overheating without external control systems. However, the lack of user control and fixed transition temperature can lead to suboptimal performance under varying climatic conditions or user preferences. Additionally, achieving high visible transmittance while maintaining strong solar modulation remains a key technical challenge. Thermochromic systems respond passively to temperature but offer limited controllability (Wu et al., 2023).

Photochromic Glazing (Readiness: emerging). Photochromic glazing changes its optical properties in response to incident solar radiation, typically darkening under high irradiance and returning to a transparent state when radiation decreases. The effect is driven by reversible chemical reactions within photochromic compounds embedded in the glazing material. From a functional standpoint, photochromic systems primarily respond to light intensity (rather than temperature or user input), leading to automatic modulation of visible transmittance. While this can reduce glare and solar gains, the response is not directly optimized for thermal performance, as it may not align with indoor cooling or heating needs (Granqvist, 2014). The lack of independent control over visible and infrared transmittance limits the effectiveness of photochromic glazing compared to spectrally selective or electrochromic systems. Additionally, response times and long-term material stability remain areas of development.

Liquid Crystal / Suspended Particle Devices (SPD) (Readiness: medium). Liquid crystal (LC) and suspended particle device (SPD) glazing are electrically switchable technologies that control light transmission through reorientation of particles or molecules under an applied electric field (Ghosh et al., 2024). In LC systems, liquid crystal molecules align to allow or block light transmission, while in SPD systems, suspended particles align to modulate light passage. From a physical perspective, these systems primarily affect visible transmittance and glare by changing the scattering or absorption of light. Unlike electrochromic glazing, their impact on solar heat gain is more limited, as they do not selectively control infrared radiation to the same extent. These technologies offer fast switching times (seconds), making them suitable for applications requiring rapid control of privacy or glare. However, their energy performance benefits are generally lower than EC systems, and continuous power may be required to maintain certain states.

3.3.2 Shading devices

Shading systems modulate solar radiation and affect cooling demand, daylighting, and visual comfort (Tzempelikos and Athinenitis, 2007). Performance depends on geometry, optical properties, placement, and control strategy.

3.3.2.1 External shading

Overhangs (Horizontal Projections) (Readiness: strong). Overhangs are fixed horizontal shading elements positioned above windows, designed to block direct solar radiation based on solar geometry. Their effectiveness relies on the seasonal variation of solar altitude, allowing them to block high sun while permitting lower winter sun to enter the space. From a physical perspective, overhangs reduce solar heat gains by intercepting direct beam radiation before it reaches the glazing surface. Their performance depends on geometric parameters such as projection depth, window height, and orientation. Properly dimensioned overhangs can significantly reduce cooling loads without compromising winter solar gains (Granqvist, 2014). They are passive systems requiring no control or maintenance and are particularly effective on south-facing façades in mid-latitude climates. Case study: validated through simulation and monitored building studies showing significant cooling load reductions in office buildings (Granqvist, 2014). Effective in reducing solar gains based on solar geometry, particularly for south-oriented façades (Granqvist, 2014).

Vertical Fins (Readiness: strong). Vertical fins are fixed shading elements installed on the sides of windows, primarily designed to block low-angle solar radiation from east and west orientations. Unlike overhangs, they are effective when the sun is closer to the horizon. From a solar control perspective, vertical fins reduce direct solar gains by obstructing lateral solar incidence, which is particularly critical in cooling-dominated climates. Their effectiveness depends on depth, spacing, and orientation relative to the façade (Granqvist, 2014). They are often used in combination with horizontal shading to provide comprehensive solar control across different orientations.

Louvers (Fixed or Adjustable) (Readiness: strong). Louvers are slatted shading systems composed of horizontal or vertical blades that can be either fixed or adjustable. Adjustable (dynamic) louvers allow continuous control of solar penetration and daylight distribution by modifying blade angle. From a physical standpoint, louvers control both direct and diffuse solar radiation. By adjusting the tilt angle, they can reflect, absorb, or transmit incoming radiation, enabling a balance between solar protection and daylight availability. Reflective louvers can also redirect daylight deeper into the space, improving indoor illuminance distribution. Dynamic louvers, when integrated with control systems, can optimize energy performance by responding to solar position and indoor conditions (Granqvist, 2014).

Screens and Meshes (Readiness: medium). Screens and meshes are shading systems made of perforated materials or textile fabrics installed externally to reduce solar radiation while maintaining partial visual connection with the exterior. Their performance is primarily determined by the openness factor, material reflectance, and transmittance. From a physical perspective, these systems reduce solar gains by partially blocking and diffusing incident radiation. Unlike opaque shading, they allow a portion of light to pass through, resulting in softer daylight and reduced glare. However, their effectiveness in limiting heat gains is lower compared to fully opaque external shading systems. They are particularly suitable for retrofit applications due to ease of installation and flexibility and provide diffuse shading and reduce solar gains while maintaining visual connection with the exterior (Bellia et al., 2013).

Roller Shutters / External Blinds (Readiness: strong). Roller shutters and external blinds are movable shading systems installed outside the glazing, capable of fully or partially blocking solar radiation. These systems can be manually operated or automated, allowing dynamic control of solar gains and daylight (Roca-Musach et al., 2023). From a heat transfer perspective, external placement is highly effective because solar radiation is intercepted before reaching the glazing, preventing heat from entering the building. When fully deployed, these systems can significantly reduce SHGC at the system level and improve thermal insulation, particularly during nighttime. In addition to thermal benefits, they provide glare control, privacy, and improved acoustic insulation. However, their performance depends on control strategy and user behaviour.

3.3.2.2 Internal shading

Venetian Blinds (Internal) (Readiness: strong). Venetian blinds are internal shading devices composed of adjustable horizontal slats, typically made of aluminum, wood, or plastic, which can be tilted to control the amount and direction of incoming light. Their primary function is to regulate daylight penetration and glare while maintaining a degree of visual connection with the exterior. From a physical perspective, venetian blinds interact with solar radiation after it has passed through the glazing. As a result, a portion of the solar energy is already transmitted indoors before being reflected, absorbed, or redistributed by the slats. This limits their effectiveness in reducing cooling loads compared to external shading systems. However, by adjusting slat angle, blinds can redirect daylight toward the ceiling, improving indoor light distribution and reducing glare. The thermal performance of venetian blinds depends on slat reflectance, angle, and control strategy. Highly reflective slats can reduce absorbed heat and improve daylight redirection, while automated control can enhance performance by adapting to solar position and indoor conditions (Granqvist, 2014). Venetian blinds are widely used in retrofit applications due to their low cost, ease of installation, and flexibility.

Roller Shades and Curtains (Readiness: strong). Roller shades and curtains are internal shading systems consisting of continuous fabric layers that can be deployed to cover glazing surfaces. Their performance depends on fabric properties such as solar transmittance, reflectance, absorptance, and openness factor. From a physical standpoint, these systems reduce solar radiation entering the occupied space by absorbing and reflecting part of the transmitted energy. However, similar to other internal shading devices, solar radiation has already passed through the glazing before interacting with the shading layer, limiting their effectiveness in reducing heat gains compared to external systems. Highly reflective or metallized fabrics can improve performance by reflecting solar radiation back toward the glazing, partially reducing heat transfer to the interior. Open-weave fabrics allow visual connection and daylight penetration while reducing glare, whereas opaque fabrics provide stronger solar protection and privacy. Roller shades and curtains are particularly attractive in retrofit scenarios due to their low cost, ease of installation, and wide range of available configurations. Their effectiveness is strongly influenced by user behaviour or control strategies.

3.3.2.3 Internal (between-glass) shading

Between-glass shading (Readiness: medium). Between-glass shading systems consist of shading devices (typically venetian blinds or pleated fabrics) installed within the cavity of insulating glazing units (IGUs) (Sun et al., 2016). The shading element is sealed between the panes, protected from environmental exposure such as dust, wind, and mechanical wear. From a physical perspective, these systems intercept solar radiation within the glazing cavity, meaning that solar energy has already passed through the outer pane before interacting with the shading device. As a result, their thermal performance is intermediate between external and internal shading systems: more effective than internal devices (which act entirely inside the conditioned space), but less effective than external shading (which blocks radiation before it enters the glazing system). The thermal behavior depends on the position of the shading layer within the IGU, the optical properties of the slats or fabric (reflectance, absorptance, transmittance), and the ventilation conditions of the cavity (sealed vs ventilated). Absorbed solar radiation can lead to increased temperatures within the glazing unit, which may affect both thermal performance and durability. Between-glass shading systems offer significant advantages in terms of durability and maintenance, as the protected environment prevents dirt accumulation and reduces mechanical degradation. They also provide stable optical performance over time and can be integrated with manual or automated control systems. However, limitations include reduced flexibility for maintenance or replacement, potential overheating of the cavity, and somewhat lower solar control effectiveness compared to external shading systems.

3.3.2.4 Control strategies

Control strategies are a critical component in the performance of shading systems, as they determine how and when shading devices respond to environmental conditions. Their effectiveness directly influences energy consumption, visual comfort, and occupant satisfaction. Rule-based control represents the most widely implemented approach, relying on predefined thresholds such as solar irradiance, indoor illuminance, or temperature. These systems are relatively simple, robust, and easy to implement, but they may not achieve optimal performance under highly variable conditions (Granqvist, 2014). Sensor-based (closed-loop) control improves upon this by using real-time feedback from indoor environmental parameters (e.g., illuminance levels, glare indices, or operative temperature). This allows shading devices to respond dynamically to actual conditions within the space, enhancing both energy efficiency and occupant comfort (Granqvist, 2014). Predictive control represents a more advanced approach, integrating weather forecasts, occupancy patterns, and building performance models to anticipate future conditions and optimize shading operation accordingly. While this strategy offers the highest potential for performance optimization, its implementation is more complex and currently limited to pilot projects and advanced building automation systems (US Department of Energy, 2023).

3.3.3 References

Aguilar-Santana, J. L., Jarimi, H., Velasco-Carrasco, M., & Riffat, S. (2020). Review on window-glazing technologies and future prospects. International Journal of Low-Carbon Technologies, 15(1), 112–120. https://doi.org/10.1093/ijlct/ctz032

Baetens, R., Jelle, B. P., & Gustavsen, A. (2010). Properties, requirements and possibilities of smart windows for dynamic daylight and solar energy control. Solar Energy Materials and Solar Cells, 94(2), 87–105. https://doi.org/10.1016/j.solmat.2009.08.021

Bellia, L., De Falco, F., & Minichiello, F. (2013). Effects of solar shading devices on energy requirements of standalone office buildings for Italian climates. Applied Thermal Engineering, 54(1), 190–201. https://doi.org/10.1016/j.applthermaleng.2013.01.039

Ghosh, A., Hafnaoui, R., Mesloub, A., Elkhayat, K., Albaqawy, G., Alnaim, M. M., & Mayhoub, M. S. (2024). Active smart switchable glazing for smart city: A review. Journal of Building Engineering, 84, 108644. https://doi.org/10.1016/j.jobe.2024.108644

Granqvist, C. G. (2014). Electrochromics for smart windows: Oxide-based thin films and devices. Thin Solid Films, 564, 1–38. https://doi.org/10.1016/j.tsf.2014.02.002

Grynning, S., Gustavsen, A., Time, B., & Jelle, B. P. (2013). Windows in the buildings of tomorrow: Energy losers or energy gainers? Energy and Buildings, 61, 185–192. https://doi.org/10.1016/j.enbuild.2013.02.029

International Organization for Standardization. (2017a). Thermal performance of windows, doors and shutters—Calculation of thermal transmittance—Part 1: General (ISO 10077-1:2017).

International Organization for Standardization. (2017b). Energy performance of buildings—Thermal, solar and daylight properties of building components and elements—Part 1: Simplified calculation method of the solar and daylight characteristics for solar protection devices combined with glazing (ISO 52022-1:2017).

Jelle, B. P., Hynd, A., Gustavsen, A., Arasteh, D., Goudey, H., & Hart, R. (2012). Fenestration of today and tomorrow: A state-of-the-art review and future research opportunities. Solar Energy Materials and Solar Cells, 96, 1–28. https://doi.org/10.1016/j.solmat.2011.08.010

Roca-Musach, M., Garcia-Nevado, E., Alonso-Montolio, C., Cabillo, I. C., & Roura, H. C. (2023). Comparison of the thermal effect of two automatic controls of roller shutters in an academic space. In J. Littlewood, R. J. Howlett, & L. C. Jain (Eds.), Sustainability in energy and buildings 2022 (Vol. 336). Springer. https://doi.org/10.1007/978-981-19-8769-4_25

Sun, Y., Wu, Y., Wilson, R., & Lu, S. (2016). Experimental measurement and numerical simulation of the thermal performance of a double glazing system with an interstitial Venetian blind. Building and Environment, 103, 111–122. https://doi.org/10.1016/j.buildenv.2016.03.028

Tzempelikos, A., & Athienitis, A. K. (2007). The impact of shading design and control on building cooling and lighting demand. Solar Energy, 81(3), 369–382. https://doi.org/10.1016/j.solener.2006.06.015

U.S. Department of Energy. (2023, September 29). EnergyPlus engineering reference (Version 23.2.0).

Wu, S., Sun, H., Duan, M., Mao, H., Wu, Y., Zhao, H., & Lin, B. (2023). Applications of thermochromic and electrochromic smart windows: Materials to buildings. Cell Reports Physical Science, 4(5), 101370. https://doi.org/10.1016/j.xcrp.2023.101370

3.4 Natural Ventilation of Buildings and Spatial Uncertainties of Microclimate Conditions due to Different Urban Planning and Landscaping

This section should be cited as:

Zhang, L., Zhang, X. (2026). Natural ventilation of buildings and spatial uncertainties of microclimate conditions due to different urban planning and landscaping. In: A Systematic Review of Passive Energy Conservation Measures and Probabilistic Assessment under Changing Climate in Urban Settings, CIB W040 Report, CIB General Secretariat.

3.4.1 Natural ventilation of buildings and key parameters

3.4.1.1 Problem Statement

The increasing urban density and climate variability have intensified the need for sustainable passive design strategies that balance occupant comfort with environmental impact, as buildings account for a significant portion of global energy use and carbon emissions (X. Xie et al., 2023). According to the United Nations Environment Programme (UNEP), buildings and the construction sector accounted for 37% of global energy- and process-related CO_2 emissions in 2022 (UNEP, 2024). Mechanical ventilation systems commonly account for a noticeable share of building energy use, especially in dense urban settings where cooling demand is high. In this context, natural ventilation becomes an important means to alleviate part of this energy burden while still ensuring acceptable indoor environmental quality.

Natural ventilation can enhance indoor air quality, improve thermal comfort, and reduce energy demand, especially in regions with mild or warm climates. After establishing this general significance, specific design indicators (including façade geometry and WWR) can be meaningfully introduced as key determinants influencing natural ventilation effectiveness. Furthermore, the applicability and effectiveness of natural ventilation differ across climate regions. In general, it plays a more prominent role in climates where outdoor conditions frequently fall within a comfortable range, allowing buildings to rely more on naturally driven airflow. In such regions, natural ventilation can reduce the need for mechanical conditioning and contribute to improved thermal comfort.

Therefore, this section introduces the typologies and governing mechanisms of natural ventilation, synthesizes evidence on how façade and building geometry parameters affect airflow and comfort across urban contexts, highlights unresolved gaps under climate change, and outlines methodological considerations for robust evaluation.

3.4.1.2 Typologies and Mechanisms of Natural Ventilation

Natural ventilation represents a fundamental passive cooling strategy that utilizes natural forces to drive airflow without mechanical assistance, offering significant potential for energy savings and improved indoor thermal comfort and environmental quality (R. A. Ali et al., 2023). Effective use of several natural ventilation strategies can be achieved through the optimization of building geometry design and window-to-wall ratios, as each type operates through distinct mechanisms and responds differently to architectural configurations. While larger window-to-wall ratios (WWR) allow more air to enter the space and therefore appear favourable for natural ventilation, excessively large WWR can also introduce drawbacks such as overheating/cooling, increased solar gains, and glare. These negative impacts may offset ventilation benefits, meaning that WWR should be optimized rather than simply maximized. The conceptual diagram of the several types of natural ventilation, classified by driving force and opening orientation, is shown in Figure 3.4.1.

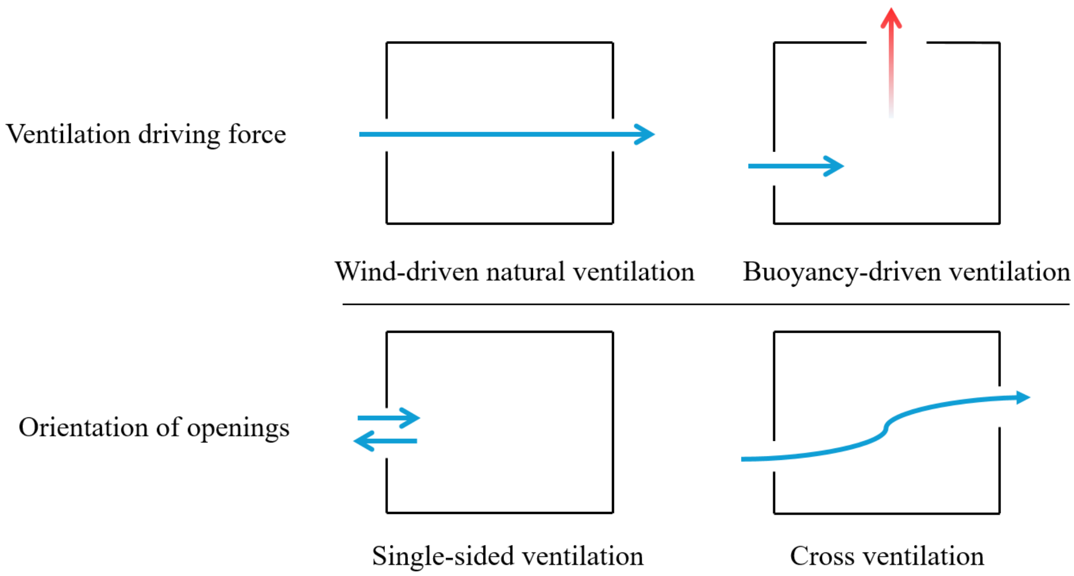

Figure 3.4.1 Conceptual diagram of different types of natural ventilation

Wind-driven natural ventilation operates through pressure differentials created by wind flow around buildings, with fresh air injections occurring through high-pressure windward openings and exhaust through low-pressure leeward openings (Cui et al., 2015). This mechanism is highly dependent on external wind conditions, with effectiveness varying significantly based on wind speed, direction, and building orientation (Karava et al., 2007). Research demonstrates that wind-driven systems are particularly sensitive to building geometry and opening configurations, with facade porosity and opening design playing crucial roles in determining air change rates (Cui et al., 2015).

Buoyancy-driven ventilation, commonly known as the stack effect, operates through density differences between indoor and outdoor air caused by temperature variations (X. Gao et al., 2022). This mechanism creates natural pressure gradients that drive airflow from lower to higher elevations within buildings, with warm air rising and exiting through upper openings while cooler air enters through lower openings (P. F. Linden et al., 1990).

Single-sided ventilation involves airflow through openings located on a single facade, relying on wind pressure difference and thermal buoyancy effects to drive air exchange (T. S. Larsen & Heiselberg, 2007). While this configuration is often necessary in dense urban environments or buildings with limited facade access, it typically provides lower ventilation rates compared to cross ventilation systems. Research indicates that single-sided ventilation performance is significantly influenced by opening size, position, external wind conditions, and the transient airflow pattern around buildings (T. Yang et al., 2006; H. Y. Zhong et al., 2022).

Cross ventilation represents the most efficient natural ventilation strategy, involving airflow through multiple openings positioned on different building facades (Jiang et al., 2023). This system combines both wind-driven and buoyancy-driven forces to create continuous airflow patterns through interior spaces, with effectiveness depending on the relative positioning and sizing of inlet and outlet openings (Derakhshan & Shaker, 2017; Jia Li, 2023). Compared to single-sided ventilation, cross ventilation can more effectively enhance the air exchange rate, improve thermal comfort, accelerate the removal of indoor pollutants, and is better suited to the climatic conditions of tropical regions (Aflaki et al., 2015).

Despite extensive investigations into the mechanisms of various natural ventilation types, several limitations remain. Research gaps persist in understanding the coupled effects of multiple ventilation mechanisms in complex urban settings, the influence of diverse climatic regions on ventilation performance, (Andrian & Craske, 2023; Bastide et al., 2014; Jia Li, 2023) and the consistency between field measurements and numerical simulations (H. Hu et al., 2022). A broad consensus within the literature is that natural ventilation holds substantial potential for improving indoor air quality, enhancing thermal comfort, and reducing energy demand, with building geometry, window-to-wall ratios, and opening configurations identified as the critical determinants of effectiveness. However, in highly polluted urban environments such as Delhi, natural ventilation may be intentionally minimized to prevent outdoor pollutants from degrading indoor air quality (e.g., $PM_{2.5}$), indicating that its applicability is context-dependent (Nihar et al., 2023).

3.4.1.3 Influence of Design Parameters

The effectiveness of these natural ventilation types is fundamentally linked to building design parameters, particularly window-to-wall ratios and building geometry (Ragab et al., 2025), which directly influence pressure distributions, airflow patterns, and thermal dynamics within the built environment. Recent studies quantify the energy-saving potential associated with window-to-wall ratio (WWR). Tawfeeq & Qaradaghi reported that optimizing WWR in hot-summer Mediterranean climates can reduce energy use intensity by 1.2-15 kWh/m² depending on building orientation (Tawfeeq & Qaradaghi, 2024). Li et al. (2021) showed that higher WWR significantly increases cooling electricity demand, from 19.6 kWh at 20% WWR to 461.9 kWh at 100% WWR on a typical summer day. These results illustrate that WWR is a critical design parameter for energy efficiency (J. Li et al., 2021).

In the period following 2010, studies have evolved from focusing on isolated building parameters to integrating urban morphology and microclimate interactions, highlighting the importance of building orientation, aspect ratios, and façade openings in optimizing ventilation performance (Adeli et al., 2019).

Research consistently demonstrates that building orientation, aspect ratio, and WWR significantly affect natural ventilation potential and indoor thermal comfort, with optimized configurations leading to improved air change rates and reduced energy consumption (Adeli et al., 2019; Ziabari et al., 2019).

3.4.1.4 Building Geometry and Urban Morphology

Regarding building geometry parameters, building orientation and layout, length-to-width, and height-to-width ratios are frequently identified as critical factors that influence the potential for natural ventilation and the distribution of airflow (W. Zhong et al., 2023). Modifying building corners and adding vertical voids can improve ventilation by changing wind flow patterns and pressure distribution (Hakim et al., 2025; Juan et al., 2023). Some studies suggested using building shape classifications to systematically assess how different geometric features affect ventilation performance (S. Li et al., 2023). Moreover, building layout patterns play a key role in influencing ventilation performance and microclimate conditions, especially in high-density areas (Deng et al., 2024; Juan et al., 2023; Toren & Sharmin, 2024). The influence of neighboring buildings and urban density on wind pressure coefficients and ventilation was emphasized, with denser configurations often reducing ventilation potential (Leite & Frota, 2014; S. Zhang et al., 2024).

3.4.1.5 Window-to-Wall Ratio (WWR)

WWR is the proportion of window area to the exterior wall area and a key design parameter influencing airflow rates, thermal comfort, and building energy performance (Adeli et al., 2019; Al Rikabi et al., 2022). Findings suggest that moderate increases in WWR enhance ventilation rates and indoor air quality; however, excessive WWR may result in overheating and greater occupant discomfort (Krithigadevi V & K. Bhagyasri, 2023; Rajput & Thomas, 2023). Beyond thermal comfort considerations, high WWR configurations may also introduce additional risks, such as moisture accumulation and potential deterioration of building envelopes (M. Ali, Oladokun, Osman, Mohd Din, et al., 2016; M. Ali, Oladokun, Osman, Samsuddin, et al., 2016; Magrini et al., 2017).

Optimal WWR values differ according to climate zone and building typology, with common recommendations suggesting a range of 20% to 40% to achieve a balance between ventilation performance and energy efficiency (Adeli et al., 2019; Pathirana et al., 2019). A study integrates WWR considerations with advanced façade technologies, including radiative cooling and phase change materials, to mitigate thermal impacts (X. Xie et al., 2024).

3.4.1.6 Contextual Variations and Knowledge Gaps

Despite extensive research on natural ventilation, a specific knowledge gap persists regarding the combined influence of building geometry and WWR on ventilation efficiency within dense urban contexts, especially under changing climatic conditions (S. Zhang et al., 2024; Zhao et al., 2024). Some studies emphasize the role of window design and orientation in enhancing airflow and thermal comfort (Abdullah & Alibaba, 2022; Fontenelle et al., 2021). Meanwhile, other studies emphasize the complex interactions between urban morphology, building density, and microclimate, which can either enhance or obstruct natural ventilation. (Z. Gao & He, 2024; S. Li et al., 2023; Zeng et al., 2024). The optimal WWR is still under debate. Although numerical simulation and optimization studies have investigated the optimal window-to-wall ratio (WWR) for different climates and building types, a comprehensive review covering all scenarios is still lacking. Existing research indicates that optimal WWR depends on climate, orientation, glazing type, and building function. For instance, Alsehail & Almhafdy (2020) highlighted the climate- and orientation-dependence of WWR; (Sayadi et al., 2021) suggested 40-50% for warm climates and higher values in cold climates; Goia reported 30-45% for most European office buildings (Goia, 2016). These studies collectively indicate that optimal WWR must be determined through a context-specific evaluation of climatic and building factors. Results vary depending on the climate zone and the building typology (Rana et al., 2022). Due to the absence of a unified understanding and systematic framework for these complex factors, the practical use of passive ventilation strategies in urban design and architecture remains limited (Bienvenido-Huertas et al., 2023; Coşar et al., 2023).

3.4.1.7 Methodological Review and Limitations

Regarding methodological approaches, the integration of advanced CFD simulations with on-site measurements or wind tunnel experiments has been commonly used to analyze airflow characteristics and ventilation performance. Several studies employed Reynolds-Averaged Navier-Stokes (RANS) models and parametric CFD simulations to obtain more comprehensive insights (Rajput & Thomas, 2023; Zhao et al., 2024; W. Zhong et al., 2023). Typical outputs extracted from CFD studies include wind resource assessment, cross-ventilation potential, and thermal comfort improvements resulting from temperature differentials. To reduce computational cost, simplified natural ventilation network models (e.g., those implemented in ClimateStudio or EnergyPlus) can also be employed to efficiently estimate air changes per hour (ACH). Hybrid simulation frameworks, which integrate multi-scale urban modeling, parametric CFD, and building energy simulations, provide a more comprehensive understanding of ventilation in complex urban morphologies by linking large-scale wind patterns with building-scale indoor performance (X. Yin & Muhieldeen, 2024).

Despite these advances, several sources of uncertainty can affect CFD results and potentially lead to discrepancies with actual performance. Key uncertain input parameters include boundary conditions (e.g., inflow wind speed and direction), building geometry and surface properties (e.g., window sizes, façade roughness), turbulence modeling (e.g., RANS vs LES) and turbulence parameters (e.g., turbulence intensity, kinetic energy, dissipation rate), as well as indoor settings such as window opening and occupant behavior.

Additionally, the complexity and resource intensity of simulations restrict their routine use in practice. Simplifications such as periodic boundary conditions or regular building layouts may overlook real-world variability, reducing the applicability of the results. (Gough, 2017; Zhao et al., 2024). Inconsistencies in turbulence modeling and boundary-condition settings can also affect comparability (Tarkhan et al., 2022).

3.4.1.8 Practical and Operational Implications

Moreover, variability in selected comfort metrics and evaluation criteria across studies leads to inconsistent assessments of ventilation effectiveness. (Shimonosono et al., 2023) investigated sixty naturally ventilated office buildings in Japan and pointed out that there are several common characteristics in the design and operation. Most buildings set the effective natural ventilation opening area to around 0.1-0.5% of the room area. The control of the openings depends on temperature conditions, especially when the outdoor temperature is lower than the indoor temperature. This rule does not vary according to building latitude or construction year. As shown in Figure 3.4.2, temperature-related criteria such as the lower limit of outdoor temperature and the condition (Outdoor temperature < Indoor temperature) are the most frequently used, indicating that temperature difference is the dominant factor in operating natural ventilation. In addition, Shimonosono et al. reported that the operation of openings is often simplified, with limited intermediate adjustment of the opening ratio. The authors suggest that future natural ventilation systems should adopt the concept of “opening ratio” to improve indoor thermal environment control. This approach is considered especially effective in regions like Hokkaido (Japan), where summer climate is cool.

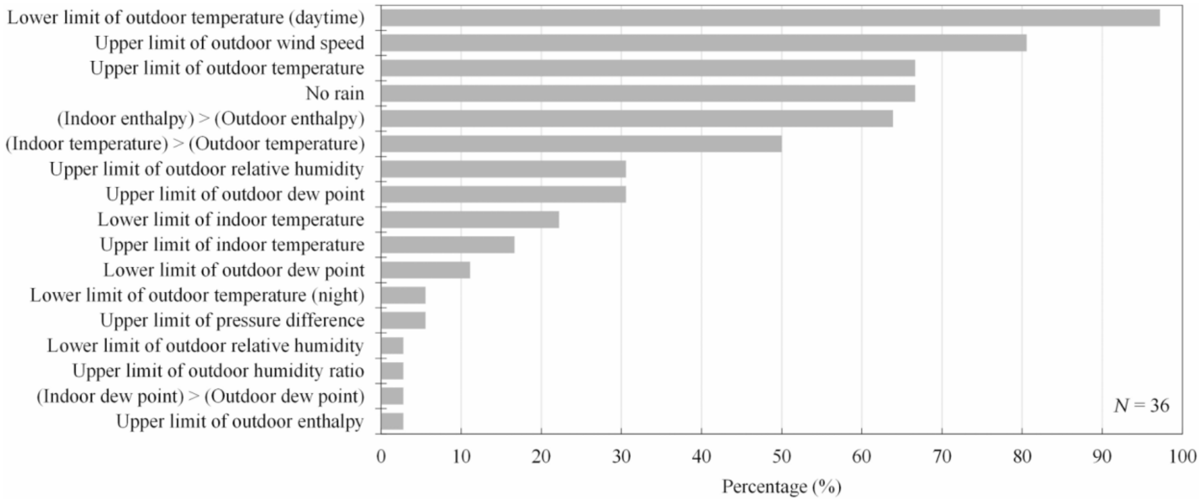

Figure 3.4.2 Percentage of criteria used for opening natural ventilation openings in 36 buildings surveyed (Shimonosono et al., 2023)

Furthermore, considering the influence of outdoor moisture, future control strategies should integrate humidity or enthalpy-based parameters. When the outdoor humidity or dew point is high, unregulated natural ventilation may lead to excessive indoor moisture and potential condensation risks, especially in regions with humid summers (Debata & Ogura, 2025). Therefore, combining temperature-based and humidity-based controls could enhance both thermal and moisture comfort.

3.4.1.9 Summary of Natural Ventilation

In summary, natural ventilation operates through distinct mechanisms whose effectiveness is strongly shaped by window-to-wall ratios and building geometry. While cross ventilation shows superior performance, the optimal configurations of WWR and geometry remain context-dependent notably under changing climatic conditions. For example, Younes et al. (2024) found that in a Mediterranean climate the number of comfortable hours achievable through natural ventilation drops by 40%, falling to 26% in the worst-case future scenario, indicating that warming and altered outdoor conditions reduce natural ventilation potential.

At the community or neighborhood scale, studies on multi-scale urban natural ventilation and climate adaptation illustrate that urban spatial layout (including wind corridors and building height/density) plays a major role in natural ventilation performance across blocks rather than just within individual buildings (S. Zhang et al., 2024).

Furthermore, the layout and aerodynamic configuration of buildings, for example, orientation relative to prevailing winds significantly influence indoor and outdoor airflow pathways. Miao & Lau (2023) found that when linear building blocks are aligned parallel to the prevailing wind direction, they obstruct airflow less, whereas perpendicular or oblique orientations significantly reduce wind speed in street-canyon areas.

Given these findings, methodological and practical limitations remain, including inconsistent metrics, a shortage of field studies under future climate scenarios, and limited community-scale data. There is therefore a clear need for more integrated, climate-responsive, and neighbourhood-scale studies to advance the applicability of passive ventilation strategies in urban environments.

3.4.2 Spatial uncertainties of microclimate conditions due to different urban planning and landscaping

3.4.2.1 Problem statement

Research on the climatic impacts of urban planning and landscaping has emerged as a critical area of inquiry due to the increasing challenges posed by urban heat islands (UHI) and climate change. 2023; Nuruzzaman, 2015). This section provides an overview of probabilistic assessments of passive energy-saving measures in urban environments under climate change, covering both urban-scale analyses. It includes various urban characteristics, local climate zones, overall roughness, albedo, and green coverage. Neighborhood-scale studies focus on landscape elements such as trees, water bodies, shading structures, and pavements that may create distinct microclimatic conditions. The structure of this section is illustrated in Figure 3.4.3.

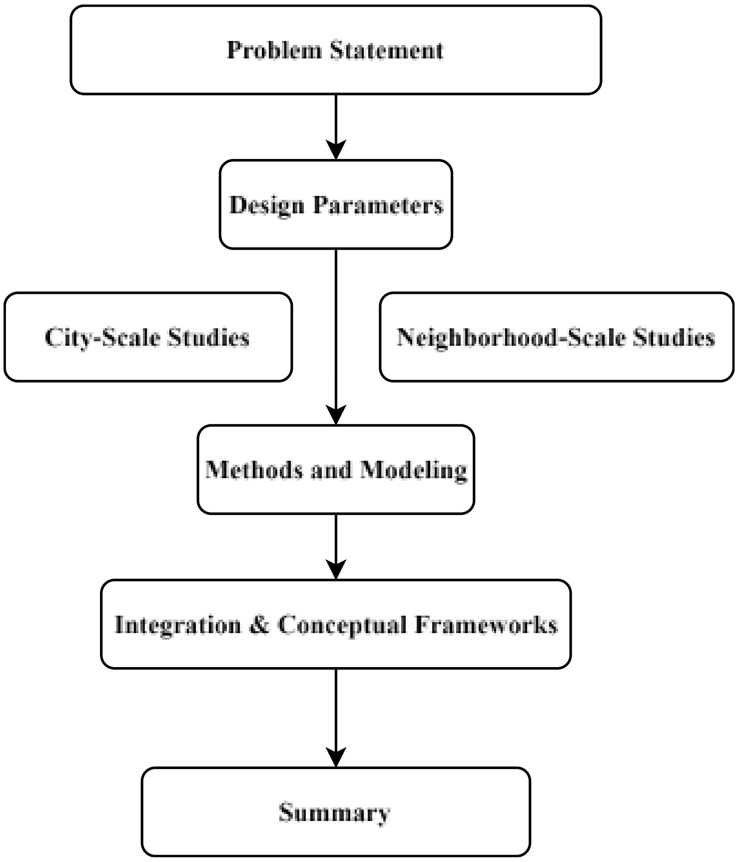

Figure 3.4.3 Diagram of the Structure of Section 3.4.2

Urban green and blue spaces, including trees, parks, and water bodies, have been identified as essential for mitigating elevated temperatures, improving thermal comfort, and enhancing urban resilience (Cherif et al., 2024; Kumar et al., 2024). Additionally, a 0.1 °C decrease in daily maximum temperature corresponds to an average 3.0% reduction in heat-related mortality (Santamouris & Osmond, 2020). This section aims to synthesize current knowledge on how urban planning and landscaping affect spatial climate uncertainty, focusing on trees, water bodies, shading structures, and pavements.

3.4.2.2 City-Scale Studies

The Local Climate Zone (LCZ) framework defines regions of relatively uniform surface cover, structure, material, and human activity, each typically spanning hundreds of meters and producing characteristic thermal responses, LCZ mapping is often based on the conceptual scale of hundreds of meters to several kilometers (Stewart & Oke, 2012), and in practice a grid resolution of 100-150 m has been shown to be a good compromise for classification (Bechtel et al., 2015).

High-albedo materials are most effective in LCZs characterized by high building density and extensive impervious surfaces. Specifically, compact high-rise, compact mid-rise, and compact low-rise zones (LCZ 1-3), as well as open low-rise and other densely built low-rise areas (LCZ 4-6), exhibit the greatest potential for temperature reduction through reflective surfaces. These LCZs absorb substantial solar radiation during daytime, resulting in higher surface and air temperatures, which can be mitigated by increasing albedo. Empirical and modeling studies support this strategy: (Santamouris, 2014b) noted that reflective materials are particularly effective in dense urban fabrics, while (Luo et al., 2024) that increasing surface reflectivity can effectively reduce urban temperatures, with the magnitude of cooling varying across different urban forms and LCZ types.

Urban vegetation and blue-green spaces are widely recognized as effective strategies to mitigate urban heat. (Cai et al., 2024) found that increasing the proportion of blue-green space in certain LCZ types, specifically LCZ 6 (open low-rise) and LCZ 9, effectively reduces land surface temperatures. Their analysis indicates that targeted greening interventions in these urban forms can provide significant cooling benefits.

Urban heat mitigation strategies, such as increasing vegetation or implementing high-albedo surfaces, can reduce local ambient temperatures, which in turn affects building energy demand. Lower ambient temperatures reduce cooling loads and can improve overall building energy performance. (Santamouris, 2014b) indicates that even moderate reductions in urban air temperature can significantly decrease cooling energy requirements, although the magnitude depends on building type, HVAC systems, and local climate conditions. This highlights that microclimate interventions at the urban scale can have measurable impacts on building performance assessments.

Different LCZs exhibit distinct microclimates due to variations in building density, height, and land cover. Therefore, using a single airport weather dataset may not accurately represent conditions across all urban zones, and LCZ-specific climate data are recommended for more precise building performance simulations.

The influence of input parameter uncertainty, such as tree leaf area density (LAD) or surface solar properties (e.g., albedo and emissivity), on urban microclimate and building performance simulations remains largely unexplored. Due to the lack of systematic studies quantifying how these uncertainties propagate to differences between modeled and observed outcomes, it is recommended that future work conduct sensitivity and uncertainty analyses to assess the impact of LAD and surface properties on simulation accuracy.

In the field of urban morphological classification, the studies have utilized LCZ (Local Climate Zone) classification or analogous urban morphology frameworks, often combining remote sensing and machine learning techniques to achieve high accuracy and fine spatial detail (Pauly & Ferrero, 2024; Yin & Zhao, 2024; Yu et al., 2025). However, traditional LCZ classifications typically emphasize structural characteristics while overlooking urban functions and metabolic elements, which limits their ability to fully capture microclimatic variations (Park et al., 2024).

In studies quantifying urban surface characteristics, remote sensing has been used to map albedo and land cover properties (Bechtel et al., 2015), Numerical modeling is used to systematically investigate and perturb the local urban climate, including airflow, air temperature, and urban surface energy transfer processes (Schrijvers, 2020), and The hybrid approach combining remote sensing and the WRF-UCM model has been used to simulate urban microclimates and the Urban Heat Island effect at city scale, showing that updated land-use data from remote sensing improves model accuracy in reproducing observed temperature patterns (G. Chen et al., 2016). It should be noted that many of these studies were conducted in hot, humid climates, where shading from trees and the presence of water bodies strongly influence urban temperatures.

In addition to surface characteristics, urban green cover also plays a critical role in modulating microclimate. Xie et al. evaluated vegetation types, density, and spatial distribution, finding that dense tree cover and water bodies provide the most significant cooling effects (J. Xie et al., 2024). Joshi and Teller (Joshi & Teller, 2024) proposed that greening alone may be insufficient to mitigate urban-scale UHI, especially under future climate scenarios with increased heat and drought stress. Zhang et al.'s study points out that there is a lack of consensus on optimal greening configurations, and socio-economic as well as vulnerability factors have not been adequately incorporated into greening assessments (R. Zhang et al., 2023).

3.4.2.3 Neighbourhood-Scale Studies

Urban planning and landscaping significantly influence spatial climate variability at the neighbourhood scale, particularly through elements such as trees, water bodies, shading structures, and pavements. Trees and water bodies reduce local temperatures and enhance microclimate regulation, while shading structures mitigate solar radiation impacts. Pavements often increase heat retention, contributing to spatial climate uncertainty. Integrating these elements is crucial for effective urban climate management.

The studies have quantitatively assessed temperature reductions attributable to landscape elements, considering both thermal comfort and climatic metrics. In terms of thermal comfort, Yang Wei et al. reported that the greatest decrease in Physiological Equivalent Temperature (PET) achieved through proposed landscape designs reaches approximately 12 °C (W. Yang et al., 2018). In terms of climatic temperature, Rocco Pace et al. found that for every 10% increase or decrease in tree canopy cover, the hourly maximum ambient air temperature changes inversely by approximately 0.2 °C (Pace et al., 2023). Trees and green spaces consistently show strong cooling effects, often exceeding those of water bodies and pavements, though water bodies contribute significantly through evaporation (Y. Hu et al., 2023; Jandaghian & Colombo, 2024; L. T. Xie & Cai, 2015). Combined interventions, such as cool pavements with tall trees or green roofs with vegetation, enhance cooling beyond single elements (Alcazar et al., 2016).

However, from the perspective of natural ventilation, dense trees and green spaces can also reduce wind speeds and impede air renewal. For example, (Niu et al., 2023) reported that the presence of trees around a building could decrease ventilation flow rates by 32 %. In a microclimate study, (Feng et al., 2023) found that beneath the canopies of four tree species, relative humidity was 3-11% higher than at a nearby weather station during summer, and even higher in winter (10-20%), indicating that urban trees can significantly increase local humidity through transpiration. (F. Li et al., 2022) found that trees located on the windward side of buildings tend to reduce local wind velocity, resulting in higher $PM_{2.5}$ concentrations at the pedestrian level. (Hewitt et al., 2019). Therefore, in certain urban contexts, such sheltering effects may offset some of the cooling benefits provided by vegetation. Consequently, the optimization of landscape interventions should not only consider cooling effects but also balance airflow and ventilation conditions to maximize overall urban comfort.

The spatial configuration of landscape elements also strongly influences cooling efficiency. Studies indicate that edge density, patch shape, and distribution patterns significantly affect microclimate outcomes (Maimaitiyiming et al., 2014; Silveira et al., 2024; Z. Wu & Zhang, 2018). Fragmented and elongated green spaces often provide broader cooling zones compared to large, contiguous patches (Ghosh & Das, 2018). Moreover, the spatial scale of analysis influences the explanatory power of vegetation and water cover on surface temperature, with smaller scales showing stronger effects (X. Lin et al., 2025; Y. Wang et al., 2017).

Finally, urban heat mitigation has direct implications for public health and social equity. Green and blue infrastructure can reduce heat-related morbidity and mortality, particularly benefiting vulnerable populations disproportionately affected by heat stress (Kwon et al., 2024; L. Larsen, 2015). Research emphasizes the importance of inclusive planning processes that prioritize heat mitigation in marginalized communities.

3.4.2.4 Methods and Modelling

Several studies have employed advanced numerical models to simulate urban microclimates and assess cooling scenarios, often integrating LCZ classification for more detailed spatial resolution. Commonly used models include WRF, ENVI-MET, and MUKLIMO_3 (Joshi & Teller, 2024; Martinelli et al., 2024; Pauly & Ferrero, 2024; Polydoros et al., 2023). As shown in Figure 3.4.4, the combination of multi-source remote sensing data with machine learning techniques has enhanced the accuracy of urban morphology and thermal environment assessments (Lu et al., 2024; H. Yu, Zhang, & Yu, 2025). However, the computational complexity and high data requirements of these high-resolution models have limited their widespread application in urban-scale planning (J. Chen et al., 2024).

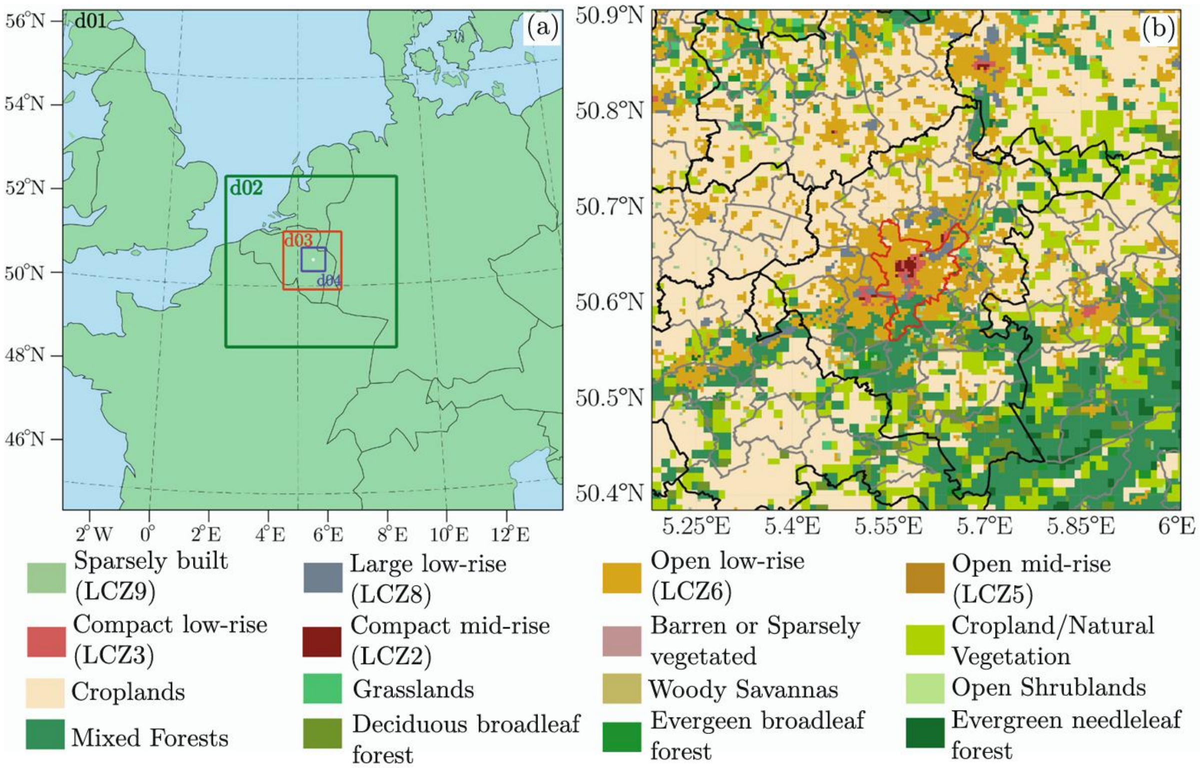

Figure 3.4.4 (a) The WRF model domain setup with four nested domains having resolutions of 9 km, 3 km, 1 km, and 333 m; (b) Urban land-use categories in the innermost domain (d04) after adding LCZ data from WUDAPT. Black borders indicate provinces, gray borders indicate municipalities, and the red border marks the Liège city boundary **(Joshi & Teller, 2024)**

Diverse methodological approaches, including remote sensing, computational fluid dynamics (CFD), machine learning, and microclimate simulation tools such as ENVI-met, InVEST, and TARGET, are used to quantify cooling effects and guide urban design decisions (J. Chen et al., 2024; Y. Hu et al., 2023; Ji et al., 2024; Qureshi et al., 2023; Silveira et al., 2024). These models enable scenario testing and optimization of green and blue infrastructure layouts, improving the precision of heat mitigation strategies across different spatial scales. Empirical field measurements are often employed to validate model results, reinforcing the reliability of interventions (Del Serrone et al., 2022; Nastos et al., 2024). To provide a clear overview of the input requirements and associated uncertainties for each model, the key parameters of the various modeling approaches are summarized in Tables 3.4.1 – 3.4.4:

Table 3.4.1 Letter-Based Parameters Used in ENVI-met and Their Sources of Uncertainty

Parameter	Full Name	Purpose	Sources of Uncertainty
LAD	Leaf Area Density	Canopy drag, radiation attenuation, transpiration	Species variation; seasonal change; measurement difficulty
LAI	Leaf Area Index	Shading and evapotranspiration	Remote-sensing retrieval error; heterogeneous canopy structure
α	Surface Albedo	Shortwave reflectance	Surface aging, moisture, soiling

Parameter	Full Name	Purpose	Sources of Uncertainty
ε	Surface Emissivity	Longwave radiation emission	Literature variability; material degradation
h_c	Canopy Height	Aerodynamic and shading effects	Growth, pruning, seasonal variability
R_s	Surface/Stomatal Resistance	Controls transpiration	Weather dependence; plant stress
R_n	Net Radiation	Surface energy balance	Cloud variability; simplified radiation schemes
T_s	Surface Temperature	Surface energy and heat exchange	Spatial material heterogeneity
T_a	Air Temperature	Atmospheric input	Street-level micro-variation
RH	Relative Humidity	ET and microclimate processes	Local humidity fluctuations
K	Incoming Shortwave Radiation	Radiative forcing	Cloud and aerosol variability
L	Longwave Radiation	Longwave exchange	Atmospheric composition, temperature profile

Table 3.4.2 Letter-Based Parameters Used in CFD (RANS/LES) Models and Their Sources of Uncertainty

Parameter	Full Name	Purpose	Sources of Uncertainty
k	Turbulent Kinetic Energy	Turbulence intensity	Boundary condition uncertainty
εt	Turbulent Dissipation Rate	Turbulence energy decay	Empirical model dependency
ω	Specific Dissipation Rate	Turbulence closure	Sensitive to model constants
νt	Eddy Viscosity	Turbulent mixing	Highly model dependent
$u(z)$	Wind Speed Profile	Inflow boundary condition	Urban roughness causes profile deviation
z_0	Roughness Length	Aerodynamic roughness	City morphology simplified into one parameter
θ	Potential Temperature	Buoyancy and atmospheric stability	Measurement scarcity; temporal variability
C_p	Heat Capacity	Material thermal storage	Simplified representation of multilayer structures
λ (*ks*)	Thermal Conductivity	Heat conduction	Depends on moisture and material heterogeneity
T_s	Surface Temperature	Thermal boundary	Strong spatial variations; solar exposure
q''	Heat Flux	Surface heat forcing	Hard to measure; parameterization uncertainty

Parameter	Full Name	Purpose	Sources of Uncertainty
ρ	Air Density	Buoyancy and heat transfer	Influenced by temperature variability

Table 3.4.3 Letter-Based Parameters Used in the TARGET Urban Cooling Model and Their Sources of Uncertainty

Parameter	Full Name	Purpose	Sources of Uncertainty
LAI	Leaf Area Index	Controls shading and radiative attenuation	Seasonal variability; retrieval uncertainty
α	Albedo	Surface reflectance	Aging, weathering, contamination
ε	Emissivity	Longwave radiation	Material and measurement variability
K	Shortwave Radiation	Radiative input	Cloud cover; atmospheric conditions
T_a	Air Temperature	Background climate	Spatial heterogeneity
RH	Relative Humidity	Evaporative cooling	Local moisture variability
u	Wind Speed	Convective exchange	Strong turbulence in street canyons
T_s	Surface Temperature	Radiative balance	Spatial heterogeneity in urban materials

Table 3.4.4 Letter-Based Parameters Used in the InVEST Urban Cooling Model and Their Sources of Uncertainty

Parameter	Full Name	Purpose	Sources of Uncertainty
NDVI	Normalized Difference Vegetation Index	Vegetation fraction, cooling potential	Satellite resolution; atmospheric correction
EVI	Enhanced Vegetation Index	Vegetation structure	Sensor noise; algorithm dependency
LAI	Leaf Area Index	ET and vegetation cooling	Seasonal and spatial variation
α	Albedo	Surface reflectivity	Imaging time; material variability
LST	Land Surface Temperature	Baseline cooling assessment	Thermal IR retrieval error
T_a	Reference Air Temperature	Cooling estimation	Limited representativeness of stations
RH	Relative Humidity	ET-related processes	Spatial gradients

3.4.2.5 Integration and Conceptual Frameworks

The integration of green and blue infrastructure is increasingly recognized as a key strategy for enhancing urban thermal resilience. Synergistic deployment of green and blue elements addresses both heat stress and environmental quality, contributing to urban sustainability. Integrated approaches consider multiple ecosystem services, balancing cooling performance with co-benefits such as air quality improvement and biodiversity support. Research highlights the need for coordinated planning to optimize the distribution and interaction of these infrastructures across spatial scales for maximum thermal comfort and environmental benefits (de la Barrera & Reyes-Paecke, 2021; Kumar et al., 2024; Pereira et al., 2023; Q. Wu et al., 2024).

Several studies have developed conceptual frameworks that link urban green infrastructure (UGI), spatial configuration, and microclimate regulation, providing a theoretical basis for understanding the relationships between landscape elements and spatial climate outcomes (Clark et al., 2010; Ji et al., 2024b). Spatial configuration refers to the composition and arrangement of elements, which determine their cooling efficiency and interactions with urban morphology (Maimaitiyiming et al., 2014; Y. Wang et al., 2017). These frameworks support the evaluation of planning interventions aimed at reducing thermal uncertainty and improving urban microclimates (X. Lin et al., 2025).

3.4.2.6 Summary and Future Outlook

Despite extensive research, spatial climate uncertainty in urban environments remains inadequately addressed, particularly regarding the influence of specific landscape elements on microclimate variability. While the cooling effects of green spaces and water bodies have been quantified, knowledge gaps persist in understanding the combined and configuration-dependent impacts of these elements on urban thermal heterogeneity (Ghosh & Das, 2018; Silveira et al., 2024). Controversies exist over the relative effectiveness of different green infrastructure types, such as street trees versus parks (Qureshi et al., 2023), and potential trade-offs between cooling performance and pollutant dispersion (Q. Wu et al., 2024). Future research should develop integrated, multi-disciplinary frameworks that encompass ecological, morphological, climatic, and social dimensions to optimize landscape interventions. Such an integrated approach will support urban planners in creating climate-resilient, thermally comfortable, and sustainable urban environments that are responsive to local conditions and evolving climate challenges.

3.4.3 References

A. Sharbaf, S., & Schneider-Marin, P. (2025). Cost-benefit analysis of sustainable upgrades in existing buildings: A critical review. *Energy and Buildings*, *328*, 115142. https://doi.org/10.1016/j.enbuild.2024.115142

Abdullah, H. K., & Alibaba, H. Z. (2022). A Performance-Based Window Design and Evaluation Model for Naturally Ventilated Offices. *Buildings*, *12*(8), 1141–1141. https://doi.org/10.3390/BUILDINGS12081141

Abuku, M., Janssen, H., & Roels, S. (2009). Impact of wind-driven rain on historic brick wall buildings in a moderately cold and humid climate: Numerical analyses of mould growth risk, indoor climate and energy consumption. *Energy and Buildings*, *41*(1), 101–110. https://doi.org/10.1016/j.enbuild.2008.07.011

Adeli, M. M., Sarhaddi, F., & Farahat, S. (2019). Parametric Study of the Impact of Windows to Wall Ratio on Reduction of Energy Consumption and Environmental Impact of a Zero-Energy Building in Different Orientations. *Applied and Computational Mechanics*, *50*(2), 295–302. https://doi.org/10.22059/JCAMECH.2019.288460.424

Aflaki, A., Mahyuddin, N., Al-Cheikh Mahmoud, Z., & Baharum, M. R. (2015). A review on natural ventilation applications through building façade components and ventilation openings in tropical climates. *Energy and Buildings*, *101*, 153–162. https://doi.org/10.1016/J.ENBUILD.2015.04.033

Aït Oumeziane, Y., Moissette, S., Bart, M., Collet, F., Pretot, S., & Lanos, C. (2017). Influence of hysteresis on the transient hygrothermal response of a hemp concrete wall. *Journal of Building Performance Simulation*, *10*(3), 256–271. https://doi.org/10.1080/19401493.2016.1216166

Akhavan Shams, S., Ge, H., & Wang, L. (2024). Hygrothermal modeling in mass timber constructions: Recent advances and machine learning prospects. *Journal of Building Engineering*, *96*, 110500. https://doi.org/10.1016/j.jobe.2024.110500

Al Rikabi, I. J., Abuelnour, M. A., Omara, A. A. M., Ismail, N. A., Ani, F. N., & Abuelnuor, A. A. A. (2022). A numerical Study of the Effect of Façade Opening on Nighttime Ventilation of a Low-Energy Building. *8th IEC 2022 - International Engineering Conference: Towards Engineering Innovations and Sustainability*, 129–135. https://doi.org/10.1109/IEC54822.2022.9807454

Alazazmeh, A., & Asif, M. (2021). Commercial building retrofitting: Assessment of improvements in energy performance and indoor air quality. *Case Studies in Thermal Engineering*, *26*, 100946. https://doi.org/10.1016/j.csite.2021.100946

Alcazar, S. S., Olivieri, F., & Neila, J. (2016). Green roofs: Experimental and analytical study of its potential for urban microclimate regulation in Mediterranean–continental climates. *Urban Climate*, *17*, 304–317. https://doi.org/10.1016/J.UCLIM.2016.02.004

Ali, M., Oladokun, M. O., Osman, S. B., Mohd Din, S. A., Ibrahim, M. S., & Yusof, F. (2016). Hygrothermal performance of building envelopes in the tropics under operative conditions: condensation and mould growth risk appraisal. *Jurnal Teknologi*, *78*(5), 271–279. https://doi.org/10.11113/JT.V78.8309

Ali, M., Oladokun, M. O., Osman, S. B., Samsuddin, N., & Hamzah, H. A. (2016). Moisture condensation on building envelopes in differential ventilated spaces in the tropics: Quantitative assessment of influencing factors. *MATEC Web of Conferences*, *66*. https://doi.org/10.1051/MATECCONF/20166600089

Ali, R. A., Megahed, N. A., Shahda, M. M., & Hassan, A. M. (2023). Natural ventilation as a passive cooling strategy for multi-story buildings: analytic vertical skycourt formations. *City, Territory and Architecture*, *10*(1), 1–16. https://doi.org/10.1186/S40410-023-00212-6/TABLES/1

Alsehail, A., & Almhafdy, A. (2020). The Effect of Window-to-Wall Ratio (WWR) and Window Orientation (WO) on the Thermal Performance: A preliminary overview. *Environment-Behaviour Proceedings Journal*, *5*(15), 165–173. https://doi.org/10.21834/EBPJ.V5I15.2500

Amaripadath, D., & Sailor, D. J. (2024). Reassessing energy-efficient passive retrofits in terms of indoor environmental quality in residential buildings in the United States. *Energy and Buildings*, *319*, 114564. https://doi.org/10.1016/j.enbuild.2024.114564

Amorim, M., de Freitas, V. P., & Torres, I. (2024). Influence of Moisture on the Energy Performance of Retrofitted Walls - Experimental Assessment and Validation of an Hygrothermal Model. *International Journal of Architectural Heritage*, *18*(3), 477–491. https://doi.org/10.1080/15583058.2022.2157777

Andrian, V., & Craske, J. (2023). Stochastic models of ventilation driven by opposing wind and buoyancy. *Proceedings of the Royal Society A: Mathematical, Physical and Engineering Sciences*, *479*(2276). https://doi.org/10.1098/rspa.2023.0170

Antretter, F., Sauer, F., Schöpfer, T., & Holm, A. (2011). Validation of hygrothermal whole building simulation software. *Proceedings of Building Simulation 2011*, 1694–1701.

Anwar, A., Younis, M., & Ullah, I. (2020). Impact of Urbanization and Economic Growth on CO2 Emission: A Case of Far East Asian Countries. *International Journal of Environmental Research and Public Health*, *17*(7), 2531. https://doi.org/10.3390/ijerph17072531

ASHRAE. (1967). *ASHRAE Handbook 1967 Fundamentals*. ASHRAE.

Asturias-Schaub, L. R., & Gil-Alana, L. A. (2023). CO2 emissions in Latin America: a time series perspective based on fractional integration. *Environmental Science and Pollution Research*, *30*(50), 109585–109605. https://doi.org/10.1007/s11356-023-29987-4

Athauda, R. S., Asmone, A. S., & Conejos, S. (2023). Climate Change Impacts on Facade Building Materials: A Qualitative Study. *Sustainability*, *15*(10), 7893. https://doi.org/10.3390/su15107893

Azkorra, Z., Pérez, G., Coma, J., Cabeza, L. F., Bures, S., Álvaro, J. E., Erkoreka, A., & Urrestarazu, M. (2015). Evaluation of green walls as a passive acoustic insulation system for buildings. *Applied Acoustics*, *89*, 46–56. https://doi.org/10.1016/J.APACOUST.2014.09.010

Bakkour, A., Ouldboukhitine, S. E., Biwole, P., & Amziane, S. (2025). Modeling heat and moisture transfer in bio-based wall structures using the finite element method: Application to straw walls in varied climatic conditions. *Journal of Building Engineering*, *104*. https://doi.org/10.1016/j.jobe.2025.112263

Bastide, A., Lucas, F., & Boyer, H. (2014). *Impact of the atmospheric boundary layer profile on the ventilation of a cubic building with two large opposite openings*. https://arxiv.org/pdf/1409.7080

Bastien, D., & Winther-Gaasvig, M. (2018). Influence of driving rain and vapour diffusion on the hygrothermal performance of a hygroscopic and permeable building envelope. *Energy*, *164*(46), 288–297. https://doi.org/10.1016/j.energy.2018.07.195

Bayat Pour, M., Niklewski, J., Naghibi, A., & Frühwald Hansson, E. (2024a). A literature review of probabilistic hygrothermal assessment for building envelopes. *Building and Environment*, *261*, 111756. https://doi.org/10.1016/j.buildenv.2024.111756

Bayat Pour, M., Niklewski, J., Naghibi, A., & Frühwald Hansson, E. (2024b). A literature review of probabilistic hygrothermal assessment for building envelopes. In *Building and Environment* (Vol. 261). Elsevier Ltd. https://doi.org/10.1016/j.buildenv.2024.111756

Bechtel, B., Alexander, P. J., Böhner, J., Ching, J., Conrad, O., Feddema, J., Mills, G., See, L., & Stewart, I. (2015). Mapping Local Climate Zones for a Worldwide Database of the Form and Function of Cities. *ISPRS International Journal of Geo-Information 2015, Vol. 4, Pages 199-219*, *4*(1), 199–219. https://doi.org/10.3390/IJGI4010199

Belloum, R., Agoudjil, B., Chennouf, N., & Boudenne, A. (2022). Hygrothermal performance assessment of a bio-based building made with date palm concrete walls. *Building and Environment*, *223*. https://doi.org/10.1016/j.buildenv.2022.109467

Benmahiddine, F., Bennai, F., Charaka, A., Hamami, A. E. A., Tahakourt, A., & Belarbi, R. (2024). Multi-scale analysis of the effects of hysteresis on the hydrothermal behaviour of bio-based materials: Application to hemp concrete. *Construction and Building Materials*, *411*. https://doi.org/10.1016/j.conbuildmat.2023.134107

Berardi, U. (2017). A cross-country comparison of the building energy consumptions and their trends. *Resources, Conservation and Recycling*, *123*, 230–241. https://doi.org/10.1016/j.resconrec.2016.03.014

Bielawski, J., Papis, B. K., Krajewski, G., & Węgrzyński, W. (2024). An exploratory investigation into moisture content and wind impact on the fire behaviour of modular living walls. *Fire Safety Journal*, *142*, 104024. https://doi.org/10.1016/J.FIRESAF.2023.104024

Bienvenido-Huertas, D., de la Hoz-Torres, M. L., Aguilar, A. J., Tejedor, B., & Sánchez-García, D. (2023). Holistic overview of natural ventilation and mixed mode in built environment of warm climate zones and hot seasons. *Building and Environment*, *245*. https://doi.org/10.1016/J.BUILDENV.2023.110942

Blanco, I., & Convertino, F. (2023). Thermal performance of green façades: research trends analysis using a science mapping approach. *Sustainability*, *15*(13), 9981. https://doi.org/10.3390/su15139981

Blocken, B., & Carmeliet, J. (2000). Driving rain on building envelopes-I. Numerical estimation and full-scale experimental verification. *Journal of Thermal Envelope and Building Science*, *24*(1), 61–85.

Blocken, B., & Carmeliet, J. (2004). A review of wind-driven rain research in building science. *Journal of Wind Engineering and Industrial Aerodynamics*, *92*, 1079–1130. https://doi.org/10.1016/j.jweia.2004.06.003

Blocken, B., & Carmeliet, J. (2006). The influence of the wind-blocking effect by a building on its wind-driven rain exposure. *Journal of Wind Engineering and Industrial Aerodynamics*, *94*(2), 101–127. https://doi.org/10.1016/j.jweia.2005.11.001

Blocken, B., & Carmeliet, J. (2007). Validation of CFD simulations of wind-driven rain on a low-rise building facade. *Building and Environment*, *42*(7), 2530–2548. https://doi.org/10.1016/j.buildenv.2006.07.032

Cabeza, L. F., Bai, Q., Bertoldi, P., Kihila, J. M., Lucena, A. F. P., Mata, E., Mirasgedis, S., Novikova, A., & Saheb, Y. (2022). Buildings. In P. R. Shukla, J. Skae, R. Slade, A. Al Khourdajie, R. Van Diemen, D. McCollum, M. Pathak, S. Some, P. Vyas, R. Fradera, M. Belkacemi, A. Hasija, G. Lisboa, S. Luz, & J. Malley (Eds.), *Climate Change 2022 - Mitigation of Climate Change. Contribution of Working Group III to the Sixth Assessment Report of the Intergovernmental Panel on Climate Change* (pp. 953–1048). Cambridge University Press. https://doi.org/10.1017/9781009157926.011

Cai, Y., Gao, C., Pan, W., Chen, Y., & Wu, Z. (2024). Research on Optimal Cooling Landscape Combination and Configuration Based on Local Climate Zones—Fuzhou, China. *Sustainability (Switzerland)* , *16*(6), 2367. https://doi.org/10.3390/SU16062367/S1

Chabada, M., & Juras, P. (2025). Numerical Study: Substrate Thickness and Type of Roof Structure and Their Impact on the Thermal Behavior of Green Roofs. *Buildings 2025*, *Vol. 15*, *Page 3240*, *15*(17), 3240. https://doi.org/10.3390/BUILDINGS15173240

Chaudhry, D. (2024). Climate change and health of the urban poor: The role of environmental justice. *The Journal of Climate Change and Health*, *15*, 100277. https://doi.org/10.1016/j.joclim.2023.100277

Chen, G., Zhao, L., & Mochida, A. (2016). Urban Heat Island Simulations in Guangzhou, China, Using the Coupled WRF/UCM Model with a Land Use Map Extracted from Remote Sensing Data. *Sustainability 2016*, *Vol. 8*, *Page 628*, *8*(7), 628. https://doi.org/10.3390/SU8070628

Chen, J., Bach, P. M., Nice, K. A., & Leitão, J. P. (2024). Investigating the efficacy of a fast urban climate model for spatial planning of green and blue spaces for heat mitigation. *Science of The Total Environment*, *955*, 176925. https://doi.org/10.1016/J.SCITOTENV.2024.176925

Chen, Q., Li, B., & Liu, X. (2013). An experimental evaluation of the living wall system in hot and humid climate. *Energy and Buildings*, *61*, 298–307. https://doi.org/10.1016/j.enbuild.2013.02.030

Chen, W., Pan, J., Quan, J., Wei, H., & Wang, W. (2026). Scalable impact of urban green infrastructure on urban climate: A critical review. In *Renewable and Sustainable Energy Reviews* (Vol. 226). Elsevier Ltd. https://doi.org/10.1016/j.rser.2025.116259

Cherif, N., Lopes, H., & Silva, L. (2024). *The extent of the impact of green spaces on urban heat islands: A meta-analysis of research using remote sensing between 2010 and 2023*. https://assets-eu.researchsquare.com/files/rs-4534390/v1/81dfb491-79bf-4282-a154-c0f30372858e.pdf

Chung, D., Wen, J., & Lo, L. C. J. (2023). Examining the impact of stochastic multi-year weather and air infiltration on hygrothermal moisture risks. *Journal of Building Physics*, *47*(1), 4–35. https://doi.org/10.1177/17442591231163459

Chung, D., Wen, J., & Lo, L. J. (2020). Development and verification of the open source platform, HAM-Tools, for hygrothermal performance simulation of buildings using a stochastic approach. *Building Simulation*, *13*(3), 497–514. https://doi.org/10.1007/s12273-019-0594-5

Clark, C., Busiek, B., River, P. A.-C. of the F., & 2010, undefined. (2010). Quantifying thermal impacts of green infrastructure: Review and gaps. *CiteseerC Clark, B Busiek, P AdriaensCities of the Future/Urban River Restoration Conference 2010, 2010•Citeseer*. https://citeseerx.ist.psu.edu/document?repid=rep1&type=pdf&doi=e97c126c135bed02963b680a5ba3775bb3aa69ff

Coelho, G. B. A., Silva, H. E., & Henriques, F. M. A. (2018). Calibrated hygrothermal simulation models for historical buildings. *Building and Environment*, *142*, 439–450. https://doi.org/10.1016/j.buildenv.2018.06.034

Collins, S., Kuoppamäki, K., Kotze, D. J., & Lü, X. (2017). Thermal behavior of green roofs under Nordic winter conditions. *Building and Environment*, *122*, 206–214. https://doi.org/10.1016/J.BUILDENV.2017.06.020

COMSOL. (n.d.). Retrieved July 3, 2024, from https://www.comsol.com/

Coşar, M., Harputlugil, G. U., & De Wilde, P. (2023). Rethinking natural ventilation strategies in buildings through simulation. *Building Simulation Conference Proceedings*, *18*, 2196–2203. https://doi.org/10.26868/25222708.2023.1462

Cui, S., Cohen, M., Stabat, P., & Marchio, D. (2015). CO2 tracer gas concentration decay method for measuring air change rate. *Building and Environment*, *84*, 162–169. https://doi.org/10.1016/J.BUILDENV.2014.11.007

D'Agostino, D., Becchio, C., Crespi, G., & Corgnati, S. P. (2023). Assessment of passive and active buildings resilience to gas supply disruption in winter across European climates. *Sustainable Cities and Society*, *92*, 104461. https://doi.org/10.1016/j.scs.2023.104461

Dang, X., Guimarães, A. S., Sarkany, A., Laukkarinen, A., Xu, B., Vanderschelden, B., Rode, C., Xia, C., Feng, C., Whitman, C., Deckers, D., Yang, H., Fechner, H., Sharma, H., Ge, H., Xie, H., Zhang, H., Vandemeulebroucke, I., Mazura, J., ... Roels, S. (2025). A state-of-the-art empirical round robin validation of heat, air and moisture (HAM) models. *Building and Environment*, *276*, 112867. https://doi.org/10.1016/j.buildenv.2025.112867

Das, S., Choudhury, M. R., Chatterjee, B., Das, P., Bagri, S., Paul, D., Bera, M., & Dutta, S. (2024). Unraveling the urban climate crisis: Exploring the nexus of urbanization, climate change, and their impacts on the environment and human well-being – A global perspective. *AIMS Public Health*, *11*(3), 963–1001. https://doi.org/10.3934/publichealth.2024050

de la Barrera, F., & Reyes-Paecke, S. (2021). Green Infrastructure to Mitigate Extreme Temperatures in Cities. *Urban Microclimate Modelling for Comfort and Energy Studies*, 403–417. https://doi.org/10.1007/978-3-030-65421-4_19

de Oliveira Santos, T. D., Pacheco, F. A. L., & Fernandes, L. F. S. (2024). A systematic analysis on the efficiency and sustainability of green facades and roofs. *Science of The Total Environment*, *932*, 173107. https://doi.org/10.1016/J.SCITOTENV.2024.173107

de Wit, S., & Augenbroe, G. (2002). Analysis of uncertainty in building design evaluations and its implications. *Energy and Buildings*, *34*(9), 951–958. https://doi.org/10.1016/S0378-7788(02)00070-1

Debata, Y., & Ogura, D. (2025). Effects of Airtightness and Ventilation on the Humidity Environment of Non-residential Spaces in Detached Houses. *Lecture Notes in Civil Engineering*, *555 LNCE*, 3–9. https://doi.org/10.1007/978-981-97-8317-5_1

Del Serrone, G., Peluso, P., & Moretti, L. (2022a). Evaluation of Microclimate Benefits Due to Cool Pavements and Green Infrastructures on Urban Heat Islands. *Atmosphere 2022, Vol. 13, Page 1586*, *13*(10), 1586. https://doi.org/10.3390/ATMOS13101586

Del Serrone, G., Peluso, P., & Moretti, L. (2022b). Evaluation of Microclimate Benefits Due to Cool Pavements and Green Infrastructures on Urban Heat Islands. *Atmosphere*, *13*(10), 1586–1586. https://doi.org/10.3390/ATMOS13101586

DELPHIN. (n.d.). Retrieved March 29, 2025, from https://bauklimatik-dresden.de/

Deng, J. Y., Xia, Y., Lao, H., Ye, Y., Wang, Z., & Jiang, H. (2024). Natural ventilation potential of teaching building complexes with different block shapes and layout patterns. *Journal of Building Engineering*, *96*, 110420–110420. https://doi.org/10.1016/J.JOBE.2024.110420

Derakhshan, S., & Shaker, A. (2017a). Numerical study of the cross-ventilation of an isolated building with different opening aspect ratios and locations for various wind directions. *International Journal of Ventilation*, *16*(1), 42–60. https://doi.org/10.1080/14733315.2016.1252146;WEBSITE:WEBSITE:TFOPB;PAGEGROUP:STRING:PUBLICATION

Derakhshan, S., & Shaker, A. (2017b). Numerical study of the cross-ventilation of an isolated building with different opening aspect ratios and locations for various wind directions. *International Journal of Ventilation*, *16*(1), 42–60. https://doi.org/10.1080/14733315.2016.1252146

Duan, Z., Omrany, H., & Zuo, J. (2025). Impact of climate change on energy performance and energy conservation measures effectiveness in Australian office buildings. *Energy*, *319*, 134956. https://doi.org/10.1016/j.energy.2025.134956

El Menchawy, A. S., Elkholy, M. A., & Mohamed, A. F. A. (2025). Applying green roof in an educational building in the hot arid zone to achieve thermal comfort. *Journal of Umm Al-Qura University for Engineering and Architecture 2025*, 1–15. https://doi.org/10.1007/S43995-025-00209-X

Elaouzy, Y., & El Fadar, A. (2022). Energy, economic and environmental benefits of integrating passive design strategies into buildings: A review. *Renewable and Sustainable Energy Reviews*, *167*, 112828. https://doi.org/10.1016/j.rser.2022.112828

Elnagar, E., Düvier, C., Batra, Z., Christoffersen, J., Mandin, C., Schweiker, M., & Wargocki, P. (2024). Creating a comprehensive framework for design, construction and management of healthy buildings. *Energy and Buildings*, *324*, 114883. https://doi.org/10.1016/j.enbuild.2024.114883

EnergyPlus. (n.d.). Retrieved July 3, 2024, from https://energyplus.net/

Erkal, A., D'Ayala, D., & Sequeira, L. (2012). Assessment of wind-driven rain impact, related surface erosion and surface strength reduction of historic building materials. *Building and Environment*, *57*, 336–348. https://doi.org/10.1016/j.buildenv.2012.05.004

Feng, X., Wen, H., He, M., & Xiao, Y. (2023). Microclimate effects and influential mechanisms of four urban tree species underneath the canopy in hot and humid areas. *Frontiers in Environmental Science*, *11*, 1108002. https://doi.org/10.3389/FENVS.2023.1108002/BIBTEX

Ferroukhi, M. Y., Abahri, K., Belarbi, R., & Limam, K. (2017). Integration of a hygrothermal transfer model for envelope in a building energy simulation model: experimental validation of a HAM–BES co-simulation approach. *Heat and Mass Transfer/Waerme- Und Stoffuebertragung*, *53*(6), 1851–1861. https://doi.org/10.1007/s00231-016-1944-9

Ferroukhi, M. Y., Djedjig, R., Limam, K., & Belarbi, R. (2016). Hygrothermal behavior modeling of the hygroscopic envelopes of buildings: A dynamic co-simulation approach. *Building Simulation*, *9*(5), 501–512. https://doi.org/10.1007/s12273-016-0292-5

Fontenelle, M. R., Bastos, L. E. G., & Lorente, S. (2021). Natural ventilation for office building retrofit in dense urban context under hot and humid climate. *Ambiente Construído*, *21*(2), 67–87. https://doi.org/10.1590/S1678-86212021000200515

Foroushani, S. S. M., Ge, H., & Naylor, D. (2014). Effects of roof overhangs on wind-driven rain wetting of a low-rise cubic building: A numerical study. *Journal of Wind Engineering and Industrial Aerodynamics*, *125*, 38–51. https://doi.org/10.1016/j.jweia.2013.10.007

Gangolells, M., Gaspar, K., Casals, M., Ferré-Bigorra, J., Forcada, N., & Macarulla, M. (2020). Life-cycle environmental and cost-effective energy retrofitting solutions for office stock. *Sustainable Cities and Society*, *61*, 102319. https://doi.org/10.1016/j.scs.2020.102319

Gao, X., Yang, C., Chen, L., Lu, N., Li, A., & Meng, F. (2022). Review on buoyancy-driven natural ventilation in an enclosure with various types of heat sources. *E3S Web of Conferences*, *356*, 03062. https://doi.org/10.1051/E3SCONF/202235603062

Gao, Z., & He, B. J. (2024). A review of classified regional ventilation strategies based on urban morphology. *IOP Conference Series*, *1363*(1), 012075–012075. https://doi.org/10.1088/1755-1315/1363/1/012075

Ge, H. (2015). Influence of time resolution and averaging techniques of meteorological data on the estimation of wind-driven rain load on building facades for Canadian climates. *Journal of Wind Engineering and Industrial Aerodynamics*, *143*, 50–61. https://doi.org/10.1016/j.jweia.2015.04.019

Ge, H., Chiu, V., & Stathopoulos, T. (2017). Effect of overhang on wind-driven rain wetting of facades on a mid- rise building : Field measurements. *Building and Environment*, *118*, 234–250. https://doi.org/10.1016/j.buildenv.2017.03.034

Ge, H., Deb Nath, U. K., & Chiu, V. (2017). Field measurements of wind-driven rain on mid- and high-rise buildings in three Canadian regions. *Building and Environment*, *116*, 228–245. https://doi.org/10.1016/j.buildenv.2017.02.016

Gholamalipour, P., Ge, H., & Stathopoulos, T. (2022). Wind-driven rain (WDR) loading on building facades: A state-of-the-art review. *Building and Environment*, *221*, 109314. https://doi.org/10.1016/j.buildenv.2022.109314

Gholamalipour, P., Ge, H., & Stathopoulos, T. (2024a). CFD modeling of Wind-Driven Rain (WDR) on a mid-rise building in an urban area. *Journal of Wind Engineering and Industrial Aerodynamics*, *245*. https://doi.org/10.1016/j.jweia.2023.105637

Gholamalipour, P., Ge, H., & Stathopoulos, T. (2024b). Impact of upstream buildings on Wind-Driven Rain Loading: Refining Obstruction Factor in ISO semi-empirical model based on CFD. *Journal of Building Engineering*, *97*, 110717. https://doi.org/10.1016/J.JOBE.2024.110717

Gholamalipour, P., Stathopoulos, T., & Ge, H. (2025). Refined ISO model for Wind-Driven Rain (WDR) on buildings: Machine Learning-based approach. *Building and Environment*, 113522. https://doi.org/10.1016/j.buildenv.2025.113522

Ghosh, S., & Das, A. (2018). Modelling urban cooling island impact of green space and water bodies on surface urban heat island in a continuously developing urban area. *Modeling*

Earth Systems and Environment, *4*(2), 501–515. https://doi.org/10.1007/S40808-018-0456-7/TABLES/8

Glaser H. (1958). Simplified calculation of vapor diffusion through layered walls with precipitation of water and ice. *Refrigeration Technology*, *10*(11), 358–364.

Goia, F. (2016). Search for the optimal window-to-wall ratio in office buildings in different European climates and the implications on total energy saving potential. *Solar Energy*, *132*, 467–492. https://doi.org/10.1016/J.SOLENER.2016.03.031

González-Torres, M., Pérez-Lombard, L., Coronel, J. F., Maestre, I. R., & Yan, D. (2022). A review on buildings energy information: Trends, end-uses, fuels and drivers. *Energy Reports*, *8*, 626–637. https://doi.org/10.1016/j.egyr.2021.11.280

Gough, H. (2017). *Effects of meteorological conditions on building natural ventilation in idealised urban settings*. https://centaur.reading.ac.uk/id/eprint/71951

Hagentoft, C.-E. (2017). Reliability of energy efficient building retrofitting - probability assessment of performance and cost (Annex 55, RAP-RETRO). *Energy and Buildings*, *155*, 166–171. https://doi.org/10.1016/j.enbuild.2017.09.007

Hakim, M. N., Ekasiwi, S. N. N., & Samodra, F. X. T. B. (2025). Design parameters for enhancing passive ventilation using vertical void in hot humid climate with high density. *IOP Conference Series*, *1439*(1), 012028–012028. https://doi.org/10.1088/1755-1315/1439/1/012028

Harbiankova, A., & Manso, M. (2025). Integrating green roofs and green walls to enhance buildings thermal performance: A literature review. *Building and Environment*, *270*, 112524. https://doi.org/10.1016/J.BUILDENV.2025.112524

Hens, H. L. S. C. (2015). Combined heat, air, moisture modelling: A look back, how, of help? *Building and Environment*, *91*, 138–151. https://doi.org/10.1016/j.buildenv.2015.03.009

Hilbrecht, R., Cruickshank, C. A., Baldwin, C., & Scharf, N. (2025). A Rapid Review of Hygrothermal Performance Metrics for Innovative Materials in Building Envelope Retrofits. *Energies*, *18*(18), 5016. https://doi.org/10.3390/en18185016

Hittle, D. (1977). *The Building Loads Analysis and System Thermodynamics (BLAST) Program: Vol I: User's manual*.

Hu, H., Kikumoto, H., Ooka, R., Lin, C., & Zhang, B. (2022). Comprehensive validation of experimental and numerical natural ventilation predictions based on field measurement with experimental house. *Building and Environment*, *207*, 108433. https://doi.org/10.1016/J.BUILDENV.2021.108433

Hu, X., Zhang, H., & Yu, H. (2023). Numerical simulation study on the hygrothermal performance of building exterior walls under dynamic wind-driven rain condition.

Building Simulation 2023 17:2, *17*(2), 207–221. https://doi.org/10.1007/s12273-023-1076-3

Hu, Y., Wang, C., & Li, J. (2023). Assessment of Heat Mitigation Services Provided by Blue and Green Spaces: An Application of the InVEST Urban Cooling Model with Scenario Analysis in Wuhan, China. *Land 2023*, *Vol. 12*, *Page 963*, *12*(5), 963. https://doi.org/10.3390/LAND12050963

Hung, Y. C. (2024). A review of Monte Carlo and quasi-Monte Carlo sampling techniques. In *Wiley Interdisciplinary Reviews: Computational Statistics* (Vol. 16, Number 1). John Wiley and Sons Inc. https://doi.org/10.1002/wics.1637

IEA. (2023). *Net Zero Roadmap- A Global Pathway to Keep the 1.5 degree C Goal in Reach*.

IEA. (2024). *World energy outlook 2024*.

IPCC. (2023). *Climate Change 2023: Synthesis Report, Summary for Policymakers. Contribution of Working Groups I, II and III to the Sixth Assessment Report of the Intergovernmental Panel on Climate Change [Core Writing Team, H. Lee and J. Romero (eds.)]. IPCC, Geneva, Switzerland.* https://doi.org/10.59327/IPCC/AR6-9789291691647.001

J. R. Philip, & D. A. De Vries. (1957). Moisture movement in porous materials under temperature gradients. *Eos, Transactions American Geophysical Union*, *38*(2), 222–232. https://doi.org/10.1029/TR038i002p00222

Jandaghian, Z., & Colombo, A. (2024). The Role of Water Bodies in Climate Regulation: Insights from Recent Studies on Urban Heat Island Mitigation. *Buildings 2024*, *Vol. 14*, *Page 2945*, *14*(9), 2945. https://doi.org/10.3390/BUILDINGS14092945

Janssen, H. (2013). Monte-Carlo based uncertainty analysis: Sampling efficiency and sampling convergence. *Reliability Engineering and System Safety*, *109*, 123–132. https://doi.org/10.1016/j.ress.2012.08.003

Ji, L., Shu, C., Gaur, A., Wang, L., & Lacasse, M. (2024a). A state-of-the-art review of studies on urban green infrastructure for thermal resilient communities. *Building and Environment*, *257*, 111524. https://doi.org/10.1016/J.BUILDENV.2024.111524

Ji, L., Shu, C., Gaur, A., Wang, L., & Lacasse, M. (2024b). A state-of-the-art review of studies on urban green infrastructure for thermal resilient communities. *Building and Environment*, *257*, 111524. https://doi.org/10.1016/J.BUILDENV.2024.111524

Jia Li. (2023). Research on Building Design Methods Based on Natural Ventilation. *Design*, *08*(03), 1515–1521. https://doi.org/10.12677/DESIGN.2023.83181

Jia, S., Weng, Q., Yoo, C., Xiao, H., & Zhong, Q. (2024). Building energy savings by green roofs and cool roofs in current and future climates. *Npj Urban Sustainability 2024 4:1*, *4*(1), 1–13. https://doi.org/10.1038/s42949-024-00159-8

Jiang, Z., Kobayashi, T., Yamanaka, T., & Sandberg, M. (2023). A literature review of cross ventilation in buildings. *Energy and Buildings*, *291*, 113143. https://doi.org/10.1016/J.ENBUILD.2023.113143

Johari, F., Peronato, G., Sadeghian, P., Zhao, X., & Widén, J. (2020). Urban building energy modeling: State of the art and future prospects. In *Renewable and Sustainable Energy Reviews* (Vol. 128). Elsevier Ltd. https://doi.org/10.1016/j.rser.2020.109902

Joshi, M. Y., & Teller, J. (2024). Assessing urban heat island mitigation potential of realistic roof greening across local climate zones: A highly-resolved weather research and forecasting model study. *Science of The Total Environment*, *944*, 173728. https://doi.org/10.1016/J.SCITOTENV.2024.173728

Juan, Y. H., Li, Z., Lee, Y. T., Wen, C. Y., & Yang, A. S. (2023). Effect of wind-based climate-responsive design on city breathability of a compact high-rise city. *Journal of Building Engineering*, *78*. https://doi.org/10.1016/J.JOBE.2023.107773

Jurgilevich, A., Käyhkö, J., Räsänen, A., Pörsti, S., Lagström, H., Käyhkö, J., & Juhola, S. (2023). Factors influencing vulnerability to climate change-related health impacts in cities – A conceptual framework. *Environment International*, *173*, 107837. https://doi.org/10.1016/j.envint.2023.107837

Kaczmarek, A. (2025). A State-of-the-Art Review of Retrofit Interventions in Low-Emission School Buildings Located in Cool Temperate Climates. *Buildings*, *15*(10), 1620. https://doi.org/10.3390/buildings15101620

Kalagasidis, A. S. (2004). *HAM-Tools: an integrated simulation tool for heat, air and moisture transfer analyses in building physics*. Chalmers Tekniska Hogskola (Sweden).

Kamel, E., & Memari, A. (2022). Residential Building Envelope Energy Retrofit Methods, Simulation Tools, and Example Projects: A Review of the Literature. *Buildings*, *12*(7), 954. https://doi.org/10.3390/buildings12070954

Karava, P., Stathopoulos, T., & Athienitis, A. K. (2007). Wind-induced natural ventilation analysis. *Solar Energy*, *81*(1), 20–30. https://doi.org/10.1016/J.SOLENER.2006.06.013

Kayll, D. G. (2001). The role of the building envelope professional in the aftermath of Vancouver's Leaky Condominium Crisis. *Thermal Performance of the Exterior Envelopes of Whole Buildings*, 1–5.

Kokatnur, T., Ferreira, S., Akkoç, B. K., Markarian, E., Nojedehi, P., Qiblawi, S., Sewraj, K., Gunay, B., O'Brien, W., Papineau, M., Schweiker, M., Harputlugil, G. U., & Azar, E. (2025). A review of passive design strategies and their effect on thermal resilience in low-income households. *Energy and Buildings*, *348*, 116508. https://doi.org/10.1016/j.enbuild.2025.116508

Kong, G., Hu, S., & Yang, Q. (2023). Uncertainty method and sensitivity analysis for assessment of energy consumption of underground metro station. *Sustainable Cities and Society*, *92*. https://doi.org/10.1016/j.scs.2023.104504

Kotze, D. J., Kuoppamäki, K., Niemikapee, J., Mesimäki, M., Vaurola, V., & Lehvävirta, S. (2020). A revised terminology for vegetated rooftops based on function and vegetation. *Urban Forestry and Urban Greening*, *49*, 126644. https://doi.org/10.1016/j.ufug.2020.126644

Kotzen, B., Galea, E. R., Mosco, S., Wang, Z., Ewer, J., & Jia, F. (2023). Fire safety risks of external living walls and implications for regulatory guidance in England. *Fire Safety Journal*, *139*(1), 103816. https://doi.org/10.1016/j.firesaf.2023.103816

Kousis, I., & Santamouris, M. (2025). Assessing long-term effectiveness of passive cooling strategies in the built environment under climate change. *Solar Energy*, *302*, 114038. https://doi.org/10.1016/j.solener.2025.114038

Krithigadevi V, & K. Bhagyasri. (2023a). Impact of orientation, aspect ratio, WWR on natural ventilation of non-high-rise residential building in a warm-humid climate. *Sustainability, Agri, Food and Environmental Research*. https://doi.org/10.7770/SAFER-V12N-ART783

Krithigadevi V, & K. Bhagyasri. (2023b). Impact of orientation, aspect ratio, WWR on natural ventilation of non-high-rise residential building in a warm-humid climate. *Sustainability, Agri, Food and Environmental Research*. https://doi.org/10.7770/SAFER-V12N-ART783

Krithigadevi V, & K. Bhagyasri. (2023c). Impact of orientation, aspect ratio, WWR on natural ventilation of non-high-rise residential building in a warm-humid climate. *Sustainability, Agri, Food and Environmental Research*. https://doi.org/10.7770/SAFER-V12N-ART783

Kubilay, A., Derome, D., Blocken, B., & Carmeliet, J. (2014a). High-resolution field measurements of wind-driven rain on an array of low-rise cubic buildings. *Building and Environment*, *78*, 1–13. https://doi.org/10.1016/j.buildenv.2014.04.004

Kubilay, A., Derome, D., Blocken, B., & Carmeliet, J. (2014b). Numerical simulations of wind-driven rain on an array of low-rise cubic buildings and validation by field measurements. *Building and Environment*, *81*, 283–295. https://doi.org/10.1016/J.BUILDENV.2014.07.008

Kubilay, A., Derome, D., Blocken, B., & Carmeliet, J. (2015). Wind-driven rain on two parallel wide buildings: field measurements and CFD simulations. *Journal of Wind Engineering and Industrial Aerodynamics*, *146*, 11–28. https://doi.org/10.1016/j.jweia.2015.07.006

Kukk, V., Kers, J., Kalamees, T., Wang, L., & Ge, H. (2022). Impact of built-in moisture on the design of hygrothermally safe cross-laminated timber external walls: A stochastic approach. *Building and Environment*, *226*. https://doi.org/10.1016/j.buildenv.2022.109736

Kumar, P., Debele, S. E., Khalili, S., Halios, C. H., Sahani, J., Aghamohammadi, N., Andrade, M. de F., Athanassiadou, M., Bhui, K., Calvillo, N., Cao, S. J., Coulon, F., Edmondson, J. L., Fletcher, D., Dias de Freitas, E., Guo, H., Hort, M. C., Katti, M., Kjeldsen, T. R., … Jones, L. (2024). Urban heat mitigation by green and blue infrastructure: Drivers, effectiveness, and future needs. *Innovation*, *5*(2). https://doi.org/10.1016/J.XINN.2024.100588/ASSET/B819D1D0-BE70-4CDA-9FBE-C6AA223A84E2/MAIN.ASSETS/GR3.JPG

Künzel, H., & Dewsbury, M. (2022). Moisture control design has to respond to all relevant hygrothermal loads. *UCL Open Environment*, *4*. https://doi.org/10.14324/111.444/ucloe.000037

Künzel, H. M. (1995). *Simultaneous heat and moisture transport in building components : one- and two-dimensional calculation using simple parameters*. Fraunhofer Institute of Building Physics.

Kutty, N. A., Barakat, D., Darsaleh, A. O., & Kim, Y. K. (2023). A Systematic Review of Climate Change Implications on Building Energy Consumption: Impacts and Adaptation Measures in Hot Urban Desert Climates. *Buildings*, *14*(1), 13. https://doi.org/10.3390/buildings14010013

Kwon, T. K., Kim, T. H., & Lim, Y. S. (2024). Exploring the Heat Mitigation Effects of Urban Climate Adaptation Facilities. *Sustainability*, *16*(22), 9919–9919. https://doi.org/10.3390/SU16229919

Larsen, L. (2015). Urban climate and adaptation strategies. *Frontiers in Ecology and the Environment*, *13*(9), 486–492. https://doi.org/10.1890/150103/ABSTRACT

Larsen, T. S., & Heiselberg, P. (2007). *Single-sided Natural Ventilation Driven by a Combination of Wind Pressure and Temperature Difference*: (p. 145). Sendai International Centre, Graduate School of Engineering, Tohoku University. https://vbn.aau.dk/en/publications/single-sided-natural-ventilation-driven-by-a-combination-of-wind-

LBNL Simulation Research Group. (1977). *DOE-1 COMPUTER PROGRAM FOR BUILDING ENERGY ANALYSIS*.

Leite, R. C. V, & Frota, A. B. (2014). THE WIND AND THE CITY: EVALUATING THE LIMITS TO APPLY NATURAL VENTILATION FOR THERMAL COMFORT IN DENSE URBAN SETTLEMENTS USING A COMPUTATIONAL FLUID DYNAMICS TOOL. *Blucher Mechanical Engineering Proceedings*, *1*(1). www.proceedings.blucher.com.br/evento/10wccm

Li, D., Han, P., Li, K., Di, Q., & Duan, Y. (2024). A Study on the Impact of Urbanization Level on Carbon Emissions Based on the STIRPAT Model: A Case Study of Five Major Urban Agglomerations in Northern China. *Sustainability*, *16*(14), 6134. https://doi.org/10.3390/su16146134

Li, F., Rubinato, M., Zhou, T., Li, J., & Chen, C. (2022). Numerical simulation of the influence of building-tree arrangements on wind velocity and PM2.5 dispersion in urban communities. *Scientific Reports*, *12*(1), 16378. https://doi.org/10.1038/S41598-022-20455-6

Li, H., Zhao, Y., Wang, C., Ürge-Vorsatz, D., Carmeliet, J., & Bardhan, R. (2024). Cooling efficacy of trees across cities is determined by background climate, urban morphology, and tree trait. *Communications Earth & Environment*, *5*(1), 754. https://doi.org/10.1038/s43247-024-01908-4

Li, J., Zheng, B., Bedra, K. B., Li, Z., & Chen, X. (2021). Evaluating the effect of window-to-wall ratios on cooling-energy demand on a typical summer day. *International Journal of Environmental Research and Public Health*, *18*(16). https://doi.org/10.3390/IJERPH18168411

Li, S., Xiao, Q., Teng, M., Qiu, X., Xu, W., Liu, H., Wu, X., & Wu, C. (2023). A comprehensive morphological classification scheme for local ventilation performance zones in spatially heterogeneous urban areas. *Developments in the Built Environment*, *15*, 100202–100202. https://doi.org/10.1016/J.DIBE.2023.100202

Libralato, M., De Angelis, A., Tornello, G., Saro, O., D'Agaro, P., & Cortella, G. (2021). Evaluation of Multiyear Weather Data Effects on Hygrothermal Building Energy Simulations Using WUFI Plus. *Energies*, *14*(21), 7157. https://doi.org/10.3390/en14217157

Liddo, F. Di, Amoruso, P., Tajani, F., Morano, P., & Stara, F. (2025). Urban redevelopment and decarbonization challenges. An overview from the real estate market perspective. *Energy and Buildings*, *343*, 115914. https://doi.org/10.1016/j.enbuild.2025.115914

Lin, X., Cui, Y., Hao, S., Zhu, C., Zhang, P., & Zhao, H. (2025). Influence of urban landscape pattern on summer surface temperature and its spatial scale effects. *Geocarto International*, *40*(1). https://doi.org/10.1080/10106049.2024.2441370

Lin, Y., Huang, T., Yang, W., Hu, X., & Li, C. (2023). A Review on the Impact of Outdoor Environment on Indoor Thermal Environment. *Buildings*, *13*(10), 2600. https://doi.org/10.3390/buildings13102600

Linden, P. F., Lane-Serff, G. F., & Smeed, D. A. (1990). Emptying filling boxes: the fluid mechanics of natural ventilation. *Journal of Fluid Mechanics*, *212*, 309–335. https://doi.org/10.1017/S0022112090001987

Liu, W., Engel, B. A., Feng, Q., & Li, R. (2022). Simulating annual runoff retention performance of extensive green roofs: A comparison of four climatic regions in China. *Journal of Hydrology*, *610*, 127871. https://doi.org/10.1016/j.jhydrol.2022.127871

Liyanage, D. R., Hewage, K., Hussain, S. A., Razi, F., & Sadiq, R. (2024a). Climate adaptation of existing buildings: A critical review on planning energy retrofit strategies for future climate. *Renewable and Sustainable Energy Reviews*, *199*, 114476. https://doi.org/10.1016/j.rser.2024.114476

Liyanage, D. R., Hewage, K., Hussain, S. A., Razi, F., & Sadiq, R. (2024b). Climate adaptation of existing buildings: A critical review on planning energy retrofit strategies for future climate. *Renewable and Sustainable Energy Reviews*, *199*, 114476. https://doi.org/10.1016/j.rser.2024.114476

Lu, L., Guo, H., Weng, Q., Bartesaghi-Koc, C., Osmond, P., & Li, Q. (2024). A transferable approach to assessing green infrastructure types (GITs) and their effects on surface urban heat islands with multi-source geospatial data. *Remote Sensing of Environment*, *306*, 114119. https://doi.org/10.1016/J.RSE.2024.114119

Luikov, A. V. (1966). *Heat and mass transfer in capillary-porous bodies* (P. W. B. Harrison & W. M. Pun, Eds.). Pergamon Press.

Luikov, A. V. (1975). Systems of differential equations of heat and mass transfer in capillary-porous bodies . *International Journal of Heat and Mass Transfer*, *18*(1), 1–14.

Luo, J., Xu, T., & Yan, C. (2024). Seasonal variation in vegetation cooling effect and its driving factors in a subtropical megacity. *Building and Environment*, *266*, 112065. https://doi.org/10.1016/J.BUILDENV.2024.112065

Macdonald, I., & Strachan, P. (2001). Practical application of uncertainty analysis. *Energy and Buildings*, *33*(3), 219–227. https://doi.org/10.1016/S0378-7788(00)00085-2

Magrini, A., Lazzari, S., Marenco, L., & Guazzi, G. (2017). A procedure to evaluate the most suitable integrated solutions for increasing energy performance of the building's envelope, avoiding moisture problems. *International Journal of Heat and Technology*, *35*(4), 689–699. https://doi.org/10.18280/IJHT.350401

Maimaitiyiming, M., Ghulam, A., Tiyip, T., Pla, F., Latorre-Carmona, P., Halik, Ü., Sawut, M., & Caetano, M. (2014). Effects of green space spatial pattern on land surface temperature: Implications for sustainable urban planning and climate change adaptation. *ISPRS Journal of Photogrammetry and Remote Sensing*, *89*, 59–66. https://doi.org/10.1016/J.ISPRSJPRS.2013.12.010

Manso, M., & Castro-Gomes, J. (2015). Green wall systems: A review of their characteristics. *Renewable and Sustainable Energy Reviews*, *41*, 863–871. https://doi.org/10.1016/J.RSER.2014.07.203

Manso, M., Teotónio, I., Silva, C. M., & Cruz, C. O. (2021). Green roof and green wall benefits and costs: A review of the quantitative evidence. *Renewable and Sustainable Energy Reviews*, *135*, 110111. https://doi.org/10.1016/j.rser.2020.110111

Månsson, L.-G. (1998). *Calculation of energy and environmental performance of buildings*. Energy Conservation in Buildings and Community Systems Programme.

Mark Bomberg. (1974). *Moisture flow through porous building materials* [PhD Thesis]. Lund University.

Martinelli, A., Carlucci, F., Climate, F. F.-, & 2024, undefined. (2024). On the role of the building envelope on the urban heat island mitigation and building energy performance in Mediterranean cities: A case study in southern. *Mdpi.ComA Martinelli, F Carlucci, F FioritoClimate, 2024•mdpi.Com*. https://www.mdpi.com/2225-1154/12/8/113

MATLAB. (n.d.). Retrieved August 20, 2025, from https://www.mathworks.com/?s_tid=gn_logo

Matthews, R. S., Bury, M. R. C., & Redfearn, D. (1996). Investigation of dynamic water penetration tests for curtain walling. *Journal of Wind Engineering and Industrial Aerodynamics*, *60*(1–3), 1–16. https://doi.org/10.1016/0167-6105(96)00020-7

Miao, Y., & Lau, S. S. Y. (2023). Effect of Linear Building Blocks on the Wind Environment of Streets between High-Rise Buildings A case of Hong Kong. *International Review for Spatial Planning and Sustainable Development*, *11*(3), 63–77. https://doi.org/10.14246/IRSPSD.11.3_63

Nastos, P. T., Polychroni, I., Nastou, M.-P. P., Charalampopoulos, I., Solomos, S., & Zerefos, S. (2024). *Improving urban design to address human thermal discomfort in urban agglomerations characterized by different microclimatic conditions*. https://doi.org/10.5194/EMS2024-574

Nihar, K., Nutkiewicz, A., & Jain, R. K. (2023). Natural ventilation versus air pollution: assessing the impact of outdoor pollution on natural ventilation potential in informal settlements in India. *Environmental Research: Infrastructure and Sustainability*, *3*(2), 025002. https://doi.org/10.1088/2634-4505/ACC88F

Niu, S., Liu, X., Wang, A., Chen, L., Zhou, X., Shi, X., Yang, L., & Jin, X. (2023). Research on the influence of outdoor trees on natural ventilation performance of an academic building. *Building Simulation 2023 16:6*, *16*(6), 927–946. https://doi.org/10.1007/S12273-022-0977-X

Not yet built for purpose: Global building sector emissions still high and rising. (2024, March 7). https://www.unep.org/news-and-stories/press-release/not-yet-built-purpose-global-building-sector-emissions-still-high?utm_source=chatgpt.com

Ode Sang, Å., Thorpert, P., & Fransson, A. M. (2022). Planning, Designing, and Managing Green Roofs and Green Walls for Public Health – An Ecosystem Services Approach. *Frontiers in Ecology and Evolution*, *10*, 804500. https://doi.org/10.3389/FEVO.2022.804500/FULL

Oh, S., & Haberl, J. S. (2016). Origins of analysis methods used to design high-performance commercial buildings: Whole-building energy simulation. *Science and Technology for the Built Environment*, *22*(1), 118–137. https://doi.org/10.1080/23744731.2015.1063958

Ouldboukhitine, S. E., Bakkour, A., Khiati, S., & Belarbi, R. (2025). Modular green walls: A sustainable architectural solution for energy efficiency in oceanic climates. *Energy and Buildings*, *342*, 115850. https://doi.org/10.1016/J.ENBUILD.2025.115850

Pace, R., Chiocchini, F., Sarti, M., Endreny, T. A., Calfapietra, C., & Ciolfi, M. (2023). Integrating Copernicus land cover data into the i-Tree Cool Air model to evaluate and map urban heat mitigation by tree cover. *European Journal of Remote Sensing*, *56*(1). https://doi.org/10.1080/22797254.2022.2125833

Pajek, L., Potočnik, J., & Košir, M. (2022). The effect of a warming climate on the relevance of passive design measures for heating and cooling of European single-family detached buildings. *Energy and Buildings*, *261*, 111947. https://doi.org/10.1016/j.enbuild.2022.111947

Pan, Y., Zhu, M., Lv, Y., Yang, Y., Liang, Y., Yin, R., Yang, Y., Jia, X., Wang, X., Zeng, F., Huang, S., Hou, D., Xu, L., Yin, R., & Yuan, X. (2023). Building energy simulation and its application for building performance optimization: A review of methods, tools, and case studies. *Advances in Applied Energy*, *10*, 100135. https://doi.org/10.1016/j.adapen.2023.100135

Panchalingam, K., Rasheed, E. O., & Rotimi, J. O. B. (2024). Cost-Related Drivers and Barriers of Passivhaus: A Systematic Literature Review. *Sustainability*, *16*(15), 6510. https://doi.org/10.3390/su16156510

Pang, Z., O'Neill, Z., Li, Y., & Niu, F. (2020). The role of sensitivity analysis in the building performance analysis: A critical review. In *Energy and Buildings* (Vol. 209). Elsevier Ltd. https://doi.org/10.1016/j.enbuild.2019.109659

Panico, S., Larcher, M., Herrera Avellanosa, D., Baglivo, C., Troi, A., & Maria Congedo, P. (2023). Hygrothermal simulation challenges: Assessing boundary condition choices in retrofitting historic European buildings. *Energy and Buildings*, *297*, 113464. https://doi.org/10.1016/j.enbuild.2023.113464

Park, S., Lee, S., & Oh, K. (2024). Defining and Verifying New Local Climate Zones with Three-Dimensional Built Environments and Urban Metabolism. *Land 2024, Vol. 13, Page 1461*, *13*(9), 1461. https://doi.org/10.3390/LAND13091461

Pathirana, S., Rodrigo, A., & Halwatura, R. (2019a). Effect of building shape, orientation, window to wall ratios and zones on energy efficiency and thermal comfort of naturally ventilated houses in tropical climate. *International Journal of Energy and Environmental Engineering*, *10*(1), 107–120. https://doi.org/10.1007/S40095-018-0295-3

Pathirana, S., Rodrigo, A., & Halwatura, R. (2019b). Effect of building shape, orientation, window to wall ratios and zones on energy efficiency and thermal comfort of naturally ventilated houses in tropical climate. *International Journal of Energy and Environmental Engineering*, *10*(1), 107–120. https://doi.org/10.1007/S40095-018-0295-3

Pauly, L., & Ferrero, E. (2024). *Numerical Experimentation to Study the Influence of Various Urban Features on Microclimate Using Different Urban Scenarios * https://doi.org/10.5194/EMS2024-210

Peng, L. L. H., Yang, X., He, Y., Hu, Z., Xu, T., Jiang, Z., & Yao, L. (2019). Thermal and energy performance of two distinct green roofs: Temporal pattern and underlying factors in a subtropical climate. *Energy and Buildings*, *185*, 247–258. https://doi.org/10.1016/j.enbuild.2018.12.040

Pereira, C., Flores-Colen, I., & Mendes, M. P. (2023). Guidelines to reduce the effects of urban heat in a changing climate: Green infrastructures and design measures. *Sustainable Development*, *32*(1), 57–83. https://doi.org/10.1002/SD.2646

Pérez-Bella, J. M., Domínguez-Hernández, J., López-Julián, P. L., Salesa-Bordabana, Á., & Orna-Carmona, M. (2024). Closing the gap between traditional wind-driven rain studies and the performance-based design of building façades: Case study of the Netherlands. *Building and Environment*, *248*, 111083. https://doi.org/10.1016/j.buildenv.2023.111083

Polydoros, A., Cartalis, C., Kotroni, V., Lavouvardos, K., Agathangelidis, I., Giannaros, C., Saliari, M., & Galanaki, E. (2023). *Modelling assessment of the potential of adaptation measures to mitigate urban heat in future climate conditions*. https://doi.org/10.5194/EGUSPHERE-EGU23-15871

Posani, M., Veiga, R., & Freitas, V. (2023). Post-Insulating traditional massive walls in Southern Europe: A moderate thermal resistance can be more effective than you think. *Energy and Buildings*, *295*, 113299. https://doi.org/10.1016/j.enbuild.2023.113299

Qin, M., & Yang, J. (2016). Evaluation of different thermal models in EnergyPlus for calculating moisture effects on building energy consumption in different climate conditions. *Building Simulation*, *9*(1), 15–25. https://doi.org/10.1007/s12273-015-0263-2

Qureshi, A. M., Rachid, A., & Bartlett, D. (2023). Quantifying the cooling effect of urban heat stress interventions. *International Journal of Global Warming*, *30*(1), 60–80. https://doi.org/10.1504/IJGW.2023.130493;SUBPAGE:STRING:ABSTRACT;REQUESTEDJOURNAL:JOURNAL:IJGW;ISSUE:ISSUE:10.1504/IJGW.2023.30.ISSUE-1;WGROUP:STRING:PUBLICATION

Ragab, A., Hassieb, M. M., & Mohamed, A. F. (2025). Exploring the impact of window design and ventilation strategies on air quality and thermal comfort in arid educational buildings. *Scientific Reports 2025 15:1*, *15*(1), 19596-. https://doi.org/10.1038/s41598-025-01362-y

Rajput, T. S., & Thomas, A. (2023). Analyzing the effects of passive design strategies on building ventilation performance and thermal comfort using simulation-based approach.

E3S Web of Conferences, *396*, 02023–02023. https://doi.org/10.1051/E3SCONF/202339602023

Rana, J., Hasan, R., Sobuz, H. R., & Tam, V. W. Y. (2022a). Impact assessment of window to wall ratio on energy consumption of an office building of subtropical monsoon climatic country Bangladesh. *International Journal of Construction Management*, *22*(13), 2528–2553. https://doi.org/10.1080/15623599.2020.1808561

Rana, J., Hasan, R., Sobuz, H. R., & Tam, V. W. Y. (2022b). Impact assessment of window to wall ratio on energy consumption of an office building of subtropical monsoon climatic country Bangladesh. *International Journal of Construction Management*, *22*(13), 2528–2553. https://doi.org/10.1080/15623599.2020.1808561

Rao, P., Torreggiani, D., Tassinari, P., Rötzer, T., Pauleit, S., & Rahman, M. A. (2025). Do urban green spaces cool cities differently across latitudes? Spatial variability and climatic drivers of vegetation-induced cooling. *Sustainable Cities and Society*, *130*, 106513. https://doi.org/10.1016/j.scs.2025.106513

Recart, C., & Sturts Dossick, C. (2022). Hygrothermal behavior of post-retrofit housing: A review of the impacts of the energy efficiency upgrade strategies. *Energy and Buildings*, *262*, 112001. https://doi.org/10.1016/j.enbuild.2022.112001

Santamouris, M. (2014a). Cooling the cities – A review of reflective and green roof mitigation technologies to fight heat island and improve comfort in urban environments. *Solar Energy*, *103*, 682–703. https://doi.org/10.1016/j.solener.2012.07.003

Santamouris, M. (2014b). Cooling the cities – A review of reflective and green roof mitigation technologies to fight heat island and improve comfort in urban environments. *Solar Energy*, *103*, 682–703. https://doi.org/10.1016/J.SOLENER.2012.07.003

Santamouris, M., Ding, L., Fiorito, F., Oldfield, P., Osmond, P., Paolini, R., Prasad, D., & Synnefa, A. (2017). Passive and active cooling for the outdoor built environment – Analysis and assessment of the cooling potential of mitigation technologies using performance data from 220 large scale projects. *Solar Energy*, *154*, 14–33. https://doi.org/10.1016/j.solener.2016.12.006

Santamouris, M., & Osmond, P. (2020a). Increasing Green Infrastructure in Cities: Impact on Ambient Temperature, Air Quality and Heat-Related Mortality and Morbidity. *Buildings 2020, Vol. 10, Page 233*, *10*(12), 233. https://doi.org/10.3390/BUILDINGS10120233

Santamouris, M., & Osmond, P. (2020b). Increasing Green Infrastructure in Cities: Impact on Ambient Temperature, Air Quality and Heat-Related Mortality and Morbidity. *Buildings*, *10*(12), 233. https://doi.org/10.3390/BUILDINGS10120233

Santamouris, M., & Vasilakopoulou, K. (2021). Present and future energy consumption of buildings: Challenges and opportunities towards decarbonisation. *E-Prime - Advances in*

Electrical Engineering, Electronics and Energy, *1*, 100002. https://doi.org/10.1016/j.prime.2021.100002

Sayadi, S., Hayati, A., & Salmanzadeh, M. (2021). Optimization of Window-to-Wall Ratio for Buildings Located in Different Climates: An IDA-Indoor Climate and Energy Simulation Study. *Energies 2021*, *Vol. 14*, *Page 1974*, *14*(7), 1974. https://doi.org/10.3390/EN14071974

Scherz, M., Hoxha, E., Maierhofer, D., Kreiner, H., & Passer, A. (2023). Strategies to improve building environmental and economic performance: an exploratory study on 37 residential building scenarios. *The International Journal of Life Cycle Assessment*, *28*(7), 828–842. https://doi.org/10.1007/s11367-022-02073-6

Schrijvers, P. (2020). *urban climate at street scale: analysis and adaptation*. https://repository.tudelft.nl/file/File_47ce81bf-2d6c-4d75-9f7d-89b669e4e282

Schroderus, S., Kuurola, P., Kempe, M., Fedorik, F., Leivo, V., & Haverinen-Shaughnessy, U. (2025). Impacts of building energy retrofits on energy consumption, indoor environment, and hygrothermal performance in future climate scenarios. *Energy and Buildings*, *347*, 116413. https://doi.org/10.1016/j.enbuild.2025.116413

Seidu, S., Chan, D. W. M., & Taiwo, R. (2025). Integrating green and grey infrastructure systems in dense urban regions: a synthesis of critical barriers and effective implementation guidelines. *Clean Technologies and Environmental Policy*. https://doi.org/10.1007/s10098-025-03309-3

Shafique, M., Kim, R., & Rafiq, M. (2018). Green roof benefits, opportunities and challenges – A review. *Renewable and Sustainable Energy Reviews*, *90*, 757–773. https://doi.org/10.1016/j.rser.2018.04.006

Shimonosono, K., Sasaki, Y., & Kohri, K. (2023). Exploring the impact of opening ratio on indoor thermal environment: A study on natural ventilation design. *Japan Architectural Review*, *6*(1), e12381. https://doi.org/10.1002/2475-8876.12381;JOURNAL:JOURNAL:24758876

Silveira, C., Dias, A., Amaral, F., … G. de G.-S. C. and, & 2024, undefined. (2024). The importance of private gardens and their spatial composition and configuration to urban heat island mitigation. *ElsevierC Silveira, ATC Dias, FG Amaral, G de Gois, N PistónSustainable Cities and Society, 2024•Elsevier*. https://www.sciencedirect.com/science/article/pii/S2210670724004141

Stewart, I. D., & Oke, T. R. (2012). Local climate zones for urban temperature studies. *Bulletin of the American Meteorological Society*, *93*(12), 1879–1900. https://doi.org/10.1175/BAMS-D-11-00019.1

Sun, S., Kensek, K., Noble, D., & Schiler, M. (2016). A method of probabilistic risk assessment for energy performance and cost using building energy simulation. *Energy and Buildings*, *110*, 1–12. https://doi.org/10.1016/j.enbuild.2015.09.070

Synnefa, A., Dandou, A., Santamouris, M., Tombrou, M., & Soulakellis, N. (2008). On the Use of Cool Materials as a Heat Island Mitigation Strategy. *Journal of Applied Meteorology and Climatology*, *47*(11), 2846–2856. https://doi.org/10.1175/2008JAMC1830.1

Tabatabaee, S., Ashour, M., Mohandes, S. R., Sadeghi, H., Mahdiyar, A., Hosseini, M. R., & Ismail, S. (2022). Deterrents to the adoption of green walls: a hybrid fuzzy-based approach. *Engineering, Construction and Architectural Management*, *29*(9), 3460–3479. https://doi.org/10.1108/ECAM-04-2021-0286

Tajuddeen, I., & Sajjadian, S. M. (2024). Climate change and the built environment - a systematic review. *Environment, Development and Sustainability*. https://doi.org/10.1007/s10668-024-04962-2

Tariku, F. (2008). *Whole building heat and moisture analysis*. Concordia University.

Tarkhan, N., Mokhtar, S., Weber, R. E., & Reinhart, C. (2022). Natural Ventilation In A Warming Climate: An Evaluation Of Computational Simulation Methods And Metrics. *Proceedings of the 2022 Annual Modeling and Simulation Conference, ANNSIM 2022*, 694–705. https://doi.org/10.23919/ANNSIM55834.2022.9859527

Tawfeeq, H., & Qaradaghi, A. M. A. (2024). Optimising Window-to-Wall Ratio for Enhanced Energy Efficiency and Building Intelligence in Hot Summer Mediterranean Climates. *Sustainability (Switzerland)*, *16*(17). https://doi.org/10.3390/SU16177342

Terblanche, R. (2025). Incorporating Vegetation into Building Design. In *Sustainable Built Environment for People and Society* (4). IntechOpen. https://doi.org/10.5772/intechopen.1010089

The World Bank. (2024). *Mapping energy efficiency: a global dataset on building code effectiveness and compliance*.

Tiago, P., Leal, A. I., & Silva, C. M. (2024). Assessing Ecological Gains: A Review of How Arthropods, Bats and Birds Benefit from Green Roofs and Walls. *Environments*, *11*(4), 76. https://doi.org/10.3390/ENVIRONMENTS11040076/S1

Tijskens, A., Janssen, H., & Roels, S. (2023). Probabilistic hygrothermal assessment of various timber frame wall compositions. *Building and Environment*, *243*. https://doi.org/10.1016/j.buildenv.2023.110619

Toren, B. I., & Sharmin, T. (2024). *Urban Geometry and Microclimate of Street Canyons in Cold Semi-Arid Climate*. https://doi.org/10.5194/EMS2024-898

TRNSYS. (n.d.). Retrieved July 3, 2024, from https://www.trnsys.com/

UN-HABITAT. (2022). *World Cities Report 2022- Envisaging the Future of Cities*.

United Nations Environment Programme. (2025). *Global Status Report for Buildings and Construction 2024/2025*.

Van der Borght, R., & Pallares Barbera, M. (2023). How urban spatial expansion influences CO2 emissions in Latin American countries. *Cities*, *139*, 104389. https://doi.org/10.1016/j.cities.2023.104389

Van Linden, S., & Van Den Bossche, N. (2022). Review of rainwater infiltration rates in wall assemblies. *Building and Environment*, *219*, 109213. https://doi.org/10.1016/j.buildenv.2022.109213

van Schijndel, A. W. M. (2007). *Integrated heat air and moisture modeling and simulation*. https://doi.org/10.6100/IR622370

Vereecken, E., Van Gelder, L., Janssen, H., & Roels, S. (2015). Interior insulation for wall retrofitting - A probabilistic analysis of energy savings and hygrothermal risks. *Energy and Buildings*, *89*, 231–244. https://doi.org/10.1016/j.enbuild.2014.12.031

Viecco, M., Jorquera, H., Sharma, A., Bustamante, W., Fernando, H. J. S., & Vera, S. (2021). Green roofs and green walls layouts for improved urban air quality by mitigating particulate matter. *Building and Environment*, *204*, 108120. https://doi.org/10.1016/J.BUILDENV.2021.108120

Vijayaraghavan, K. (2016). Green roofs: A critical review on the role of components, benefits, limitations and trends. *Renewable and Sustainable Energy Reviews*, (57), 740–752. https://doi.org/10.1016/j.rser.2015.12.119

Vox, G., Blanco, I., Convertino, F., & Schettini, E. (2022). Heat transfer reduction in building envelope with green façade system: A year-round balance in Mediterranean climate conditions. *Energy and Buildings*, *274*, 112439. https://doi.org/10.1016/j.enbuild.2022.112439

Waddicor, D. A., Fuentes, E., Sisó, L., Salom, J., Favre, B., Jiménez, C., & Azar, M. (2016). Climate change and building ageing impact on building energy performance and mitigation measures application: A case study in Turin, northern Italy. *Building and Environment*, *102*, 13–25. https://doi.org/10.1016/j.buildenv.2016.03.003

Wang, C., Wang, X., Causone, F., Yang, Y., Gao, N., Ye, Y., Li, P., & Shi, X. (2025). Addressing uncertainty to achieve stability in urban building energy modeling: A comparative study of four possible approaches. *Building and Environment*, *267*. https://doi.org/10.1016/j.buildenv.2024.112197

Wang, X., Berrah, N., Mathur, S., & Vinuya, F. (2012). *Winds of Change: East Asia's Sustainable Energy Future*. World Bank.

Wang, Y., Zhan, Q., & Ouyang, W. (2017). Impact of Urban Climate Landscape Patterns on Land Surface Temperature in Wuhan, China. *Sustainability 2017*, *Vol. 9*, *Page 1700*, *9*(10), 1700. https://doi.org/10.3390/SU9101700

Woloszyn, M., & Rode, C. (2008). Tools for performance simulation of heat, air and moisture conditions of whole buildings. *Building Simulation*, *1*(1), 5–24. https://doi.org/10.1007/s12273-008-8106-z

Wu, Q., Huang, Y., Irga, P., Kumar, P., Li, W., Wei, W., Shon, H. K., Lei, C., & Zhou, J. L. (2024). Synergistic control of urban heat island and urban pollution island effects using green infrastructure. *Journal of Environmental Management*, *370*, 122985–122985. https://doi.org/10.1016/J.JENVMAN.2024.122985

Wu, Z., & Zhang, Y. (2018a). Spatial Variation of Urban Thermal Environment and Its Relation to Green Space Patterns: Implication to Sustainable Landscape Planning. *Sustainability 2018*, *Vol. 10*, *Page 2249*, *10*(7), 2249. https://doi.org/10.3390/SU10072249

Wu, Z., & Zhang, Y. (2018b). Spatial variation of urban thermal environment and its relation to green space patterns: implication to sustainable landscape planning. *Sustainability*, *10*(7), 2249. https://doi.org/10.3390/SU10072249

WUFI Plus. (n.d.). Retrieved July 3, 2024, from https://wufi.de/en/software/wufi-plus/

WUFI Pro 6.8. (n.d.). Retrieved March 29, 2025, from https://wufi.de/en/

Xiao, Z., Lacasse, M. A., Dragomirescu, E., & Defo, M. (2023). Projected changes of wind-driven rain and moisture load in wall assemblies across Canada. *Journal of Wind Engineering and Industrial Aerodynamics*, *238*, 105446. https://doi.org/10.1016/j.jweia.2023.105446

Xie, J., Zhou, S., Chung, L. C. H., & Chan, T. O. (2024). Evaluating land-surface warming and cooling environments across urban–rural local climate zone gradients in subtropical megacities. *Building and Environment*, *251*, 111232. https://doi.org/10.1016/J.BUILDENV.2024.111232

Xie, L. T., & Cai, G. Y. (2015). Impact of land cover types and components on urban heat. *Https://Doi.Org/10.1117/12.2207452*, *9808*, 226–235. https://doi.org/10.1117/12.2207452

Xie, X., Luo, Z., Grimmond, S., & Sun, T. (2023). Impact of building density on natural ventilation potential and cooling energy saving across Chinese climate zones. *Building and Environment*, *244*. https://doi.org/10.1016/J.BUILDENV.2023.110621

Xie, X., Xu, B., Fei, Y., Chen, X. ni, Pei, G., & Ji, J. (2024a). Passive energy-saving design strategy and realization on high window-wall ratio buildings in subtropical regions. *Renewable Energy*, *229*. https://doi.org/10.1016/J.RENENE.2024.120709

Xie, X., Xu, B., Fei, Y., Chen, X. ni, Pei, G., & Ji, J. (2024b). Passive energy-saving design strategy and realization on high window-wall ratio buildings in subtropical regions. *Renewable Energy*, *229*. https://doi.org/10.1016/J.RENENE.2024.120709

Yan, J., Zhang, S., Zhang, J., Zhang, S., Zhang, C., Yang, H., Wang, R., & Wei, L. (2022). Stormwater retention performance of green roofs with various configurations in different climatic zones. *Journal of Environmental Management*, *319*, 115447. https://doi.org/10.1016/J.JENVMAN.2022.115447

Yang, S., Wang, L. (Leon), Stathopoulos, T., & Marey, A. M. (2023). Urban microclimate and its impact on built environment – A review. *Building and Environment*, *238*, 110334. https://doi.org/10.1016/j.buildenv.2023.110334

Yang, T., Wright, N. G., Etheridge, D. W., & Quinn, A. D. (2006). A Comparison of CFD and Full-scale Measurements for Analysis of Natural Ventilation. *International Journal of Ventilation*, *4*(4), 337–348. https://doi.org/10.1080/14733315.2005.11683713

Yang, W., Lin, Y., & Li, C. Q. (2018). Effects of Landscape Design on Urban Microclimate and Thermal Comfort in Tropical Climate. *Advances in Meteorology*, *2018*(1), 2809649. https://doi.org/10.1155/2018/2809649

Yin, H., & Zhao, X. (2024). Urban heat island analysis based on high resolution measurement data: A case study in Beijing. *Sustainable Cities and Society*, *106*, 105389. https://doi.org/10.1016/J.SCS.2024.105389

Yin, X., & Muhieldeen, M. W. (2024). Evaluation of cooling energy saving and ventilation renovations in office buildings by combining bioclimatic design strategies with CFD-BEM coupled simulation. *Journal of Building Engineering*, *91*. https://doi.org/10.1016/J.JOBE.2024.109547

Younes, J., Ghaddar, N., & Ghali, K. (2024). Impact assessment of climate change on naturally ventilated residential buildings in Lebanon 'Overheating risk under future climate scenarios. *E3S Web of Conferences*, *562*. https://doi.org/10.1051/E3SCONF/202456207001

Yu, H., Zhang, C., & Yu, L. (2025). Do Different Urban Morphologies Have Consistent Patterns on Urban Heat Islands in Different Cities and Scales? A Local Climate Zone Exploration. *IEEE Journal of Selected Topics in Applied Earth Observations and Remote Sensing*, *18*, 2429–2443. https://doi.org/10.1109/JSTARS.2024.3517837

Yu, H., & Zhang, H. (2025). A new method for predicting wind-driven rain catch ratios on building facades in urban residential areas using machine learning models. *Building and Environment*, *270*, 112467. https://doi.org/10.1016/j.buildenv.2024.112467

Yu, H., Zhang, H., & Feng, C. (2025). Wind-driven rain under typhoon conditions: distribution analysis, semi-empirical model optimization, and predictive model development. *Building and Environment*, *283*(8046), 113394. https://doi.org/10.1016/j.buildenv.2025.113394

Yu, S., Cui, Y., Shao, Y., & Han, F. (2019). Research on the comprehensive performance of hygroscopic materials in an office building based on energyplus. *Energies*, *12*(1). https://doi.org/10.3390/en12010191

Yu, S., Liu, X., Li, Y., He, S., Yao, Y., & Sun, S. (2023). Experimental and numerical simulation study on hygrothermal migration of damaged envelope walls during wind-driven rain. *Building and Environment*, *243*, 110653. https://doi.org/10.1016/J.BUILDENV.2023.110653

Zeng, L., Zhang, X., Lu, J., Li, Y., Hang, J., Hua, J., Zhao, B., & Ling, H. (2024). Influence of Various Urban Morphological Parameters on Urban Canopy Ventilation: A Parametric Numerical Study. *Atmosphere*, *15*(3). https://doi.org/10.3390/ATMOS15030352

Zhang, K., Garg, A., Mei, G., Jiang, M., Wang, H., Huang, S., & Gan, L. (2022). Thermal performance and energy consumption analysis of eight types of extensive green roofs in subtropical monsoon climate. *Building and Environment*, *216*, 108982. https://doi.org/10.1016/J.BUILDENV.2022.108982

Zhang, M., Qin, M., Rode, C., & Chen, Z. (2017). Moisture buffering phenomenon and its impact on building energy consumption. *Applied Thermal Engineering*, *124*, 337–345. https://doi.org/10.1016/j.applthermaleng.2017.05.173

Zhang, R., Yang, J., Ma, X., Xiao, X., Society, J. X.-S. C. and, & 2023, undefined. (2023). Optimal allocation of local climate zones based on heat vulnerability perspective. *Elsevier*. https://www.sciencedirect.com/science/article/pii/S2210670723005929

Zhang, S., Fang, X., Cheng, C., Chen, J., Guo, F., Yu, Y., & Yang, S. (2024). *Research on multi-scale urban natural ventilation climate guidance: A case study in the Shijiazhuang metropolitan area*. https://doi.org/10.21203/RS.3.RS-3807647/V1

Zhang, X., Riaz Ahmad, M., & Chen, B. (2020). Numerical and experimental investigation of the hygrothermal properties of corn stalk and magnesium phosphate cement (MPC) based bio-composites. *Construction and Building Materials*, *244*. https://doi.org/10.1016/j.conbuildmat.2020.118358

Zhang, Y., Yang, Y., Zhang, L., Zhao, C., Yan, J., Liu, M., & Zhao, L. (2022). Seasonal variation in leaf area index and its impact on the shading effects of vertical green facades in subtropical areas. *Building and Environment*, *225*, 109629. https://doi.org/10.1016/J.BUILDENV.2022.109629

Zhao, Y., Zhang, X., Ling, H., Jia, S., Yang, X., Zhang, Y., Zhao, B., & Hua, J. (2024). Utilizing periodic boundary conditions to save computational resources for assessing building natural ventilation in urban areas. *Urban Climate*, *55*. https://doi.org/10.1016/J.UCLIM.2024.101925

Zhong, H. Y., Sun, Y., Shang, J., Qian, F. P., Zhao, F. Y., Kikumoto, H., Jimenez-Bescos, C., & Liu, X. (2022). Single-sided natural ventilation in buildings: a critical literature review.

Building and Environment, *212*, 108797. https://doi.org/10.1016/J.BUILDENV.2022.108797

Zhong, W., Pan, Y., Xiao, W., & Zhang, T. (2023). Identifying bioclimatic techniques for sustainable low-rise high-density residential units: Comparative analysis on the ventilation performance of vernacular dwellings in China. *Journal of Building Engineering*, *80*, 108008–108008. https://doi.org/10.1016/J.JOBE.2023.108008

Ziabari, S., Zolfagharzadeh, H., J, F. A. M. J.-S. Ontol. Int., & 2019, undefined. (2019). Comparative study on the influence of window to wall ratio on energy consumption and ventilation performance in office building of temperate humid climate: a. *Sid.IrSS Ziabari, H Zolfagharzadeh, F Asadi Malek Jahan, S SalavatianSpace Ontol. Int. J, 2019•sid.Ir*. https://www.sid.ir/fileserver/je/53000120190203.pdf

3.5 Impact of Urban Planning and Landscaping on Energy and Thermal Comfort Performance of Buildings

This section should be cited as:

Ortner, F.P., Aydin, E.E., Govindarajan, P. (2026). Impact of urban planning and landscaping on energy and thermal comfort performance of buildings. In: A Systematic Review of Passive Energy Conservation Measures and Probabilistic Assessment under Changing Climate in Urban Settings, CIB W040 Report, CIB General Secretariat.

3.5.1 Introduction

This section reviews literature on urban energy conservation to examine how urban planning and landscaping influence energy and thermal performance. Urban planning is an interdisciplinary field concerned with the design, organization, and management of land use and the built environment (Alesaily et al., 2025). Urban planning policies shape the 'urban fabric' of a city: the distinct spatial and material configurations of buildings, streets, and open spaces. The study of the physical structure and form of cities is referred to as urban morphology (Biljecki and Chow, 2022). Climate, culture, and policy influence morphological outcomes and are, in turn, reshaped by evolving climatic and societal challenges, including climate-change mitigation.

Heating-dominated contexts such as the United Kingdom and the European Union have seen extensive research on retrofitting building stocks to improve energy conservation and support net-zero commitments (Ascione et al., 2017). Several researchers across the globe have scrutinized the impact of urban morphology and landscape to determine whether specific design characteristics promote energy efficiency and well-being or require retrofitting to achieve desirable outcomes. Accordingly, this review is organized into two thematic strands: i) urban morphology and energy conservation measures and, ii) retrofitting strategies within the urban fabric.

Firstly, urban morphology, encompassing form (Li et al., 2025), configuration (Leng et al., 2020; Li and Gou, 2025) , and density (Abu Dab'at and Alqadi, 2024; Aydin et al., 2024; Chokhachian et al., 2020), plays a decisive role in shaping building and urban performance across dimensions such as energy efficiency and liveability. It is also imperative to introduce the concept of the urban microclimate within the context of urban morphology. Urban microclimate influences and is reshaped by morphological conditions; this bidirectional relationship affects liveability through parameters such as outdoor thermal comfort and wind flow, which are examined in this report.

Secondly, retrofitting strategies involving urban landscaping such as greenery on walls, green and cool roofs, tree canopies, water bodies, reflective pavements, and albedo adjustments in urban canyons were frequent topics of study. For instance, the LUSH programme in Singapore (URA, 2017) illustrates how urban landscaping interventions can enhance energy performance and well-being outcomes.

As cities confront densification, climate change, and energy transitions, it is critical to understand how morphology influences performance across climates. Uninformed design interventions have demonstrated cascading environmental impacts across various climates, where rising thermal comfort standards have substantially increased energy demand and associated carbon emissions, ultimately exacerbating urban heat island effects and posing risks to human health and well-being (Aydin et al. 2024). These complexities demand region and climate specific design strategies that follow a passive-first, actively optimized approach (Feng et al., 2019) to minimize adverse microclimatic impacts.

Climate and region-specific analyses must be conducted across multiple spatial scales—micro, meso, and macro — to understand the bidirectional relationship between building performance and urban microclimate. Coupling urban microclimate models with building performance models is increasingly recognized as a key research direction for enabling a data-driven approach to climate-adaptive architectural and urban design. For example, urban morphological characteristics can be used to generate localized weather data by refining generalized climatic datasets (e.g., EPW files), which can then be used to evaluate building energy and thermal performance (Yang et al. 2012).

The remainder of this section describes the literature collection and screening process, outlines the methods and tools employed in the reviewed studies, and presents the key findings. Section 2 provides a discussion and synthesis covering relevant theoretical frameworks, wind and thermal comfort performance, and the advantages of climate-specific urban morphology. Section 3 examines retrofitting strategies at three scales—building, street, and urban canopy—while the conclusion summarizes key research gaps and proposes future directions.

3.5.2 Overview of how the review was conducted

This review synthesizes insights from about 60 peer-reviewed research articles that collectively examine how urban morphology and landscaping influence design performance. Relevant studies were retrieved from Google Scholar using the keywords "urban morphology" and "design performance," with a publication window beyond 2017 and supplemented with a small number of manual inclusions. Table 3.5.1 illustrates the selected literature spans diverse climatic contexts, including China, Seattle, Palestine, Germany, and several African cities. Additionally, type of analysis, tools and morphological characters assessed are documented in Table 3.5.1. Across these studies, urban form parameters like Floor Area Ratio (FAR), building site coverage (BSC), and green or open space ratios (GSR, OSR) are consistently highlighted as key determinants to energy and daylight performance.

Table 3.5.1 Literature summary on urban morphological characteristic evaluated, climate zone and tools utilised.

Article	Climate Location	Scale of analysis & programme	Urban morphological character	Type of analysis & Tools
		Hot/ Hot-Humid/Hot-Dry Climate		
Makki et al. (2019)	hot-dry climate; Medina of Fes (Fes el Bali), Morocco	Urban block → superblock → urban patch; 5 × 5 superblock derived from a traditional Fes block	Block clustering and density variation; courtyard size and distribution; building height variation; adjacent open space area; elevated public open spaces; upper-level connectivity (skyways); distance between open spaces; solar exposure at street level	Multi-objective evolutionary optimisation; parametric modelling in Grasshopper 3D; SPEA-2 algorithm via Octopus plugin; statistical analysis of fitness values; Pareto front analysis; normal distribution analysis across generations
Peng et al. (2017)	Nanjing, China; (hourly weather data from Nanjing weather station used)	Urban public plot / cluster scale;	Floor Area Ratio (FAR); Building Site Coverage (BSC); Building height; Building location and configuration; Incident wind direction	CFD-based comparative simulation; steady RANS using standard k-ε turbulence model; Phoenics 2015; IMERSOL radiation model; Boussinesq approximation
Zhu, S. et al. (2024)	Hot-humid, subtropical; Guangzhou, China	Urban block scale; individual buildings and collective block layouts; Program: Office buildings	building length & width, number of floors, building spacing, orientation; Floor Area Ratio (FAR), building density, surface-to-volume ratio (S/V), street height-to-width ratio (H/W), sky view factor (SVF)	Parametric simulation study; Latin Hypercube Sampling; EnergyPlus (EUI); Ladybug/Honeybee (UTCI); scatter-matrix correlation analysis (MATLAB); global sensitivity analysis using RBD-FAST (SALib via GH-CPython); comparative analysis across six block typologies
Aydin et al. (2024)	Tropical (Singapore)	Urban block scale (residential)	Street orientation, building spacing, density	Microclimate and thermal comfort simulation; Urban Weather Generator (UWG)
Shareef, S. and	Hot-humid climate	Urban canyon / neighbourhood scale	Urban fabric density, canyon geometry, surface materials	ENVI-MET and IES-VE

Altan, H. (2022)				
Eshraghi et al. (2025)	dry-arid climate (Tehran, Iran)	Urban block scale; residential, office, and commercial (retail) buildings	Building shape, FAR, building coverage ratio, building density, building height, number of stories, building length and width, street width, site length, green space ratio, window-to-wall ratio (fixed per use), commercial ratio, residential ratio, rotation, distances and heights of neighbouring buildings (8 directions)	Parametric UBEM simulations + machine learning + explainable AI; Rhino–Grasshopper with Ladybug, Dragonfly, Honeybee, Urban Weather Generator (UWG), OpenStudio/EnergyPlus; ML models (XGBoost, Random Forest, CatBoost, LightGBM, ANN, KNN, SVM); SHAP sensitivity analysis; statistical analysis (R^2, RMSE, ANOVA)
		Mediterranean/ Warm-Temperate Climate		
Abu Dab'at et al. (2024)	Mediterranean climate; (Hebron, Palestine)	Neighbourhood-scale urban patterns (33,000 m² each); single mixed-use prototype building (residential + ground-floor commercial)	Floor Space Index (FSI ≈ FAR), Ground Space Index (GSI ≈ site coverage), Open Space Ratio (OSR), Average building height (L)	GIS-based urban morphology analysis; K-means clustering; comparative building energy simulation using **DesignBuilder**
Elzeni et al. (2022)	Not specified;	Neighbourhood and urban canyon scale	Streets: connectivity, integration, choice, permeability; Plots: openness, compactness, diversity; Buildings: V/A, S/V, GSI, FSI, BDF, VHurb, FAI, Hbuild; Open spaces: porosity, sinuosity, occlusivity, sky view factor (SVF), urban canyon index (UCI), rugosity (RU)	Conceptual and comparative literature review
		Temperate Climate		
Ahn et al (2019)	Temperate oceanic climate (Seattle, USA)	Neighbourhood level; multi-family residential buildings	Horizontal compactness, vertical density, variation in building heights	Spatial regression; Moran's I test for spatial autocorrelation GeoDa (spatial regression, Moran's I); GIS datasets from Washington Geospatial Data Archive (WAGDA) and Seattle Open Data
Leng et al. (2020)	Temperate climate (Harbin, China)	Neighborhood scale (residential)	building site cover (BSC), floor area ratio (FAR), building height (BH), road height-width ratio	Spatial analysis; statistical correlation; GIS-based morphological metrics

			(RHR), total wall surface area (WSA), and lower green space ratio (GSR)	
Chokhachian et al. (2020)	Temperate–cold climate (Germany)	District scale (mixed-use)	Density, height-to-width ratio, canyon geometry, compactness	Ladybug
		Cold / Cross Climate comparative studies		
Golany (1996)	hot-humid, cold-humid, hot-dry, cold-dry, seashore strips, mountain slopes;	Urban and neighborhood scale; primarily residential and mixed-use (residential, commercial, educational, open spaces)	Urban form (compact, dispersed, clustered); site selection (altitude, slope, wind, orientation, proximity to water); street orientation and width; land-use integration vs. segregation; open space size and distribution; vegetation and evapotranspiration; earth-sheltered habitats	Theoretical and comparative analysis based on indigenous settlements and climatic principles
Li, X. and Gou, Z. (2025)	Hague, Singapore, Tallinn, Berlin, Montreal, Vienna, Vantaa, and Zurich	Urban block scale (residential district)	Building density, Floor area ratio, Average building height, High coefficient of variation, Average building shape factor, Mean surface area, Bulk volume, Mean volume, Building occupancy Space Crowding, Windward area coefficient factor	Ladybug tools, rhino and grasshopper
Li et al. (2025)	(i) severe cold, (ii) cold, (iii) hot-summer and cold-winter, (iv) hot-summer and warm-winter; 26- Chinese Cities	Macro-scale (city-wide); residential buildings and public buildings	Building density, floor area ratio, aggregation, homogeneity, functional distribution, urban orientation, building height uniformity (rugosity), sky view factor, shading factor, shape coefficient (surface-area-to-volume ratio)	Empirical statistical analysis; Pearson correlation analysis; GIS-based processing using ArcGIS 10.7 and Excel 2016

In parallel, another set of studies were obtained via searching "*green roof*", "*cool roof*", "*water bodies*", "*albedo effect*"; "*tree canopy*" impacting "*building energy*" and "*indoor thermal comfort*" in Google Scholar. The filtered studies examine the role of landscaping including i) trees (Li et al., 2024; Tsoka et al., 2021; Czekajlo et al., 2023; Flowers and Huang, 2024; Ge et al., 2024; Wu et al., 2024; Fu et al., 2025; Meili et al., 2025; Pastore et al., 2017; Balogun et al., 2014; Hsieh et al., 2018; Ravazdezh and Rivers, 2025), ii) green roofs and walls (GhaffarianHoseini et al., 2013; Bera et al., 2025; Harbiankova and Manso, 2025; Charoenkit and Yiemwattana, 2016; Yang et al., 2025; Perini and Magliocco, 2014; Berardi, 2016; Coma et al., 2017; Li et al., 2019),

iii) water bodies, and iv) materials in shaping building thermal performance and comfort. Table 3 and Table 4 below summarises the research articles focusing on urban fabric retrofitting.

3.5.3 Summary on Methods Employed

Studies investigating the impact of urban morphology on microclimate and energy conservation employed a range of methods, from correlation and regression analyses to advanced sensitivity testing (Leng et al., 2020; Eshraghi et al., 2025; Li and Gou, 2025). In accordance with the conceptual framework distinguishing micro-, meso-, and macro-scales, the modeling approaches can be categorized as follows:

i) Micro-scale models resolve pedestrian-level thermal comfort, radiative exchange, airflow, and material effects. Tools such as ENVI-MET, OpenFOAM, Fluent, and CityFFD are widely used to evaluate the interaction between morphology, shading, albedo, evapotranspiration, and ventilation (Tsoka et al., 2021; Flowers & Huang, 2024; Ge et al., 2024; Fu et al., 2025). A handful of such simulation studies are validated with observational data (Ge et al., 2024; Fu et al., 2025; Berardi, 2016). ENVI-MET is frequently employed for design-stage studies due to lower modeling thresholds, whereas CFD platforms such as OpenFOAM and Fluent offer higher accuracy at greater computational cost.

ii) At the meso-scale, models such as Weather Research and Forecasting (WRF) and Global Environmental Multiscale (GEM) (Marey et al., 2025) simulate regional climate dynamics and provide boundary conditions that account for synoptic weather patterns and urban heat island intensification (Falasca et al., 2019; Jandaghian & Berardi, 2020). These outputs are increasingly coupled with micro-scale models and urban energy tools to propagate meteorological uncertainty.

iii) Building-scale effects of urban morphology are commonly assessed using EnergyPlus, OpenStudio, DesignBuilder, and the City Energy Analyst, supported by GIS-based morphology extraction and Rhino–Grasshopper parametric modeling workflows (Makki et al., 2019). Several studies employ Urban Building Energy Modeling (UBEM) techniques or analyze geo-referenced datasets to characterize operational energy demand at district scale (Ferrando et al., 2020).

iv) Coupled models link microclimate simulations with building energy models through intermediate weather correction tools such as the Urban Weather Generator (UWG) (Aydin et al., 2024 & Yang et al, 2012) or through explicit coupling between tools such as Urban Tethys-Chloris (UT&C) coupled with EnergyPlus (Meili et al., 2025). A few studies incorporated empirical monitoring of material-level impacts, comparing the performance of different building materials across climates (e.g., Bakhshoodeh et al., 2022; Wu et al., 2024; Ravazdezh & Rivers, 2025; Coma et al., 2017; Zhao et al., 2025; Schade et al., 2021; Zhou et al., 2024; Liu et al., 2022).

v) More recent studies integrate probabilistic analysis through Monte Carlo sampling, Bayesian inference, and surrogate-assisted uncertainty propagation (Prataviera et al., 2022; Roth et al., 2020) to quantify the sensitivity and likelihood of performance outcomes. Explainable AI frameworks such as Shapley Additive Explanations (SHAP) and Recursive Feature Elimination (RFE) have also been adopted to rank morphological drivers including window-to-wall ratio, density metrics, and building geometry (Li and Gou, 2025).

Across the literature, EnergyPlus remains the most widely used building energy simulation engine, whereas microclimate and CFD tools dominate urban heat studies. The distinction between scales and tool categories is essential for avoiding methodological conflation and ensuring that performance assessments remain aligned with the physical processes under investigation.

The following section discusses morphological and landscaping characteristics in greater detail, examining how individual parameters influence urban energy conservation across climates.

3.5.4 Urban Morphology and Energy Conservation Measures

The role of urban morphology is examined with a clear definition of its components and how different morphological characteristics have been leveraged across climatic zones. Beyond energy conservation, factors such as wind flow, ventilation, and outdoor thermal comfort, which indirectly affect energy performance, are also discussed in this section.

3.5.4.1 Theoretical Frameworks linking Morphology, Urban Microclimate, and ECM

Urban morphology is a broad and abstract concept; consequently, research in this domain employs theoretical frameworks to unpack morphological characteristics through parameters such as density, building height, spacing, orientation, and green space. These parameters are typically assessed against key indicators like energy consumption, daylight availability, and thermal comfort to understand how form shapes performance.

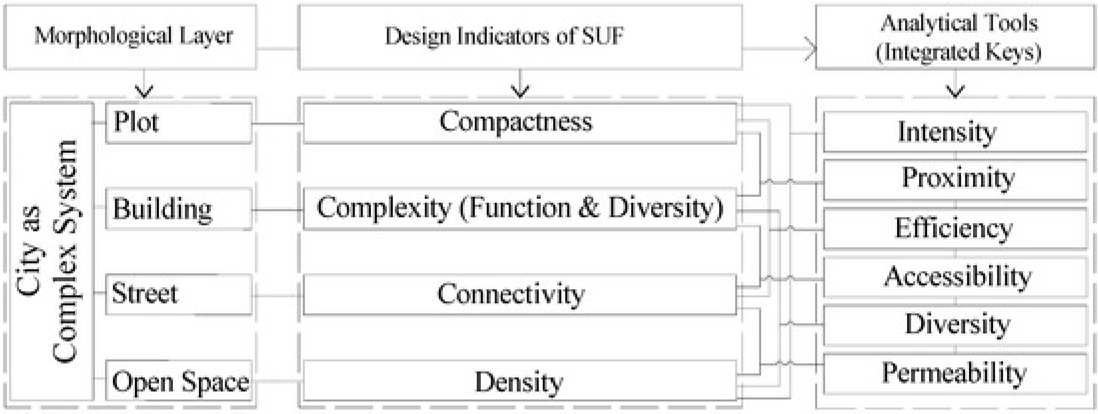

Figure 3.5.1 Theoretical framework quantifying urban morphology as six analytical tool reproduced from Mobaraki and Oktay Vehbi (2022)

Mobaraki and Oktay Vehbi (2022), for example, proposed a theoretical framework linking urban morphology to sustainable urban form through typo-morphological layers of plots, buildings, streets, and open spaces across micro, meso, and macro scales. As shown in Figure 3.5.1, their primarily theoretical work highlighted six analytical tools, including intensity, proximity, efficiency, accessibility, diversity, and permeability, as critical for evaluating sustainability performance of urban form, encompassing environmental, social, and spatial dimensions (including but not limited to energy conservation). For further details on urban morphological indicators readers are directed to Global Building Morphology indicator study (Biljecki and Chow, 2022)

In contrast, studies such as Elzeni, Elmokadem and Badawy, (2022) and Eshraghi et al., 2025) moved beyond theoretical frameworks to offer analytical metrics that can be directly deployed in evaluation of urban morphology, including vertical and horizontal compactness, surface-to-volume ratio (S/V) also referred to as form factor, and other quantifiable indices. Additional papers defined appropriate scales for analysing the impact of urban morphology on microclimate: Leng et al., (2020) applied a 150 m urban boundary for office buildings, while Ahn and Sohn, (2019) showed that residential microclimatic effects are most significant within 50–100 m.

3.5.4.2 Urban Morphology on Wind and Thermal Comfort Performance

In addition to urban morphology's role in energy conservation, it is necessary to examine its influence on wind and outdoor thermal comfort performance. As discussed earlier, urban morphology cannot be considered in isolation from the urban microclimate; the two interact dynamically and mutually shape environmental outcomes. This interaction has direct implications for the broader question of urban energy demand. In this context, outdoor thermal comfort can be interpreted as a design constraint operating within the wider umbrella of energy performance objectives.

Multiple studies demonstrated the strong influence of urban morphology on ventilation and outdoor comfort. (Peng et al., 2019, 2017) examined ventilation efficiency by fixing FAR and varying BSC, showing that performance is not linearly related to BSC: both tower and slab forms can succeed or fail depending on their arrangement. They found that intermediate BSC (~44%) with channeling layouts provides the best balance, as lowering average building height enhances turbulent diffusion and wind channeling only when blockage is minimized. Zhu *et al.*, (2024), analyzing hot-humid Guangzhou, linked morphology to both building energy use and outdoor thermal comfort (UTCI). They reported that while orientation and spacing had limited impact on UTCI, plan dimensions could reduce energy use by 20–36%. FAR, S/V ratio, and building height significantly influenced both energy and comfort, with shading from taller buildings lowering UTCI only in isolated cases. A positive correlation was observed between energy consumption and UTCI, indicating that less shaded forms increased both thermal stress and energy demand.

3.5.4.3 Advantages of climate-specific urban morphologies

Several studies highlight the climate-dependent role of urban morphology in building energy performance. Li et al., (2025) in their analysis across 26 different climates within China, found that in severe cold regions, stronger building aggregation reduced heat loss and lowered energy consumption, while in cold regions, greater variation in building orientation reduced heating demand by improving ventilation effects. Conversely, Li et al., (2025) highlight that a higher form factors and complex building shapes increased heating, cooling, and lighting loads, particularly in hot-summer and cold-winter climates.

Leng et al., (2020), focusing on a severe cold city, also reported that greater BSC, higher FAR, taller buildings, deeper canyons, and reduced GSR lowered heating demand, indicating compact vertical forms (a point or a tower building) perform more efficiently than horizontally spanned buildings (slab building). Extending this to a global scale covering tropical, oceanic, humid continental, and subarctic climates, Li and Gou, (2025) compared 240 residential districts across eight cities (Hague, Singapore, Tallinn, Berlin, Montreal, Vienna, Vantaa, and Zurich) and identified height, volume, shape factor, windward coefficient, and surface-to-volume ratio as key determinants of energy self-sufficiency. They showed that complex shapes increase energy demand but expand Photovoltaic potential, while larger volumes improve thermal capacity; in Nordic cities height and volume dominated, whereas in tropical, high-density contexts form factors (or the footprint compactness) were most critical.

Multiple studies address how compactness of urban form, characterised by low S/V ratio, may improve efficiency in cold climates but exacerbate heating or cooling loads in more temperate contexts. Earlier theoretical work by Golany, (1996) also emphasized climate-specificity, suggesting compact layouts perform better in stressful climates (hot-dry and cold-dry), but advocated dispersed green spaces, mixed land uses, and evapotranspiration to enhance comfort. Abu Dab'at and Alqadi, (2024) focusing on a heating-dominated Mediterranean context, found that compact forms (high FAR and BSC, low OSR) reduced solar access in winter, raising heating demand, but provided shading benefits in summer. Ahn and Sohn, (2019) in temperate Seattle, observed that higher BSC and lower vertical height variation were linked to reduced residential energy use. Chokhachian *et al.*, (2020) showed that in temperate Munich, extreme density with narrow canyons consistently worsened both heating and cooling loads, whereas intermediate to wide canyons balanced UHI mitigation with solar and daylight access, with an optimal FAR of about 4.

Although clustered forms are generally advantageous in cooling-dominated climates and dispersed typologies benefit heating-dominated contexts, studies on BSC, density, orientation, and canyon depth reveal unresolved questions about their optimal balance, with performance outcomes highly dependent on climate and scale. Similarly, while higher density often correlates with increased energy use due to occupancy and economic activity, its spatial configuration largely determines performance outcomes (Li et al., 2025). The reviewed studies also reveal two key research gaps: (i) limited examination of seasonal variability within the same climate and region, and (ii) insufficient cross-scale analysis linking morphological characteristics to microclimatic processes and, in turn, to building energy and thermal performance. These gaps constrain the development of more generalizable climate-specific urban design strategies.

3.5.5 Retrofitting Strategies in Urban Fabric

Urban fabric is the spatial and material composition of the built environment, including buildings, streets, and open spaces, which collectively shape the city's form, function, and environmental performance (Maretto et al., 2023). This section summarizes the findings across the reviewed literature of the impact of retrofit of various elements of the urban fabric on urban microclimate and ECM in (i) building level, and (ii) street and street canyon level. Table 3.5.2 summarizes design strategies and consideration while retrofitting urban fabric for energy efficiency.

Table 3.5.2 Key takeaways from retrofitting urban fabric employing different strategies.

Strategy	Cooling Impact	Considerations
Green roof & walls	Reduce roof surface temperatures & improves comfort; reduces cooling loads by 3-37%	Living walls outperform facades; irrigation enhances evapotranspiration.
Cool roofs	High-albedo coatings lower roof & air temperatures, reducing energy demand	Effectiveness varies by colour & climate; may increase glare & discomfort
Trees	Shade & evapotranspiration lower cooling loads (20-50% for well-placed trees)	Evergreens may increase winter heating demand; species & placement must match climate
Water bodies	Evaporative cooling reduces surrounding air temperatures; urban cooling islands	Placement along prevailing winds enhances cooling; integrate with green spaces
Urban albedo (pavement, street, building walls)	Cool pavements & high-albedo surfaces reduce heat storage & lower energy demand	Excessive reflectivity may increase glare & pedestrian discomfort; balance needed

3.5.5.1 *Building Level Material Strategies*

The building level material retrofitting strategies are discussed in two categories namely, greenery integration in walls and green and cool roofs. Table 3.5.3 summarises the literature discussing building level material strategies categorised across climate, methods, design parameters and observed outcomes.

Table 3.5.3 Literature summary on urban retrofitting strategies at building material level; categorised across climate, methods, design parameters and observed outcomes.

Article	Climate	Methods	Tested design parameters	Performance Outcome
Coma et al., 2017	Mediterranean	Experimental study for living and green facades	Living walls versus green facade	58.9% energy saving with living walls in summer season, 33.8% with green facades
Bakhshoodeh et al., 2022	Mediterranean	Comparison for 3 facade types for 2 orientations	Green facade, shade sail, plain wall	4.4°C and 1.7°C reduction for north-facing and west-facing facade surface temperature
Perini & Magliocco, 2014	Mediterranean	Vegetation density analysis through simulation	Green roof, ground vegetation	3-37% cooling load reduction
Baniassadi et al., 2018	Mediterranean	Comparative study via simulation tool	Ceiling R value, Window U value, window SHGC, Wall R value, air exchange rate, building orientation,	4-24% cooling energy savings up to a 20% reduction in discomfort hours with high albedo material

			window-to-wall ratio	
Karimi et al., 2022	Temperate and humid	Simulation study of living walls and green facades	Building form and foliage species	**3.62 - 4.43 kWh/m²** total energy reduction
Berardi, 2016	Continental climate	Green roof analysis with measurement and simulation	Leaf area index, soil depth	1.8-20.9% energy reduction; 22-36% indoor discomfort reduction
Zhao et al., 2024	Multiple climates in China	Comparative cool roof study via simulation	Cool roof pigments and their reflectivity	5.5% energy reduction, 14°C surface air temp. reduction by blue cool roof
-Schade et al., 2021	Subarctic	Real data collection and data analysis	Green roof versus black roof compared in different seasons	Black roofs ~10°C warmer than green roofs in summer, green roof is better insulator in summer

3.5.5.2 Greenery Integration on Walls

Green façades (plants rooted at ground level) and living walls (vegetation supported by external layers) represent two main wall-greening approaches (Harbiankova & Manso, 2025). In temperate and humid climates, total building energy consumption (heating and cooling energy) for simplified building varied in a range of 3.62 to 4.43 kWh/m², influenced by building form and foliage species (Karimi et al., 2022). Real-world data experimented and collected through three 27 m^3 cubicles in Mediterranean climate show living walls outperform green façades, reducing cooling demand by 58.9% versus 33.8% (Coma et al., 2017). For green façades, irrigation enhanced evapotranspirative cooling, achieving reductions of 4.4 °C and 1.7 °C for north-facing and west-facing facade surface temperature in Mediterranean climates (Bakhshoodeh et al., 2022).

3.5.5.3 Green and Cool Roofs

Green roofs effectively reduce building energy use in retrofitting studies (Berardi, 2016; Pastore et al., 2017). In continental climates, higher Leaf Area Index (LAI) improved microclimate cooling, while soil depth (30 cm, LAI = 2) reduced building energy consumption by 1.8–2.9% and lowered top-floor indoor discomfort by 22–36% (Berardi, 2016). In Mediterranean climates, ground vegetation improved outdoor comfort, while green roofs decreased cooling loads by 3–37%, depending on coverage and building density (Perini & Magliocco, 2014).

A cool roof is produced by applying a reflective coating that combines high solar reflectance (albedo) with high thermal emittance, thereby reflecting most incoming radiation and minimizing heat retention (Elnabawi et al., 2022). Cool roofs have been widely studied as retrofitting strategies at building and urban scales. Elnabawi et al.'s (2022) review study highlighted their dual benefits at both scales, reducing energy demand, roof surface temperatures, and indoor discomfort at the building scale, while lowering near-surface air temperatures, carbon emissions, and outdoor heat stress at the urban scale.

Zhao et al. (2024) demonstrated that performance varies by climate, with blue-coloured cool roofs in hot summer/warm winter regions reducing surface air temperature by up to 14.0 °C, while achieving a maximum energy use reduction of 5.5% compared to conventional roofs in other climates. In Mediterranean climate, Baniassadi et al. (2018) reported 24–41% cooling energy savings for low-performance buildings and up to a 20% reduction in discomfort hours in non-conditioned buildings when high-albedo roofs were applied. Additionally, Schade et al. (2021) showed that in subarctic climates, black roofs were ~10 °C warmer than green roofs in summer, but both performed similarly in winter, with green roofs offering negligible thermal benefits despite potential value for other ecological functions.

3.5.5.4 Street Level Strategies

Street Level Strategies are summarized across four categories: tree canopy, water body, pavements, and street canyon. Table 3.5.4 presents a summary of street level strategies adopted in literature.

Table 3.5.4 Literature summary on urban retrofitting strategies at street level; categorised across climate, methods, design parameters and observed outcomes.

Article	Climate	Method	Tested design parameters	Performance Outcome
Flowers & Huang, 2024	humid-subtropical	Monthly simulation method comparions	Tree and season: street tree presence and absence scenarios for 6 months	Building surface temperature reduction by 9.5% and cooling demand reduction by 16.7%
Wu et al., 2024	humid-subtropical	Measurement of a test bed for street canyon	Tree and aspect ratio	5.1–8.2°C surface cooling with trees
Hsieh et al., 2018	subtropical monsoon	Measurement & simulation	3 tree types, distance to buildings	Tree shading and transpiration reduced cooling loads by 10.3–15.2%
Liu et al., 2022	subtropical humid monsoon	Simulation	Location, season: 6 measurement points in building block at differing heights	3:1 green-to-water ratio minimized winter heating energy loads in residential buildings, 1:2 green-to-water ratio reduced summer cooling energy loads
`Falasca et al., 2019	humid subtropical climate	simulation	Settlement comparions (Rural, suburban, urban), high albedo materials on none/roof/all surfaces	High-albedo materials (0.7) applied to all surfaces in the urban canyon reduced energy demand by up to 5% during heatwaves but negatively affected pedestrian thermal comfort

Pastore et al., 2017	mediterranean	Multi-scale simulation comparison	Outdoor vegetation, low-e glazing, living walls, green roof	Up to 4.8°C reduced peak indoor air temperature using combined vegetation, 54% cooling energy saving using high leaf area density trees (2.5 m^2/m^3)
Salvati et al., 2022	temperate	Experimental model for real time measurement and simulation	3 locations for different road and facade albedo and vegetation scenarios	Road albedo of 0.6 raised wall surface temperatures by ~3°C and indoor operative temperatures by ~0.5°C
Jandaghian and Berardi, 2020	temperate continental	Measurement and simulation	6 different reflective surfaces, 3 locations	Albedo to 0.65 for roofs, 0.60 for walls, and 0.45 for ground surfaces reduced cooling energy demand by about 10%
Ravazdezh & Rivers, 2025	humid-continental climates	Regression model	Tree canopy coverage	10% tree canopy increase within 12m of homes decreased annual electricity use by 29%
Xu et al., 2019	humid continental	Measurement and simulation	4 locations (in relation to water bodies and trees)	43.6 kWh energy saving potential during hot summer days at 3pm by combining water bodies with green spaces

3.5.5.5 *Tree Canopy*

Tree canopy integration has been widely studied as a strategy to mitigate cooling loads by reducing solar exposure and enhancing evapotranspiration. Conceptually, tree canopies provide varying effects across seasonal changes and different climatic conditions. For instance, Meili et al. (2025) conducted a comparative analysis of tree impacts on energy demand in seven climates. They found that in hot-humid contexts, cooling benefits from trees were partly offset by increased humidity, which raised dehumidification energy demand. In cold-arid cities, evergreen vegetation increased building heating load by up to 7.16% on sunny winter days due to shading and wind effects (Ge et al., 2024). These findings indicate that effective outcomes depend on aligning tree species and placement with urban morphology and climate, since dense planting in enclosed, humid spaces may reduce cooling efficacy and thermal comfort (Li et al., 2024; Yang et al., 2025).

Tree shading provides significant long-term benefits under future climate scenarios. In hot-humid climates, 60 years of tree growth reduced cooling demand by 15.5% (Fu et al., 2025), while in temperate climates, planting strategies lowered cooling demand by 19–48% depending on canopy density; without trees, 2050 projections showed a 73–77% increase (Czekajlo et al., 2023).

Many papers included climate-specific findings for tree canopy impact on the urban and building cooling. In the Mediterranean, combined vegetation strategies reduced peak indoor air temperature by up to 4.8 °C (Pastore et al., 2017), and continuous high-density tree rows (Leaf Area Density (LAD) = 2.5 m^2/m^3) achieved cooling energy savings up to 54% (Tsoka et al., 2021). In humid-subtropical settings, trees lowered building surface temperatures by 9.5% and cooling demand by 16.7% in Taipei (Flowers & Huang, 2024). Street-canyon experiments with trees showed 5.1–8.2 °C surface cooling but also reduced wind velocity by 63.6% and raised vapor pressure by 2.77 hPa, potentially impairing comfort (Wu et al., 2024). In subtropical monsoon and humid-continental climates, tree shading and transpiration reduced cooling loads by 10.3–15.2% in Nanjing (Hsieh et al., 2018), while in Ottawa, a 10% canopy increase within 12.5 m of homes decreased annual electricity use by 29% and summer afternoon demand by 15% (Ravazdezh & Rivers, 2025).

3.5.5.6 Water Bodies

Water bodies contribute significantly to micro-scale cooling through evaporation and the absorption of shortwave radiation (Xu et al., 2019). Consequently, their integration into urban landscapes serves as a viable mitigation strategy against the urban heat island effect (Zhou et al., 2024). The effectiveness of water fountains can be further enhanced when they are positioned along prevailing wind directions, which facilitates the spatial distribution of cooling benefits (Tang et al., 2025).

At the building scale, combining water bodies with green spaces indicated up to 43.6 kWh energy saving potential during hot summer days at 3pm in humid continental climates (Xu et al., 2019). In subtropical humid monsoon regions, a 3:1 green-to-water ratio minimized winter heating energy loads in residential buildings, while a 1:2 ratio most effectively reduced summer cooling energy loads, indicating seasonal complementarities between green spaces and water bodies (Liu et al., 2022).

3.5.5.7 Pavement

Pavement material selection influences thermal comfort and urban heat island through both the material's permeability (Zhou et al., 2025) and heat reflectivity (Kappou et al., 2022). In their review, Kappou et al. (2022) elaborated on the performance of cool pavements, highlighting how increased albedo, evaporative cooling, and reduced heat conduction can decrease heat storage in pavement materials.

3.5.5.8 Albedo in Street Canyon

Salvati et al. (2022) introduced the concept of urban canyon albedo, showing that in London's temperate climate, higher road reflectivity combined with lower façade reflectivity at ground level can mitigate UHI. They found, however, that a road albedo of 0.6 risked overheating, raising wall surface temperatures by ~3 °C and indoor operative temperatures by ~0.5 °C. Similarly, Falasca et al. (2019) found that high-albedo materials (0.7) applied to all surfaces in the urban canyon reduced energy demand by up to 5% during heatwaves but negatively affected pedestrian thermal comfort, underscoring the trade-off between energy savings and outdoor comfort. At the building scale, Jandaghian and Berardi (2020) showed that increasing albedo to 0.65 for roofs, 0.60 for walls, and 0.45 for ground surfaces reduced cooling energy demand by about 10%, equivalent to savings of up to 2 W/m^2 in HVAC systems.

3.5.6 Overview of Key Findings

The literature highlights two dominant aspects shaping urban energy conservation: local microclimatic conditions and morphological configurations. These two aspects operate interdependently, as urban morphology alters local climatic patterns by modifying wind direction and speed, and by influencing solar incidence through urban occlusion. Such microclimatic modifications subsequently affect the performance of buildings embedded within the urban fabric, underlining the importance of climate and context specific strategies for the design of urban morphology. Reviewed papers demonstrate the extent to which climatic factors including wind, sun path, air temperature, and relative humidity are modified by the urban fabric (Shareef and Altan, 2022) and produce resultant changes in building performance.

While no universal design solution exists, several climate-specific patterns emerge. For instance, compact urban forms, characterized by clustered buildings, are generally effective in hot climates by reducing direct solar exposure and leveraging mutual shading to lower cooling loads. In contrast, dispersed forms are more suitable in cold climates, as they enhance solar access during winter. Beyond density, nuances in building shape, urban canyon geometry, and related morphological factors significantly affect performance and require careful consideration across climate zones.

Landscaping interventions have also received considerable attention. Tree canopies have been widely studied as a strategy to mitigate cooling loads by providing shade and enhancing evapotranspiration. However, evergreen vegetation can increase winter heating demand due to excessive shading and reduced airflow. Seasonal variability further complicates performance, with studies showing that the balance between greenery and water bodies can differently affect heating and cooling loads in warm–humid climates (Liu et al., 2022). Similarly, urban canyon albedo studies show that while reflective surfaces can mitigate UHI, they may also increase indoor and outdoor discomfort (Salvati et al., 2022), underscoring the need for holistic retrofitting approaches.

3.5.7 Conclusion

This review summarizes how elements of the urban morphology shape energy performance and liveability, with strategies varying across climatic zones. The review highlights four key future considerations. Firstly, while compact clusters reduced cooling loads in hot climates and dispersed forms enhanced solar access in cold climates, conflicting findings on site coverage, density, and canyon depth highlight unresolved questions about their optimal balance. Secondly, despite the growing attention to urban morphology and building performance, the generation of localized microclimatic boundary conditions prior to building energy simulation remains largely unaddressed. The prevalent use of generic EPW files overlooks intra-urban climatic variability, potentially biasing early-stage design decisions. Addressing this gap by integrating microclimate modelling as a precursor to building performance assessment offers a pathway toward more reliable, climate-responsive urban design workflows. Thirdly, the research showed limited treatment of seasonal variability, climate change, and dynamic urban growth, with most studies focused on static forms. Future research should prioritize case-based guidance for existing cities, linked to planning regulations that anticipate future climatic conditions. Lastly, for greenery-based strategies, integrated modeling across multiple performance metrics, context-specific testing, and empirical validation of vegetation dynamics remain critical. Similarly, studies on cool roofs, pavements, and water bodies must adopt multi-scale, empirical, and holistic approaches to deliver effective urban cooling strategies that balance comfort, energy, resource use, and resilience.

3.5.8 References

3.5.8.1 Urban Morphology

Abu Dab'at, A. and Alqadi, S. (2024) "The impact of urban morphology on energy demand of a residential building in a Mediterranean climate," Energy and Buildings, 325, p. 114989. Available at: https://doi.org/10.1016/j.enbuild.2024.114989.

Ahn, Y. and Sohn, D.-W. (2019) "The effect of neighbourhood-level urban form on residential building energy use: A GIS-based model using building energy benchmarking data in Seattle," Energy and Buildings, 196, pp. 124–133. Available at: https://doi.org/10.1016/j.enbuild.2019.05.018.

Ascione, F., Bianco, N., De Stasio, C., Mauro, G.M., Vanoli, G.P., 2017. Artificial neural networks to predict energy performance and retrofit scenarios for any member of a building category: A novel approach. Energy 118, 999–1017. https://doi.org/10.1016/j.energy.2016.10.126

Aydin, E.E. et al. (2024) "Climate-responsive urban planning through generative models: Sensitivity analysis of urban planning and design parameters for urban heat island in Singapore's residential settlements," Sustainable Cities and Society, 114, p. 105779. Available at: https://doi.org/10.1016/j.scs.2024.105779.

Biljecki, F., Chow, Y.S., 2022. Global Building Morphology Indicators. Computers, Environment and Urban Systems 95, 101809. https://doi.org/10.1016/j.compenvurbsys.2022.101809

Chokhachian, A. et al. (2020) "Urban performance and density: Generative study on interdependencies of urban form and environmental measures," Sustainable Cities and Society, 53, p. 101952. Available at: https://doi.org/10.1016/j.scs.2019.101952.

Elzeni, M., Elmokadem, A. and Badawy, N.M. (2022) "Classification of urban morphology indicators towards urban generation," Port-Said Engineering Research Journal, 26(1), pp. 43–56.

Eshraghi, P. et al. (2025) "Adopting explainable-AI to investigate the impact of urban morphology design on energy and environmental performance in dry-arid climates," Advances in Building Energy Research, 19(4), pp. 497–531. Available at: https://doi.org/10.1080/17512549.2025.2513280.

Feng, W. et al. (2019) "A review of net zero energy buildings in hot and humid climates: Experience learned from 34 case study buildings," Renewable and Sustainable Energy Reviews, 114, p. 109303. Available at: https://doi.org/10.1016/j.rser.2019.109303.

Ferrando, M., Causone, F., Hong, T., Chen, Y., 2020. Urban building energy modeling (UBEM) tools: A state-of-the-art review of bottom-up physics-based approaches. Sustainable Cities and Society 62, 102408. https://doi.org/10.1016/j.scs.2020.102408

Golany, G.S. (1996) "Urban design morphology and thermal performance," Atmospheric Environment, 30(3), pp. 455–465. Available at: https://doi.org/10.1016/1352-2310(95)00266-9.

Leng, H. et al. (2020) “Urban morphology and building heating energy consumption: Evidence from Harbin, a severe cold region city,” Energy and Buildings, 224, p. 110143. Available at: https://doi.org/10.1016/j.enbuild.2020.110143.

Li, X. and Gou, Z. (2025) “Urban morphology and energy self-sufficiency: A comparative study of residential blocks in eight global cities,” Cities, 166, p. 106240. Available at: https://doi.org/10.1016/j.cities.2025.106240.

Li, Y. et al. (2025) “Urban Form and Urban Energy Consumption at the Macro Scale in China,” Buildings, 15(16), p. 2909. Available at: https://doi.org/10.3390/buildings15162909.

Makki, M. et al. (2019) “Evolutionary algorithms for generating urban morphology: Variations and multiple objectives,” International Journal of Architectural Computing, 17(1), pp. 5–35. Available at: https://doi.org/10.1177/1478077118777236.

Marey, A., Wang, L.L., Gaur, A., Lu, H., Leroyer, S., Belair, S., 2025. Urban climate simulation for extreme heat events – A comparison between WRF and GEM. Urban Climate 63, 102570. https://doi.org/10.1016/j.uclim.2025.102570

Mobaraki, A. and Oktay Vehbi, B. (2022) “A Conceptual Model for Assessing the Relationship between Urban Morphology and Sustainable Urban Form,” Sustainability, 14(5), p. 2884. Available at: https://doi.org/10.3390/su14052884.

Peng, Y. et al. (2019) “An Investigation of the Quantitative Correlation between Urban Morphology Parameters and Outdoor Ventilation Efficiency Indices,” Atmosphere, 10(1), p. 33. Available at: https://doi.org/10.3390/atmos10010033.

Peng, Y., Gao, Z. and Ding, W. (2017) “An Approach on the Correlation between Urban Morphological Parameters and Ventilation Performance,” Energy Procedia, 142, pp. 2884–2891. Available at: https://doi.org/10.1016/j.egypro.2017.12.412.

Prataviera, E., Vivian, J., Lombardo, G., Zarrella, A., 2022. Evaluation of the impact of input uncertainty on urban building energy simulations using uncertainty and sensitivity analysis. Applied Energy 311, 118691. https://doi.org/10.1016/j.apenergy.2022.118691

Roth, J., Martin, A., Miller, C., Jain, R.K., 2020. SynCity: Using open data to create a synthetic city of hourly building energy estimates by integrating data-driven and physics-based methods. Applied Energy 280, 115981. https://doi.org/10.1016/j.apenergy.2020.115981

Shareef, S. and Altan, H. (2022) “Urban block configuration and the impact on energy consumption: A case study of sinuous morphology,” Renewable and Sustainable Energy Reviews, 163, p. 112507. Available at: https://doi.org/10.1016/j.rser.2022.112507.

Urban Redevelopment Authority. Updates to the Landscaping for Urban Spaces and High-Rises (LUSH) Programme: LUSH 3.0. Published: 09 November 2017. Circular No :URA/PB/2017/06-DCG. 2024 Oct 2. Available: https://www.ura.gov.sg/Corporate/Guidelines/Circulars/dc17-06

Yang, X., Zhao, L., Bruse, M., Meng, Q., 2012. An integrated simulation method for building energy performance assessment in urban environments. Energy and Buildings 54, 243–251. https://doi.org/10.1016/j.enbuild.2012.07.042

Zhu, S. et al. (2024) "Exploring the Impact of Urban Morphology on Building Energy Consumption and Outdoor Comfort: A Comparative Study in Hot-Humid Climates," Buildings, 14(5), p. 1381. Available at: https://doi.org/10.3390/buildings14051381.

3.5.8.2 Urban Fabric

Maretto, M., Gherri, B., Maiullari, D., Vernizzi, C., Pitanti, G., Finizza, C., & Monacelli, A. (2023). Environmental Urban Morphology: A Multidisciplinary Methodology for the Analysis of Public Spaces in Dense Urban Fabrics. *Sustainability*, *15*(23), 16493.

3.5.8.3 Greenery Integration on Walls

Harbiankova, A., & Manso, M. (2025). Integrating green roofs and green walls to enhance buildings thermal performance: A literature review. *Building and Environment*, 112524.

Karimi, K., Farrokhzad, M., Roshan, G., & Aghdasi, M. (2022). Evaluation of effects of a green wall as a sustainable approach on reducing energy use in temperate and humid areas. *Energy and Buildings*, *262*, 112014.

Coma, J., Pérez, G., de Gracia, A., Burés, S., Urrestarazu, M., & Cabeza, L. F. (2017). Vertical greenery systems for energy savings in buildings: A comparative study between green walls and green facades. *Building and environment*, *111*, 228-237.

Bakhshoodeh, R., Ocampo, C., & Oldham, C. (2022). Evapotranspiration rates and evapotranspirative cooling of green façades under different irrigation scenarios. *Energy and Buildings*, *270*, 112223.

3.5.8.4 Green and Cool Roof

Berardi, U. (2016). The outdoor microclimate benefits and energy saving resulting from green roofs retrofits. *Energy and buildings*, *121*, 217-229.

Pastore, L., Corrao, R., & Heiselberg, P. K. (2017). The effects of vegetation on indoor thermal comfort: The application of a multi-scale simulation methodology on a residential neighborhood renovation case study. *Energy and Buildings*, *146*, 1-11.

Perini, K., & Magliocco, A. (2014). Effects of vegetation, urban density, building height, and atmospheric conditions on local temperatures and thermal comfort. *Urban Forestry & Urban Greening*, *13*(3), 495-506.

Elnabawi, M. H., Alhumaidi, A., Osman, B., & Alshehhi, R. (2022). Cool roofs in hot climates: A conceptual review of modelling methods and limitations. *Buildings*, *12*(11), 1968.

Zhao, S., Hai, G., & Zhang, X. (2024). An Analysis of the Influence of Cool Roof Thermal Parameters on Building Energy Consumption Based on Orthogonal Design. *Buildings*, *14*(1), 28.

Baniassadi, A., Sailor, D. J., Crank, P. J., & Ban-Weiss, G. A. (2018). Direct and indirect effects of high-albedo roofs on energy consumption and thermal comfort of residential buildings. *Energy and Buildings*, *178*, 71-83.

Schade, J., Lidelöw, S., & Lönnqvist, J. (2021). The thermal performance of a green roof on a highly insulated building in a sub-arctic climate. *Energy and Buildings*, *241*, 110961.

Tree Canopy

Meili, N., Zheng, X., Takane, Y., Nakajima, K., Yamaguchi, K., Chi, D., ... & Fatichi, S. (2025). Modeling the effect of trees on energy demand for indoor cooling and dehumidification across cities and climates. *Journal of Advances in Modeling Earth Systems*, *17*(3), e2024MS004590.

Ge, J., Wang, Y., Zhou, D., Gu, Z., & Meng, X. (2024). Effects of urban vegetation on microclimate and building energy demand in winter: An evaluation using coupled simulations. *Sustainable Cities and Society*, *102*, 105199.

Li, H., Zhao, Y., Wang, C., Ürge-Vorsatz, D., Carmeliet, J., & Bardhan, R. (2024). Cooling efficacy of trees across cities is determined by background climate, urban morphology, and tree trait. *Communications Earth & Environment*, *5*(1), 754.

Yang, C., Xie, M., & Mendis, T. (2025). Evaluating the role of urban trees on building energy use: a global literature review. *Landscape and Urban Planning*, *264*, 105475.

Fu, H., Jiao, Y., Deng, L., & Wang, W. (2025). Dynamic impacts of vegetation growth and urban development on microclimate and building energy consumption. *Sustainable Cities and Society*, *126*, 106382.

Czekajlo, A., Alva, J., Szeto, J., Girling, C., & Kellett, R. (2023). Impact of 2050 tree shading strategies on building cooling demands. *Buildings & Cities*, *4*(1).

Tsoka, S., Leduc, T., & Rodler, A. (2021). Assessing the effects of urban street trees on building cooling energy needs: The role of foliage density and planting pattern. *Sustainable Cities and Society*, *65*, 102633.

Flowers, B., & Huang, K. T. (2024). Developing a Chained Simulation Method for Quantifying Cooling Energy in Buildings Affected by the Microclimate of Avenue Trees. *Atmosphere*, *15*(10), 1150.

Wu, Z., Shi, Y., Ren, L., & Hang, J. (2024). Scaled outdoor experiments to assess impacts of tree evapotranspiration and shading on microclimates and energy fluxes in 2D street canyons. *Sustainable Cities and Society*, *108*, 105486.

Hsieh, C. M., Li, J. J., Zhang, L., & Schwegler, B. (2018). Effects of tree shading and transpiration on building cooling energy use. *Energy and Buildings*, *159*, 382-397.

Ravazdezh, F., & Rivers, N. (2025). Quasi-experimental evidence that the urban tree canopy reduces residential energy consumption. *Energy and Buildings*, *344*, 115992.

Water Bodies

Xu, X., Liu, S., Sun, S., Zhang, W., Liu, Y., Lao, Z., ... & Zhu, J. (2019). Evaluation of energy saving potential of an urban green space and its water bodies. *Energy and Buildings*, *188*, 58-70.

Tang, L., Zheng, W., Wu, Y., Tang, L., & Zhao, Y. (2025). Evaluating the cooling performance of vegetation combined with a fountain in horizontal and vertical urban environments. *Building and Environment*, *267*, 112192.

Zhou, W., Wu, T., & Tao, X. (2024). Exploring the spatial and seasonal heterogeneity of cooling effect of an urban river on a landscape scale. *Scientific Reports*, *14*(1), 8327.

Liu, W., Zuo, B., Qu, C., Ge, L., & Shen, Q. (2022). A reasonable distribution of natural landscape: Utilizing green space and water bodies to reduce residential building carbon emissions. *Energy and Buildings*, *267*, 112150.

Pavement

Zhao, J., Lu, J., Ge, J., Fan, Y., Wang, H., Gu, M., ... & Luo, X. (2025). Influences of permeable pavements with different hydraulic properties on evaporative cooling and outdoor thermal environment: Field experiments. *Building and Environment*, *270*, 112525.

Kappou, S., Souliotis, M., Papaefthimiou, S., Panaras, G., Paravantis, J. A., Michalena, E., ... & Mihalakakou, G. (2022). Cool pavements: State of the art and new technologies. *Sustainability*, *14*(9), 5159.

Urban Canyon Albedo

Salvati, A., Kolokotroni, M., Kotopouleas, A., Watkins, R., Giridharan, R., & Nikolopoulou, M. (2022). Impact of reflective materials on urban canyon albedo, outdoor and indoor microclimates. *Building and Environment*, *207*, 108459.

Falasca, S., Ciancio, V., Salata, F., Golasi, I., Rosso, F., & Curci, G. (2019). High albedo materials to counteract heat waves in cities: An assessment of meteorology, buildings energy needs and pedestrian thermal comfort. *Building and environment*, *163*, 106242.

Jandaghian, Z., & Berardi, U. (2020). Analysis of the cooling effects of higher albedo surfaces during heat waves coupling the Weather Research and Forecasting model with building energy models. *Energy and Buildings*, *207*, 109627.

3.6 Urban Moisture Distribution and its Impact on Thermal Comfort

This section should be cited as:

Teng, X., Fan, Y. (2026). Urban moisture distribution and its impact on thermal comfort. In: A Systematic Review of Passive Energy Conservation Measures and Probabilistic Assessment under Changing Climate in Urban Settings, CIB W040 Report, CIB General Secretariat.

3.6.1 Factors influencing moisture transfer and diffusion

The transfer and evaporation of moisture into the atmosphere primarily occur through the processes of evaporation and transpiration (Miralles et al., 2025; Sinha et al., 2025). Water in the soil, permeable pavements, rain stored over impervious surfaces, rivers and lakes are sources for evaporation (Guida et al., 2025; Qin et al., 2025). The higher the water vapor deficiency is, the faster the evaporation rate. Wind also accelerates evaporation by carrying away heat and moisture, enhancing the transfer of water vapor into the atmosphere (Liu et al., 2025b). When the surface temperature of a building or ground is low, water vapor in the air may condense into water droplets, releasing latent heat and thus altering the local water vapor concentration (Liu et al., 2025a). The transpiration of plants contributes to moisture transfer, as they release water vapor through stomata on their leaves, increasing local moisture (Wang et al., 2025). The physical processes, influenced by urban morphology, building materials, urban greenery, water bodies and the characteristics of urban underlying surfaces, collectively shape the distribution and variation of urban moisture.

3.6.1.1 Urban morphology

The urban dry island (Cao et al., 2024) and urban moisture island (Wu et al., 2025) effects coexist as spatiotemporally heterogeneous phenomena. Conventional understanding suggests that urban areas are typically drier than surrounding non-urban areas (Lokoshchenko, 2017), characterizing the urban dry island effect. It is mainly due to the significantly higher proportion of impervious surfaces in urban areas compared to rural areas. The water on urban impervious surfaces evaporates quickly a period after the rainfall, while the permeable surfaces in rural areas can retain water in their pores, allowing for a longer water evaporation process.

Shortly after the rainfall, surface water accumulation increases and impervious surfaces evaporate a significant amount of water, raising the water vapor concentration (Zhou et al., 2021). The expansion of artificial lakes, wetlands and other water bodies in urban areas enhances evaporation, further increasing water vapor. Human activities, such as industrial production and domestic water use, contribute to higher water vapor content in the atmosphere. The urban heat island effect also intensifies evaporation (Huang and Song, 2023). These factors also collectively contribute to the formation of urban moisture islands, characterized by higher moisture content in urban areas compared to rural areas (Shi et al., 2019). The relative humidity variation over time for Hong Kong experiences a yearly increase in humidity due to limited airflow, insufficient ventilation and sea breeze (Huang and Song, 2023). Insufficient ventilation prevents effective moisture diffusion, causing moisture to linger in the air and resulting in localized water vapor accumulation. The urban form density and street layout significantly influences the water vapor transfer and evaporation process, shaping the spatial distribution of water vapor in cities (Wang et al., 2021). Yang et al. (Yang et al., 2021) highlighted that high-density cities experience increased local moisture. Correa et al. (Correa et al., 2012) demonstrated that the canyon effect exacerbates water vapor accumulation due to limited ventilation. Enhanced urban ventilation aids in moisture removal, increasing the diffusion rate of water vapor and enhancing the efficiency water evaporation from surfaces into the atmosphere (Seppänen and Kurnitski, 2009).

Research showed that ventilation corridors, by promoting air circulation, effectively regulate local moisture distribution (Gu et al., 2020). The lower temperature in green space ventilation corridors results in weaker evapotranspiration, leading to the lower content of water vapor compared to dispersed vegetated area (Jiang et al., 2018). On the other hand, ventilation corridors also influence water evaporation through air flow. Air flow helps remove accumulated water vapor (Onabanjo et al., 2023; Wang et al., 2021), increasing water vapor deficiency in the ventilation corridors and thus facilitate evapotranspiration. The impact of ventilation corridors on moisture distribution is influenced by factors such as climate conditions and corridor design parameters (e.g., width and orientation). The layout of streets and ventilation corridors align with the prevailing wind direction to enhance air movement and facilitate water vapor dispersion (Gong et al., 2023; Ng, 2009).

3.6.1.2 Building materials

Building materials significantly alter the local humidity distribution in cities by influencing water evaporation and water vapor condensation processes (Torres-Rivas et al., 2018). The hygroscopicity, thermal conductivity and surface properties of different materials determine their ability to regulate moisture transfer, influencing the urban microclimate's humidity and thermal environment. Li et al. (Li and Luo, 2024) conducted capillary water absorption experiments on seven traditional and novel porous building materials (expanded polystyrene, extruded polystyrene, foam glass, expanded perlite, cement mortar, clay brick and gypsum board). The results showed that the density and porosity of building materials influence their capillary absorption rate and water retention capacity. Clay bricks exhibited the highest capillary absorption rate, which may lead to indoor moisture condensation.

The building surface will become wet after rainfall. Dense materials (such as concrete and asphalt) have low porosity and limited internal water storage. Surface water evaporates quickly, leading to a faster drying rate (Jerjen et al., 2015). In contrast, porous bricks and green building materials, with their higher porosity, can store more water internally. Through capillary action, the water in these materials evaporates more slowly, resulting in a slower drying rate and prolonged evaporation process (Dos Santos and Mendes, 2009). At lower temperatures, non-hygroscopic materials like metal and glass tend to form condensate on their surfaces, reducing the content of outdoor water vapor. However, during the condensation, the relative humidity is high due to the lower temperature as the near-surface air presents saturated conditions.

3.6.1.3 Urban greenery and water bodies

Natural elements (urban greenery and water bodies) not only mitigate the urban heat island effect but also optimize the thermal and moisture conditions around buildings. Urban greenery and water bodies significantly influence water vapor transfer and water evaporation by modulating local temperature and wind patterns (Lin and Li, 2025; Manapragada and Natanian, 2025; Ming et al., 2025).

The urban greening system encompasses four main components, namely green walls (often referred to as vertical greening), green roofs, park green spaces, and street trees. Related studies have shown that the distance between green structures and walls influences the humidity levels and the drying process of the walls (Edelman et al., 2019). The temperature and humidity regulation effect of green façades is significantly influenced by the moisture content of the substrate (Abdo and Huynh, 2021). A summary of previous studies on the summer shading, cooling, humidifying and energy-saving effects of vertical greening is shown in Table A1 of Appendix A (Peng et al., 2020). As for Green roofs, they can also regulate urban temperature and humidity through evapotranspiration (Jim, 2014). Vegetation types, irrigation systems and wind speed significantly influence evaporation efficiency and plant transpiration on green roofs (Cirkel et al., 2018; Tabares-Velasco and Srebric, 2009). The water content in the soil directly impacts plant transpiration (Furr and Reeve, 1945). When soil moisture drops below the wilting point, plants are unable to transpire and eventually wilt. Urban parks, through their strong transpiration, enhance the transfer of more water vapor to the atmosphere, increasing the air humidity (Kim and Coseo, 2018).

Due to high specific heat and evaporative cooling (Wong et al., 2016), water bodies significantly influence the surrounding thermal environment and relative humidity (Indumati et al., 2009; Yang et al., 2020). The air above water bodies remains cooler than over built-up areas in daytime, driving natural convection such as sea or lake breezes that transport cool moist air to adjacent zones (Manteghi et al., 2015), as shown in Figure 3.6.1a. In calm and clear weather during nighttime, a heat dome with humid and hot regions can form above the water body (Figure 3.6.1b). The temperature and humidity inside the dome are significantly higher than in surrounding areas (Saaroni and Ziv, 2003; Theeuwes et al., 2013).

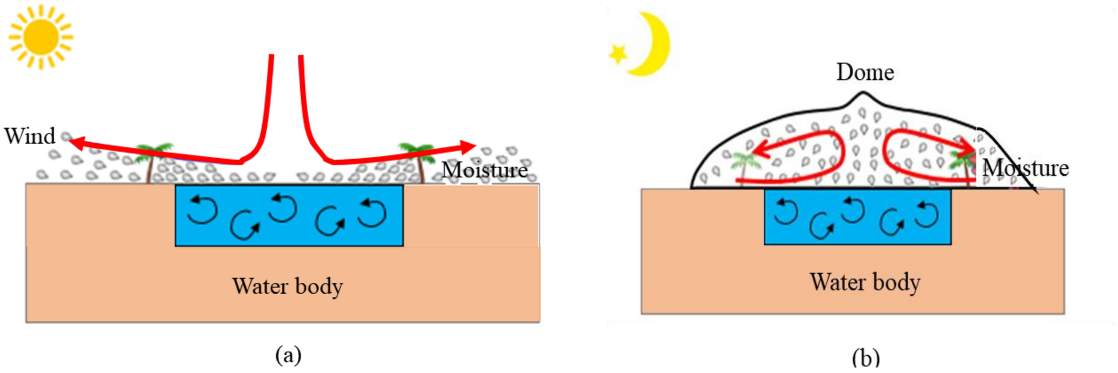

Figure 3.6.1. Impact of water bodies on surrounding moisture environments. (a) Daytime condition. (b) Nighttime condition.

3.6.1.4 The characteristics of urban underlying surfaces

Impervious surfaces (such as asphalt and concrete) differ significantly from natural soils in their physical properties, influencing the evaporation process in urban areas. Immediately after rainfall, most of the water runs off over impervious surfaces, while the remaining limited water evaporates fast, leading to the disappearance of evaporative cooling. Natural soils promote evaporation and increase water vapor with their higher porosity and moisture retention capacity (Amooh and Bonsu, 2015). Soil physical properties, such as sand content, initial moisture and dry density, significantly influence the rate of water evaporation (An et al., 2018). Studies have shown that lower soil porosity results in lower evaporation efficiency within the soil (Liao et al., 2021).

In clear weather, water retained in the permeable pavements can evaporate into the urban air. High porosity permeable paving materials (such as permeable bricks, permeable asphalt, permeable gravel and grass paving bricks) have a significant evaporation and moisture-enhancing effect (Fwa et al., 2015). To achieve the maximum evaporative effect of permeable pavements, it is crucial to keep a sufficient water supply. The water can come from retained moisture in the base layers, as well as external rainfall or artificial watering. With climate change, heatwaves are becoming more frequent globally. Watering road surfaces is one of the few adaptive outdoor temperature and humidity regulation measures (dynamic approach). Study found that in Zurich, Switzerland, during heatwave conditions, watering for 10 minutes (with a water volume of 6 mm) between 8:00 and 10:00 in the morning ensures the maximum cooling effect for 24 hours (Kubilay et al., 2020). The influences of various factors on moisture are summarized in Table B1 of Appendix B.

3.6.2 Spatial non-uniformity of urban moisture distribution

The spatial distribution of moisture in cities shows significant non-uniformity. Data from a single weather station cannot fully reflect the humidity conditions across the entire city. This non-uniformity is mainly influenced by factors such as urban morphology, building materials, urban greenery, water bodies distribution and the characteristics of the underlying surface. Due to these varying factors, there is a marked difference in moisture levels across different regions, requiring the deployment of multiple weather stations to comprehensively capture its spatial variations. To achieve a comprehensive understanding of humidity variation across these regions, both fixed and mobile monitoring methods can be utilized. Data from fixed stations are more suitable for studying long-term humidity trends (Yang et al., 2017). Mobile monitoring methods can capture the spatial distribution of humidity more comprehensively. Mobile measurement data analysis may be limited to relatively short observation periods. The development of the low-altitude economy and IoT can help to improve long-term monitoring with high spatial-temporal resolution. To investigate the spatial heterogeneity of humidity distribution, researchers developed humidity prediction models and created datasets with varying spatial resolutions. Yang et al. (Yang et al., 2013) developed a physically based analytical spatial air temperature and humidity model (PASATH). Razafimaharo et al. (Razafimaharo et al., 2020) developed a daily high-resolution temperature and relative humidity dataset (HYRAS) for Germany and its catchment areas, spanning from 1951 to 2015, with a spatial resolution of 5 km×5 km.

3.6.3 The impact of moisture on thermal comfort

Thermal comfort significantly influences an individual's physiological health, psychological stress and work performance. Humidity, as a key environmental factor, influences both thermal sensation and comfort (Bueno et al., 2021; Lan et al., 2011; Li et al., 2021). Under high temperature conditions, high humidity exacerbates heat stress by inhibiting sweating and skin evaporation, increasing the sensation of thermal discomfort (Amaripadath et al., 2023; Berglund, 1997; Jing et al., 2013). In hot summers, reducing air temperature enhances thermal comfort, while increasing relative humidity reduces it. Therefore, the overall impact of humidity on outdoor thermal comfort requires precise quantification. Two commonly used parameters are Wet Bulb Globe Temperature (WBGT) (Stull, 2011) and Physiological Equivalent Temperature (PET) (Höppe, 1999). The WBGT is a weighted average of the ambient, wet-bulb and globe temperatures (Liu et al., 2025c). The WBGT is simplified by Eq. (3.6.1) (Stull, 2011).

$$\begin{aligned}\mathrm{WBGT}=&T\,arctan[\,0.151977(RH+8.313659)^{1/2}]+arctan(T+RH)-arctan(\,RH-1.676331)\\&+0.00391838(RH)^{3/2}\times arctan(\,0.023101RH)-4.686035\end{aligned} \tag{3.6.1}$$

where RH [%] represent the relative humidity. T [°C] is the air temperature.

To assess heat risks associated with urban heat island and urban moisture island effects, a heat index (HI) combining air temperature and relative humidity was introduced by Eq. (3.6.2) (Rothfusz and Headquarters, 1990). Research also used discomfort index (H) calculated by Eq. (3.6.3) (Masterton and Richardson, 1981) to assess thermal comfort related to temperature and relative humidity. Zheng et al. incorporated land surface temperature into the thermal comfort index to assess the impact of microclimate on thermal comfort. The modified thermal comfort index (MTHI) is defined by Eq. (3.6.5) (Zheng et al., 2022). Besides, studies incorporated the variations in temperature and humidity specific to coastal areas into the heat index equation, deriving a modified evaluation index to assess the impact of water bodies on human comfort in coastal zones. The standard formula for the heat index is outlined in Eq. (3.6.6) (Oke, 1982). Studies also adopted UTCI as a thermal comfort evaluation index, with key variables such as wind speed, air temperature, relative humidity and mean radiant temperature influencing its calculation (Thapa et al., 2024).

$$\begin{aligned}HI=&-8.784695+1.61139411\times T+2.338549\times RH-0.14611605\times T\times RH\\&-1.2308094\times10^{-2}\times T^2-1.6424828\times10^{-2}\times RH^2+2.211732\times10^{-3}\times T^2\times RH\\&+7.2546\times10^{-4}\times T\times RH^2-3.582\times10^{-6}\times T^2\times RH^2\end{aligned} \tag{3.6.2}$$

$$H=T+\frac{5}{9}\times(e-10) \tag{3.6.3}$$

$$e=6.112\times(RH/1000)\times10^{[7.5\times T/(237.7+T)]} \tag{3.6.4}$$

$$MTHI=0.10 \times (T - 0.55 \times (1 - RH) \times (T - 14.50)) \times (2.25 + 0.67 \times LST) \quad (3.6.5)$$

$$E_t = T - 0.55(1 - RH)(T - 14.5) \quad (3.6.6)$$

where *e* denotes [kPa] the pressure of water vapor. *LST* [° C] is the land surface temperature.

Urban morphology and street layout play a significant role in influencing temperature and humidity, which impacts thermal comfort. Du et al. (Du et al., 2022) found that the highest urban moisture island intensity occurs in coastal areas (LCZ10) during the daytime, where the difference between the HI and the air temperature at 2 m reaches 5.4 °C, resulting in poor thermal comfort. At nighttime, the highest difference (6.6 °C) occurs in high-density areas (LCZ1), as the peak urban heat island intensity intensifies the impact of the urban moisture island on thermal comfort. Wide streets promote airflow, lowering humidity. However, stronger solar radiation during the day leads to higher temperatures, which negatively influence thermal comfort (Qaid and Ossen, 2015).

Water bodies lower the temperature through evaporation, enhancing thermal comfort. However, the increase in humidity may reduce thermal comfort (Deng et al., 2022; Gunawardena et al., 2017). The impacts of water bodies on thermal comfort also need a comprehensive consideration of both temperature and humidity. Zhao and Fong (Zhao and Fong, 2017) found through numerical simulations in Hong Kong that water bodies pose a risk of reducing thermal comfort during the day due to the high humidity. A related study showed that in urban parks in Tabriz, Iran, water body evaporation can lower air temperature but increase humidity, which reduces thermal comfort (Teshnehdel et al., 2022). Proper landscape planning enhances the water body's effect on human comfort. In Ahmedabad, India, the temperature and PET index on the western side of Kankaria Lake were 0.2 °C and up to 1.44 °C lower, respectively, compared to the eastern side during seven days in October (Gajjar and Devi, 2019).

In addition to temperature reduction, trees provide important shade effects that contribute to improved thermal comfort. Under tree canopies, air temperature and PET can decrease by 0.6° C and 0.1-1.6° C with higher thermal comfort, respectively (subtropical, Hong Kong, Cheung and Jim, 2018, (Cheung and Jim, 2018)). A study by De Abreu-Harbich et al. (De Abreu-Harbich et al., 2015) found that different tree species could reduce 76-89% of solar radiation between 10:00 and 14:00 (under the canopy, Campinas, Brazil), while also lowering air temperature by 0.7-2.8° C. Relative humidity increased by 0.5%-10.4%. A study in Shenyang, China, by Miao et al. (Miao et al., 2022) found that in summer, street trees could reduce PET from 46.3°C to 44.2°C to improve thermal comfort. While in autumn, it increased from 36.4 °C to 37.5 °C.

When considering urban heat mitigation strategies, permeable pavements can be beneficial in cooling through evaporation. However, the increase in humidity they generate may also elevate heat stress, potentially compromising thermal comfort. Zhao et al. (Zhao et al., 2025) found that irrigation of permeable pavements improves thermal comfort, reducing the UTCI difference with impermeable surfaces by 0.4°C. Materials like grass and travertine can lower heat stress, which showed grass with a PET score of 25.9 °C (Irmak et al., 2017). Regular watering in arid regions, such as Lanzhou, can significantly enhance thermal comfort by regulating both humidity and temperature (Liu et al., 2022). The impacts of humidity on thermal comfort are summarized in Table C1 of Appendix C.

3.6.4 Summary

Urban moisture distribution plays a critical role in shaping thermal comfort, influenced by various factors such as urban morphology, building materials, greenery, water bodies and underlying surface characteristics. The interplay between moisture and temperature significantly impacts human thermal comfort, with high humidity exacerbating heat stress during hot conditions. Urban moisture islands driven by impervious surfaces, limited ventilation and human activities further intensify these effects. Strategies such as enhancing urban ventilation, optimizing green infrastructure and utilizing permeable pavements can mitigate these challenges by regulating humidity and temperature. However, the trade-offs between cooling effects and increased humidity must be carefully managed to ensure improved thermal comfort. Looking ahead, as global temperatures rise and heatwaves become more frequent, cities must adopt adaptive measures to address the dual challenges of heat and humidity. Future research should focus on developing integrated urban planning strategies that balance humidity and temperature regulation with thermal comfort. This includes optimizing ventilation corridors, expanding green and blue infrastructure and utilizing advanced materials with improved moisture and temperature management properties. Besides, leveraging emerging technologies such as IoT and low-altitude monitoring systems can enhance the precision of humidity and temperature data collection, enabling more effective urban climate management. By prioritizing these approaches, cities can better adapt to a warming climate and enhance the resilience and comfort of urban environments.

3.6.5 References

Abdo, P., Huynh, B.P., 2021. An experimental investigation of green wall bio-filter towards air temperature and humidity variation. Journal of Building Engineering 39, 102244.

Alsaad, H., Hartmann, M., Hilbel, R., Voelker, C., 2022. The potential of facade greening in mitigating the effects of heatwaves in Central European cities. Building and Environment 216, 109021.

Amaripadath, D., Rahif, R., Velickovic, M., Attia, S., 2023. A systematic review on role of humidity as an indoor thermal comfort parameter in humid climates. Journal of Building Engineering 68, 106039.

Amooh, M.K., Bonsu, M., 2015. Effects of soil texture and organic matter on evaporative loss of soil moisture. J. Glob. Agric. Ecol 3, 152-161.

An, N., Tang, C.-S., Xu, S.-K., Gong, X.-P., Shi, B., Inyang, H.I., 2018. Effects of soil characteristics on moisture evaporation. Engineering Geology 239, 126-135.

Berglund, L., 1997. Thermal and non-thermal effects of humidity on comfort. Journal of the Human-Environment System 1, 35-45.

Berretta, C., Poë, S., Stovin, V., 2014. Moisture content behaviour in extensive green roofs during dry periods: The influence of vegetation and substrate characteristics. Journal of Hydrology 511, 374-386.

Bueno, A.M., de Paula Xavier, A.A., Broday, E.E., 2021. Evaluating the connection between thermal comfort and productivity in buildings: A systematic literature review. A Systematic Literature Review 11, 244.

Cameron, R.W., Taylor, J.E., Emmett, M.R., 2014. What's 'cool'in the world of green façades? How plant choice influences the cooling properties of green walls. Building and Environment 73, 198-207.

Cao, J., Li, M., Yang, X., Zhang, R., Wang, M., 2024. The impact of urban dry island on building energy consumption is overlooked compared to urban heat island in cold climate. Energy and Buildings 320, 114655.

Chen, Q., Li, B., Liu, X., 2013. An experimental evaluation of the living wall system in hot and humid climate. Energy and Buildings 61, 298-307.

Cheung, P.K., Jim, C.Y., 2018. Comparing the cooling effects of a tree and a concrete shelter using PET and UTCI. Building and Environment 130, 49-61.

Cirkel, D.G., Voortman, B.R., Van Veen, T., Bartholomeus, R.P., 2018. Evaporation from (blue-) green roofs: Assessing the benefits of a storage and capillary irrigation system based on measurements and modeling. Water 10, 1253.

Coma, J., Pérez, G., de Gracia, A., Burés, S., Urrestarazu, M., Cabeza, L.F., 2017. Vertical greenery systems for energy savings in buildings: A comparative study between green walls and green facades. Building and Environment 111, 228-237.

Correa, E., Ruiz, M.A., Canton, A., Lesino, G., 2012. Thermal comfort in forested urban canyons of low building density. An assessment for the city of Mendoza, Argentina. Water Resources Research 58, 219-230.

Cuce, E., 2017. Thermal regulation impact of green walls: An experimental and numerical investigation. Applied Energy 194, 247-254.

De Abreu-Harbich, L.V., Labaki, L.C., Matzarakis, A., 2015. Effect of tree planting design and tree species on human thermal comfort in the tropics. Landscape and Urban Planning 138, 99-109.

De Jesus, M.P., Lourenço, J.M., Arce, R.M., Macias, M., 2017. Green façades and in situ measurements of outdoor building thermal behaviour. Building and Environment 119, 11-19.

Deng, X., Cao, Q., Wang, L., Wang, W., Wang, S., Wang, L., 2022. Understanding the impact of urban expansion and lake shrinkage on summer climate and human thermal comfort in a land-water mosaic area. Atmospheres 127, e2021JD036131.

Djedjig, R., Belarbi, R., Bozonnet, E., 2017. Experimental study of green walls impacts on buildings in summer and winter under an oceanic climate. Energy and Buildings 150, 403-411.

Dos Santos, G.H., Mendes, N., 2009. Heat, air and moisture transfer through hollow porous blocks. International Journal of Heat and Mass Transfer 52, 2390-2398.

Du, R., Song, J., Huang, X., Wang, Q., Zhang, C., Brousse, O., Chan, P.W., 2022. High-resolution regional modeling of urban moisture island: mechanisms and implications on thermal comfort. Building and Environment 207, 108542.

Edelman, H., Pakkala, T., Tuominen, E., Köliö, A., Jauni, M., Pentti, M., Kiviste, M., Vinha, J., Lehvävirta, S., 2019. Moisture Safety of Green Facades. Alue Ja Ympäristö 48, 55-68.

Eumorfopoulou, E., Kontoleon, K., 2009. Experimental approach to the contribution of plant-covered walls to the thermal behaviour of building envelopes. Building and Environment 44, 1024-1038.

Furr, J., Reeve, J., 1945. The range of soil moisture percentages through which plants undergo permanent wilting in some soils from semi-arid, irrigated areas. J. Agric. Res 71, 149-170.

Fwa, T., Lim, E., Tan, K., 2015. Comparison of permeability and clogging characteristics of porous asphalt and pervious concrete pavement materials. Transportation Research Record 2511, 72-80.

Gajjar, H., Devi, J.J., 2019. Assessment of role of water body on thermal comfort in ahmedabad, India, IOP Conference Series: Earth and Environmental Science. IOP Publishing, p. 012023.

Giannopoulou, K., Livada, I., Santamouris, M., Saliari, M., Assimakopoulos, M., Caouris, Y., 2014. The influence of air temperature and humidity on human thermal comfort over the greater Athens area. Sustainable Cities and Society 10, 184-194.

Gonçalves, T.D., Brito, V., Vidigal, F., Matias, L., Faria, P., 2015. Evaporation from porous building materials and its cooling potential. Journal of Materials in Civil Engineering 27, 04014222.

Gong, D., Dai, X., Zhou, L., 2023. Satellite-Based optimization and planning of urban ventilation corridors for a healthy microclimate environment. Sustainability 15, 15653.

Gu, K., Fang, Y., Qian, Z., Sun, Z., Wang, A., 2020. Spatial planning for urban ventilation corridors by urban climatology. Ecosystem Health and Sustainability 6, 1747946.

Guida, G., Vespo, V.S., Musso, G., Della Vecchia, G., 2025. The role of hydraulic and thermal properties of soil in evaporation: a numerical insight. Environmental Geotechnics 12, 34-51.

Gunawardena, K.R., Wells, M.J., Kershaw, T., 2017. Utilising green and bluespace to mitigate urban heat island intensity. Science of the Total Environment 584-585, 1040-1055.

Guo, A., Yue, W., Yang, J., Li, M., Xie, P., He, T., Zhang, M., Yu, H., 2023. Quantifying the impact of urban ventilation corridors on thermal environment in Chinese megacities. Ecological Indicators 156, 111072.

Haggag, M., Hassan, A., Elmasry, S., 2014. Experimental study on reduced heat gain through green façades in a high heat load climate. Energy and Buildings 82, 668-674.

Hoelscher, M.-T., Nehls, T., Jänicke, B., Wessolek, G., 2016. Quantifying cooling effects of facade greening: Shading, transpiration and insulation. Energy and Buildings 114, 283-290.

Höppe, P., 1999. The physiological equivalent temperature–a universal index for the biometeorological assessment of the thermal environment. International Journal of Biometeorology 43, 71-75.

Huang, X., Song, J., 2023. Urban moisture and dry islands: spatiotemporal variation patterns and mechanisms of urban air humidity changes across the globe. Environmental Research Letters 18, 103003.

Indumati, S., Oza, R., Mayya, Y., Puranik, V., Kushwaha, H., 2009. Dispersion of pollutants over land–water–land interface: Study using CALPUFF model. Atmospheric Environment 43, 473-478.

Irmak, M.A., Yilmaz, S., Dursun, D., 2017. Effect of different pavements on human thermal comfort conditions. Atmósfera 30, 355-366.

Jerjen, I., Poulikakos, L.D., Plamondon, M., Schuetz, P., Luethi, T., Flisch, A., 2015. Drying of porous asphalt concrete investigated by X-ray computed tomography. Physics Procedia 69, 451-456.

Jiang, Y., Song, D., Shi, T., Han, X., 2018. Adaptive analysis of green space network planning for the cooling effect of residential blocks in summer: A case study in Shanghai. Sustainability 10, 3189.

Jiao, Y., Zhu, G., Lu, S., Ye, L., Qiu, D., Meng, G., Wang, Q., Li, R., Chen, L., Wang, Y., 2024. The cooling effect of oasis reservoir-riparian forest systems in arid regions. Water Resources Research 60, e2024WR038301.

Jim, C.Y., 2014. Air-conditioning energy consumption due to green roofs with different building thermal insulation. Applied Energy 128, 49-59.

Jim, C.Y., 2015. Thermal performance of climber greenwalls: Effects of solar irradiance and orientation. Applied Energy 154, 631-643.

Jing, S., Li, B., Tan, M., Liu, H., 2013. Impact of relative humidity on thermal comfort in a warm environment. Indoor and Built Environment 22, 598-607.

Katsoulas, N., Antoniadis, D., Tsirogiannis, I., Labraki, E., Bartzanas, T., Kittas, C., 2017. Microclimatic effects of planted hydroponic structures in urban environment: measurements and simulations. International Journal of Biometeorology 61, 943-956.

Kim, G., Coseo, P., 2018. Urban park systems to support sustainability: the role of urban park systems in hot arid urban climates. Forests 9, 439.

Kontoleon, K., Eumorfopoulou, E., 2010. The effect of the orientation and proportion of a plant-covered wall layer on the thermal performance of a building zone. Building and Environment 45, 1287-1303.

Koyama, T., Yoshinaga, M., Hayashi, H., Maeda, K.-i., Yamauchi, A., 2013. Identification of key plant traits contributing to the cooling effects of green façades using freestanding walls. Building and Environment 66, 96-103.

Kubilay, A., Derome, D., Carmeliet, J., 2019. Impact of evaporative cooling due to wetting of urban materials on local thermal comfort in a street canyon. Sustainable Cities and Society 49, 101574.

Kubilay, A., Ferrari, A., Derome, D., Carmeliet, J., 2020. Smart wetting of permeable pavements as an evaporative-cooling measure for improving the urban climate during heat waves. Journal of Building Physics 45, 36-66.

Lan, L., Wargocki, P., Lian, Z., 2011. Quantitative measurement of productivity loss due to thermal discomfort. Energy and Buildings 43, 1057-1062.

Li, G., Liu, C., He, Y., 2021. The effect of thermal discomfort on human well-being, psychological response and performance. Science and Technology for the Built Environment 27, 960-970.

Li, Y., Luo, D., 2024. Liquid-Water Transfer Coefficients of Porous Building Materials Under High-Humidity Conditions. Buildings 14, 3865.

Liao, Y., Cao, H.-X., Liu, X., Li, H.-T., Hu, Q.-Y., Xue, W.-K., 2021. By increasing infiltration and reducing evaporation, mulching can improve the soil water environment and apple yield of orchards in semiarid areas. Agricultural Water Management 253, 106936.

Lin, H., Li, X., 2025. The Role of Urban Green Spaces in Mitigating the Urban Heat Island Effect: A Systematic Review from the Perspective of Types and Mechanisms. Sustainability 17, 6132.

Little, J., 2021. The causes of surface condensation and mould, and the responsibility of relevant parties to alleviate them. Technological University Dublin.

Liu, Ma, Zhang, Luo, 2022. Watering on porous pavement for improvement of environmental human thermal comfort in an ecological community in arid area: A case study in Lanzhou, China. Sustainable Cities and Society 85, 104081.

Liu, B., Yu, P., Zhang, X., Wu, Y., Li, J., Wan, Y., Bai, Y., Wei, X., Liu, L., Wang, Y., 2025a. Soil moisture shapes the responses of Quercus wutaishansea forest stand transpiration to potential evapotranspiration. Journal of Hydrology 652, 132679.

Liu, X., Xu, Y., Jia, H., Zhao, Y., Hou, H., Zhang, Y., 2025b. NH3 release during the evaporation of different types of atmospheric precipitation: A case study in Changchun, China. Scientific Reports 15, 31117.

Liu, Y., Song, C., Ye, S., Lv, J., Gao, P., 2025c. Daily Max Simplified Wet-Bulb Globe Temperature and its Climate Networks for Teleconnection Study, 1940–2022. Scientific Data 12, 584.

Lokoshchenko, M.A., 2017. Urban heat island and urban dry island in Moscow and their centennial changes. Journal of Applied Meteorology and Climatology 56, 2729-2745.

Manapragada, N.V.S.K., Natanian, J., 2025. Urban Microclimate and Energy Modeling: A Review of Integration Approaches. Sustainability 17, 3025.

Manteghi, G., bin Limit, H., Remaz, D., 2015. Water bodies an urban microclimate: A review. Modern Applied Science 9, 1.

Masterton, J.M., Richardson, F., 1981. Humidex: a method of quantifying human discomfort due to excessive heat and humidity. CABI Databases.

Mazzali, U., Peron, F., Romagnoni, P., Pulselli, R.M., Bastianoni, S., 2013. Experimental investigation on the energy performance of Living Walls in a temperate climate. Building and Environment 64, 57-66.

Miao, C., Li, P., Huang, Y., Sun, Y., Chen, W., Yu, S., 2022. Coupling outdoor air quality with thermal comfort in the presence of street trees: a pilot investigation in Shenyang, Northeast China. Journal of Forestry Research, 1-9.

Ming, T., Hu, Y., Shi, T., Li, Y., Hu, S., Yang, D., Lv, B., Peng, C., Chen, Y., 2025. Effect of Blue–Green Infrastructure in Mitigating Microenvironmental Heat Islands: Field-and Simulation-Based Insights. Atmosphere 16, 134.

Miralles, D.G., Bonte, O., Koppa, A., Baez-Villanueva, O.M., Tronquo, E., Zhong, F., Beck, H.E., Hulsman, P., Dorigo, W., Verhoest, N.E., 2025. GLEAM4: global land evaporation and soil moisture dataset at 0.1 resolution from 1980 to near present. Scientific Data 12, 416.

Ng, E., 2009. Policies and technical guidelines for urban planning of high-density cities–air ventilation assessment (AVA) of Hong Kong. Building and Environment 44, 1478-1488.

Oke, T.R., 1982. The energetic basis of the urban heat island. Quarterly Journal of the Royal Meteorological Society 108, 1-24.

Onabanjo, A.A., Olanipekun, L.O., Olanipekun, D.O., 2023. EFFECTS OF INDOOR AIR QUALITY, HUMIDITY AND TEMPERATURE ON EMPLOYEES HEALTH AND PERFORMANCE. Web of Humanities: Journal of Social Science and Humanitarian Research 1, 8-18.

Pan, L., Chu, L., 2016. Energy saving potential and life cycle environmental impacts of a vertical greenery system in Hong Kong: A case study. Building and Environment 96, 293-300.

Paramita, B., Matzarakis, A., 2019. Urban morphology aspects on microclimate in a hot and humid climate. Geographica Pannonica 23.

Peng, L.L., Jiang, Z., Yang, X., Wang, Q., He, Y., Chen, S.S., 2020. Energy savings of block-scale facade greening for different urban forms. Applied Energy 279, 115844.

Pérez, G., Coma, J., Sol, S., Cabeza, L.F., 2017. Green facade for energy savings in buildings: The influence of leaf area index and facade orientation on the shadow effect. Applied Energy 187, 424-437.

Perini, K., Bazzocchi, F., Croci, L., Magliocco, A., Cattaneo, E., 2017. The use of vertical greening systems to reduce the energy demand for air conditioning. Field monitoring in Mediterranean climate. Energy and Buildings 143, 35-42.

Perini, K., Ottelé, M., Fraaij, A., Haas, E., Raiteri, R., 2011. Vertical greening systems and the effect on air flow and temperature on the building envelope. Building and Environment 46, 2287-2294.

Pirouz, B., Palermo, S.A., Turco, M., 2021. Improving the efficiency of green roofs using atmospheric water harvesting systems (an innovative design). Water 13, 546.

Pulselli, R., Pulselli, F., Mazzali, U., Peron, F., Bastianoni, S., 2014. Emergy based evaluation of environmental performances of Living Wall and Grass Wall systems. Energy and Buildings 73, 200-211.

Qaid, A., Ossen, D.R., 2015. Effect of asymmetrical street aspect ratios on microclimates in hot, humid regions. International Journal of Biometeorology 59, 657-677.

Qin, X., Yuan, X., Tabari, H., Hamdi, R., 2025. Severe constraints on water vapor diffusion due to the shrinkage of the Aral Sea. Atmospheric Research 318, 108008.

Razafimaharo, C., Krähenmann, S., Höpp, S., Rauthe, M., Deutschländer, T., 2020. New high-resolution gridded dataset of daily mean, minimum, and maximum temperature and relative humidity for Central Europe (HYRAS). Theoretical & Applied Climatology 142.

Rothfusz, L.P., Headquarters, N.S.R., 1990. The heat index equation (or, more than you ever wanted to know about heat index). Fort Worth, Texas: National Oceanic and Atmospheric Administration, National Weather Service, Office of Meteorology 9023, 640.

Saaroni, H., Ziv, B., 2003. The impact of a small lake on heat stress in a Mediterranean urban park: the case of Tel Aviv, Israel. International Journal of Biometeorology 47, 156-165.

Seppänen, O., Kurnitski, J., 2009. Moisture control and ventilation, WHO guidelines for indoor air quality: dampness and mould. World Health Organization.

Serra, V., Bianco, L., Candelari, E., Giordano, R., Montacchini, E., Tedesco, S., Larcher, F., Schiavi, A., 2017. A novel vertical greenery module system for building envelopes: The results and outcomes of a multidisciplinary research project. Energy and Buildings 146, 333-352.

Shi, L., Luo, Z., Matthews, W., Wang, Z., Li, Y., Liu, J., 2019. Impacts of urban microclimate on summertime sensible and latent energy demand for cooling in residential buildings of Hong Kong. Energy 189, 116208.

Sinha, R., Peláez-Vico, M.Á., Pascual, L.S., Thibivilliers, S., Libault, M., Huang, S.-S.C., Fritschi, F.B., Zandalinas, S.I., Mittler, R., 2025. The differential transpiration response of plants to stress. Philosophical Transactions B 380, 20240241.

Starke, P., Göbel, P., Coldewey, W., 2010. Effects of different water-permeable pavement designs on evaporation rates, Novatech 2010-7ème Conférence internationale sur les techniques et stratégies durables pour la gestion des eaux urbaines par temps de pluie/7th International Conference on sustainable techniques and strategies for urban water management. GRAIE, Lyon, France, pp. 1-10.

Stull, R., 2011. Wet-bulb temperature from relative humidity and air temperature. Journal of Applied Meteorology and Climatology 50, 2267-2269.

Šuklje, T., Medved, S., Arkar, C., 2016. On detailed thermal response modeling of vertical greenery systems as cooling measure for buildings and cities in summer conditions. Energy 115, 1055-1068.

Tabares-Velasco, P.C., Srebric, J., 2009. The Role of Plants in the Reduction of Heat Flux through Green Roofs: Laboratory Experiments. Ashrae Transactions 115, 793-802.

Takebayashi, H., Danno, H., Tozawa, U., 2022. Study on strategies to implement adaptation measures for extreme high temperatures into the street canyon. Atmosphere 13, 946.

Tan, C.L., Wong, N.H., Jusuf, S.K., 2014. Effects of vertical greenery on mean radiant temperature in the tropical urban environment. Landscape and Urban Planning 127, 52-64.

Teshnehdel, S., Gatto, E., Li, D., Brown, R.D., 2022. Improving outdoor thermal comfort in a steppe climate: Effect of water and trees in an urban park. Landsc Urban Plan 11, 431.

Thapa, S., Rijal, H.B., Zaki, S.A., 2024. District-wise evaluation of meteorological factors and outdoor thermal comfort in India using UTCI–Insight into future climatic scenario. Sustainable Cities and Society 116, 105840.

Theeuwes, N.E., Solcerová, A., Steeneveld, G.J., 2013. Modeling the influence of open water surfaces on the summertime temperature and thermal comfort in the city. Journal of Geophysical Research: Atmospheres 118, 8881-8896.

Thomsit-Ireland, F., Essah, E.A., Hadley, P., Blanuša, T., 2020. The impact of green facades and vegetative cover on the temperature and relative humidity within model buildings. Building and Environment 181, 107009.

Torres-Rivas, A., Palumbo, M., Haddad, A., Cabeza, L.F., Jiménez, L., Boer, D., 2018. Multi-objective optimisation of bio-based thermal insulation materials in building envelopes considering condensation risk. Applied Energy 224, 602-614.

Tu, D., Tang, J., Zhang, Z., Sun, H., 2023. Thermal environment optimization in a large space building for energy-saving. Case Studies in Thermal Engineering 51, 103649.

Vox, G., Blanco, I., Schettini, E.J.B., Environment, 2018. Green façades to control wall surface temperature in buildings. Building and Environment 129, 154-166.

Wang, R., Yang, Q., Deng, Z., Nian, W., 2025. The research on soil-plant-climate interactions: An integrated assessment of water management and drought resilience. Advances in Resources Research 5, 456-476.

Wang, X., Li, H., Sodoudi, S., 2022. The effectiveness of cool and green roofs in mitigating urban heat island and improving human thermal comfort. Building and Environment 217, 109082.

Wang, Z., Song, J., Chan, P.W., Li, Y., 2021. The urban moisture island phenomenon and its mechanisms in a high-rise high-density city. International Journal of Climatology 41, E150-E170.

Wong, N.H., Kumakura, E., Jusuf, S.K., Chigusa, K., 2016. Experimental Study on the Influence of Urban Water Body on Thermal Environment at Outdoor Scale Model. Procedia Engineering 169, 191-198.

Wong, N.H., Kwang Tan, A.Y., Chen, Y., Sekar, K., Tan, P.Y., Chan, D., Chiang, K., Wong, N.C., 2010. Thermal evaluation of vertical greenery systems for building walls. Building and Environment 45, 663-672.

Wu, T., Chen, Z., Zhou, S., Huang, R., Xing, P., Li, S., Qiao, R., Wu, Z., 2025. Joint evaluation of urban built environment's driving patterns on urban heat island (UHI) and urban moisture island (UMI). Sustainable Cities and Society 127, 106450.

Xu, J., Wei, Q., Huang, X., Zhu, X., Li, G., 2010. Evaluation of human thermal comfort near urban waterbody during summer. Building and Environment 45, 1072-1080.

Yan, H., Wu, F., Dong, L., 2018. Influence of a large urban park on the local urban thermal environment. Science of the Total Environment 622, 882-891.

Yang, F., Yuan, F., Qian, F., Zhuang, Z., Yao, J., 2018. Summertime thermal and energy performance of a double-skin green facade: A case study in Shanghai. Sustainable Cities and Society 39, 43-51.

Yang, J., Zhao, Y., Zou, Y., Xia, D., Lou, S., Guo, T., Zhong, Z., 2022a. Improving the thermal comfort of an open space via landscape design: a case study in hot and humid areas. Atmosphere 13, 1604.

Yang, L., Liu, X., Qian, F., 2020. Research on water thermal effect on surrounding environment in summer. Energy and Buildings 207, 109613.

Yang, P., Ren, G., Hou, W., 2017. Temporal–spatial patterns of relative humidity and the urban dryness island effect in Beijing City. Journal of Applied Meteorology and Climatology 56, 2221-2237.

Yang, Q., Dai, F., Beecham, S., 2022b. The influence of evaporation from porous concrete on air temperature and humidity. Journal of Environmental Management 306, 114472.

Yang, S., Li, S., Chen, B., Xie, Z., Peng, J., 2021. Responses of heat stress to temperature and humidity changes due to anthropogenic heating and urban expansion in South and North China. Frontiers in Earth Science 9, 673943.

Yang, Y., Endreny, T.A., Nowak, D.J., 2013. A physically based analytical spatial air temperature and humidity model. Journal of Geophysical Research: Atmospheres 118, 10,449-410,463.

Yin, H., Kong, F., Middel, A., Dronova, I., Xu, H., James, P., 2017. Cooling effect of direct green façades during hot summer days: An observational study in Nanjing, China using TIR and 3DPC data. Building and Environment 116, 195-206.

Zhan, Q., Gao, S., Xiao, Y., Yang, C., Wu, Y., Fan, Z., Wu, J., Zhan, M., 2020. Impact mechanism and improvement strategy on urban ventilation, urban heat island and urban pollution island: A case study in Xiangyang, China. International Review for Spatial Planning and Sustainable Development 8, 68-86.

Zhang, Y., Dai, M., 2022. Analysis of the cooling and humidification effect of multi-layered vegetation communities in urban parks and its impact. Atmosphere 13, 2045.

Zhao, J., Lu, J., Ge, J., Fan, Y., Wang, H., Gu, M., Xue, Y., Zhao, Y., Lv, G., Lin, H., 2025. Influences of permeable pavements with different hydraulic properties on evaporative cooling and outdoor thermal environment: Field experiments. Building and Environment 270, 112525.

Zhao, T.F., Fong, K.F., 2017. Characterization of different heat mitigation strategies in landscape to fight against heat island and improve thermal comfort in hot–humid climate (Part I): Measurement and modelling. Sustainable Cities and Society 32, 523-531.

Zheng, X., Zhang, N., Wang, X., 2022. Development of a modified thermal humidity index and its application to human thermal comfort of urban vegetation patches. Ecosystem Health and Sustainability 8, 2130095.

Zhou, J., Liu, J., Chu, Q., Wang, H., Shao, W., Luo, Z., Zhang, Y., 2021. Mechanisms and empirical modeling of evaporation from hardened surfaces in urban areas. International Journal of Environmental Research and Public Health 18, 1790.

Appendix A. A summary of previous studies on the summer shading, cooling, humidifying and energy-saving effects of vertical greening

Table A1 A review of prior research on the summer shading, cooling, humidifying and energy-saving benefits of vertical greening.

Ref	Research region	Climate [a]	Method [b]	Green area (m^2)	Influential factors	Results [c]
(Eumorfopoulou and Kontoleon, 2009)	Thessaloniki, Greece	Cfa	E	N/A	N/A	MT_w=1.9-5.3
(Tan et al., 2014)	Singapore	Af	E	N/A	N/A	MT_w=8.9
(Jim, 2015)	Hong Kong	Cfa	E	1136	Orientation, weather	MT_w=5
(Yin et al., 2017)	Nanjing, China	Cfa	E	N/A	Canopy structure	MT_w=8
(Katsoulas et al., 2017)	Arta, Greece	Csa	S	N/A	Leaf area density	MT_w=8
(Vox et al., 2018)	Bari, Italy	Csa	E	1.55	weather	MT_w=8
(Cuce, 2017)	Nottingham, UK	Cfb	E	N/A	Weather	MT_w=3.5-6.1
(Koyama et al., 2013)	Nagoya, Japan	Cfa	E	1.62	Plant species	MT_w=3.7-11.3
(Cameron et al., 2014)	Reading, UK	Cfb	E	2.88	Plant species	MT_w=9.2-9.9; MT_a=3
(De Jesus et al., 2017)	Madrid, Spain	Csa	E	456	N/A	MT_a=2.5-2.9
(Wong et al., 2010)	Singapore	Af	E	32	Plant species	MT_w=4.4-11.6; MT_a=3.3
(Hoelscher et al., 2016)	Berlin, Germany	Cfb	E	N/A	Plant species	MT_w=10.5-15.5; MT_a=0
(Perini et al., 2011)	Three cities in Netherland	Cfb	E	N/A	Green-facade type	MT_w=1.2-5; MT_a=0, MT_{la}=-1.1

(Šuklje et al., 2016)	Ljubljana, Slovenia	Cfb	E	3	Green-facade structure	MT_w=29-34; MT_{la}=-7
(Yang et al., 2018)	Shanghai, China	Cfa	E	N/A	Orientation	MT_w=9; MT_{la}=0.2-5.5
(Djedjig et al., 2017)	La Rochelle, France	Cfb	E	6.2	N/A	MT_w=15; M_{RH}=50%
(Pérez et al., 2017)	Lleida, Spain	Csa	E	N/A	Orientation	MT_w=17.6; M_{RH}=7%
(Chen et al., 2013)	Wuhan, China	Cfa	E	6.25	N/A	MT_w=20.8
(Coma et al., 2017)	Catalonia, Spain	Csa	E	27	Orientation, green-facade type	MT_w=4.6-16.5
(Perini et al., 2017)	Sestri Ponente, Italy	Csa	E	50	N/A	MT_w=20
(Mazzali et al., 2013)	Three cities in Italy	Cfb, Cfa, Csa	E	9-30.2	N/A	MT_w=12-20
(Pan and Chu, 2016)	Hong Kong	Cfa	E	8.22	N/A	MT_w=8
(Serra et al., 2017)	Turin, Italy	Cfa	E	N/A	N/A	MT_w=23
(Haggag et al., 2014)	Al-Ain City, UAE	BWh	E+ S	12	N/A	MT_w=13
(Pulselli et al., 2014)	Siena, Italy	Csa	S	98	Green-facade type, insulation, air-gap width	MT_w=6.4
(Kontoleon and Eumorfopoulou, 2010)	Thessaloniki, Greece	BSk	S	30	Orientation, foliage percentage, wall structure	MT_w=1.7-16.9

[a] According to the KÖppen-Geiger classification.

[b] E: experiment; S: Simulation.

[c] T_a: air temperature (℃). T_w: wall surface temperature (℃). MT_w: daily maximum T_a reduction (℃). MT_{la}: daily maximum T_w reduction in the cavity layer (℃, negative values denote a warming effect). M_{RH}: daily maximum increase in relative humidity (%).

Appendix B. Summary of factors influencing urban moisture

Table B1 Summary of factors influencing urban moisture.

Ref	Research region	Influential factors	Results
(Huang and Song, 2023)	Hong Kong	High-density cities	Increase moisture
(Yang et al., 2021)	South and north China	High-density cities	Increase moisture
(Correa et al., 2012)	Mendoza, Argentina	Canyon effect	Increase moisture
(Paramita and Matzarakis, 2019)	Bandung, Indonesia	Canyon streets (hot and humid climate)	Increase moisture
(Tu et al., 2023)	Cang Zhou, Hebei Province	Increase building spacing	Decrease moisture
(Zhan et al., 2020)	Xiangyang, China	Urban ventilation	Decrease moisture
(Kubilay et al., 2019)	Zurich, Switzerland	Highly moisture permeability porous materials	Increase moisture
(Guo et al., 2023)	Chinese megacities	Water-based corridors	Increase moisture
(Jiang et al., 2018)	Shanghai, China	Green space ventilation corridors	Decrease moisture
(Gonçalves et al., 2015)	N/A	Building materials (natural stone and ceramic brick, summer)	Increase moisture
(Yang et al., 2022b)	N/A	Dense materials (concrete and asphalt)	Decrease moisture
(Little, 2021)	All over Ireland	Non-hygroscopic materials (metal and glass)	Increase moisture
(Thomsit-Ireland et al., 2020)	N/A	Green wall (summer)	M_{RH}=11%
		Green wall (winter)	M_{RH}=-5.7%
(Alsaad et al., 2022)	Stuttgart, Germany	Living wall	M_{RH}=5.07%

(Cirkel et al., 2018)	Amsterdam, the Netherland	Green roof (C3 sedum plants)	Increase moisture
(Pirouz et al., 2021)	The Mediterranean region	Green roof (soil moisture, summer)	Increase or decrease moisture
(Yan et al., 2018)	Beijing, China	Trees	Increase moisture
(Zhang and Dai, 2022)	Beijing, China	Multi-layered vegetation (canopy density)	Increase moisture
(De Abreu-Harbich et al., 2015)	Southeast of Brazil	Trees (tropics)	M_{RH}=0.5-10.4%
(Theeuwes et al., 2013)	N/A	Water bodies	Increase moisture
(Jiao et al., 2024)	Lanzhou, China	Oasis effect (arid regions)	Increase moisture
(Starke et al., 2010)	N/A	Permeable pavement	Increase moisture
(Fwa et al., 2015)	N/A	High porosity permeable (permeable bricks, permeable gravel and grass paving bricks)	Increase moisture

Note: M_{RH} [%] represents the relative humidity change. A positive value indicates an increase, while a negative value indicates a decrease.

Appendix C. A review of the influences of humidity on thermal comfort

Table C1 A review of the influences of humidity on thermal comfort.

Ref	Research region	Influential factors	Humidity	Temperature	Thermal comfort
(Jing et al., 2013)	Chongqing, China	N/A	High	High	Reduce
(Du et al., 2022)	Hong Kong, China	Sea breeze	Increase	High	Reduce
(Qaid and Ossen, 2015)	Putrajaya Boulevard, Malaysia (hot and humid regions)	Compact urban forms and narrow street layouts	Increase	Increase	Reduce
(Takebayashi et al., 2022).	Kobe city	Wide streets	Decrease	Decrease	Improve
(Giannopoulou et al., 2014)	Athens area	Southerly wind	Increase	High	Reduce
(Liu et al., 2025b	Amoy and Hsia-men, China	Sea breeze	Increase	High (Heatwaves)	Reduce (Humidity intensifies heatwaves)
(Zheng et al., 2022)	Beijing, China	Reducing the distance from rivers or increasing plant density	Decrease	Decrease	Improve
(Gunawardena et al., 2017)	N/A	Water bodies	Increase	Moderate	Reduce
(Zhao and Fong, 2017)	Hong Kong, China (hot–humid climate)	Water bodies	Increase	High	Reduce
(Xu et al., 2010)	Shanghai, China	10-20 m from the water’s edge	Increase	Decrease	Improve
(Teshnehdel et al., 2022)	Tabriz, Iran	Water bodies	Increase	Decrease	Reduce

(Deng et al., 2022)	Wuhan, China	Lake shrinkage	Decrease	Increase	Reduce
(Cheung and Jim, 2018)	Hong Kong, China	Trees	Increase	Decrease	Improve (Reduce PET)
(Miao et al., 2022)	Shenyang, China	Trees	Increase	Decrease	Improve (Reduce PET)
(Yang et al., 2022a)	Guangzhou, China (Subtropical coast)	Increasing tree leaf area density	Increase	Decrease	Improve (Reduce PET)
(Gobatti et al., 2025)	Zurich, Switzerland	Increasing tree cover and maintaining high soil moisture	Increase	Decrease	Improve (Reduce UTCI)
(Wang et al., 2022)	Berlin, Germany	Green roofs	Increase	Decrease (Heatwaves)	Improve
(Berretta et al., 2014)	The University of Sheffield's Green Roof Centre	Green roofs	Increase	Decrease	Reduce
(Zhao et al., 2025)	Zhangzhou, Fujian, China	Permeable pavements	Increase	Decrease	Improve (Reduce UTCI)
(Irmak et al., 2017)	The Ata botanical garden, Erzurum	Permeable pavements	Increase	Decrease	Improve (Reduce PET)
(Liu et al., 2022)	Lanzhou, China	Permeable pavements (regular watering)	Increase	Decrease	Improve

4 HAM Tools and Probabilistic Approach for Building Performance Assessment

This section should be cited as:

Shams, S.A., Yan, S., Karatas, A., Wang, L., Ge, H. (2026). HAM tools and probabilistic approach for building performance assessment. In: A Systematic Review of Passive Energy Conservation Measures and Probabilistic Assessment under Changing Climate in Urban Settings, CIB W040 Report, CIB General Secretariat.

4.1 HAM tools

This section reviews the common tools used in hygrothermal simulations and evaluates their potential for probabilistic applications. Although the term “HAM Tools” could refer to a broad spectrum of tools capable of simulating heat, air, and moisture transfer phenomena, in this report, the term “HAM Tools” specifically denotes the software packages that offer predefined material models, boundary conditions, climate management, and building-specific abstractions including building envelope and energy systems. These tools are utilized for performing building envelope or whole building heat, air, and moisture simulations.

In the past decades, simulation software has been widely used to investigate the heat, air and moisture (HAM) phenomena in and around buildings, and assess the performance of passive design/retrofit strategies. The calculation of moisture migration phenomena in building envelopes can be traced back to 1950s, when Glaser applied steady-state methods to calculate vapor transfer through wall assembly (Glaser H., 1958); this was followed by several studies on calculating coupled heat and moisture phenomena, including capillary suction and liquid transport in 1960s and1970s (Luikov, 1966, 1975; Bomberg, 1974). The heat and moisture modelling framework constructed from 1950s to 1970s, plus the inspiration of capillary flow theory from soil science(Philip & De Vries, 1957), built up the foundation of HAM Tools’ originating decade of 1980s. The 1990s and 2000s witnessed a broad application of the HAM Tools. Two pivotal international IEA-EBC activities, namely ANNEX 24 (1991-1995) and ANNEX 41 (2004-2007), significantly facilitated the extensive adoption of HAM Tools. ANNEX 24 provided an overview of 29 HAM tools developed during 1980s, among which DIM and WUFI2 later evolved into today’s most widely used commercial tools- Delphin and WUFI (Bauklimatik Dresden, 2026; Fraunhofer IBP, 2026). While WUFI Pro (Fraunhofer IBP, 2026) is among the widely used HAM tools for analysing building components such as wall assemblies(Dang et al., 2025), WUFI Plus (Fraunhofer IBP, 2026) is frequently applied tool at the whole-building scale (Coelho et al., 2018; Libralato et al., 2021; Posani et al., 2023). The WUFI Plus can undertake whole building heat and moisture simulation (Antretter et al., 2011), however, the closed software ecosystem prohibited stochastic simulations for probabilistic assessment, it does not allow users to call the simulation solver in other programming environment and prohibit varying the input parameters outside of WUFI. On the other hand, Delphin, which was developed by the Technical University of Dresden, can be utilized in other programming environments, making it frequently used for stochastic simulations (Zhao et al., 2021; Wang et al., 2021; Kukk et al., 2022). In addition to WUFI and DELPHIN, there are also non-commercialized hygrothermal simulation tools developed to investigate the heat and moisture transfer behaviors of building envelope systems, such as MATCH (Rode, 1990) and LATENITE (Karagiozis, 1993).

IEA ANNEX 41 (2004-2007) is an international research activity that was focused on whole building hygrothermal analysis, Woloszyn and Rode provided a comprehensive review of the whole building hygrothermal analysis tools developed/tested during IEA ANNEX 41 (Woloszyn & Rode, 2008). Tools such as HAM-Tools (Kalagasidis, 2004) and HAMFitPlus (Tariku, 2008) were developed to model coupled heat, air, and moisture transfer across the building envelope, accounting for interactions between indoor and outdoor environments, and typical HVAC systems. These tools incorporated the hygric properties of building materials for whole-building simulations but generally required external solvers such as Matlab/Simulink (*MathWork*, *2026*) for numerical implementation. Another example is HAMLab (van Schijndel, 2007), which uses the COMSOL (*COMSOL*, 2026) environment as its numerical solver. This integration allows HAMLab to utilize COMSOL's finite element method (FEM) capabilities to solve the governing coupled PDEs for room-level HAM modelling, bridging high-level building physics abstractions with robust numerical computation.

Nevertheless, most of the IEA ANNEX 41 tools were rarely used for probabilistic assessments of building performance. More importantly, many were either research-focused or institution-specific and have since become obsolete or are no longer supported. As of 2026, only a few tools, such as WUFI Plus (Fraunhofer IBP, 2026), WUFI Pro (Fraunhofer IBP, 2026), Delphin (Bauklimatik Dresden, 2026) , remain actively used in academia or industry (Akhavan et al., 2024).

In parallel with the evolution of HAM modelling in buildings, energy modelling developed along a separate trajectory. In 1960s, ASHRAE Fundamental handbook firstly included the total equivalent temperature difference (TETD) method for heating/cooling load calculation of buildings (ASHRAE, 1967). Driven by the oil crisis in 1970s, the U.S. Army Construction Engineering Research Laboratory (CERL) and Lawrence Berkeley National Laboratory (LBNL) developed two programs that can simulate dynamic thermal behavior of buildings: the Building Loads Analysis and System Thermodynamics (BLAST), and DOE-1(Hittle, 1977; LBNL Simulation Research Group, 1977). The ANNEX 21 (1988-1993) perhaps can be considered as the counterpart of ANNEX 24 in thermal/energy modelling, this international research program has compared thermal/energy simulation programs from 24 research groups (Månsson, 1998). Oh and Haberl conducted a deep review of the origins of the most widely used building energy simulation programs and the analysis methods of thermal envelope loads used in the software to analyze high-performance commercial buildings in the United States (Oh & Haberl, 2016). However, they did not consider the moisture transfer analysis methods and the programs that integrated heat and moisture transfer.

EnergyPlus (*National Laboratory of the Rockies, 2026*) is the most widely used software for whole-building energy assessments (Pang et al., 2020). Through its Heat and Moisture Transfer (HAMT) model, which is fundamentally based on Künzel's model (Künzel, 1995), the effects of coupled heat and moisture transfer can be incorporated into building energy simulations. The accuracy and applicability of this model have been evaluated against measurements in the literature (Belloum et al., 2022; Yang et al., 2016; Yu et al., 2019).

The ESP-r program was originally developed in the mid 1970s at the University of Strathclyde. Designed as an integrated simulation environment, ESP-r enables holistic analysis of building energy, airflow, and environmental performance through a modular, physics-based approach (Clarke, 2001). ESP-r incorporates capabilities for simulating coupled heat, air, and moisture (HAM) transfer processes within building envelope systems and building spaces, and the HAM transfer was integrated with HVAC systems (Clarke, 2013). This enables detailed investigation of whole building HAM behaviors, and coordination of passive/active energy conservation measures.

TRNSYS (*TRNSYS*, 2026), another widely used energy performance assessment tool, can be applied for whole-building hygrothermal simulations. On its own, TRNSYS employs a simplified representation of hygrothermal transfers. However, more advanced modelling can be achieved by coupling TRNSYS with COMSOL. This co-simulation strategy has been adopted in several studies reported in the literature (Benmahiddine et al., 2024; Ferroukhi et al., 2016, 2017). In this co-simulation approach, COMSOL is responsible for solving the partial differential equations governing coupled heat and moisture transfer within building components, while TRNSYS performs the multizone energy simulation of the building.

In a recent study, (Chung et al., 2020) developed and verified an augmented version of HAM-Tools platform for 1-D hygrothermal analysis of building envelopes, by adding wind-driven rain and ventilated air gaps, this platform was developed based on MATLAB-SIMULINK. The tool was validated against WUFI Pro 6.1 through eight ventilated wall scenarios that varied in climate conditions, wall configurations, and materials. Ultimately, the authors proposed that HAM-Tools is appropriate for stochastic simulations, given its open platform nature. Later, (Chung et al., 2023) applied the augmented HAM-Tools (Chung et al., 2020) to investigate the effects of stochastic multi-year weather data and probabilistic air infiltration on hygrothermal risks in wood-framed wall assemblies. However, the capability of this augmented model for whole-building simulation has yet to be explored and requires further study.

Hygrothermal models have also been implemented in general-purpose programming languages, such as Python and FORTRAN (Aït Oumeziane et al., 2017; Bakkour et al., 2025; Zhang et al., 2020; Dong et al., 2020). The programming tools and simulation environment such as MATLAB were also used to develop the hygrothermal models and undertake hygrothermal simulations (Akhavan Shams et al., 2025). However, these implementations are typically developed for specific research purposes and remain largely personal or project-based tools. In contrast, the focus of the present review is on software platforms that are widely used, accessible, actively maintained, and available to the broader research and professional communities.

Table 4.1 presents commonly used simulation tools for evaluating the hygrothermal performance of buildings. The tools are compared across several key aspects relevant to large-scale building assessments, including their ability to model passive measures (such as add on insulation, cool materials, green envelopes and natural ventilation), integrate HVAC systems, couple with CFD for urban physics, and support or enable stochastic simulations.

Table 4.1 A comparison of commonly used HAM simulation Tools

Tool	Coupled heat and moisture (simulation scale)	Passive measures modelling	HVAC integration	CFD coupling	Stochastic simulation via scripting tools	Post-processing for performance metrics assessment
WUFI Plus	Yes (whole building)	Insulation, cool materials, green envelopes, natural ventilation	Yes (simple profiles)	No	No	Mold growth; Wood decay; Corrosion; Freeze damage of building envelopes
WUFI Pro	Yes (component level)	Insulation, cool materials, green envelopes	No (simple profiles)	No	No	Mold growth; Wood decay; Corrosion; Freeze damage of building envelopes
DELPHIN	Yes (component level)	Insulation, cool materials, green envelopes (via scripts)	No	No	Yes	Yes
COMSOL	Yes (component level and whole building)	Insulation, cool materials, green envelopes (costume physics), natural ventilation (via CFD)	No (can be modeled, complex and requires expertise)	Yes	Yes	No
EnergyPlus	Yes, using HAMT Model (whole building)	Insulation, cool materials, green envelopes (EcoRoof model), natural ventilation (AirflowNetwork)	Yes (Typical systems)	Yes (Coupling with CFD tools such as fluent)	Yes	Energy of whole building
TRNSYS	No (possible with COMSOL co-simulation)	Insulation, cool materials, green envelopes (costume modules), natural ventilation (TRNFlow/COMIS)	Yes	Yes (with COMIS or coupling with COMSOL)	Yes	No
IES-VE	NO	Insulation, cool materials, green envelopes, natural ventilation (MacroFlo)	Yes	Yes	No	Thermal comfort índices and Energy Performance

DeST	No (Whole building)	Insulation, cool materials, natural ventilation	Yes	Yes	NO	Thermal comfort índices and Energy Performance
ESP-r	Yes (whole building)	Insulation, cool materials, green envelope (programmable), natural ventilation	Yes	Yes	Yes	Thermal comfort and Energy Performance

In summary, the tools developed for HAM simulations are robust enough to simulate various heat, air and moisture transfer phenomena in buildings and different types of passive energy conservation measures. However, the tools that can couple with interior and exterior microclimate behaviors are still limited; and those can undertake stochastic simulation for probabilistic analysis are limited. Some of the tools have been widely adopted by industry, such as WUFI, Delphin, EnergyPlus (DesignBuilder or OpenStudio), and ESP-r and IES-VE, however, the probabilistic assessment is still not widely adopted by industry.

In the future work, more case studies that couple energy/hygrothermal and interior/exterior environment conditions, particularly with consideration of moisture migration might be useful for multi-objective assessment of passive energy conservation measures. Faster simulation methods, such as machine learning, might be useful to accelerate computational speed, and enable stochastic simulations with considering more uncertain parameters for probabilistic assessment, as showed by (Tijskens et al., 2023). The workflow should be integrated with BIM tools, for the industrial practitioners to adopt the coupling approaches and stochastic approaches for multi-objective performance assessment of passive energy conservation measures.

4.2 Probabilistic approach

The probabilistic assessment of building performance is mainly achieved by Monte Carlo or Quasi-Monte Carlo based stochastic simulations. In Monte Carlo simulation, input parameters are sampled randomly according to predefined probability distributions, which generally requires a very large number of runs to achieve statistical convergence. The early works of stochastic building performance simulations typically employ the Monte Carlo approach(de Wit & Augenbroe, 2002; Macdonald & Strachan, 2001). By contrast, Quasi-Monte Carlo methods use low-discrepancy sequences instead of purely random sampling, which improves the uniformity of the sampling space and often accelerates convergence for high-dimensional problems (Hung, 2024). In Monte Carlo or Quasi-Monte Carlo methods, input parameters are considered as stochastic variables, each parameter is assigned with a given probability distribution. These distributions are then sampled through various techniques (Monte Carlo, such as random sampling or Quasi-Monte Carlo, such as Latin Hypercube Sampling) to perform stochastic simulation (Janssen, 2013). The resulting data set is subsequently used for uncertainty analysis, sensitivity analysis, and risk assessment.

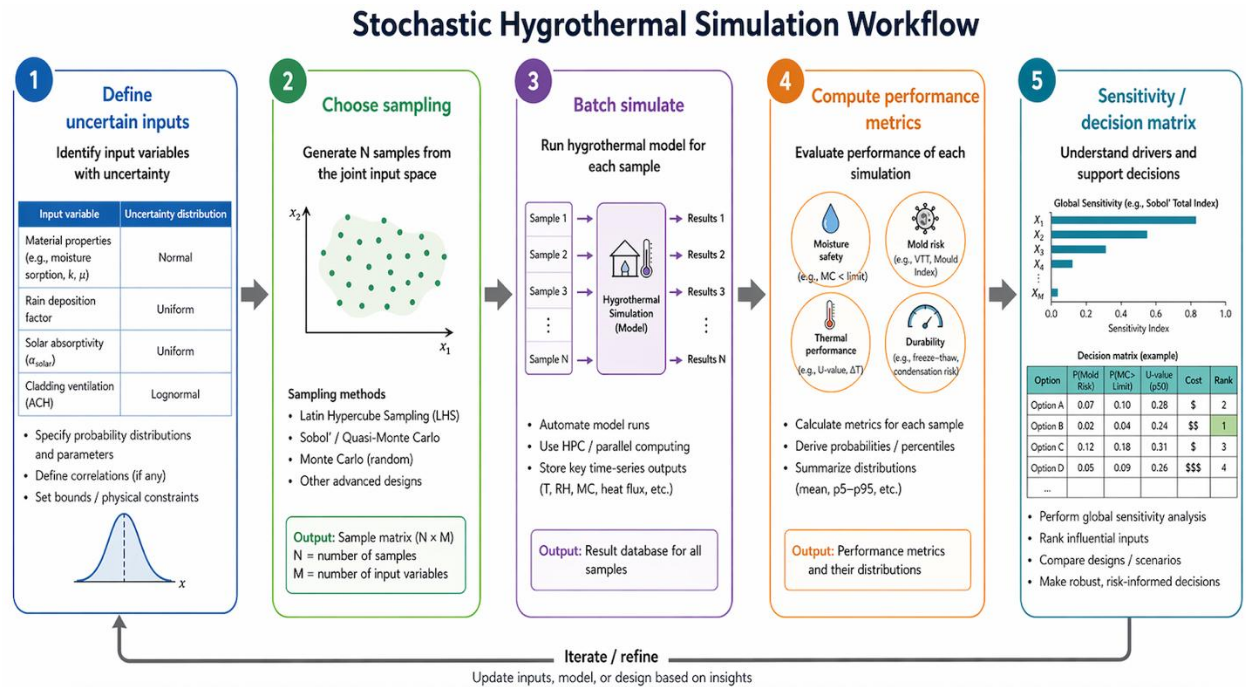

Figure 4.1 A general workflow for stochastic hygrothermal simulation

While earlier programs like Annex 24 focused on the fundamentals of HAM modeling, Annex 55 (2015)—specifically Subtask 2, Probabilistic tools—established the framework for the probabilistic assessment of energy-saving retrofits. This international effort was instrumental in moving the field beyond deterministic 'pass/fail' criteria toward a more nuanced understanding of reliability under uncertainties. Subtask 2 identified a suite of five essential toolsets for this transition: qualitative exploration, uncertainty propagation, sensitivity analysis, metamodeling, and economic optimization. The program adapted qualitative tools from the field of risk assessment but shifted their focus from binary hazard identification to a gradual evaluation of performance through the concepts of gains and costs. By providing these methodological foundations, Annex 55 enabled the reliability-based analysis and sensitivity testing techniques that underpin contemporary hygrothermal research.

Some studies in the literature have also applied probabilistic simulations by defining predetermined stochastic scenarios, where each scenario represents a specific realization (set) of sampled input features. These features may include variations in climate conditions, occupancy behavior, or retrofit strategies (Bayat Pour et al., 2024b). However, the present report focuses on Monte Carlo and Quasi-Monte Carlo–based stochastic simulations, which represent the main and most widely used class of probabilistic methods in building performance analysis. (Tijskens et al., 2023) utilized a convolutional neural network metamodel to conduct over 135,000 simulations to evaluate how different timber frame walls perform regarding mould growth and interstitial condensation. The study demonstrated that relying solely on the vapour diffusion resistance (sd-ratio) is insufficient for ensuring moisture safety. The findings revealed that moisture buffering, either in the insulation material (e.g., cellulose) or the weather barrier (e.g., wood-based boards), is a more decisive factor in preventing condensation run-off than the s-ratio itself.

Table 4.2 is a summary of Monte Carlo or Quasi-Monte Carlo based stochastic simulation. The stochastic simulations have been applied for both energy/thermal analysis of whole building and hygrothermal analysis of building envelope system. For energy/thermal analysis of whole building, most of the studies set energy use and indoor air temperature as target performance, reflecting energy and thermal comfort performance; for hygrothermal analysis of building envelope system, the total moisture content of the wall assembly or deterioration indicator, such as number of freeze thaw cycle and mold growth index (Ojanen et al., 2010), of wall components were generally set as target performance, reflecting moisture safety performance.

For whole building energy/thermal analysis, most studies considered thermal properties of building envelope materials, internal heat gains, and HVAC system parameters as stochastic variables. In contrast, for building envelope hygrothermal analyses, the focus was on the hygrothermal properties of building materials, boundary conditions, and climate data as stochastic variables.

Most of the whole building analysis adopted Monte Carlo sampling without sampling design, i.e., random draws are taken directly from the input distributions. This so-called basic random sampling (BRS) is simple to implement but requires a very large number of runs to achieve convergence, making it computationally expensive. In contrast, some studies in recent years have applied Latin Hypercube Sampling (LHS) (Kong et al., 2023; Sun et al., 2016), which stratifies each input distribution into intervals of equal probability and ensures that the full range of variability is represented. Compared to BRS, LHS achieves better coverage of the input space and typically converges with fewer samples.

According to (Bayat Pour et al., 2024b), efficiency varies significantly across sampling approaches. BRS is widely used but suffers from slow convergence and high computational cost. LHS, a frequently applied technique in hygrothermal research, provides more uniform and unbiased coverage, requiring fewer samples to reach stable results. Similarly, BRS and LHS are the widely used sampling methods in building energy performance analyses, according to (Pang et al., 2020). On the other hand, QMC methods (e.g. Sobol), based on low-discrepancy, have also gained attention for their improved space-filling properties and faster convergence in both hygrothermal and thermal assessment studies. Overall, while random sampling remains common in whole-building applications, more advanced techniques such as LHS and QMC offer a clear advantage in terms of accuracy and computational efficiency for probabilistic building performance assessments.

Based on the summary presented in Table 4.2, some limitations and knowledge gaps were also found in previous literatures. First, most whole building energy/thermal analysis generally do not consider the moisture transfer behavior in building envelope components, although some of the studies have already demonstrated the moisture transfer in building envelope components could considerably impact on the energy/thermal performance of whole building through deterministic simulation study (Amorim et al., 2024; M. Zhang et al., 2017). Second, there is a lack of probabilistic hygrothermal assessments of building envelope systems focusing on energy/thermal performance. Although some of the hygrothermal studies investigated the impact of building envelope design parameters on heat loss of the wall assembly (Sun et al., 2016; Vereecken et al., 2015), no further analyses were conducted to investigate their impact on energy use and indoor thermal comfort performance. Finally, although recent years have seen increasing applications of probabilistic approaches to assess uncertainty in urban-scale building energy performance (Johari et al., 2020; C. Wang et al., 2025), there is still a lack of studies investigating the hygrothermal performance of building envelope systems at urban scale. In fact, some of the input parameters for hygrothermal modelling are highly influenced by microclimate conditions. The temporal distributions of these parameters for a given wall assembly should be determined based on microclimate parameters. For example, the rain penetration rate of wall assembly is related to the intensity of wind driven rain (WDR) and driving rain wind pressure (DRWP) on a wall. The empirical equation can be established through watertightness test to describe such relationship (S. Van Linden & Van Den Bossche, 2022; Xiao et al., 2023). the spatial distribution of the WDR and DRWP could be obtained through large scale field measurements (Pérez-Bella et al., 2024).

Table 4.2 A compilation of Monte-Carlo or Quasi Monte-Carlo based stochastic simulations

Reference	**Simulation objective**	**Scale**	**Software**	**Target performance**	**Type of stochastic variables**	**Sampling method**
(Moon & Augenbroe, 2005)	Hygrothermal	Whole Building	Energyplus; COMIS; WUFI	Mould growth	Air mass Flow coefficient; moisture source; external convective heat transfer coefficient; wind exponent; insulation conductivity	LHS
(Sulaiman & Olsina, 2014)	Hygrothermal	Whole building	HAMBASE; MATLAB	Hygrothermal comfort	Climate conditions	BRS
(Zhao et al., 2011)	Hygrothermal	Wall	DELPHIN; Python	Total moisture content	Hygrothermal properties; Boundary conditions	BRS
(Defraeye et al., 2013)	Hygrothermal	Wall	A custom finite-element HAM model	Drying rate, surface temperature, Relative humidity	Hygrothermal properties	BRS
(Marincioni et al., 2018)	Hygrothermal	Wall	DELPHIN; R	Mould growth index	Hygric properties; Boundary conditions; Layer thicknesses	LHS
(Wang & Ge, 2018)	Hygrothermal	Wall	DELPHIN; MATLAB	Total moisture content; Mould growth index	Hygric properties	LHS

(Hou et al., 2019)	Hygrothermal	Wall	DELPHIN	Heat loss; Freeze thaw cycle	Hygrothermal properties; Climate conditions; Boundary conditions	BRS; LHS; QMC (Sobol; Niederreiter-Xing sequence; Lattice sequence)
(Wang et al., 2021)	Hygrothermal	Wall	DELPHIN	Mould growth index	Hygrothermal properties; Boundary conditions	QMC (Sobol)
(Zhao et al., 2021)	Hygrothermal	Wall	DELPHIN	Relative humidity; Total moisture content	Hygrothermal properties; Boundary conditions; Layer thicknesses	LHS
(Kukk et al., 2022)	Hygrothermal	Wall	DELPHIN; MATLAB	Mould growth index	Hygrothermal properties; Climate conditions; Thicknesses, Initial moisture content	LHS
(Chung et al., 2023)	Hygrothermal	Wall	HAM-Tools	Total moisture content	Hygrothermal properties; Climate conditions; Boundary conditions; Air infiltration	LHS
(Kahangi Shahreza et al., 2024)	Hygrothermal	Wall	DELPHIN	Mould growth index; Total moisture content	Hygrothermal properties; Climate conditions; Rain leakage	LHS
(Bayat Pour & Abdul Hamid, 2024)	Hygrothermal	Wall	DELPHIN	Mould growth index	Hygrothermal properties; Boundary conditions; Replacement scenarios	LHS
(Hagentoft, 2017)	Hygrothermal	Attic	-	Mould growth index	Hygrothermal properties; Hygrothermal loads; Climate conditions; Operation factors; Economic variables	BRS
(Hopfe & Hensen, 2011)	Energy	Whole building	VA114; Matlab; SimLab	Energy consumption; Indoor air temperature	Thermal properties; Internal heat gains; Occupancy; Airtightness; Sizes and thicknesses	BRS
(Heo et al., 2012)	Energy	Whole building	EnergyPlus; SimLab	Gas energy use; Indoor air temperature	Thermal properties; Internal heat gains; Ventilation/Infiltration; Heating system	LHS
(Shen & Tzempelikos, 2013)	Energy	Whole building	EnergyPlus; SimLab	Energy consumption	Thermal properties; Shading and window design properties	LHS
(Menberg et al., 2016)	Energy	Whole building	TRNSYS; MATLAB	Annual heating demand	Thermal properties; Internal heat gains; Heating system	QMC (Sobol)

(Sun et al., 2016)	Energy	Whole building	EnergyPlus; jEPlus; JESS	Energy consumption; Total utility cost	Thermal properties; Internal heat gains; HVAC system; Window design properties; Infiltration	LHS
(Bordbari et al., 2018)	Energy	Whole building	EnergyPlus; MATLAB	Energy consumption; Energy cost; Thermal comfort	Thermal properties; HVAC system, Occupancy	BRS
(Delgarm et al., 2018)	Energy	Whole building	EnergyPlus; MATLAB; jEPlus	Cooling, heating, and electricity demand; Total electricity consumption	Thermal properties; Glazing; Overhang	QMC (Sobol)
(Zhu et al., 2020)	Energy	Whole building	EnergyPlus; R	Gas use; Electricity use	Thermal properties; Internal heat gains; HVAC system parameters	LHS; QMC (Sobol)
(Lu et al., 2021)	Energy	Whole building	Rhino (Grasshopper); EnergyPlus; R	Energy use intensity	Thermal properties; Internal heat gains; Air infiltration; Window design properties; Heating, cooling and lighting system; Occupant behavior	LHS
(Carpino et al., 2022)	Energy	Whole building	DesignBuilder; EnergyPlus	Net primary energy demand	Thermal properties; Occupant behavior	LHS
(Kong et al., 2023)	Energy	Whole building	DeST	Peak cooling load; Annual energy demand	Equipment and occupant behavior; Climate conditions;	LHS
(Sengupta et al., 2024)	Energy	Whole building	Modelica	Thermal resilience performance	Thermal properties; Airtightness; Shading properties; Cooling system; Occupant behavior	LHS
(Tian & Chai, 2025)	Energy	Whole building	Glodon; Python	Life cycle carbon emissions; Life cycle cost	Thermal properties; Window design properties; Climate data; HVAC system parameters; Lighting system, occupant behaviour	LHS

4.3 Evidence-based HAM design under uncertainty

Although probabilistic assessment helps address uncertainties in HAM design, there is a growing need for evidence-based HAM design to further reduce these uncertainties in practical applications. Evidence-based HAM design under uncertainty is an emerging but still evolving field in building science. In recent years, significant progress has been made in developing probabilistic frameworks to evaluate mould growth, material degradation, and moisture safety in building envelopes (Almeida & Barreira, 2018; Calle et al., 2020; Wang et al., 2021; Pietrzyk et al., 2004; Vereecken et al., 2015). These advances have been supported by stochastic simulation techniques and strengthened by empirical evidence from field measurements, such as monitored wall assemblies and infiltration studies (Calle et al., 2020; Wang & Ge, 2018; Yan et al., 2025). Together, these efforts have improved the reliability and physical realism of hygrothermal models and laid a foundation for uncertainty-aware performance assessment.

Nevertheless, the application of these probabilistic approaches in practical HAM design and retrofit decision-making remains limited. Most existing studies focus on uncertainty analysis or sensitivity testing, while relatively few dynamically update the probabilistic outcomes based on the real-world monitoring, which can dynamically adjust the outcomes, support robust and reliable design or retrofit solutions. Recent research has begun to narrow this gap by integrating long-term monitoring data with stochastic modelling and by incorporating multi-year climate variability into hygrothermal simulations (Chung et al., 2023; Gradeci et al., 2018). Although these approaches represent promising steps toward evidence-based and uncertainty-informed design, they are still in the early stages of development.

4.3.1 Evidence-based HAM design

Evidence-based HAM design integrates empirical data from laboratory and field studies with coupled heat, air, and moisture models within a quantified uncertainty framework to derive reliability metrics such as the probabilities of mould growth, condensation, and freeze–thaw damage. It moves beyond deterministic checks by employing calibrated models and advanced techniques which include sensitivity analysis, Bayesian inference, and surrogate modelling to enhance computational efficiency and support more informed design decisions. Comprehensive data inputs are essential for HAM simulations, encompassing material properties (e.g., density, porosity, thermal conductivity), outdoor and indoor climatic conditions (e.g., temperature, humidity, wind, radiation, ventilation, occupancy), surface and boundary parameters (e.g., heat and vapour transfer coefficients, rain deposition, air change rates), and hygrothermal functions describing thermal and moisture transport and storage behaviors.

Several studies have advanced the scientific reliability of HAM simulations through rigorous experimental validation and model calibration. In 2013, Spitz et al. conducted detailed measurements of temperature and humidity across multiple layers of a full-scale wooden-frame test house in France under real climatic conditions to evaluate HAM simulations using EnergyPlus. Their findings emphasized the importance of accurately characterizing material properties, moisture content, and air infiltration to enhance model calibration and improve the prediction of hygrothermal behavior (Spitz et al., 2013). In 2014, Fox investigated the hygrothermal performance of highly insulated wood-frame walls with controlled air leakage through full-scale field experiments at the University of Waterloo. Continuous monitoring of temperature, relative humidity, moisture content, and heat flux enabled the evaluation of condensation and mould risks and supported WUFI-based model calibration, thereby improving predictive accuracy and informing durable wall design (Fox, 2014). Subsequently, in 2019, Calle et al. examined rainwater infiltration in non-insulated brick cavity walls to refine HAM simulations by developing infiltration functions derived from experimental testing under varying workmanship and pressure conditions. Their study revealed that moisture transfer was primarily governed by surface runoff and construction defects rather than air pressure, leading to more realistic and physically representative hygrothermal predictions (Calle et al., 2020). Together, these studies illustrate the growing integration of experimental evidence into HAM modelling, thereby strengthening its predictive capability for assessing building hygrothermal performance.

4.3.2 Quantify and reduce uncertainty

Building on experimental evidence, recent studies have advanced HAM modelling by incorporating stochastic frameworks that quantify simulation uncertainties using observational and experimental data. This trend has been driven by advances in low-cost sensing technologies and the rapid development of computational methods that enable probabilistic analysis.

In 2012, Zhao developed a statistical and experimental framework to improve the reliability of HAM modelling. Laboratory experiments were conducted to measure key hygrothermal properties of materials such as brick, plaster, and mortar, including moisture storage, vapor permeability, and liquid water transport. The measured data were statistically analyzed to create generalized material datasets and incorporated into a Monte Carlo based probabilistic HAM model. This approach enhanced the reliability of HAM simulations in predicting building durability, thermal efficiency, and mold growth under uncertain material and boundary conditions (Zhao, 2012).

In 2024, Andres Arcones et al. developed a Bayesian calibration framework that explicitly accounts for model bias and measurement noise to improve the reliability of simulation-based predictions. Using temperature measurements from a transient thermal experiment on reinforced concrete, they compared several likelihood formulations, including Approximate Bayesian Computation, Global Moment Matching, and Relative Global Moment Matching, to evaluate uncertainty propagation. Their results showed that incorporating model bias directly into the inference process enhances parameter calibration accuracy and leads to more reliable predictions of heat and moisture transfer behavior (Andres Arcones et al., 2024). In the same year, Ryan et al. developed a probabilistic framework to evaluate moisture-induced degradation risks in wood-frame building envelopes under uncertain material, design, and climatic conditions. By combining hygrothermal simulations with Response Surface Methodology and Bayesian analysis, they quantified the influence of key parameters on mold growth potential. The study found that vapor barrier permeance and cladding diffusion resistance were the most critical factors, demonstrating the value of probabilistic modelling for uncertainty-informed hygrothermal design (Ryan et al., 2024).

Bayat Pour et al. emphasized that integrating Bayesian frameworks with experimental observations can substantially reinforce evidence-based HAM design and enable more robust, uncertainty-informed decision-making in assessing building durability and moisture-related risks (Bayat Pour et al., 2024). Bayesian inference can be integrated with stochastic HAM modelling to enhance the reliability of building envelope performance predictions. Using Markov Chain Monte Carlo (MCMC) algorithms, uncertain model parameters are updated by combining prior information with experimental data to generate posterior distributions (Yan, 2024). This probabilistic calibration allows HAM models to account for both epistemic and aleatoric uncertainties. As a result, the implementation of Bayesian inference with stochastic HAM modeling could provide more accurate and evidence-based assessments of moisture risks and hygrothermal durability in building envelopes.

4.4 Urban scale assessment

At the urban scale, applying probabilistic assessments for understanding Heat and Moisture Transfer (HAM) in building stock requires a complex data-driven methodology. As Urban Building Energy Models (UBEMs) are increasingly used to simulate the energy performance of entire districts or cities by classifying buildings into archetypes defined by their age, construction type, and use, an urban-scale model specifically focused on Heat and Moisture Transfer in Buildings has yet to be developed. Such a model is crucial, as moisture dynamics not only affect energy consumption but also drive critical issues like mould growth, indoor air quality, and long-term durability of the building envelope. Addressing HAM at scale is especially urgent in the context of climate change, where rising humidity levels and more frequent extreme weather events increase the vulnerability of existing building stock.

Mold growth in residential buildings is a well-documented consequence of uncontrolled moisture accumulation, with established links to respiratory illness, allergic reactions, and structural degradation (Zhang et al., 2021; Wu & Wong, 2020). The risk is particularly elevated in aging housing stock, where deteriorating materials, limited ventilation, and deferred maintenance create conditions conducive to fungal colonization (Arthur, 2004; Annila et al., 2017). Although building envelope characteristics are recognized as primary drivers, occupant behavior and awareness also play an important and often underappreciated role: behaviors such as blocking air vents, neglecting condensation on surfaces, and deferring plumbing maintenance have been shown to accelerate mold development, particularly in high-occupancy or low-income dwellings (Prezant et al., 2008). This intersection of physical building performance and human factors makes mold risk a natural candidate for probabilistic assessment. This leads to uncertainty in both the hygrothermal boundary conditions and the occupancy-driven variables that modulate them.

A further challenge at the urban scale is the absence of a standardized, non-invasive assessment framework capable of characterizing mold risk across a diverse building stock. Existing inspection methods -- such as infrared thermography, bulk sampling, air sampling, image-recognition-based approaches, and microbial volatile organic compound (MVOC) analysis -- carry significant limitations in terms of cost, invasiveness, interpretive complexity, and spatial coverage (Wu & Wong, 2020). Infrared imaging can identify moisture anomalies but lacks specificity for mold and requires expert interpretation. Bulk sampling, while accurate, is invasive and expensive, which limits its use in community-wide screening. Air sampling, though less disruptive, is sensitive to transient environmental conditions and may fail to capture mold growth within enclosed cavities. These practical constraints reinforce the need for scalable, data-driven approaches that can translate limited inspection data into neighbourhood-level risk profiles, precisely the kind of output that could be generated by coupling urban-scale hygrothermal simulation with field-calibrated probabilistic models.

A step in this direction was taken by Salehi et al. (2025), who developed a localized mold-risk profile for 17 aging residential buildings in Southwest Chicago by integrating occupant survey data, professional mold inspection results, and contractor remediation proposals. Mold severity was quantified using a Mold Severity Index (MSI) based on colony-forming unit (CFU/m^3) concentrations from air and surface sampling, classified into low, medium, and high risk thresholds consistent with WHO indoor air quality guidelines (Heseltine & Rosen, 2009). Mold was confirmed in 13 of the 17 homes, with 77% exhibiting high contamination levels (≥1000 CFU/m^3). The study found that mold prevalence correlated strongly with building age, hygroscopic materials such as wood and brick, limited passive ventilation, and lower household income. These factors collectively define the kinds of building archetypes that an urban-scale HAM model would need to represent. Moreover, 85% of residents in mold-confirmed homes were unaware of its presence prior to inspection, highlighting the limits of occupant-reported data and reinforcing the need for simulation-driven predictive tools that can identify at-risk dwellings without relying on self-reported observations. These findings provide an empirical basis for parameterizing probabilistic mold-risk models at the neighborhood scale, and illustrate how field-calibrated inspection data can be used to support evidence-based decision-making by housing authorities, public health officials, and municipal planners (Salehi et al., 2025).

As a conclusion, there is a need for a combination of HAM simulation software, field data, and machine learning approach that can integrate detailed hygrothermal simulations with probabilistic risk assessment to create actionable predictions at urban scale. These insights are intended for decision-support tools for city planners, public health officials, and community organizations. Ultimately, such approaches can guide cities in prioritizing retrofits, targeting vulnerable communities, and designing resilient, healthy, and energy-efficient urban environments for the long term.

4.5 References

Aït Oumeziane, Y., Moissette, S., Bart, M., Collet, F., Pretot, S., & Lanos, C. (2017). Influence of hysteresis on the transient hygrothermal response of a hemp concrete wall. Journal of Building Performance Simulation, 10(3), 256–271. https://doi.org/10.1080/19401493.2016.1216166

Akhavan Shams, S., Ge, H., & Wang, L. (2024). Hygrothermal modeling in mass timber constructions: Recent advances and machine learning prospects. Journal of Building Engineering, 96, 110500. https://doi.org/10.1016/j.jobe.2024.110500

Akhavan Shams, S., Ge, H., & Wang, L. (2025). Effect of Hysteresis on Modeling Hygrothermal Performance of Hempcrete Wall Assemblies. In S. Amziane, R. D. Toledo Filho, M. Y. R. da Gloria, & J. Page (Eds.), Bio-Based Building Materials - Proceedings of ICBBM 2025 (pp. 850–860). Springer, Cham. https://doi.org/10.1007/978-3-031-92777-5_68

Almeida, R. M. S. F., & Barreira, E. (2018). Monte Carlo Simulation to Evaluate Mould Growth in Walls: The Effect of Insulation, Orientation, and Finishing Coating. Advances in Civil Engineering, 2018(1). https://doi.org/10.1155/2018/8532167

Amorim, M., de Freitas, V. P., & Torres, I. (2024). Influence of Moisture on the Energy Performance of Retrofitted Walls - Experimental Assessment and Validation of an Hygrothermal Model. International Journal of Architectural Heritage, 18(3), 477–491. https://doi.org/10.1080/15583058.2022.2157777

Andrés Arcones, D., Weiser, M., Koutsourelakis, P.-S., & Unger, J. F. (2026). Embedded model form uncertainty quantification with measurement noise for Bayesian model calibration. Data-Centric Engineering, 7, e7. https://doi.org/10.1017/dce.2025.10035

Annila, P. J., Hellemaa, M., Pakkala, T. A., Lahdensivu, J., Suonketo, J., & Pentti, M. (2017). Extent of moisture and mould damage in structures of public buildings. Case Studies in Construction Materials, 6, 103–108. https://doi.org/10.1016/j.cscm.2017.01.003

Antretter, F., Sauer, F., Schopfer, T., & Holm, A. (2011). Validation of hygrothermal whole building simulation software. Proceedings in Building Simulation 2011, 1694–1701.

Arthur, R. (2004). Damp Indoor Spaces and Health. Institute of Medicine: Committee on Damp Indoor Spaces and Health. The National Academy Press. Washington, DC.

ASHRAE. (1967). ASHRAE Handbook 1967 Fundamentals. ASHRAE.

Bakkour, A., Ouldboukhitine, S.-E., Biwole, P., & Amziane, S. (2025). Modeling heat and moisture transfer in bio-based wall structures using the finite element method: Application to straw walls in varied climatic conditions. Journal of Building Engineering, 104, 112263. https://doi.org/10.1016/j.jobe.2025.112263

Bauklimatik Dresden. (2026, May). Delphin 6.1.7. Https://Bauklimatik-Dresden.de/En/Software/Delphin/.

Bayat Pour, M., & Abdul Hamid, A. (2024). Towards a sustainable decision analysis approach for moisture-safe building envelope design. Journal of Building Engineering, 97, 110955. https://doi.org/10.1016/j.jobe.2024.110955

Bayat Pour, M., Niklewski, J., Naghibi, A., & Frühwald Hansson, E. (2024). A literature review of probabilistic hygrothermal assessment for building envelopes. Building and Environment, 261, 111756. https://doi.org/10.1016/j.buildenv.2024.111756

Belloum, R., Agoudjil, B., Chennouf, N., & Boudenne, A. (2022). Hygrothermal performance assessment of a bio-based building made with date palm concrete walls. Building and Environment, 223, 109467. https://doi.org/10.1016/j.buildenv.2022.109467

Benmahiddine, F., Bennai, F., Charaka, A., Hamami, A. E. A., Tahakourt, A., & Belarbi, R. (2024). Multi-scale analysis of the effects of hysteresis on the hydrothermal behaviour of bio-based materials: Application to hemp concrete. Construction and Building Materials, 411, 134107. https://doi.org/10.1016/j.conbuildmat.2023.134107

Bomberg, M. (1974). Moisture flow through porous building materials [PhD Thesis]. Lund University.

Bordbari, M. J., Seifi, A. R., & Rastegar, M. (2018). Probabilistic energy consumption analysis in buildings using point estimate method. Energy, 142, 716–722. https://doi.org/10.1016/j.energy.2017.10.091

Calle, K., Coupillie, C., Janssens, A., & Van Den Bossche, N. (2020). Implementation of rainwater infiltration measurements in hygrothermal modelling of non-insulated brick cavity walls. Journal of Building Physics, 43(6), 477–502. https://doi.org/10.1177/1744259119883909

Carpino, C., Bruno, R., Carpino, V., & Arcuri, N. (2022). Uncertainty and sensitivity analysis to moderate the risks of energy performance contracts in building renovation: A case study on an Italian social housing district. Journal of Cleaner Production, 379, 134637. https://doi.org/10.1016/j.jclepro.2022.134637

Chung, D., Wen, J., & Lo, L. C. J. (2023). Examining the impact of stochastic multi-year weather and air infiltration on hygrothermal moisture risks. Journal of Building Physics, 47(1), 4–35. https://doi.org/10.1177/17442591231163459

Chung, D., Wen, J., & Lo, L. J. (2020). Development and verification of the open source platform, HAM-Tools, for hygrothermal performance simulation of buildings using a stochastic approach. Building Simulation, 13(3), 497–514. https://doi.org/10.1007/s12273-019-0594-5

Clarke, J. (2013). Moisture flow modelling within the ESP-r integrated building performance simulation system. Journal of Building Performance Simulation, 6(5), 385–399. https://doi.org/10.1080/19401493.2013.777117

Clarke, J. A. (1985). Energy Simulation in Building Design. CRC Press.

Coelho, G. B. A., Silva, H. E., & Henriques, F. M. A. (2018). Calibrated hygrothermal simulation models for historical buildings. Building and Environment, 142, 439–450. https://doi.org/10.1016/j.buildenv.2018.06.034

COMSOL. (2026, May). COMSOL Multiphysics. Https://Www.Comsol.Com/.

de Wit, S., & Augenbroe, G. (2002). Analysis of uncertainty in building design evaluations and its implications. Energy and Buildings, 34(9), 951–958. https://doi.org/10.1016/S0378-7788(02)00070-1

Dang, X., Guimarães, A. S., Sarkany, A., Laukkarinen, A., Xu, B., Vanderschelden, B., ... & Roels, S. (2025a). A state-of-the-art empirical round robin validation of heat, air and moisture (HAM) models. Building and Environment, 276, 112867.

Defraeye, T., Blocken, B., & Carmeliet, J. (2013). Influence of uncertainty in heat–moisture transport properties on convective drying of porous materials by numerical modelling. Chemical Engineering Research and Design, 91(1), 36–42. https://doi.org/10.1016/j.cherd.2012.06.011

Delgarm, N., Sajadi, B., Azarbad, K., & Delgarm, S. (2018). Sensitivity analysis of building energy performance: A simulation-based approach using OFAT and variance-based sensitivity analysis methods. Journal of Building Engineering, 15, 181–193. https://doi.org/10.1016/j.jobe.2017.11.020

Dong, W., Chen, Y., Bao, Y., & Fang, A. (2020). A validation of dynamic hygrothermal model with coupled heat and moisture transfer in porous building materials and envelopes. Journal of Building Engineering, 32, 101484. https://doi.org/10.1016/j.jobe.2020.101484

Ferroukhi, M. Y., Abahri, K., Belarbi, R., & Limam, K. (2017). Integration of a hygrothermal transfer model for envelope in a building energy simulation model: experimental validation of a HAM–BES co-simulation approach. Heat and Mass Transfer, 53(6), 1851–1861. https://doi.org/10.1007/s00231-016-1944-9

Ferroukhi, M. Y., Djedjig, R., Limam, K., & Belarbi, R. (2016). Hygrothermal behavior modeling of the hygroscopic envelopes of buildings: A dynamic co-simulation approach. Building Simulation, 9(5), 501–512. https://doi.org/10.1007/s12273-016-0292-5

Fox, M. J. (2014). Hygrothermal performance of highly insulated wood frame walls with air leakage: Field measurements and simulations [Master's Thesis]. Ryerson University, Toronto, Canada.

Fraunhofer IBP. (2026a, May). WUFI Plus 3.5. Https://Wufi.de/En/Software/Wufi-Plus/.

Fraunhofer IBP. (2026b, May). WUFI Pro 7.0. Https://Wufi.de/En/Software/Wufi-Pro/.

Glaser H. (1958). Simplified calculation of vapor diffusion through layered walls with precipitation of water and ice. Refrigeration Technology, 10(11), 358–364.

Gradeci, K., Labonnote, N., Time, B., & Köhler, J. (2018). A probabilistic-based methodology for predicting mould growth in façade constructions. Building and Environment, 128, 33–45. https://doi.org/10.1016/j.buildenv.2017.11.021

Hagentoft, C.-E. (2017). Reliability of energy efficient building retrofitting - probability assessment of performance and cost (Annex 55, RAP-RETRO). Energy and Buildings, 155, 166–171. https://doi.org/10.1016/j.enbuild.2017.09.007

Heo, Y., Choudhary, R., & Augenbroe, G. A. (2012). Calibration of building energy models for retrofit analysis under uncertainty. Energy and Buildings, 47, 550–560. https://doi.org/10.1016/j.enbuild.2011.12.029

Heseltine, E., & Rosen, J. (2009). WHO guidelines for indoor air quality: Dampness and mould. World Health Organization.

Hittle, D. (1977). The Building Loads Analysis and System Thermodynamics (BLAST) Program: Vol I: User's manual.

Hopfe, C. J., & Hensen, J. L. M. (2011). Uncertainty analysis in building performance simulation for design support. Energy and Buildings, 43(10), 2798–2805. https://doi.org/10.1016/j.enbuild.2011.06.034

Hou, T., Nuyens, D., Roels, S., & Janssen, H. (2019). Quasi-Monte Carlo based uncertainty analysis: Sampling efficiency and error estimation in engineering applications. Reliability Engineering & System Safety, 191, 106549. https://doi.org/10.1016/j.ress.2019.106549

Hung, Y. (2024). A review of Monte Carlo and quasi-Monte Carlo sampling techniques. WIREs Computational Statistics, 16(1). https://doi.org/10.1002/wics.1637

Janssen, H. (2013). Monte-Carlo based uncertainty analysis: Sampling efficiency and sampling convergence. Reliability Engineering & System Safety, 109, 123–132. https://doi.org/10.1016/j.ress.2012.08.003

Johari, F., Peronato, G., Sadeghian, P., Zhao, X., & Widén, J. (2020). Urban building energy modeling: State of the art and future prospects. Renewable and Sustainable Energy Reviews, 128, 109902. https://doi.org/10.1016/j.rser.2020.109902

Kahangi Shahreza, S., Bayat Pour, M., & Abdul Hamid, A. (2024). Towards rational decision-making on repointing to mitigate moisture damage in building envelopes: A probabilistic study. Developments in the Built Environment, 19, 100510. https://doi.org/10.1016/j.dibe.2024.100510

Kalagasidis, A. S. (2004). HAM-Tools: An integrated simulation tool for heat, air and moisture transfer analyses in building physics [PhD Thesis]. Chalmers University of Technology, Gothenburg, Sweden.

Karagiozis, A. (1993). Overview of the 2-D Hygrothermal Heat-Moisture Transport Model LATENITE.

Kong, G., Hu, S., & Yang, Q. (2023). Uncertainty method and sensitivity analysis for assessment of energy consumption of underground metro station. Sustainable Cities and Society, 92, 104504. https://doi.org/10.1016/j.scs.2023.104504

Kukk, V., Kers, J., Kalamees, T., Wang, L., & Ge, H. (2022). Impact of built-in moisture on the design of hygrothermally safe cross-laminated timber external walls: A stochastic approach. Building and Environment, 226, 109736. https://doi.org/10.1016/j.buildenv.2022.109736

Künzel, H. M. (1995). Simultaneous heat and moisture transport in building components: One- and two-dimensional calculation using simple parameters. Fraunhofer Institute of Building Physics, Fraunhofer, Germany.

LBNL Simulation Research Group. (1977). DOE-1 COMPUTER PROGRAM FOR BUILDING ENERGY ANALYSIS.

Libralato, M., De Angelis, A., Tornello, G., Saro, O., D'Agaro, P., & Cortella, G. (2021). Evaluation of Multiyear Weather Data Effects on Hygrothermal Building Energy Simulations Using WUFI Plus. Energies, 14(21), 7157. https://doi.org/10.3390/en14217157

Lu, S., Wang, C., Fan, Y., & Lin, B. (2021). Robustness of building energy optimization with uncertainties using deterministic and stochastic methods: Analysis of two forms. Building and Environment, 205, 108185. https://doi.org/10.1016/j.buildenv.2021.108185

Luikov, A. V. (1966). Heat and mass transfer in capillary-porous bodies (P. W. B. Harrison & W. M. Pun, Eds.). Pergamon Press.

Luikov, A. V. (1975). Systems of differential equations of heat and mass transfer in capillary-porous bodies . International Journal of Heat and Mass Transfer, 18(1), 1–14.

Macdonald, I., & Strachan, P. (2001). Practical application of uncertainty analysis. Energy and Buildings, 33(3), 219–227. https://doi.org/10.1016/S0378-7788(00)00085-2

Månsson, L.-G. (1998). Calculation of energy and environmental performance of buildings. Energy Conservation in Buildings and Community Systems Programme. (IEA ANNEX 21)

Marincioni, V., Marra, G., & Altamirano-Medina, H. (2018). Development of predictive models for the probabilistic moisture risk assessment of internal wall insulation. Building and Environment, 137, 257–267. https://doi.org/10.1016/j.buildenv.2018.04.001

MathWorks. (2026, May). Matlab/Simulink. Https://Www.Mathworks.Com/Products/Simulink.Html.

Moon, H. J., & Augenbroe, G. (2005). A mixed simulation approach to analyze mold growth under uncertainty. The Ninth International IBPSA Conference, 785–792.

National Laboratory of the Rockies. (2026, May). EnergyPlus 26.1.0. Https://Energyplus.Net/.

Oh, S., & Haberl, J. S. (2016). Origins of analysis methods used to design high-performance commercial buildings: Whole-building energy simulation. Science and Technology for the Built Environment, 22(1), 118–137. https://doi.org/10.1080/23744731.2015.1063958

Ojanen, T., Viitanen, H., Peuhkuri, R., Lahdesmaki, K., Vinha, J., & Salmien, K. (2010). Mold growth modeling of building structures using sensitivity classes of materials. Proceedings in Buildings XI Conference.

Pang, Z., O'Neill, Z., Li, Y., & Niu, F. (2020). The role of sensitivity analysis in the building performance analysis: A critical review. Energy and Buildings, 209, 109659. https://doi.org/10.1016/j.enbuild.2019.109659

Pérez-Bella, J. M., Domínguez-Hernández, J., López-Julián, P. L., Salesa-Bordabana, Á., & Orna-Carmona, M. (2024). Closing the gap between traditional wind-driven rain studies and the performance-based design of building façades: Case study of the Netherlands. Building and Environment, 248, 111083. https://doi.org/10.1016/j.buildenv.2023.111083

Philip, J. R., & De Vries, D. A. (1957). Moisture movement in porous materials under temperature gradients. Eos, Transactions American Geophysical Union, 38(2), 222–232. https://doi.org/10.1029/TR038i002p00222

Pietrzyk, K., Kurkinen, K., & Hagentoft, C.-E. (2004). An Example of Application of Limit State Approach for Reliability Analysis of Moisture Performance of a Building Component. Journal of Thermal Envelope and Building Science, 28(1), 9–26. https://doi.org/10.1177/1097196304041993

Posani, M., Veiga, R., & Freitas, V. (2023). Post-Insulating traditional massive walls in Southern Europe: A moderate thermal resistance can be more effective than you think. Energy and Buildings, 295, 113299. https://doi.org/10.1016/j.enbuild.2023.113299

Prezant, B. (2008). Recognition, Evaluation, and Control of Indoor Mold. AIHA.

Rode, C. (1990). Combined heat and moisture transfer in building constructions. Technical University of Denmark.

Ryan, B., Bristow, D., & Mukhopadhyaya, P. (2024). A probabilistic approach for risk assessment of moisture-related degradation of building envelopes. Journal of Building Physics, 48(2), 168–196. https://doi.org/10.1177/17442591241261078

Salehi, P., Pipim, C., & Karatas, A. (2025). Integrating household characteristics, mold inspection and remediation data to develop localized mold-risk profiles for residential buildings. In J. M. Branco et al. (Eds.), ICMB 2025, LNCE 776 (pp. 553–567). Springer Nature Switzerland AG. https://doi.org/10.1007/978-3-032-09054-6_44

Sengupta, A., Al Assaad, D., Berk Kazanci, O., Shinoda, J., Breesch, H., & Steeman, M. (2024). Building and system design's impact on thermal resilience to overheating during heatwaves: An uncertainty and sensitivity analysis. Building and Environment, 265, 112031. https://doi.org/10.1016/j.buildenv.2024.112031

Shen, H., & Tzempelikos, A. (2013). Sensitivity analysis on daylighting and energy performance of perimeter offices with automated shading. Building and Environment, 59, 303–314. https://doi.org/10.1016/j.buildenv.2012.08.028

SPITZ, C., WOLOSZYN, M., CATHERINE, B., & MATTHIEU, L. (2013, August 28). Simulating Combined Heat And Moisture Transfert With Energyplus: Uncertainty Study And Comparison With Experimental Data. Proceedings of BS2013. https://doi.org/10.26868/25222708.2013.2472

Sulaiman, H., & Olsina, F. (2014). Comfort reliability evaluation of building designs by stochastic hygrothermal simulation. Renewable and Sustainable Energy Reviews, 40, 171–184. https://doi.org/10.1016/j.rser.2014.07.162

Sun, S., Kensek, K., Noble, D., & Schiler, M. (2016). A method of probabilistic risk assessment for energy performance and cost using building energy simulation. Energy and Buildings, 110, 1–12. https://doi.org/10.1016/j.enbuild.2015.09.070

Tariku, F. (2008). Whole building heat and moisture analysis [PhD Thesis]. Concordia University, Montreal, Canada.

Tian, Y., & Chai, K. (2025). Building design and operation multi-objective optimization: Energy costs vs. Emissions. Energy and Buildings, 329, 115225. https://doi.org/10.1016/j.enbuild.2024.115225

Tijskens, A., Janssen, H., & Roels, S. (2023). Probabilistic hygrothermal assessment of various timber frame wall compositions. Building and Environment, 243, 110619. https://doi.org/10.1016/j.buildenv.2023.110619

TRNSYS. (2026, May). Transient System Simulation Tool. Https://Www.Trnsys.Com/.

Van Linden, S., & Van Den Bossche, N. (2022). Review of rainwater infiltration rates in wall assemblies. Building and Environment, 219, 109213. https://doi.org/10.1016/j.buildenv.2022.109213

van Schijndel, A. W. M. (2007). Integrated heat air and moisture modeling and simulation [PhD Thesis]. Eindhoven University of Technology, Eindhoven, Netherlands.

Vereecken, E., Van Gelder, L., Janssen, H., & Roels, S. (2015). Interior insulation for wall retrofitting – A probabilistic analysis of energy savings and hygrothermal risks. Energy and Buildings, 89, 231–244. https://doi.org/10.1016/j.enbuild.2014.12.031

Wang, C., Wang, X., Causone, F., Yang, Y., Gao, N., Ye, Y., Li, P., & Shi, X. (2025). Addressing uncertainty to achieve stability in urban building energy modeling: A comparative study of four possible approaches. Building and Environment, 267, 112197. https://doi.org/10.1016/j.buildenv.2024.112197

Wang, L., Defo, M., Xiao, Z., Ge, H., & Lacasse, M. A. (2021). Stochastic Simulation of Mould Growth Performance of Wood-Frame Building Envelopes under Climate Change: Risk Assessment and Error Estimation. Buildings, 11(8), 333. https://doi.org/10.3390/buildings11080333

Wang, L., & Ge, H. (2018). Stochastic modelling of hygrothermal performance of highly insulated wood framed walls. Building and Environment, 146, 12–28. https://doi.org/10.1016/j.buildenv.2018.09.032

Woloszyn, M., & Rode, C. (2008). Tools for performance simulation of heat, air and moisture conditions of whole buildings. Building Simulation, 1(1), 5–24. https://doi.org/10.1007/s12273-008-8106-z

Wu, H., & Wong, J. W. C. (2020). Current challenges for shaping the sustainable and mold-free hygienic indoor environment in humid regions. Letters in Applied Microbiology, 70(6), 396–406. https://doi.org/10.1111/lam.13291

Xiao, Z., Lacasse, M. A., Dragomirescu, E., & Defo, M. (2023). Projected changes of wind-driven rain and moisture load in wall assemblies across Canada. Journal of Wind Engineering and Industrial Aerodynamics, 238, 105446. https://doi.org/10.1016/j.jweia.2023.105446

Yan, S., Zou, J., Shu, C., Berquist, J., Brochu, V., Veillette, M., Hou, D., Duchaine, C., Zhou, L. (Grace), Zhai, Z. (John), & Wang, L. (Leon). (2025). Implementing Bayesian inference on a stochastic CO2-based grey-box model. Indoor Environments, 2(1), 100079. https://doi.org/10.1016/j.indenv.2025.100079

Yan, S. (2024). Multizone modeling of airborne quanta transmission and CO2-based ventilation designs for assessing indoor exposures [PhD Thesis] Concordia University, Montreal, Canada.

Yang, J., Fu, H., & Qin, M. (2015). Evaluation of Different Thermal Models in EnergyPlus for Calculating Moisture Effects on Building Energy Consumption in Different Climate Conditions. Procedia Engineering, 121, 1635–1641. https://doi.org/10.1016/j.proeng.2015.09.194

Yu, S., Cui, Y., Shao, Y., & Han, F. (2019). Research on the Comprehensive Performance of Hygroscopic Materials in an Office Building Based on EnergyPlus. Energies, 12(1), 191. https://doi.org/10.3390/en12010191

Zhang, M., Qin, M., Rode, C., & Chen, Z. (2017). Moisture buffering phenomenon and its impact on building energy consumption. Applied Thermal Engineering, 124, 337–345. https://doi.org/10.1016/j.applthermaleng.2017.05.173

Zhang, X., Riaz Ahmad, M., & Chen, B. (2020). Numerical and experimental investigation of the hygrothermal properties of corn stalk and magnesium phosphate cement (MPC) based bio-composites. Construction and Building Materials, 244, 118358. https://doi.org/10.1016/j.conbuildmat.2020.118358

Zhang, Y., Hua, L., Liu, Q.-H., Chu, S.-Y., Gan, Y.-X., Wu, M., Bao, Y.-X., Chen, Q., & Zhang, J. (2021). Household mold exposure interacts with inflammation-related genetic variants on childhood asthma: a case–control study. BMC Pulmonary Medicine, 21(1), 114. https://doi.org/10.1186/s12890-021-01484-9

Zhao, J., Plagge, R., Nicolai, A., Grunewald, J., & Zhang, J. S. (2011). Stochastic study of hygrothermal performance of a wall assembly—The influence of material properties and boundary coefficients. HVAC&R Research, 17(4), 591–601. https://doi.org/10.1080/10789669.2011.585421

Zhao, J. (2012). Development of a novel statistical method and procedure for material characterization and a probabilistic approach to assessing the hygrothermal performance of building enclosure assemblies. [PhD Thesis]. Syracuse University, Syracuse, USA.

Zhao, J., Zhang, J. "Jensen," Grunewald, J., & Feng, S. (2021). A probabilistic-based method to evaluate hygrothermal performance of an internally insulated brick wall. Building Simulation, 14(2), 283–299. https://doi.org/10.1007/s12273-020-0702-6

Zhu, C., Tian, W., Yin, B., Li, Z., & Shi, J. (2020). Uncertainty calibration of building energy models by combining approximate Bayesian computation and machine learning algorithms. Applied Energy, 268, 115025. https://doi.org/10.1016/j.apenergy.2020.115025

5 Future Climate Data and Reference Year Selection for Building Performance Simulations

This section should be cited as:

Zou, J., Tan, Z., Wang, Liangzhu (Leon) (2026) Future climate and reference year selection for building performance simulations. In: A Systematic Review of Passive Energy Conservation Measures and Probabilistic Assessment under Changing Climate in Urban Settings, CIB W040 Report, CIB General Secretariat.

Climate change is a critical consideration in the assessment of long-term building performance, particularly regarding energy consumption and indoor thermal comfort, as well as moisture-related deteriorations due to its profound and long-lasting effects (Machard et al., 2024; Zou et al., 2023). The anticipated impacts of climate change can significantly increase the energy required for cooling buildings, with projections indicating a rise in cooling energy demand ranging from 5% to as much as 90%, depending on the Representative Concentration Pathway (RCP) scenario that ultimately unfolds (Zhai & Helman, 2019). Meanwhile, incorporating climate change impacts into building performance simulations introduces a substantial degree of uncertainty, which can influence the reliability and accuracy of the simulation outcomes. The uncertainties associated with climate change in building performance assessments can be broadly categorized as follows:

Various Global Warming scenarios:

Different RCPs or emission scenarios represent a range of possible future greenhouse gas concentrations, each leading to varying degrees of global warming. The choice of scenario directly affects projected climate conditions and, consequently, building performance predictions.

Variability in Climate Data Sources:

Climate projections are derived from a variety of Global Climate Models (GCMs) and Regional Climate Models (RCMs). Each model has its own assumptions, spatial resolutions, and methodologies, resulting in differences in the projected climate data used for building simulations.

Bias-correction and data morphing methods:

Raw climate models often require adjustment to better reflect local climate conditions. Bias-correction and data morphing methods are commonly applied, but the choice and implementation of these techniques can introduce additional uncertainty into the climate data used for simulations.

Methods of generating reference years:

To assess building performance under future climate conditions, typical or reference years are generated from climate projections. Various approaches exist for constructing these reference years, each with its own strengths and limitations, further contributing to the overall uncertainty.

A procedure of workflow of applying reference year method on future climate could found in Zou et al. (2023):

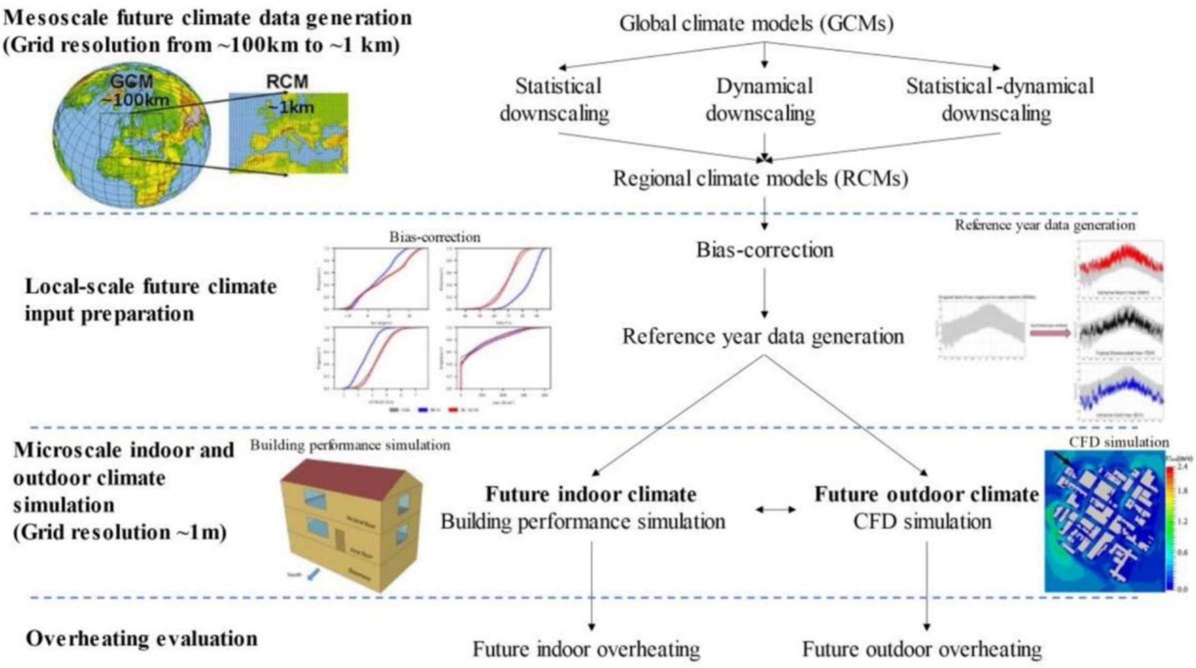

Figure 5.1 Workflow of applying reference year method on future climate data (Zou et al., 2023)

In the following sub-sections, each of these sources of uncertainty will be examined in detail. Their significance in the context of building performance simulation will be discussed, along with practical recommendations for addressing and managing these uncertainties to improve the robustness of simulation results.

5.1 Various Global Warming Scenarios

Climate change presents significant challenges to the built environment, particularly in evaluating the long-term performance and resilience of passive energy conservation measures. Reliable climate projections are crucial for assessing potential impacts on energy consumption, thermal comfort, and durability of building components under future climate conditions (Nik, 2012; Nik et al., 2021; Panico et al., 2023; Vandemeulebroucke et al., 2021; Zou, 2024; Zou et al., 2023; Zou, Wang, et al., 2025; Zou, Yu, et al., 2025). These projections are derived from Global Climate Models (GCMs), which simulate interactions among the atmosphere, oceans, and land surfaces (Randall et al., 2007). To harmonize and enhance these global modeling efforts, the Coupled Model Intercomparison Project (CMIP) (Meehl et al., 2000) coordinates climate model experiments worldwide. Scenarios differ primarily in their assumptions regarding future greenhouse gas emissions, land-use changes, and climate mitigation efforts, enabling the assessment of a wide range of possible climate outcomes. In the fifth phase (CMIP5), CMIP introduced Representative Concentration Pathways (RCPs), scenarios based on distinct greenhouse gas (GHG) emissions (Taylor et al., 2012), as shown in Fig. 5.2. Specifically, RCP 2.6 corresponds to a low-emission scenario with stringent climate mitigation efforts, RCP 4.5 and RCP 6.0 represent moderate emission scenarios with stabilization measures, and RCP 8.5 represents a high-emission, business-as-usual scenario characterized by minimal emission reductions. These scenarios enable systematic exploration of different climate futures and provide essential datasets that drive building simulations, helping designers and policymakers optimize passive measures and improve resilience of buildings to future climate conditions.

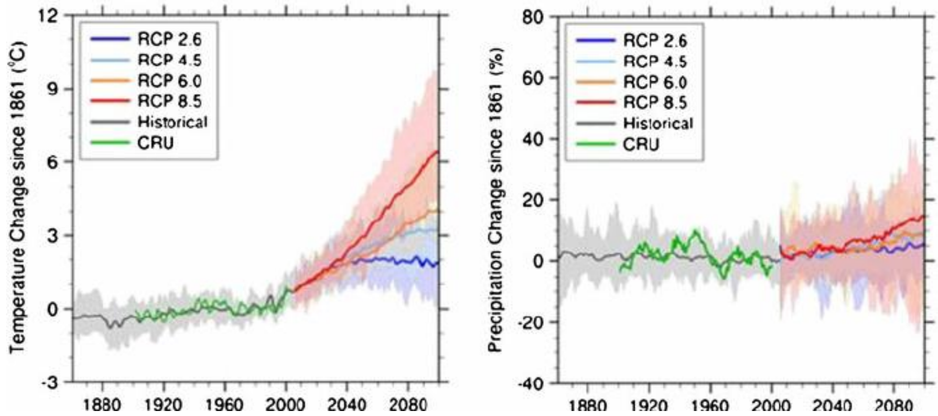

Figure 5.2 CMIP5 model based time series of temperature and precipitation anomalies (historical and projections) (Chaturvedi et al., 2014)

In CMIP6, climate modeling frameworks evolved significantly with the introduction of Shared Socioeconomic Pathways (SSPs), which replaced the purely emission-based RCPs used in CMIP5 (O'Neill et al., 2016). Unlike RCPs, SSPs integrate greenhouse gas emissions with detailed socioeconomic narratives that reflect plausible global futures—ranging from sustainable development (SSP1) to inequality-driven and fossil-fuel-intensive worlds (e.g., SSP3 and SSP5). Each SSP scenario is linked with specific emission pathways to form combined storylines (e.g., SSP1-2.6, SSP2-4.5, SSP5-8.5), enabling more holistic climate assessments that incorporate both environmental and socioeconomic dimensions. The Intergovernmental Panel on Climate Change (IPCC) Sixth Assessment Report (AR6) adopted these SSP-based scenarios and introduced substantial advancements, such as higher spatial resolution in global climate models, improved representation of extreme climate events, and tighter coupling between physical climate models and socioeconomic trends (Calvin et al., 2023; Kikstra et al., 2022; Pirani et al., 2024). These improvements are particularly valuable for urban-scale analysis, where passive energy conservation measures are sensitive to localized climate conditions and extreme heat events. The enhanced scenario framework thus supports more realistic and context-specific assessments of building performance and resilience, informing adaptive design strategies in the built environment under diverse future conditions (Kikstra et al., 2022). Figure 5.3 shows Trajectories of radiative forcing and global mean temperature (above pre-industrial levels) based on different emissions types native to the MAGICC6 model by Gidden et al. (2019).

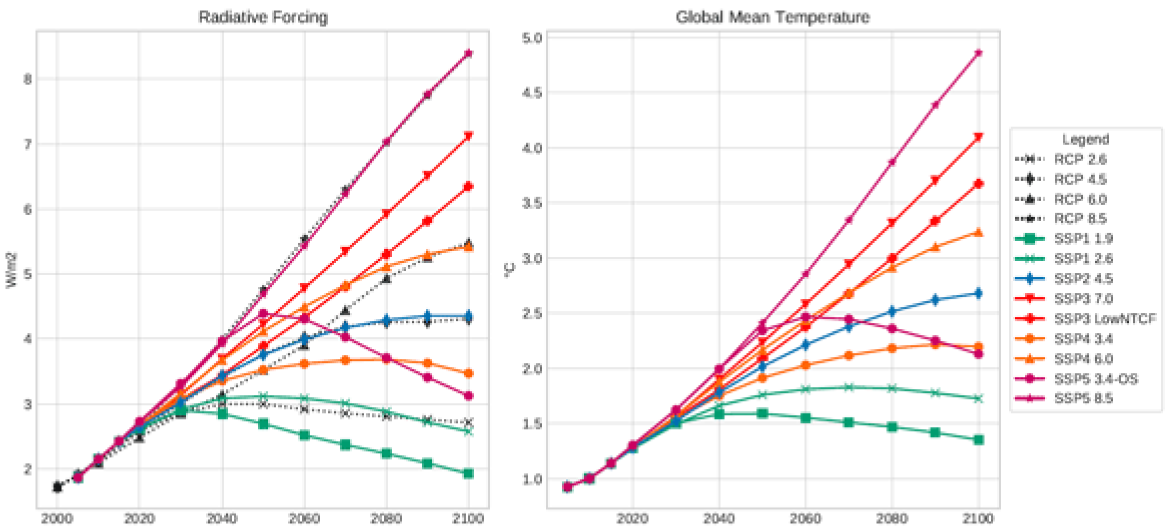

Figure 5.3 Trajectories of radiative forcing and global mean temperature (above pre-industrial levels) based on different emissions types native to the MAGICC6 model (Gidden et al., 2019).

The selection of climate scenarios—whether RCPs or SSPs—introduces significant uncertainty into building performance assessments, especially over long-term horizons. Each scenario reflects a different trajectory of greenhouse gas emissions and socioeconomic development, resulting in varying projections of temperature, humidity, and climate extremes that directly influence building performance. This scenario-driven uncertainty has profound implications for predicting building cooling demands, required heating hours, and overall energy performance across different regions. For example, according to Berardi and Jafarpur (2020), there is an average decrease of 18%–33% for the heating energy use intensity, and an average increase of 15%–126% for the cooling energy use intensity by 2070, depending on the baseline climatic file of use and building typology in Canada. Moreover, in the example of Australia, the total heating and cooling energy requirement of newly constructed 5 star hotel is projected to vary significantly in the range of −26% to 101% by 2050 and −48% to 350% by 2100 (Wang et al., 2010). Besides, based on the study of Sulzer and Christen (2024) in Europe, the projected hours of indoor heat stress will increase on average by + 379 h, + 654 h, and + 1209 h under RCP2.6, RCP4.5, and RCP8.5, respectively. These variations underscore the necessity of using multiple climate scenarios in building performance simulations (Coelho & Kraniotis, 2023). Therefore, the best practice is to assess passive strategies under a suite of plausible scenarios and transparently report the range of results, ensuring robust and adaptive design under climate uncertainty.

5.2 Variability in Climate Data Sources

Global Climate Models (GCMs) are comprehensive numerical models that simulate the Earth's climate system by representing large-scale interactions among the atmosphere, oceans, land surfaces, and cryosphere (Edwards, 2011). These models operate at relatively coarse spatial resolutions, typically on the order of hundreds of kilometers, and are primarily used to project broad, global-scale climate trends over long time periods. To provide more detailed and region-specific climate information, Regional Climate Models (RCMs) are employed. RCMs dynamically downscale the outputs from GCMs to much finer spatial resolutions—often tens of kilometers or less—allowing them to capture local climate processes, topographical effects, and land-use characteristics that are not resolved by GCMs (Rummukainen, 2010). This two-tiered modeling approach enables researchers and practitioners to obtain climate projections that are both globally consistent and locally relevant, which is essential for applications such as building performance simulations (Kikumoto et al., 2015).

The diversity of available GCMs and RCMs stems from differences in their underlying physical formulations, parameterizations, spatial and temporal resolutions, and the scientific objectives of the modeling teams that develop them (Flato et al., 2014). Each model incorporates unique assumptions about atmospheric processes, land-atmosphere interactions, and feedback mechanisms, leading to a range of possible future climate outcomes even under the same greenhouse gas emission scenario. As a result, climate projections derived from different GCMs and RCMs can vary significantly in terms of temperature, precipitation patterns, and the frequency or intensity of extreme weather events. A figure of various combinations of GCM-RCM is shown in Figure 5.4 It was reported that the choice of GCM or RCM can introduce substantial uncertainty, with up to 5 degrees due to RCM selection and 10 degrees due to GCM selection. For building performance assessments, this variability translates into substantial uncertainty in the climate data used as simulation inputs. Therefore, it is considered best practice to use an ensemble of multiple GCMs and RCMs when conducting building simulations, as this approach captures the range of plausible climate futures and supports more robust and resilient design decisions in the face of climate uncertainty.

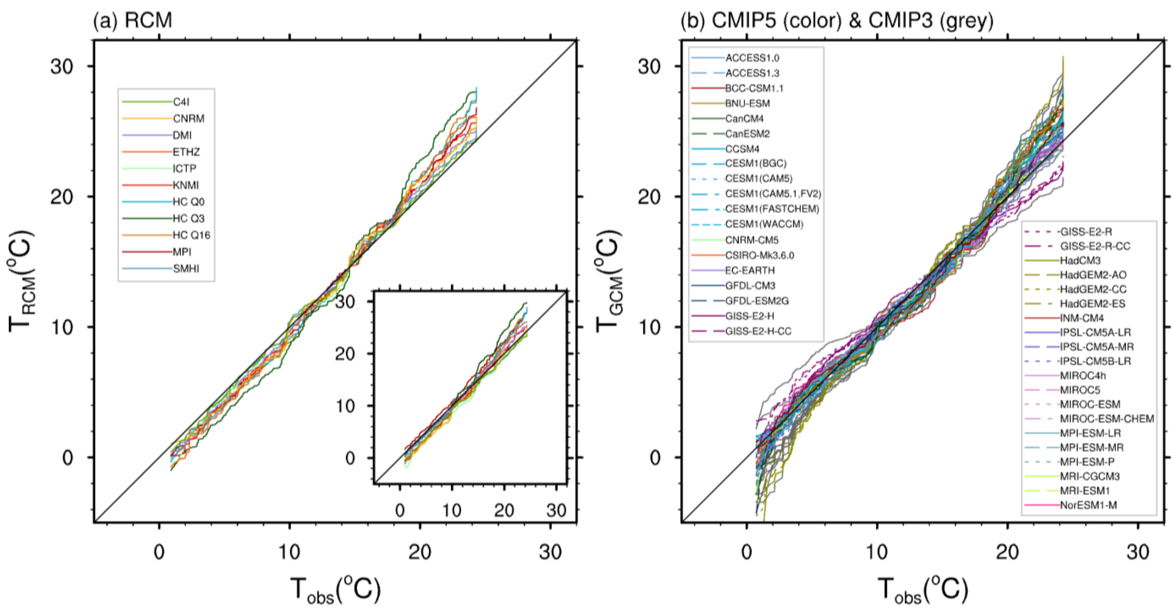

Figure 5.4 Comparison of climate projections from various RCMs and GCMs (Flato et al., 2014)

5.3 Bias-correction

Raw outputs from Global Climate Models (GCMs) and Regional Climate Models (RCMs) often exhibit systematic discrepancies—known as biases—when compared to observed local climate data (Teutschbein & Seibert, 2013). These biases can arise from the coarse spatial resolution of climate models, incomplete representation of local physical processes, and simplifications inherent in model parameterizations. For applications such as building performance simulation and urban overheating assessment, the accuracy of local climate inputs is critical as uncorrected model data can lead to significant errors in estimating future energy demand, overheating risk, and moisture-related deteriorations as well as the effectiveness of adaptation strategies. To address this, bias correction techniques are employed to statistically adjust climate model outputs so that their statistical properties closely align with historical observed data. The bias correction method aims to bridge the gap between raw climate projections and the high-quality, location-specific data required for robust impact assessments.

A wide range of bias correction methods have been developed and are now standard practice in climate impact research (Maraun, 2016). These include simple scaling and additive corrections, as well as more advanced approaches such as histogram equalization, quantile mapping, and multivariate techniques. Recent studies have demonstrated that bias correction can dramatically reduce errors in key climate variables—for example, reducing temperature bias from several degrees to near zero, and improving the accuracy of solar radiation, wind speed, and humidity projections (Maraun, 2016; Maraun et al., 2017; Zou, 2024; Zou et al., 2023). An example of raw and bias-corrected climate data is shown in Figure 5.5 Despite these improvements, bias correction methods also have limitations. They often rely on the assumption that model biases are stationary over time, which may not hold true under changing climate conditions. Furthermore, the choice of bias correction method and its implementation can introduce additional uncertainties. Therefore, it is recommended that researchers carefully select and transparently report the bias correction techniques used and consider ensemble approaches to account for residual uncertainties in future climate impact assessments.

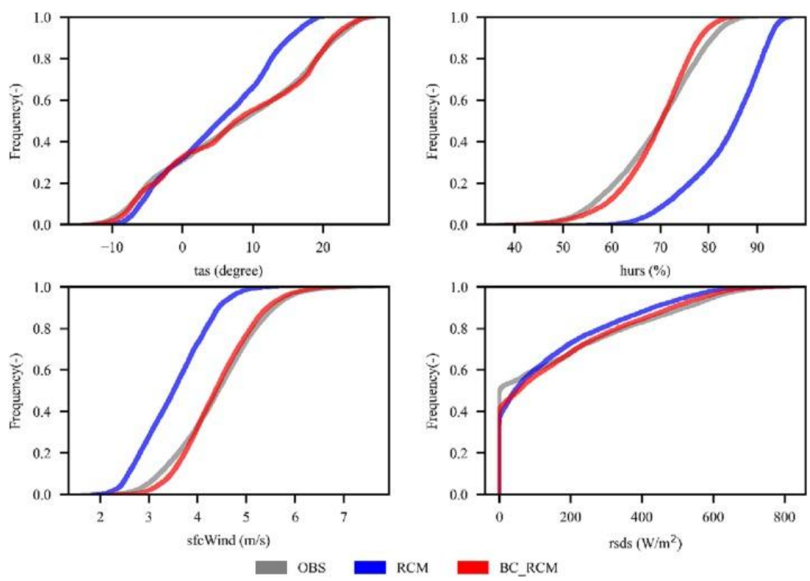

Figure 5.5 Cumulative distribution function comparison of observational (OBS), raw RCM (RCM), and bias-corrected RCM (BC_RCM) data of dry-bulb outdoor air temperature (tas), relative humidity (hurs), wind speed (sfcWind), and global solar radiation (rsds) (City: Montreal; GCM: MPI-M-MPI-ESM-LR; Time periods: 1998–2017) (Zou, Gaur, Wang, et al., 2022)

5.4 Methods of generating reference years

The reference year method is a widely adopted approach for streamlining building performance and overheating assessments under future climate scenarios (Zou, 2024; Zou, Gaur, et al., 2022a; Zou, Gaur, et al., 2022b). Given the computational intensity of simulating every year within multi-decadal climate projections, reference year methods aim to select one or a few years that are most representative of the long-term dataset or that capture specific aspects of interest, such as typical or extreme conditions. This approach enables researchers to focus on key climate characteristics while significantly reducing computational costs and repetitive simulation work. Several types of reference years have been developed for different applications (Zou et al., 2023), including the Typical Meteorological Year (TMY), which combines months from different years to best represent average conditions; and the Design Summer Year (DSY), which targets extreme summer conditions relevant for overheating risk; Moisture Reference Years, which used for assess moisture safety designs of building envelope systems (Aggarwal et al., 2022; Chung et al., 2023; Vandemeulebroucke et al., 2022). Other variants, such as the Weather Year for Energy Calculations (WYEC), International Weather Year for Energy Calculations (IWEC), and Canadian Weather Year for Energy Calculations (CWEC), use similar principles but apply different selection and weighting criteria. For more targeted assessments, methods like the Summer Reference Year (SRY) and Reference Summer Weather Year (RSWY) have been introduced to capture near-extreme or heat stress conditions, sometimes incorporating thermal comfort indices.

The process of generating reference years typically involves statistical analysis of long-term climate data, often using variables such as temperature, humidity, wind speed, and solar radiation. For example, the TMY method selects twelve months from the historical record that best represents the typical climate profile for each month, based on statistical criteria such as the cumulative distribution function (CDF) of key variables (Hall et al., 1978; Wu et al., 2025). In contrast, methods for generating extreme years (Zou, 2024; Zou, Gaur, Wang, et al., 2022), such as the Typical Downscaled Year (TDY), Extreme Cold Year (ECY), and Extreme Warm Year (EWY) as shown in Fig. 6, identify months with the least or most deviation from the long-term CDF, assembling them into a continuous year that reflects typical or extreme conditions. Recent advancements have also incorporated downscaled climate projections from Regional Climate Models (RCMs), allowing reference years to reflect future climate uncertainties and extremes. Studies have shown that these methods can efficiently capture the range of climatic projections and building energy responses, providing upper and lower bounds for future overheating risks. However, Zou et al. (2023) also highlights the need for consensus on the selection criteria and suggests that using integrated indices, such as thermal comfort metrics, may further enhance the relevance of reference years for overheating and resilience assessments.

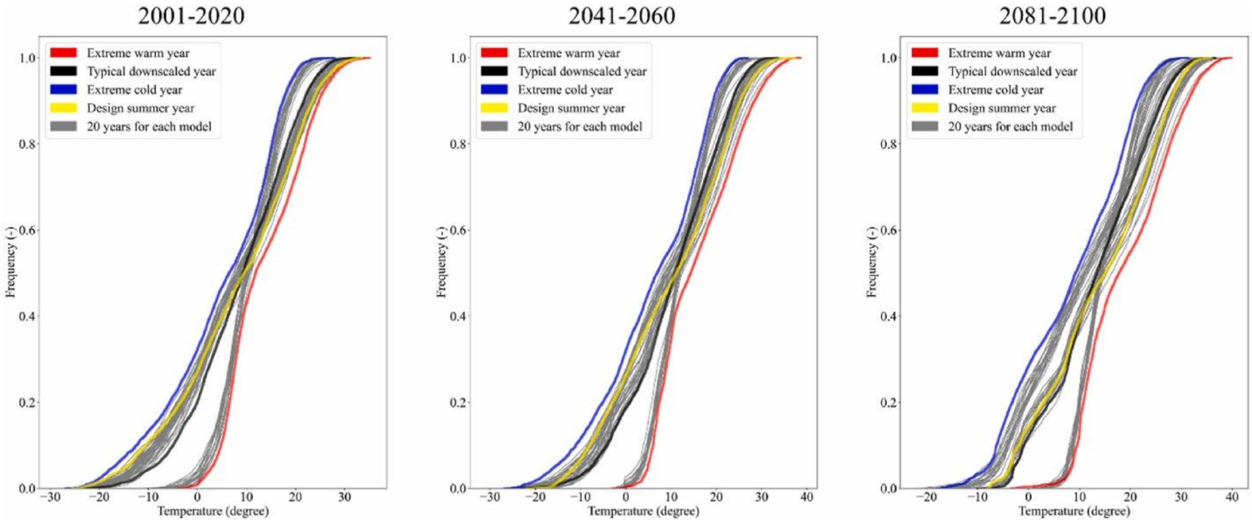

Figure 5.6 Cumulative distribution function comparison of the hourly temperature from 20 years, DSY and 1-year reference year climate data sets of TDY, ECY, and EWY in Montreal for the contemporary term, mid-term and long-term future (Zou, Gaur, Wang, et al., 2022)

5.5 References

Aggarwal, C., Ge, H., Defo, M., & Lacasse, M. A. (2022). Hygrothermal performance assessment of wood frame walls under historical and future climates using partial least squares regression. Building and Environment, 223, 109501.

Berardi, U., & Jafarpur, P. (2020). Assessing the impact of climate change on building heating and cooling energy demand in Canada. Renewable and Sustainable Energy Reviews, 121, 109681.

Calvin, K., Dasgupta, D., Krinner, G., Mukherji, A., Thorne, P. W., Trisos, C., Romero, J., Aldunce, P., Barrett, K., & Blanco, G. (2023). IPCC, 2023: Climate Change 2023: Synthesis Report. Contribution of Working Groups I, II and III to the Sixth Assessment Report of the Intergovernmental Panel on Climate Change [Core Writing Team, H. Lee and J. Romero (eds.)]. IPCC, Geneva, Switzerland. (No Title).

Chaturvedi, R., Kulkarni, A., Karyakarte, Y., Joshi, J., & Govindasamy, B. (2014). Glacial mass balance changes in the Karakoram and Himalaya based on CMIP5 multi-model climate projections. Climatic change, 123. https://doi.org/10.1007/s10584-013-1052-5

Chung, D., Wen, J., & Lo, L. C. J. (2023). Examining the impact of stochastic multi-year weather and air infiltration on hygrothermal moisture risks. Journal of Building Physics, 47(1), 4-35.

Coelho, G. B., & Kraniotis, D. (2023). Numerical investigation of mould growth risk in a timber-based facade system under current and future climate scenarios. Journal of Physics: Conference Series,

Edwards, P. N. (2011). History of climate modeling. Wiley Interdisciplinary Reviews: Climate Change, 2(1), 128-139.

Flato, G., Marotzke, J., Abiodun, B., Braconnot, P., Chou, S. C., Collins, W., Cox, P., Driouech, F., Emori, S., & Eyring, V. (2014). Evaluation of climate models. In Climate change 2013: the physical science basis. Contribution of Working Group I to the Fifth Assessment Report of the Intergovernmental Panel on Climate Change (pp. 741-866). Cambridge University Press.

Gidden, M. J., Riahi, K., Smith, S. J., Fujimori, S., Luderer, G., Kriegler, E., Van Vuuren, D. P., Van Den Berg, M., Feng, L., & Klein, D. (2019). Global emissions pathways under different socioeconomic scenarios for use in CMIP6: a dataset of harmonized emissions trajectories through the end of the century. Geoscientific Model Development, 12(4), 1443-1475.

Hall, I. J., Prairie, R., Anderson, H., & Boes, E. (1978). Generation of a typical meteorological year.

Kikstra, J. S., Nicholls, Z. R., Smith, C. J., Lewis, J., Lamboll, R. D., Byers, E., Sandstad, M., Meinshausen, M., Gidden, M. J., & Rogelj, J. (2022). The IPCC Sixth Assessment Report WGIII climate assessment of mitigation pathways: from emissions to global temperatures. Geoscientific Model Development, 15(24), 9075-9109.

Kikumoto, H., Ooka, R., Arima, Y., & Yamanaka, T. (2015). Study on the future weather data considering the global and local climate change for building energy simulation. Sustainable Cities and Society, 14, 404-413.

Machard, A., Salvati, A., P. Tootkaboni, M., Gaur, A., Zou, J., Wang, L. L., Baba, F., Ge, H., Bre, F., & Bozonnet, E. (2024). Typical and extreme weather datasets for studying the resilience of buildings to climate change and heatwaves. Scientific data, 11(1), 531.

Maraun, D. (2016). Bias correcting climate change simulations-a critical review. Current Climate Change Reports, 2(4), 211-220.

Maraun, D., Shepherd, T. G., Widmann, M., Zappa, G., Walton, D., Gutiérrez, J. M., Hagemann, S., Richter, I., Soares, P. M., & Hall, A. (2017). Towards process-informed bias correction of climate change simulations. Nature Climate Change, 7(11), 764-773.

Meehl, G. A., Boer, G. J., Covey, C., Latif, M., & Stouffer, R. J. (2000). The coupled model intercomparison project (CMIP). Bulletin of the American Meteorological Society, 81(2), 313-318.

Nik, V. M. (2012). Hygrothermal simulations of buildings concerning uncertainties of the future climate. Chalmers Tekniska Hogskola (Sweden).

Nik, V. M., Perera, A., & Chen, D. (2021). Towards climate resilient urban energy systems: a review. National Science Review, 8(3), nwaa134.

O'Neill, B. C., Tebaldi, C., Van Vuuren, D. P., Eyring, V., Friedlingstein, P., Hurtt, G., Knutti, R., Kriegler, E., Lamarque, J.-F., & Lowe, J. (2016). The scenario model intercomparison project (ScenarioMIP) for CMIP6. Geoscientific Model Development, 9(9), 3461-3482.

Panico, S., Larcher, M., Avellanosa, D. H., Baglivo, C., Troi, A., & Congedo, P. M. (2023). Hygrothermal simulation challenges: assessing boundary condition choices in retrofitting historic European buildings. Energy and Buildings, 297, 113464.

Pirani, A., Fuglestvedt, J. S., Byers, E., O'Neill, B., Riahi, K., Lee, J.-Y., Marotzke, J., Rose, S. K., Schaeffer, R., & Tebaldi, C. (2024). Scenarios in IPCC assessments: Lessons from AR6 and opportunities for AR7. npj Climate Action, 3(1), 1.

Randall, D. A., Wood, R. A., Bony, S., Colman, R., Fichefet, T., Fyfe, J., Kattsov, V., Pitman, A., Shukla, J., & Srinivasan, J. (2007). Climate models and their evaluation. In Climate change 2007: The physical science basis. Contribution of Working Group I to the Fourth Assessment Report of the IPCC (FAR) (pp. 589-662). Cambridge University Press.

Rummukainen, M. (2010). State - of - the - art with regional climate models. Wiley Interdisciplinary Reviews: Climate Change, 1(1), 82-96.

Sulzer, M., & Christen, A. (2024). Climate projections of human thermal comfort for indoor workplaces. Climatic Change, 177(2), 28.

Taylor, K. E., Stouffer, R. J., & Meehl, G. A. (2012). An overview of CMIP5 and the experiment design. Bulletin of the American Meteorological Society, 93(4), 485-498.

Teutschbein, C., & Seibert, J. (2013). Is bias correction of regional climate model (RCM) simulations possible for non-stationary conditions? Hydrology and Earth System Sciences, 17(12), 5061-5077.

Vandemeulebroucke, I., Caluwaerts, S., & Van Den Bossche, N. (2022). Decision framework to select moisture reference years for hygrothermal simulations. Building and Environment, 218, 109080.

Vandemeulebroucke, I., Defo, M., Lacasse, M., Caluwaerts, S., & Van Den Bossche, N. (2021). Canadian initial-condition climate ensemble: Hygrothermal simulation on wood-stud and retrofitted historical masonry. Building and Environment, 187, 107318.

Wang, X., Chen, D., & Ren, Z. (2010). Assessment of climate change impact on residential building heating and cooling energy requirement in Australia. Building and environment, 45(7), 1663-1682.

Wu, Y., Wang, R., Ye, L., Li, Y., Kang, X., Chen, H., Guo, Y., & Yan, D. (2025). Representative meteorological year (RMY): a novel generated weather year reflecting long-term probabilistic distribution in building energy simulation. Renewable Energy, 124528.

Zhai, Z. J., & Helman, J. M. (2019). Implications of climate changes to building energy and design. Sustainable Cities and Society, 44, 511-519.

Zou, J. (2024). Assessing Urban Overheating Under Climate Change through Representative Methods on Large Spatial and Temporal Scales Concordia University].

Zou, J., Gaur, A., & Wang, L. (2022a). A method of selecting future reference years for indoor overheating assessment. Indoor Air.

Zou, J., Gaur, A., & Wang, L. L. (2022b). Outdoor Overheating Evaluation in Montreal Using a Reference Year Method Among Future Time Periods. International Conference on Building Energy and Environment,

Zou, J., Gaur, A., Wang, L. L., Laouadi, A., & Lacasse, M. (2022). Assessment of future overheating conditions in Canadian cities using a reference year selection method. Building and Environment, 218, 109102.

Zou, J., Lu, H., Shu, C., Ji, L., Gaur, A., & Wang, L. L. (2023). Multiscale numerical assessment of urban overheating under climate projections: A review. Urban Climate, 49, 101551.

Zou, J., Wang, L., Yang, S., Lacasse, M., & Wang, L. L. (2025). Predicting long-term urban overheating and their Mitigations from nature based solutions using Machine learning and field measurements. Energy and Buildings, 338, 115720.

Zou, J., Yu, Y., Mortezazadeh, M., Lu, H., Gaur, A., & Wang, L. (2025). Evaluating climate change impacts on building level steady-state and dynamic outdoor thermal comfort. Building and environment, 112604.

International Council
for Research and Innovation
in Building and Construction

CIB is the global network for research and innovation in construction and the built environment

www.cibworld.org | secretariat@cibworld.org